Upeksha Caldera

THE ROLE OF RENEWABLE ENERGY BASED SEAWATER REVERSE OSMOSIS (SWRO) IN MEETING THE GLOBAL WATER CHALLENGES IN THE DECADES TO COME

ACTA UNIVERSITATIS LAPPEENRANTAENSIS 931

Upeksha Caldera

THE ROLE OF RENEWABLE ENERGY BASED SEAWATER REVERSE OSMOSIS (SWRO) IN MEETING THE GLOBAL WATER CHALLENGES IN THE DECADES TO COME

Dissertation for the degree of Doctor of Science (Technology) to be presented with due permission for public examination and criticism in the Auditorium of the Student Union House at Lappeenranta-Lahti University of Technology LUT, Lappeenranta, Finland on the 25th of November, 2020, at noon.

Acta Universitatis
Lappeenrantaensis 931

Supervisor Professor Christian Breyer
LUT School of Energy Systems
Lappeenranta-Lahti University of Technology LUT
Finland

Reviewers Professor Philip Davies
School of Engineering
University of Birmingham
UK

Adjunct Professor Vasilis Fthenakis
Earth and Environmental Engineering
Columbia University
USA

Opponent Professor Philip Davies
School of Engineering
University of Birmingham
UK

ISBN 978-952-335-580-4
ISBN 978-952-335-581-1 (PDF)
ISSN-L 1456-4491
ISSN 1456-4491

Lappeenranta-Lahti University of Technology LUT
LUT University Press 2020

Abstract

Upeksha Caldera
The role of renewable energy based seawater reverse osmosis (SWRO) in meeting the global water challenges in the decades to come
Lappeenranta 2020
90 pages
Acta Universitatis Lappeenrantaensis 931
Diss. Lappeenranta-Lahti University of Technology LUT
ISBN 978-952-335-580-4, ISBN 978-952-335-581-1 (PDF), ISSN-L 1456-4491, ISSN 1456-4491

Renewable energy (RE) powered desalination is rapidly gaining interest as a means to augment the increasingly stressed global water supply. This thesis introduces and describes the ways in which 100% RE-based seawater reverse osmosis (SWRO) desalination can be used to help overcome the world's water issues. Concerns within the desalination industry about switching to solely RE sources are tackled, and new ways of using desalination with better water management added. The results of this thesis clearly show that desalination demand across many regions will increase and adopting 100% RE-based desalination can help assuage global water stress. Ultimately, by addressing the issues of water stress, water demand management in the irrigation sector, and the transition to RE resources, the research establishes pathways to achieve the United Nations Sustainable Development Goals 2, 6 and 7.

The global desalination demand was estimated for the time period from 2020 to 2050, in 5-year time steps. The global desalination demand for the municipal, irrigation and industrial sectors, excluding the power sector, was found to be 4.4×10^9 m^3/day by 2050 - an almost 49-fold increase from the online capacity in 2015. This projection assumes that there is no significant improvement in the water use efficiency of the irrigation sector, the sector responsible for almost 70% of the global water withdrawals. In this thesis, scenarios were established where the irrigation efficiency of existing irrigation sites were increased under different conditions. In the most optimistic scenario, the desalination demand in 2050 was 1.7×10^9 m^3/day. In the moderate scenario, the desalination demand in 2050 fell to 3×10^9 m^3/day. The impacts of the improved water use efficiency on the global irrigation sites and the subsequent influence on the demand for desalination could be observed.

In addition to assessing the potential for desalination, the costs of running an entirely RE-based global desalination sector was analysed. The LUT Energy System modelling (ESM) tool, designed in an hourly temporal and $0.45^\circ \times 0.45^\circ$ spatial resolution, is a linear optimisation model with the objective of minimising the annual costs of the energy system. An initial overnight study, representative of the characteristics of a steady-state simulation, on a global scale for the year 2030, showed that it was possible to run 100% RE-based SWRO desalination at costs competitive with the current fossil-based desalination sector. These results were further supported by a country specific study on

the role of RE-based SWRO desalination in Iran. Despite being ranked as one of the ten most water stressed countries in the world, RE-based desalination can allow Iran to provide potable water at a cost range of 1.0 €/m^3 – 3.5 €/m^3 by the year 2030. These costs also include the water transportation costs which play a significant role due to the mountainous terrain of Iran.

The overnight results led to work on the transition pathways which allow countries to achieve an entirely RE-based desalination industry by 2050. Saudi Arabia was chosen as a case study. The transition pathway was modelled such that the current fossil fuel-based power, desalination and industrial gas sectors would be run entirely by RE resources by 2050. The installation of SWRO and the thermal Multiple Effect Distillation (MED) technologies were optimised to meet the projected desalination demand. The transition enabled the average levelised cost of water (LCOW) in Saudi Arabia to decrease from 3 €/m^3 in 2015 to 0.66 €/m^3 in 2050. The corresponding decrease in the levelised cost of electricity (LCOE) was from 139 €/MWh in 2015, assuming unsubsidised gas and oil costs, to 40 €/MWh by 2050 in a 100% RE-based energy system. Solar PV and battery storage played significant roles in enabling the Saudi Arabian transition in a cost optimised manner.

The hypothesis that desalination could provide additional flexibility to a RE-based system was also investigated. This was done by modelling the energy systems transition pathway for the desalination, power and industrial gas sectors of Saudi Arabia in integrated and non-integrated scenarios. The observed role of SWRO desalination and water storage during the Saudi Arabian transition alluded to the fact that SWRO plants do not offer the flexibility initially thought possible. Through additional analysis, it was observed that the relatively high capex of SWRO desalination plants does not allow this component to operate in a flexible way. While SWRO plants can technically be operated in a flexible manner, the results showed that it does not make economic sense to do so. The desired energy system flexibility can be offered on a lower cost level by PV power plants and battery storage, while SWRO plants are run in a baseload mode.

As SWRO desalination becomes a crucial part of the global water supply, it is necessary to be able to project the future cost trends. In this thesis, the first learning curve for SWRO capital expenditures (capex) is presented. While the learning curve has been used by different industries for cost projections, it has not yet been applied to the desalination industry. It was found that the SWRO capex has decreased by 15% for every doubling of cumulative online SWRO capacity, implying a learning rate of 15% for SWRO plants. The decreasing costs in RE technologies, coupled with the decreasing costs of SWRO plants, indicate further reduction in the water production costs.

The cumulative research findings were then adopted on a global scale for countries with desalination demand projections up to 2050. A globally prevalent LCOW range of 0.32 €/m^3 – 1.66 €/m^3 can be achieved by 2050 through 100% RE-based desalination. The global average LCOE is found to decrease drastically from 180 €/MWh in 2015 to approximately 50 €/MWh by 2050. The initial high LCOE in 2015 is due to the significant use of fossil fuels, taking into account the unsubsidised costs. The reduction in the LCOW

during the transition can be attributed to the decreasing LCOE, the elimination of the cost of fossil gas for thermal desalination by the electrification of the desalination sector, the improved efficiency and decreasing costs of desalination plants. The cost range includes the water transportation costs from the desalination plant to the demand sites which can be further inland. The results show that solar PV and battery energy storage are key RE technologies that will drive the desalination sector in the future. This indicates that most regions with water stress are also those with plentiful solar resources. The resulting costs are competitive with the conventional cost of water desalination, as well as the projected costs of traditional water treatment methods in many parts of the world. As surface water diminish, groundwater levels decline, mountain glaciers retreat and pollution and salinization threaten available resources, traditional water collection methods become threatened and expensive.

The current rhetoric in the water community is rife with discussions on managing water demand and reducing global water stress. Through our research we hope to persuade the desalination sector to latch onto the booming renewable energy sector and provide a water supply option to meet the increasing global water demand, as well as contribute to climate mitigation and consequently reduce global water stress.

Keywords: water stress, desalination, seawater reverse osmosis, renewable energy

Acknowledgements

This work was carried out in the School of Energy Systems at Lappeenranta-Lahti University of Technology LUT, Finland, between 2016 and 2020.

First, I would like to thank my supervising Professor Christian Breyer for the guidance, support and inspiration over the last few years. When I look over this manuscript, I am in awe of the work and pleased with the outcome of the last four years. Thank you for pushing me to go that extra mile and inspiring us to strive for positive change.

Second, I would like to thank all the members of the Solar Economy team – it has been a wild ride y'all. I would also like to thank Professor Thomas Dittrich, who first introduced me to Professor Christian Breyer and the concept of renewable energy based desalination. I also like to express much gratitude to the reviewers of this thesis, Professor Philip Davies and Associate Professor Vasilis Fthenakis, for their helpful comments and advice. Also, thanks to all the authors whose work this manuscript builds on. I would also like to thank the Happiness through Health initiative at LUT university for offering the wonderful group classes and the amazing crew!

I wish to express my gratitude to the Reiner Lemoine Stiftung, the Finnish Cultural Foundation and the Research Foundation of Lappeenranta University of Technology for the financial support over the last four years.

To my friends near and far, I count my blessings twice when I think of you. Anna, Lukas, Kat, Claudia, Sophie, Rose, Rohit, Viswa, thank you for the visits and support over the years. To Charlotte Aunty and Markku Uncle, thank you for all the love and support, and helping make Lappeenranta feel more like home.

My sincerest thanks to my family who have been my biggest fans, source of strength and recently some of the most passionate advocates for renewable energy systems. You continue to inspire me.

With love and gratitude,
Upeksha Caldera
March 2020
Lappeenranta, Finland

To Ammi and Thathi, for the last 31 years and counting of support
To Mali, you continue to amaze me
To Arman, there is no one else I would want to travel this journey with

Contents

List of publications

This dissertation is based on the following papers. The rights have been granted by publishers to include the papers in dissertation.

I. Caldera U, Bogdanov D, Breyer C, 2016, Local cost of seawater RO desalination based on solar PV and wind energy: A global estimate. In: Desalination, 385:207-216, DOI 10.5278/ijsepm.3305

II. Caldera U, Bogdanov D, Fasihi M, Aghahosseini A, Breyer C, 2019, Securing future water supply for Iran through 100% renewable energy powered desalination. In: International Journal of Sustainable Energy Planning and Management, 23, DOI 10.5278/ijsepm.3305

III. Caldera U, Bogdanov D, Afanasyeva S, Breyer C, 2018, Role of seawater desalination in the management of an integrated water and 100% renewable energy based power sector in Saudi Arabia. In: Water, 10, 3, DOI 10.3390/w10010003

IV. Caldera U, Breyer C, 2018, The role that battery and water storage play in Saudi Arabia's transition to an integrated 100% renewable energy power system. In: Journal of Energy Storage, 17, DOI 10.1016/j.est.2018.03.00

V. Caldera U, Breyer C, 2017, Learning Curve for Seawater Reverse Osmosis Desalination Plants: Capital Cost Trend of the Past, Present, and Future. In: Water Resources Research, 53, DOI 10.1002/2017WR021402

VI. Caldera U, Breyer C, 2019, Assessing the potential for renewable energy powered desalination for the global irrigation sector. In: Science of the Total Environment, 694, 133598, DOI 10.1016/j.scitotenv.2019.133598

VII. Caldera U, Breyer C, 2019, Strengthening the global water supply through a decarbonised global desalination sector and improved irrigation systems. In: Energy, 200, 117507, DOI 10.5278/ijsepm.3305

The publications are numbered throughout this dissertation using the Roman numerals above. Reprints of each publication are included at the end of this dissertation.

Author's contribution

Upeksha Caldera is the principal author and investigator in papers I – VII. In papers I – VII, Upeksha Caldera contributed to the conceptualisation of the research topics, aided the methods development, simulation, analysis, visualisation and wrote the original drafts. In Publication I and III, Dmitrii Bogdanov aided the methods development and carried out simulations. In Publication III, Svetlana Afanasyeva aided the methods development and further developed the visualisations. In Publication II, Arman Aghahosseini and Mahdi Fasihi provided feedback on the manuscript and assisted with the data collection.

Nomenclature

Abbreviations

a	annum
b€	billion Euro
BAU	business as usual
CAGR	cumulative annual growth rate
capex	capital expenditures
CO_2	carbon dioxide
crf	capital recovery factor
DAC	direct air capture
DEWA	Dubai Electricity and Water Authority
ESM	energy system model
FAO	Food and Agricultural Organisation
GDP	gross domestic product
HHB	hot heat burner
HPIE	highest possible irrigation efficiency
GCC	Gulf Cooperation Council
GHG	greenhouse gases
GWI	Global Water Intelligence
IPCC	Intergovernmental Panel on Climate Change
ITRPV	International Technology Roadmap for Photovoltaic
IEP	irrigation efficiency push
LCOE	levelised cost of electricity
LCOW	levelised cost of water
OECD	Organisation for Economic Co-operation and Development
opex	operational expenditures
m	meter
m^3	cubic meter
MED	multiple-effect distillation
MENA	Middle East and North Africa
MSF	multi-stage flash
Mt	million tonnes
MWh	megawatt hour
NRW	non-revenue water
RE	renewable energy
TES	thermal energy storage
USD	American dollar
PtH	power-to-heat
PtG	power-to-gas
opex	operating and maintenance expenditures
PV	photovoltaic

RO	reverse osmosis
SEC	specific energy consumption
SDG	Sustainable Development Goal
SWRO	seawater reverse osmosis
UN	United Nations
UNEP	United Nations Environment Programme
VRE	variable renewable energy
WACC	weighted average cost of capital
WHO	World Health Organisation
WRI	World Resources Institute

1 Introduction

1.1 Water –the world's most abstracted natural resource

Our relationship with water is overwhelmingly large and critically important. Civilizations have risen and perished with the access and ability to harness water resources. Where there was access to water, nomads settled, agriculture flourished, cities established, and empires formed. Where water resources depleted, chaos ensued, and civilizations crumbled (Pearce, 2018). Today, we rely on water more than we ever have. Water underpins the growth of economic and social sectors, as well as ecosystem functions, that are essential to human well-being (UNWWAP, 2015). The Food and Agricultural Organisation (FAO) (2016) reports that global water withdrawals in the last century has been increasing 1.7 times faster than the global population. Unsurprisingly, water is categorized as the most abstracted natural resource by volume, followed by sand and gravel (UNEP, 2014). History shows that freshwater resources have not lasted long and caused strife for dependent communities (Pearce, 2018). We are seeing similar events around the globe today, further exacerbated by factors like increasing demand, pollution and climate change (UNWWAP, 2019). Water is reported to be responsible for 90% of all natural disasters (WWF, 2019). During the period of 1995 – 2015, almost half of all natural disasters were either drought or flood related (WWF, 2019). So, the question raised across global communities is: how do we meet the increasing global demand for water without exhausting our natural water resources and ultimately create our own downfall? This question forms the underlying basis of this thesis.

The recent UN World Water Development Report (2019) highlights the current state of global water affairs. Water demand is reported to be growing annually by 1% since the 1980s, driven by increasing population, socioeconomic development, water demand for irrigation, and change in water use patterns. A study by Kummu et al. (2016) on the historical and future drivers of water demand reveal that the total water consumption increased from 358 km^3 per year in the 1900s to 1500 km^3 per year in the 2000s. Whilst water consumption in the 20^{th} century increased four-fold, the population living under water scarcity increased from 14% to 58% of the global population. Water scarcity is simply identified as the state when freshwater supplies cannot meet the water demand. Mekonnen and Hoekstra (2016) estimated that two-thirds of the world population experience water scarcity for at least part of a year. These results present a bleaker image of the water scarcity situation than that reported by earlier studies.

Currently, the agriculture sector (including irrigation, livestock and aquaculture) is the largest user of water, accounting for 69% of total global water withdrawals (UNWWAP, 2019). The industrial sector (including the power sector) and the municipal sector account for the remaining 19% and 12% of global water withdrawals respectively (UNWWAP, 2019). Water withdrawals refer to the extraction of water from the source for a specific use (FAO, 2010). In contrast, water consumption refers to the water that is consumed through processes such as evaporation, transpiration, incorporation in products and

contamination (FAO, 2010). Boretti and Rosa (2019) explain that the current global water withdrawals are estimated to be 4600 km^3 per year and critically near maximum sustainable levels. The authors also argue that the projections presented by the UN World Water Assessment Programme are more optimistic as the assessment is made on a global rather than on a local scale.

The Water Futures and Solutions Initiative (Burek *et al.*, 2016) project, for different socioeconomic and climate change narratives, the global water demand to increase by 20% - 33% by 2050. On a continental basis, Africa is supposed to experience the largest increase, up to 60%, but will still only account for a small share, up to 6%, of the total global water demand. Continental Asia, which presently accounts for 65% of the global water demand due to higher concentration of global irrigation sites, will continue to experience an increase in water demand accounting for 70% of the global water demand by 2050. The most intensive water demand increase is projected to occur in Africa, South America and Asia while Europe only experiences an increase in the less sustainably developed scenarios. The least increase in water demand by 2050, across all scenarios, is observed in Oceania, Central and North America. In terms of absolute water demand, China, India, United States, Russia and Pakistan account for the largest shares of the water demand in 2010 and will continue to do so in 2050.

Despite the large water demand of the agricultural sector, the industrial and municipal sectors are expected to experience steeper growth rates (UNWWAP, 2014). The 2014 UN World Water Development Report presented an increase in water demand for manufacturing, thermal electricity generation and domestic use of 400%, 140% and 130% respectively; this is the projected increase in 2050 compared to the global water demand in 2000. The corresponding cumulative annual growth rate (CAGR) for the manufacturing, thermal electricity generation and domestic are 3%, 2% and 2% respectively. However, the agricultural sector will continue to account for the largest share of the water demand and will be under increasing strain as water demand from the other sectors increase. In addition to the demands of the human defined sectors, water is required for the natural environment to survive, thrive and provide for us (UNWWAP 2014)

1.2 Freshwater is a limited natural resource

The concern is that the global demand is increasing for a finite freshwater resource which is distributed unevenly across the world (UNWWAP, 2014). Whilst we live on a blue planet with an estimated 1.4 billion km^3 of water resources, only 2.5% of this water resource (~ 35 million km^3) is available as freshwater. The remaining 97.5% is seawater. Furthermore, only 0.3% of the freshwater resource, or 90 thousand km^3, is surface freshwater water such as lakes and rivers. Nearly 69.8% of freshwater occurs as glaciers and permanent snow cover whilst the remaining 30.2% is groundwater in the form of deep and shallow basins, soil moisture and permafrost. Ultimately, less than 1% of the total freshwater resource, or 200,000 km^3 of renewable freshwater, is available for all life on Earth (UNEP, 2002). Renewable water resources are defined as the water resources

that are replenished through the natural water cycle and represent long-term average annual flow (FAO, no date). Non-renewable water refers to the groundwater resources that cannot be recharged within the human life span and are thousands of years old (FAO, no date). Groundwater is usually used during times of high water demand and low surface water availability (de Graaf *et al.*, 2014). Withdrawing groundwater beyond the natural recharge rate results in lowering of the water table and negatively impacts groundwater fed surface water. Recent research also show that over pumping of groundwater resources has substantially reduced surface water flows globally and that several watersheds have already reached their environmental limits (de Graaf *et al.*, 2019).

Various researchers have attempted to understand the use of surface water and groundwater sources annually on a global scale. Döll et al. (2012) modelled the global water withdrawals, by source, for five different demand sectors. It was found that over the time period from 1998 – 2002, groundwater sources were used to meet 35% of the total global water withdrawals. Groundwater accounted for 42%, 36% and 27% of the irrigation, domestic and manufacturing sector water withdrawals. The fraction of groundwater used for the municipal sector was highest in countries like Mongolia, Iran, Saudi Arabia, Austria, Morocco and large parts of the USA and Mexico. Groundwater for manufacturing is found to follow a similar trend to that of groundwater for domestic use. Meanwhile, groundwater for irrigation exceeded 80% of the total water withdrawals, in parts of Iran, India, Pakistan, North Africa, North America and Argentina. In contrast, groundwater use was less than 10% in regions along the Nile in Egypt, South Africa, Southeast Asia and Japan, indicating the dependence on surface water in these regions. The authors assumed that surface water was used for livestock and cooling of thermal power plants.

Wada et al. (2012) estimated that in the year 2000, 20% of the groundwater being withdrawn for irrigation was fossil groundwater - thus these groundwater resources will not be replenished once depleted. Furthermore, the contribution of fossil groundwater to the irrigation sector has tripled from 1960 to 2000. A recent study also shows that climate change is endangering the world's mountain ice that replenish surface water resources for more than a billion people, in both the Northern and Southern hemispheres (Immerzeel *et al.*, 2019). Within the framework outlined in the research, the Indus river is the most important and yet the most vulnerable. The Indus river is formed from the thick mountain glaciers and provide water to 120 million people living on the, otherwise parched, Indus plain. In addition, the region is one of the major breadbaskets of the world with the Indus basin in Pakistan being the largest contiguous irrigation project in the world (Parry *et al.*, 2016). Despite the diminishing water supply, the global water demand for irrigation, the sector that meets 45% of global food demand (Steduto *et al.*, 2018), has increased more than two-fold from 1960 to 2000 (Wada *et al.*, 2012). The World Economic Forum (no date) indicates that in a business as usual (BAU) scenario, by 2030, global water supplies will not be able to meet 40% of the total water demand. Water scarcity impedes human well-being and economic development. The UN WDDR (2019) states that at the current rate of environmental degradation and water pressure, 45% of the global gross domestic

product (GDP), 52% of the world's population and 40% of the global grain production will be at risk by 2050.

1.3 The unfolding global water crisis

In 2018, the South African city of Cape Town braced itself for 'Day Zero' when water supplies to homes and businesses would be shut off due to an unusually long period of intense drought (Welch, 2018; WRI 2018). The reservoirs were considered to be dangerously low due to the three year long drought, further exacerbated by increase in population (Welch, 2018). This crisis resulted in a report by the BBC on the 11 cities that are most likely to run out of drinking water (BBC News, 2018). The cities featured, such as London and Jakarta, are places where a water crisis occurring is uncommon. Fortunately for Cape Town, with stringent water conservation and efficiency measures, and rainfall after four years, the city has managed to avert the 'Day Zero' crisis (City Lab, 2019). Nevertheless, the conditions implemented during the drought are still in place, although less strict. However, water crises are now being felt in regions across the world. At the time of writing this thesis, Chennai, the 6th largest city in India, was facing its own 'Day Zero' (WRI, 2019b).

Recent data published by the World Resources Institute (2019a) noted 17 countries, hosting one - quarter of the global population, were facing extremely high levels of water stress. A region is said to be suffering from high water stress when the total water being withdrawn is more than 40% of the renewable water resources available (Gassert *et al.*, 2013). When a region is withdrawing more than 80% of the available renewable water resource then the region is suffering from extremely high water stress. In such a case, the region is using up fossil groundwater and reflects the situation in the 17 countries listed. It has to be noted that 12 out of the 17 countries are in the Middle East and North Africa region (WRI, 2019a). Meanwhile, 44 countries are reported to be facing high levels of water stress (WRI, 2019a). The authors (WRI, 2019a) explain that water stress is a local issue and while a country itself might not be suffering from water stress, regions within the country might be experiencing high levels of water stress. Figure 1 presents the water stress mapped for 2030 by using data provided by the World Resources Institute (Gassert *et al.*, 2013). Regions with significant water stress are prevalent in the United Sates, North Africa, Middle East, India and Eastern parts of China.

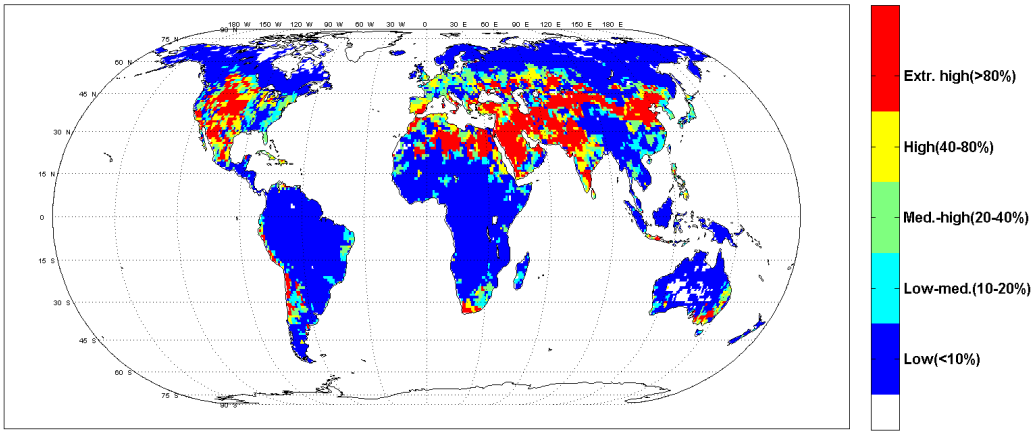

Figure 1 Water Stress Projection for 2030

Prolonged water stress manifests in the form of droughts, a natural disaster that is reported to affect an average of 55 million people around the world every year. Droughts have become increasingly challenging as they affect local water supplies, agriculture, environment, infrastructure, energy supplies and the local economy. According to the WWF (2019), the agriculture sector is most affected by droughts and water scarcity. It is reported that irrigation sites growing vital sources of food such as wheat, maize and rice are located in regions of high water stress and vulnerability to drought. According to the WWF, 22% of global wheat production are grown in areas with high to very high risk of drought. Climate change will further affect precipitation, and in conjunction with increasing pollution, exacerbates pressure on global water supplies, creating conditions for more devastating droughts. The WWF reports that 90% of global natural disasters are water related and will increase in intensity and frequency in the future.

The United Nations SDG 6 (United Nations, no date) stipulates the availability of water for all people by 2030 and the sustainable management of water resources. However, if there are no drastic changes in the current water supply and demand structures, only 60% of the total water demand will be met by 2030 (World Bank, 2019). Various organizations and researchers have discussed technological and behavioural changes that can be made to stem the increasing occurrence of water scarcity globally.

Wada et al. (2014) applied the concept of stabilization wedges, used in climate change mitigation discourse, to assess the potential for different strategies to reduce the impacts of global water stress. The strategies implemented were increasing agricultural water productivity, irrigation efficiency, water use intensity improvements in industry, limiting population increase, increasing water storage and the expansion of seawater desalination. It was found that at the rates of improvement suggested, the global population living in water stressed regions by 2050, could be decreased by 12% relative to a BAU scenario. The UNWDDR report (UNWWAP 2018) presented the concept of nature-based solutions, that rely on natural processes, to enhance the available water supply. The

solutions include concepts such as groundwater recharge, restoration of wetlands, riparian buffer risks, floodplain restoration and green roofs. According to the report, water resource management should include an appropriate portfolio of nature-based solutions and human-built infrastructure to tackle the water crisis. Other approaches being discussed and implemented are water conservation, reuse, recycling and generating large amounts of freshwater from other feed stocks (World Bank, 2019). A poll carried out by the ogranisations GlobeScan and Sustainability on the measures to be taken to overcome the global water crisis received a collection of similar responses from more than 1200 sustainability experts (Circle of Blue, 2019).

There are already observable improvements in sectoral productivity and efficiency in the water demand and supply side. However, according to the World Bank, the current rate of improvement is still too slow, and that this would only reduce the deficit between supply and demand by 1/5th in 2030 (World Bank, 2019). The report introduces and discusses the strategic role that desalination, in particular seawater based technologies, can play to close the water-supply demand gap. The authors note that as the demand for water and global water stress aggravates, desalination has become a more feasible water supply option for many nations.

1.4 The current role of seawater desalination

Desalination refers to the process of removing dissolved salts or minerals from water, thus producing freshwater from seawater or brackish water (Kucera, 2014). This method of producing freshwater has been around for thousands of years. One of the first references to seawater desalination was by Aristotle in the 4th century B.C. Aristotle is said to have written ‘saltwater, when it turns into vapor, becomes sweet and the vapor does not form saltwater again when it condenses’ (Kucera, 2014). In desalination, the saline feedwater is separated into two parts: one of that is freshwater or water with a low concentration of salt and a second part that is a brine concentrate with a higher concentration of salt than the feedwater.

Feedwater can be derived from a host of sources with various salinity factors expressed as the total dissolved solids (TDS) content. The World Health Organisation provides general guidelines on the water quality: freshwater is water with a TDS content less than 1000 parts per million (ppm), brackish water has a TDS content in the range of 1000 ppm – 35,000 ppm, whilst seawater has a TDS of 35,000 ppm or greater (Kucera, 2014). The Global Water Intelligence (GWI) group classifies brackish water to be water sources with a TDS range of 3000 ppm – 20,000 ppm while seawater to have a TDS content from 20,000 ppm - 50,0000 ppm (Virgili, 2017). Figure 2 illustrates the cumulative increase in global desalination capacity, separated by contributing feedwater sources, from 1945 until 2018. The capacities and corresponding data were obtained from the GWI database (Virgili, 2017). The cumulative global desalination capacity in 2018 is estimated to be 89,400,000 m^3/day. Seawater is the dominant feedwater source accounting for 60% of the total capacity in 2018. Brackish desalination is the next largest feedwater source with

a share of 22%. The diagram highlights the rapid growth in seawater desalination since the late 1990s, compared to the other feedwater sources.

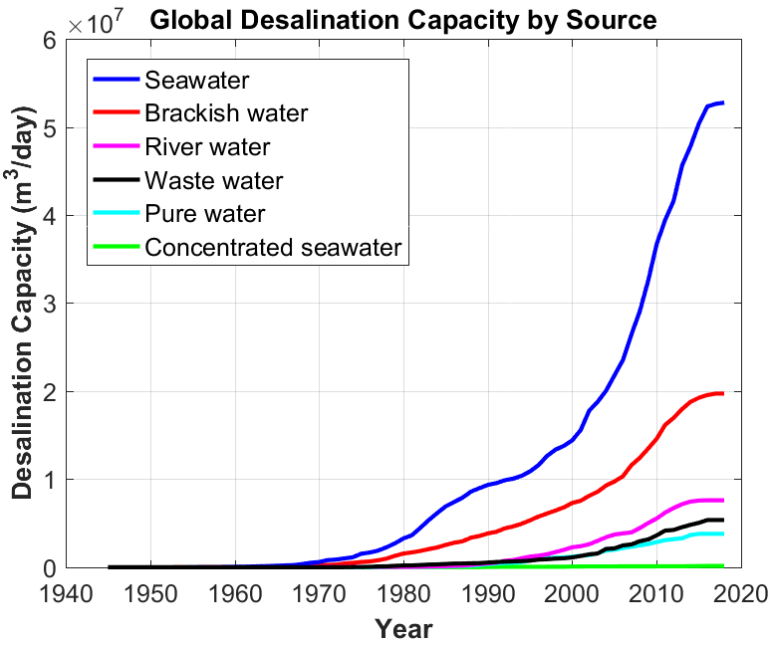

Figure 2 Global online desalination capacity by feedwater source. The feedwater sources have been categorized based on the salinity factor as defined in the GWI Desal Database

Seawater desalination is steadily being accepted as an important part of the global water supply (World Bank, 2019). The technology allows to produce 'freshwater' from the largest water body on the planet – our oceans. The solution is further supported by the fact that some of the world's largest and most populated cities lie along the coastline with easy access to the sea. From 2010 to 2016, the total desalination installations have increased annually by 9%, extending to countries where desalination was once not necessary or considered too expensive (Jia *et al.*, 2019). Market projections up to 2025 expect the upward trend to continue at a cumulative annual growth rate (CAGR) of 7% (Water Technology, 2019).

Brackish desalination is considered for projects that are further away from the coastline and where there is an availability of brackish water sources. The growth of this sector is constrained by the availability of suitable inland water sources, the extensive feedwater pre-treatment required and the disposal of brine discharge inland (World Bank, 2019). The corresponding curve in Figure 2 illustrates the slower growth of brackish desalination compared to seawater desalination (Virgili, 2017).

Regardless of the growth rates being observed and projected, over the last few years, less than 1% of the global water demand was being met by desalination (Water Technology,

2019). A key concern about desalination is that the removal of the dissolved salt from the feedwater requires significant amounts of energy, in either thermal or electric form depending on the desalination technology (UNWWAP, 2014; World Bank, 2019). The energy requirements, coupled with the higher capital costs, make desalinated water more expensive than treated surface water. This economic barrier has thwarted the growth of the global desalination sector. Until recently, desalination has been restricted to arid regions such as the Gulf Cooperation Council (GCC), where there is little surface water and an abundance of fossil fuel resources (Water Technology, 2019; World Bank, 2019). It comes as no surprise that 18% of the online desalination capacity is located in the Kingdom of Saudi Arabia (Virgili, 2017). Nevertheless, increasing water scarcity coupled together with growing water demand, in regions such as Americas and Asia, is forcing desalination into the local water supply repertoire (Water Technology, 2019; World Bank, 2019).

1.5 Motivation and objectives

Seawater desalination is expected to maintain the trend of growth and play a pivotal role in the years to come, including regions where desalination was not part of the water supply portfolio (Kucera, 2014; World Bank, 2019). While seawater desalination is becoming a necessity in many countries facing high levels of water stress, the cost of desalinated water and dependency on fossil fuels poses a significant economic barrier (UNWWAP, 2014). In addition, the burning of fossil fuels for desalination plants result in greenhouse gas emissions, further contributing to one of the causes of water scarcity – climate change. In a BAU scenario, the carbon emissions from the global desalination sector is expected to increase by 180% in 2040 (GCWDA, 2015). This is in contrast to the recent IPCC special report on Global Warming of 1.5°C (IPCC, 2018) that stipulate the need to achieve net zero greenhouse gas (GHG) emissions by 2050 in order to avoid runaway climate change chaos. Fossil fuel-based desalination hampers our efforts to achieve a net zero emissions world.

At the forefront of the discussion on climate change mitigation is the rapidly expanding renewable energy (RE) sector. The cost of RE-based technologies, including energy storage options, are in a steep state of decline and have driven the boom in installation of RE-based power plants worldwide. The investment costs of solar photovoltaics (PV) systems are reported to have decreased by 80% in the last decade, while the levelised cost of electricity (LCOE) of solar PV , onshore and offshore wind power plants have decreased by 84%, 49% & 56% respectively since 2010 (Bellini, 2019; Jansen, 2019; Vartiainen *et al.*, 2020). By the end of 2018, RE systems accounted for about 1/3 of the global power capacity (Bellini, 2019). Vartiainen et al. (2020) explain that the LCOE of utility scale solar PV in Europe, in 2019 with a weighted average cost of capital (WACC) of 7%, is cheaper than the average European spot market electricity price. The authors estimated the LCOE of utility scale PV in different European cities with varying irradiation levels such as Helsinki, London and Malaga, and compared with the local average spot market price. The authors highlight the swift pace of development within

the solar PV industry and posit PV to be the cheapest form of electricity generation everywhere, by as early as 2030.

The BloombergNEF research company indicate an 87% decrease in battery price since 2010 and project a further drop of 35% by 2023 (BloombergNEF, 2019). According to the recent analysis, the lower battery prices have helped hasten the electrification of energy sectors such as transportation. Similar observations have been echoed by Vartiainen et al. (2020) who estimate the different components of battery energy storage systems to decrease by 12% - 20% as the global cumulative battery volume doubles.

As of 2015, RE was estimated to power less than 1% of the current operational desalination plants. This is despite the fact that RE-based desalination eliminates the dependence on fossil fuels, enabling all countries to build a reliable water supply source, while eliminating emissions that lead to climate change. The current state of the desalination market highlights the disconnect between the global desalination and the RE sectors. The work presented in this thesis is motivated by the need to fill the void between the desalination and RE sectors and assess the potential for the two sectors to provide a reliable global water supply in the years to come.

The focus of the research is on the role of seawater reverse osmosis (SWRO), the technology that accounts for about quarter of the global desalination capacity and expected to retain the largest share in the years to come. The aim of this work is to generate a comprehensive and well-founded role of RE powered SWRO in meeting the increasing global water demand and respective sustainable development. In order to identify the potential for RE powered SWRO in the global water supply portfolio, the following questions were posed as research objectives:

1. There is reluctance to run SWRO desalination plants on 100% RE power systems due to the intermittent nature of renewable energy sources and consequently higher water production costs. However, with the decreasing cost of RE technologies and the global drive to achieve net zero emissions, the outlook for such systems may be different. So, can SWRO desalination plants, powered by hybrid RE power plants, produce water at costs competitive with current fossil powered SWRO plants? **(Publications I and II)**

2. Desalination systems and water storage are considered to provide flexibility to RE-based energy systems by producing freshwater that can be used as a form of indirect energy storage and provide valuable additional adjustment options. In the transition towards RE-based power systems, what are the cost-benefits of integrating desalination and water storage into the system? What is the interplay between water and battery storage in the energy transition? **(Publications III and IV)**

3. Learning curves are a very powerful tool for cost projections in dependence of expected growth of technologies. There is no well-based literature available for SWRO desalination plants (Loutatidou *et al.*, 2014; Sood *et al.*, 2014). Due to the

central role of SWRO in the future water supply of many regions of the world, it is of utmost relevance to better understand the investment cost and total desalination costs of the SWRO technology. What are the learning rates for SWRO desalination for investment costs and cost per water produced? **(Publication V)**

4. Global water demand is projected to increase and in conjunction with climate change, exacerbate the water stress situations globally. In this context, how will the desalination demand for countries vary over time? **(Publications VI and VII)**

5. Irrigated agriculture is responsible for almost 70% of the total global water withdrawals and supplements 45% of the current global food demand (Steduto *et al.*, 2018). Consequently, the water demand for irrigation is expected to rise by 11% (Steduto *et al.*, 2018). Efforts to meet the water demand increase will be challenged by depleting freshwater resources, climate change and increasing demand from the municipal and industrial sectors. Despite the diminishing freshwater resources, the global average irrigation efficiency is estimated to be as little as 33% (Jägermeyr *et al.*, 2015). This implies that there is potential to limit the global water demand by improving irrigation efficiency. What are the impacts on global water demand with the use of improved irrigation efficiency? Consequently, how do the improvements in water use efficiency translate to the desalination demand in countries with an intensive irrigation sector? **(Publications VI and VII)**

6. After projecting the global demand for desalination under different scenarios that incorporate water demand management, the next step is to identify the energy transition pathways towards RE-based seawater desalination. What are the financial and technical details of the transition pathways that can be adopted by countries with desalination demand? By addressing the issues of irrigation efficiency improvement, global water demand management, seawater desalination powered by RE, the research establishes pathways that can help achieve the United Nations (UN) SDGs 2, 6 and 7. **(Publication VII)**

1.6 Scientific contribution of the research

At the time of initiating this research work, the main impetus was to identify solutions to the growing water stress being observed in different countries. SWRO desalination offers the possibility to tap into the vast resources of the ocean to satiate our thirst. The problem is and has always been that the technology is expensive relative to traditional water treatment methods, and dependent on a steady supply of fossil fuel. To paraphrase President John F Kennedy in the 1960s, if we find a method to produce potable water from seawater it would be one of the most beneficial discoveries to humankind (World Bank, 2019).

The booming RE sector enables to create a vision of a RE powered desalination sector that is feasible and lucrative even in countries devoid of fossil resources. Literature allude to strategies where SWRO desalination plants are run with solar PV and/or wind power

plants, supported by diesel generators or the grid. However, there was no literature discussing the concepts and feasibility of achieving 100% RE-based SWRO desalination. This dissertation aims to contribute towards closing this wide research gap through the following scientific contributions:

1. A novel method to project the desalination demand in different countries based on future water stress and total demand estimates. After establishing the desalination demand projections, the global-local costs of meeting the desalination demand overnight, by 2030, through 100% RE-based SWRO desalinations plants is estimated. These results indicate if the cost of water production from such systems would be competitive with that of current fossil fuel-based SWRO plants. **(Publications I and II)**

2. This research also identifies the technical and financial aspects of transition pathways that will enable the desalination sector to achieve zero emissions by 2050 while helping to meet water demand in a cost-competitive manner. The desalination sector is extended to account for thermal desalination technologies that are lucrative in a RE-based energy system. The results can help policy makers visualize the transition on a local scale and strengthen the enabling environment to achieve the targets by 2050. **(Publications III and VII)**

3. Present a detailed study on the anticipated role of water storage and desalination as a form of additional flexibility in a 100% RE system. **(Publication IV)**

4. Analyse the historical capital investments in SWRO plants, explain the cost trends and derive a learning curve for the SWRO technology. This will be the first learning curve study done for SWRO plants. **(Publication V)**

5. Integrate improvements in water use efficiency across the irrigation sector and model the corresponding impacts on the desalination demand. Identify if RE-based SWRO desalination can be a viable water supply option to existing irrigation sites in the years to come. **(Publication VI)**

6. Model and describe the transition pathways that may be adopted by water stressed countries to meet the country's water demand up to 2050, through a combination of 100% RE-based desalination and improved water use efficiency in the irrigation sector. This will present policy makers with a blueprint to tackle the local water crisis through better water demand management and increasing supply through 100% RE desalination. **(Publication VII)**

It is hoped that the research findings will help persuade the desalination sector to latch onto the booming renewable energy sector and provide a water supply option to meet the increasing global water demand, as well as contribute to climate mitigation and consequently reduce global water stress

1.7 Structure of the dissertation

The initial chapters of this dissertation help to contextualize the study and explain the motivation for the work proposed. The subsequent chapters discuss the research objectives and the results obtained. The closing chapters provide a discussion of the research, the limitations, the scientific and practical application of the results. Chapters 1 and 2, as the opening chapters, explain the gravity of the global water crisis, the untapped potential of seawater desalination and present the motivation for the work proposed in this thesis. Chapter 3 examines the questions that arise when recasting the role of renewable energy and seawater desalination in the global water supply. Chapter 4 describes the methods utilised to answer the questions that were raised in the preceding chapter. Chapters 5, 6 and 7 analyse the results obtained and discuss the impacts of the research within a societal context.

2 Why seawater desalination?

2.1 Desalination technologies

The desalination technologies available today are broadly classified as thermal or membrane processes. Thermal desalination technologies use the distillation process where saline water is evaporated, and the water vapour condensed to produce freshwater. The heat necessary for the evaporation is produced in steam generators, boilers or waste heat steam from turbines in power stations. Common thermal desalination technologies are multi stage flash (MSF) and multiple effect distillation (MED). In membrane-based desalination technologies, the saline feedwater is desalinated through the use of a permeable membrane. A pressure greater than the osmotic pressure of the feedwater is applied forcing the separation of salt and water through the selective membrane. The most common membrane-based desalination technology is Reverse Osmosis (RO). The only energy input required is electricity (Kucera, 2014; World Bank, 2019).

The earliest seawater desalination plants are reported to be MED plants on the Netherland Antilles islands that started operations in 1928, followed by an expansion in the 1950s. MED plants comprise of a number of units where the feedwater is vaporized, under reducing pressure, by an externally provided source of steam (Al-Karaghouli *et al.*, 2013). The vapor is finally condensed to produce freshwater. Thermal energy is required in the form of heat for vaporisation and electrical energy for pumps used in the system. Table 1 lists some key operational parameters of MED plants online today (Al-Karaghouli *et al.*, 2013). The brine temperature is the temperature that the seawater is required to be heated to before passing through the MSF or MED units.

The early versions of MED desalination plants suffered from low heat transfer rates and high scaling effects (Al-Karaghouli *et al.*, 2013; Kucera, 2014). Therefore, MED plants could not be built at large scales and used for feedwater with high salinity. Large-scale seawater desalination plants became more prominent in the 1950s with the introduction of the MSF technology that overcame these issues (Al-Karaghouli *et al.*, 2013; Kucera, 2014). MSF distillation also operate in stages under reducing pressure but requires the feedwater to be at boiling point elevation. Thus, unlike MED plants, the feedwater is vaporised rapidly using the concept of 'flashing' at higher temperature without the use of heat transfer tubes. As such, MSF can be used to desalinate feedwater with low or extremely high salt concentrations with less risk of scaling. This is one of the reasons that MSF has been widely adopted, particularly in regions with high feedwater salinity like the Arabian Gulf (Al-Karaghouli *et al.*, 2013; Kucera, 2014). However, this also implies that MSF plants have higher thermal and electrical energy demand, relative to MED, as listed in Table 1.

The first commercial RO plant was established in 1965 in California, backed by an extensive desalination research funding program in the US (Kucera, 2014). By the 1980s, private funded research in this technology began to grow globally driven by concerns of

water scarcity and population growth. In SWRO, the feedwater is passed through a semi-permeable membrane at high pressure. As a result, two solutions are produced. One with freshwater, called the permeate. The second is with the high filtered salt concentration at a higher pressure, called the brine concentrate. The concentrate is generally returned to the sea. The higher the salinity of the water and lower the temperature, the greater is the pressure required. The pressure is generally provided by a high-pressure electrical pump and reused via energy recovery devices. In addition to the reverse osmosis component, SWRO plants also comprise of other facilities such as intake, pre-treatment, post-treatment and outfall sections that also require electrical energy. The total energy consumption of these stages is generally assumed to be around 1 kWh/m^3 Gulf (Al-Karaghouli *et al.*, 2013; Kucera, 2014). Typical energy data for SWRO plants are listed in Table 1.

Table 1 Average energy consumption of MED, MSF and RO plans

		MED	**MSF**	**RO**
Thermal energy input	kWh_{th}/m^3	65	85	
Electrical energy input	kWh_e/m^3	2.0 – 2.5	2.5 – 5.0	3.5 – 4.5
Feedwater		Seawater & Brackish water		
Operation temperature	°C	70	90 - 110	< 45 °C

The theoretical minimum energy required to separate freshwater, at a recovery rate of 50%, from seawater at a salinity of 35,000 ppm, is 1.06 kWh/m^3 (Elimelech *et al.*, 2011).The energy required is a function of the salinity of the feedwater and the recovery rate. According to Elimelech and Phillip (2011), pilot-scale SWRO plants are reported to have a desalination step at an energy consumption rate of 1.8 kWh/m^3 using new, high-permeability membranes with a 50% recovery rate. Even if ideal equipment were used, such as 100% efficient high-pressure pumps and energy recovery devices, the practical minimum energy required would be 1.56 kWh/m^3. However, on an industrial scale, these energy consumption values are not feasible due to the lower efficiencies of equipment used and frictional losses. Despite the deviation from the minimum energy required, Elimelech and Phillip (2011) explain that over the last 40 years, the energy consumption of the reverse osmosis stage has decreased drastically from around 15 kWh/m^3 to less than 2 kWh/m^3.

Thermal distillation in the basic single-stage form is significantly more energy intensive. This is because the process is dependent on boiling water that requires 650 kWh of thermal energy per m^3 of freshwater produced, depending on the evaporation temperature (Al-Karaghouli *et al.*, 2013). Current MSF and MED technologies overcome this issue by trying to reuse the energy through multiple stages and use the parameter Gain Output Ratio (GOR) to gauge the efficiency of the system. The GOR measures the ratio of the distillate (in kg) produced to the mass of the input steam (in kg). MED plants generally have a manufacturer design GOR range of 10 to 16 $kg_{distillate}$ / kg_{steam}, but is reported to operate in the range of 8 to 12 in the Gulf countries. MSF plants have a lower design GOR range of 8 to 12 $kg_{distillate}$ / kg_{steam}, but is reported to operate to 8 to 10 $kg_{distillate}$ / kg_{steam} in the Gulf. However, in countries with plentiful fuel resources, the preference has been to use MSF due to the lower scaling tendencies with the technology (Al-Karaghouli *et al.*, 2013; Kucera, 2014)

2.2 Observed trends

Figure 3 captures the growth of the common seawater desalination technologies from 1969 to 2015 in the GCC countries and non-GCC countries (Fulya, 2011; Caldera *et al.*, 2017; Virgili, 2017). MSF took off in the 1970s in the GCC as this was the only technology that could be implemented on a large scale and work with the highly saline feedwater in the region. In addition, the thermal energy required could be provided by the booming oil and gas industry in the region. MSF is still the dominating technology in the GCC region, accounting for approximately 62% of the installed capacity. The total online SWRO, MSF and MED capacities by 2015 in the GCC region was 23 million m^3/day. In stark contrast, in the non-GCC region, where fossil fuel resources are not abundant, MSF accounts for about 5% of the desalination capacity in the region. The total desalination capacity estimated in the non-GCC region in 2015 was 20 million m^3/day. From Figure 3 it is evident that there has been no significant change in the installed MSF capacities in the non-GCC region since the late 1990s. However, it has to be noted that over the last 10 years, the growth of MSF in the GCC region has also been plateauing.

SWRO capacities in the GCC have grown steadily over the last decade, while MED installations have slowed down since 2010. With the advances in technology and adequate pre-treatment methods, SWRO plants have proven to be able to work with the waters of the Gulf region (Fulya, 2011; Al-Karaghouli *et al.*, 2013). Also, SWRO plants have a lower energy consumption, meaning that the regional governments will have to spend less on subsiding fuel for production of water. For instance, Saudi Arabia is reported to use 1.5 million barrels of oil for the desalination sector and purchase liquid fuels and natural gas at 3% and 8% of the market price (Fthenakis *et al.*, 2016). Switching to a more electrified desalination sector will help Saudi Arabia cut back on energy consumption and according to the Smart Water Magazine (2019b), is the current path taken by the GCC countries.

SWRO has been the preferred technology in non-GCC countries and contribute to 84% of the total installed desalination capacity in the region. SWRO is less energy intensive

and is therefore more economically viable for countries without cheap fossil fuel resources. Through the analysis of SWRO application trends, it can be observed that the capacity of SWRO plants is increasing while the energy consumption is decreasing. In comparison, MED has grown at a constant rate and the cumulative installed capacity has doubled in the last decade. However, MED only contributes to 1% of the total desalination capacity in the region.

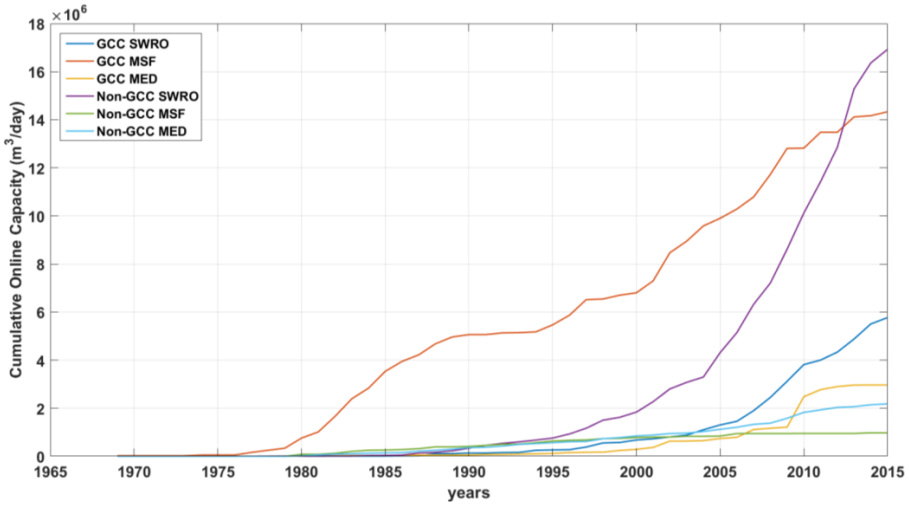

Figure 3 Global cumulative capacity trends of SWRO, MSF and MED in the GCC and non-GCC regions, from 1970 – 2015

2.3 Projected outlook for the desalination sector

According to the Global Water Intelligence (GWI) database, 1 522 504 m^3/day of seawater desalination capacity were contracted in 2015, out of which 77% were awarded to seawater reverse osmosis (SWRO) desalination plants (Virgili, 2017). A breakdown of capacity trends, as done in Figure 3, show that SWRO has dominated the desalination market over the last decade. This is owing to the continual technological improvements and the associated decline in costs. As such, SWRO is expected to continue to be the leading desalination technology. This perspective is supported by both academics and industrial analysts (Jones *et al.*, 2019; World Bank, 2019). Mayor (2019) analysed and projected the growth patterns and dynamics of the three main desalination technologies MSF, MED and RO. The results showed that the thermal technologies MSF and MED are at an advanced stage of their growth. MSF, in particular is almost at saturation level, with 83% of the growth curve achieved, while MED is at 65% and likely reach peak capacity before 2050. In contrast, RO was found to have only reached 35% of the corresponding growth curve, suggesting room for further diffusion of the technology.

Whilst there is clear consensus on the dominance of SWRO in the future desalination market, there is less clarity on what the future demand for desalination may be. Mayor (2019) projects the desalination demand up to 2050 based on logistic curves using historical data. The global cumulative capacity projected for 2050 is 1.7 x 10^8 m^3/day, with RO accounting for about 80% of the total capacity. Meanwhile, total global installed desalination capacity in 2018 is estimated to be 95.4 x 10^6 m^3/day. Thus, according to Mayor (2019) the desalination capacity would increase almost two-fold by 2050, based on past growth trends. Hanasaki et al.(2013) link gross domestic product (GDP), aridity and proximity to the shore with demand for seawater desalination. Based on these observed relationships, the production of desalinated water is projected to increase by up to 2.1 times before 2040. The demand is estimated to increase further by 6.7 – 17.3 times during the years 2041 – 2070. Nevertheless, the underlying theme is the increasing demand for seawater desalination, in particular SWRO, in the future global water supply.

Voutchkov (2013) summarises the development trends observed in SWRO systems and explains that the SWRO membranes used today are much smaller, productive and cheaper than the original counterparts (Voutchkov, 2013). Similarly, there have been other technical improvements such as installation of high-pressure pumps and energy recovery devices. These drastic advancements have driven down the cost of water production from SWRO plants. However, there are no further significant developments perceived, other than improvements in anti-fouling and scaling procedures. Voutchkov (2013) explains that while SWRO water production costs will continue to decrease, the conventional surface water treatment costs will increase due to lack of freshwater resources and stringent regulatory requirements. These costs trends are projected to further establish SWRO as a drought-proof water supply source for many water stressed communities.

In the 2011 report by Fichtner (2011), the cost of water production from conventional SWRO plants is reported to be within the range 0.4 €/m^3 to 1.9 €/m^3, assuming an exchange rate of 1.3 USD to 1 €. A recent article in Smart Water Magazine suggests a similar range of 0.4 €/m^3 to 1.2 €/m^3 for desalinated water using different technologies (Smart Water Magazine, 2019a). The 624,000 m^3/day Sorek plant in Israel is the largest SWRO plant online at present with an estimated water production cost of 0.44 €/m^3, but is to be surpassed by the 900,000 m^3/day Taweelah plant to be built near Abu Dhabi city. The cost of water production from this plant is set to be even cheaper at a cost of 0.37 €/m^3, highlighting the maturity of the technology even in the GCC region (Smart Water Magazine, 2019a; Water World, 2019b).

The municipal and industrial sectors are the largest users of desalinated water, accounting for 89% of the desalination capacity globally (World Bank, 2019). The irrigation sector, despite being the sector with the largest water demand, uses only 2% of the global desalination capacity (World Bank, 2019). The main barriers to the uptake of desalination in the irrigation sector are the high water production costs and the subsequent impact on food production costs (Quist-Jensen *et al.*, 2015). Desalinated water for irrigation requires further treatment than that for potable use, to ensure right water quality for the crop types and soil characteristics. Thus, the costs of desalinated water for irrigation can be higher

than that for potable use (Quist-Jensen *et al.*, 2015). However, countries like Spain, Israel and Australia already use desalinated water for the irrigation of high value cash crops. Spain allocates up to 22% of the total desalination capacity to the irrigation sector, with higher shares in some regions (Zarzo *et al.*, 2013). The decreasing costs and improved performance of SWRO and membrane-based water treatment systems, will further incentivise the use of desalinated water for irrigation.

A staple concern of using seawater desalination is the dependency on burning fossil fuels and the accompanying GHG emissions. Cornejo et al. (2014) explain that RO technologies have lower GHG emissions than thermal desalination technologies. However, the estimated GHG emissions footprint of seawater RO desalination (0.4–6.7 kg CO_{2eq}/m^3) is usually larger than that of brackish water RO desalination (0.4–2.5 kg CO_{2eq}/m^3) and water reuse systems (0.1–2.4 kg CO_{2eq}/m^3). Shrestha et al. (2011) found that the total CO_2 emissions of the seawater desalination sector (0.25 Mt/y) are 47.5% higher than that for water conveyance (0.17 Mt/y). The GHG footprint values vary due to the variability of location, technologies, life cycle stages, parameters considered, etc. Therefore, whilst SWRO is a lower energy consuming desalination technology, fossil based SWRO systems are not the solution to abating water scarcity.

At present only 1% of the global desalination fleet is powered by renewable energy due to the traditional view that renewable energy power plants are too expensive (World Bank, 2019). However, as the cost of renewable energy power plants and energy storage plummet (Bellini, 2019; Jansen, 2019; Vartiainen *et al.*, 2020), coupling the desalination and RE sectors becomes a more attractive option. This aspect was highlighted in a presentation by the Managing Director of the Dubai Electricity and Water Authority (DEWA) (Gulf News, 2017) who announced that Dubai would generate 1 154 000 m^3 of desalinated water a day by 2030 by capitalising on low-cost solar energy. The transition to solar energy based desalination plants, between now and 2030, is estimated to save DEWA 13 bUSD. There are also reports that the Egyptian government is assessing the feasibility of solar PV and wind powered desalination projects, together with the Saudi company ACWA that is developing the Taweelah SWRO project (Hutchins, 2020).

Despite the increasing interest in RE-based desalination, particularly SWRO, the general view, as understood from literature and industry reports, is that SWRO plants cannot be run on entirely 100% RE systems. Instead, electricity from the grid or backup diesel generators may be required to ensure that the SWRO plants are run continuously as per normal operations. In contrast, Fthenakis et al. (2016) has shown that in Saudi Arabia, the use of PV to power a 190,000 m^3/day SWRO can help save up to 43.2 million USD a year in diesel fuel subsidies.

In the following chapter, current trends within the desalination and RE sectors are used to project the potential of RE-based SWRO to meet the global water challenges. Different points are raised and discussed within the context of the research objectives.

3 Recasting the role of SWRO desalination in the global water supply

3.1 Coupling SWRO with renewable energy

The main concern of using RE resources to run desalination plants is the variability of the energy source. In general, SWRO plants are run on high full load hours, in a baseload mode, to ensure that the least cost of water production can be achieved (Semiat, 2008; Fulya, 2011). The consensus is that low water production costs cannot be obtained when run on variable renewable energy (VRE) resources and in addition, renewable energy power plants are still too expensive. The use of energy storage for the desalination sector has been disregarded so far due to the perceived higher costs. An article by Water International (2019a) likens the relationship between the renewable energy and SWRO desalination sector to a 'long engagement' and not a 'committed marriage'. In contrast, subsidized fossil fuel power plants are considered to provide more lucrative water production costs.

Electricity consumption in general contributes up to half of the final water production cost of SWRO plants. This may increase depending on the distance and the terrain type between the demand and desalination plant site. In some cases, pumping the desalinated water from the desalination plant to the demand site consumes as much, or more energy, as desalinating the seawater (Lamei *et al.*, 2008; Ghaffour *et al.*, 2013).

Due to the perceived hurdles of using 100% renewable energy based SWRO plants, literature has mostly focused on the use of RES with grid back up or diesel generator aid. As an example, the Al-Khafji SWRO desalination plant in Saudi Arabia has been designed to follow the same premise. During the day, the 60,000 m^3/day plant is powered by a neighbouring 15 MW solar PV plant, while in the evening, power from the grid is used (Water Technology, no date). However, there are yet no large scale SWRO plants that are run entirely on RES (Mito *et al.*, 2019). A recent review by Mito et al. (2019) also stress the need to couple the RE and desalination sector, but believe that the use of energy storage will increase the cost of water production. The authors instead investigate the potential to run RO plants using PV and wind, in a variable operation mode instead of baseload manner.

The objective of **Publication I** was to analyze the viability of meeting the future global desalination demand with 100% renewable energy powered SWRO plants. This was done by estimating the unit cost of water production (€/m^3) or the levelised cost of water (LCOW) for RE powered SWRO plants in 2030 and comparing it with costs of conventional SWRO desalination plants. The desalination demand was also estimated for all countries with projected water stress based on the WRI's Aqueduct Atlas (Gassert *et al.*, 2013). Figure 4 presents the SWRO desalination system envisaged in this initial work.

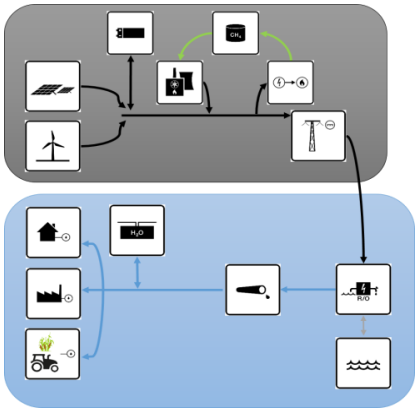

Figure 4 RE powered SWRO desalination system designed to meet the water demands of the municipal, industrial and agricultural sectors

SWRO desalination plants are powered by a cost optimised hybrid configuration of RE power plants and energy storage. High voltage direct current (DC) cables transport power to the desalination plants on the coast. The desalinated water is pumped to supply the municipal, industrial and agricultural sectors. Water storage at the site of demand ensures constant water supply. Hybrid RE plants are comprised of PV and wind power plants coupled with storage options such as batteries and power-to-gas (PtG). In **Publication I**, the feasibility of the system presented in Figure 4 is assessed for all global regions with high water stress in the year 2030.

In **Publication II** the focus shifted from the desalination demand on a global perspective to a local one, with a focus on the Middle Eastern country of Iran. Iran is continuously ranked as one of the top ten water stressed countries on the planet. Gleeson et al. (2012) show that the area of the Persian aquifer required to sustain the current groundwater withdrawals and dependent ecosystems is 10 – 20 times larger than the actual area of the Persian aquifer. A study by Joodaki et al. (2014) on groundwater in the Middle East found that from 2003 to 2012, Iran suffered the largest groundwater depletion at a rate of 25 ± 3 Gt per year. Ashraf et al. (2017) modelled the effects of water withdrawals and climate change on historical water stress in Iran and identified unsustainable water withdrawals to be the main culprit. Heightened water withdrawals, together with climate change, is projected to exacerbate the situation in the country further. Literature explains that the Iranian government has preferred the construction of dams to harness water resources (Foltz, 2002; Madani, 2014). However, research also highlight the facts that the dams have in fact caused more environmental damage by blocking water flow to rivers and destroying ecosystems (Foltz, 2002; Madani, 2014).

As of 2015, Iran had an online seawater desalination capacity of 413,000 m^3/ day, out of which 42%, 2.5% and 41% were SWRO, MSF and MED respectively (Virgili, 2017). DesalData reported that the government has taken new initiatives to expand the desalination capacity in the country due to the persistent drought and unabating water

demand (GWI - Global Water Intelligence, 2016b). Since then, the large scale 100,000 m^3/day SWRO plant in Bandar Abbas began operations providing drinking water to people in the southern region (Financial Tribune, 2018). However, the plants online are all currently powered by gas and oil power plants. In **Publication II**, the feasibility of powering future desalination demand in Iran by using the country's abundant solar and wind resources was analysed. While there are currently desalination plants located on the Caspian Sea, in **Publication II**, the Caspian Sea was excluded as a feedwater source. This is due to the perceived environmental threats of withdrawing large amounts of water from inland seas in a warming climate and the damage to ecosystems in the area (Karbassi *et al.*, 2010; Guardian, 2016). Therefore, all desalination plants for Iran were assumed to use the Persian Gulf as the feedwater source. The proposed research will enable Iran to produce water for the country without concern of fossil fuel consumption and, consequently, GHG emissions.

Publications III and **IV** explore the scenario where all desalination demand is powered by 100% renewable energy systems. However, desalination demand will increase over time and ensuring that the new plants are powered by renewable energy resources is a transitional process. The IPCC Special Report on Global Warming of 1.5C highlight the need to achieve net zero GHG emissions across all energy sectors by mid-century in order to avoid climate change chaos (IPCC, 2018). To aid this global transition, pathways that demonstrate how the desalination demand will grow over time and the energy system changes required to ensure that the desalination sector is powered solely by RES should be analysed.

The Kingdom of Saudi Arabia presents an interesting case to conduct a first study, as done in **Publication III**, on the energy transition pathway for the desalination sector. Saudi Arabia accounts for 18% of the total online global desalination capacity, meets 60% of the country's municipal water demand and 6% of the total water demand through seawater desalination (GWI, 2016a). However, the desalination sector also accounts for 30% of the country's electricity demand and consumes up to 1.5 million barrels of oil per day at subsidized local prices (Fthenakis *et al.*, 2016; Demirbas *et al.*, 2017). Therefore, it makes economic sense to run the desalination plants on RE instead of using oil and gas at a loss. In **Publication III**, the desalination demand growth for Saudi Arabia is projected up to 2050 and the energy system transition required to ensure that desalination sector will be run entirely by RES analysed.

Given the significant desalination and power sectors in the Kingdom of Saudi Arabia, the research also presents the opportunity to investigate the effects of integrating the desalination and power sectors during the energy transition. Can the desalination sector, coupled with water storage, provide additional flexibility to the RE-based power sector and reduce the final system costs? At first glance, this seems like an ideal pairing: the excess RE generation can be stored as water and at times of low RE generation, water from storage used. **Publication III** also involved the use of MSF and MED desalination technologies in the Saudi Arabian study. MSF is still the largest desalination technology in the country, accounting for 51% of the seawater desalination capacity in 2015 (Virgili,

2017). The results of this publication will also indicate the role of thermal desalination technologies during the transition of the Saudi Arabian desalination sector.

3.2 Water and energy storage in the energy system transition

The importance of energy storage in the global energy transition towards 100% renewables has been well established, both within and outside the RE community (Breyer, Bogdanov, *et al.*, 2017; Haegel *et al.*, 2019). The two key energy storage options that are most discussed about are battery energy storage and pumped hydro energy storage (PHES). According to the World Energy Council (2019), PHES currently accounts for 96.2% of the world's energy storage capacities, followed by battery storage. However, with improved power to energy ratios, Lithium-ion batteries are currently experiencing by far the fastest growth of all storage options and being implemented in small and utility-scale applications (Luo *et al.*, 2015; Haegel *et al.*, 2019). Consequently, there has been a sharp decline in the capex of batteries (Jansen, 2019; Vartiainen *et al.*, 2020). Meanwhile, there is increasing discussion about the need for strategic water storage on a larger scale in several countries.

The results of **Publication III** suggest an interplay between water and battery storage in the Saudi Arabian energy transition towards 100% RE-based desalination systems. How do the technical and financial parameters of battery and water storage influence the least cost transition path to a 100% RE-based power system? **Publication IV** probes these questions and demonstrate if it is cost-effective for Saudi Arabia to harness the increasing desalination and water storage demand to reduce the requirements for battery storage in the energy transition. In contrast, will battery storage prove to be lower cost storage option for the Saudi energy transition? Existing literature discuss the potential role of desalination and water storage in hybrid energy systems on a smaller scale (Al-Nory *et al.*, 2014; Heihsel *et al.*, 2019). In **Publication IV**, a detailed study of the role of desalination plants and water storage in a fully RE-based energy system is conducted.

3.3 SWRO cost trends

As the desalination demand and installed capacities increase, there is surging interest in the cost projections of desalination plants and the subsequent water production costs (Loutatidou *et al.*, 2014). Papapetrou et al. (2017) provides an analysis, based on two decades of relevant literature, of the methods and data necessary to determine the cost of producing desalinated water. The various factors that influence the costs of desalinated water, such as cost of land, plant capacities and energy costs, are presented. However, there is no consensus on the future cost trends, posing a problem when trying to project the costs of desalinated water.

The aim of **Publication V** is to project the capital costs of SWRO plants based on the learning curve model. The widely used and validated learning curve model draws on the concept of learning by doing and highlights the relationship between cost reduction in industries and the increase in production output. Learning curves have been used

extensively in the RE industry to project the costs of technologies such as PV and wind. However, learning curves to identify the SWRO capital cost trends have not been established within the desalination sector. Sood and Smakhtin (2014) have presented a learning curve for the cost of desalinated water, assuming 60% of the total cost is due to the opex and the remaining 40% due to the capex. Yet this does not allow to distinguish the actual impacts of the different components of SWRO plants on the final cost of water, as also highlighted by Papapetrou et al. (2017).

By using the newly established SWRO capex learning curve and the existing RE cost projections, it is possible to more accurately project the cost of desalinated water. Thus, the SWRO learning curve is a vital tool in the analysis of the potential for SWRO desalination in the decades to come.

3.4 Integrating water demand management and SWRO

If the world continues in its current path, water issues will continue to escalate, becoming widespread even in countries where once there was sufficient freshwater resources to meet local demand (UNWWAP, 2014; WWF, 2019). Seawater desalination offers countries a supply-side solution to the problem. However, various researchers and organisations attribute the unsustainable increase in freshwater withdrawals to poor management and inefficient systems, calling for better management on the water demand side (UNWWAP, 2015; Mekonnen *et al.*, 2016). The need for improvements to water use efficiency across the municipal, industrial and agricultural sectors have been stressed vehemently. For instance, according to Liemberger and Wyatt (2019), the non-revenue water (NWR) from the global municipal water network is about 126 billion m^3 a year, and is almost 3% of the total global water withdrawals. The annual losses are estimated to conservatively amount to 39 bUSD. Wada et al. (2014) suggest that a 20% increase in efficiency in domestic and industrial water use can result in a 2% decrease in the percentage of people living in water stressed regions in 2050, relative to the base scenario.

Despite the inefficiencies of the municipal and industrial sector, the biggest culprit is the global irrigation sector that accounts for 70% of the global water withdrawals and helps to meet 45% of the global food demand (Jägermeyr *et al.*, 2015). Steduto et al. (2018) explains that the remaining global food demand, until recently, has been met by rainfed cropland. However, this too is being threatened by the changing climate and recurring droughts.

Figure 5 illustrates the spread of irrigation sites globally and the corresponding beneficial irrigation efficiencies. Irrigation efficiency of a site may take several definitions. This research is based on the beneficial irrigation efficiency estimates provided by Jägermeyr et al. (2015). The beneficial irrigation efficiency is defined to be the ratio of the water transpired to the total water withdrawn from the source. The downside of this measurement unit is that the water lost to the basin which may be reused is not accounted for. The mean global area-weighted beneficial irrigation efficiency, reflecting the current distribution of irrigation systems and crops grown, is estimated to be 33%. Jägermeyr et

al. (2015) studied the global water saving potential of efficient irrigation systems and estimated that the water withdrawals can be reduced by up to 68%. Therefore, managing water withdrawals in the irrigation sector poses significant opportunities to reduce water withdrawals. However, the growth of irrigation efficiencies has been minimal, with maximum growth rates of 0.3% per year relative to the respective basis, and is not projected to be any better in the future (Hanasaki *et al.*, 2013).

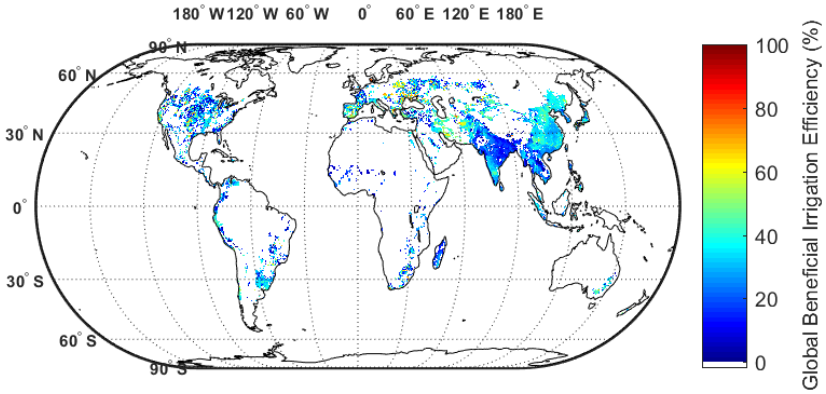

Figure 5 Global beneficial irrigation efficiency for irrigation sites growing rice, wheat and maize

Publication VI assessed the impacts on the water demand of the global irrigation sector, and the subsequent demand for desalination that can occur, if efficient irrigation systems are used. An optimistic scenario where the efficiency of the irrigation sites increases based on a logistic function, such that the efficiency of the sites by 2050 becomes 90%, was presented. This would mean the use of highly efficient sprinkler systems, that are currently only deployed in a handful of countries, would be used widely, particularly in irrigation intensive and water stressed countries.

Further, motivated by the various articles that posit desalinated water as being too expensive for irrigation, **Publication VI** analysed the costs of supplying water from 100% RE SWRO systems to existing irrigation sites in an optimistic scenario. Burn et al. (2015) explains that farmers are unwilling to pay more than 0.68 €/m^3 for irrigation water. However, as Australia continues to suffer from the longest drought in history with little sign of relief insight, farmers have had to rely on trucks carrying water for irrigation. Some estimates suggest this costs the farmers as much as 0.68 €/m^3. Meanwhile, the FAO (no date) highlights the substantial subsidies that underpin the global irrigation sector, in particular for the water and electricity use, and explains that except for a few OECD countries, most don't recover the actual costs of the irrigated water supplied. Removal of these subsidies would result in higher costs for the irrigation sector. In addition,

groundwater levels are rapidly declining, driving up the electricity consumption for water pumping and thereby the costs of irrigation. In stark contrast, RE-based SWRO can provide reliable, emissions free, water supply to irrigation sites. The main hindrance to the diffusion of the technology in the irrigation sector is the perceived higher cost of this water supply option. **Publication VI** projects the costs of water supply when RE-based SWRO is used for irrigation sites and the impacts of using improved irrigation efficiency technologies on the total water demand of the irrigation sector.

As explained by Hanasaki et al. (2013) the historical growth rate of irrigation efficiencies has been, at maximum, 0.3% per year relative to the respective basis. Therefore, the use of highly efficient irrigation systems, with an efficiency of 90% worldwide, by the year 2050, is an optimistic scenario. **Publication VII** tackles this issue by analysing two additional scenarios where the irrigation efficiencies are increased at different rates. In addition to the optimistic scenario, a 'BAU' and 'intermediate' scenario, with varying degrees of improvement in irrigation efficiency, are modelled. The corresponding impacts on the water and desalination demand for the irrigation sector, across the three scenarios are presented. To provide a comprehensive outlook, the water withdrawals and desalination demand for the irrigation, municipal and domestic sectors across the three scenarios, for the time period from 2015 to 2050, are considered.

Publication VII is a culmination of the prior research work and draws on the corresponding results. After analysing the role of better irrigation efficiency systems on the global water and desalination demand, the paper looks at how energy systems can change to ensure that the desalination demand is met solely by RE power systems by mid-century. By addressing the issues of irrigation efficiency improvement, global water demand management, seawater desalination powered by RE, the research establishes pathways that can help achieve the United Nations SDGs 2, 6 and 7.

4 Methods

4.1 Quantifying future demand for desalination

There are varying estimates of the future demand for desalination in different countries. For instance, Gao et al. (2017) project the population dependent on seawater desalination to increase three-fold by 2050. However, only the water demand of the municipal and industrial sectors were considered. Seawater desalination was disregarded as an option for the global irrigation sector. Similarly, Mayor (2019) analyses the future demand for desalination though a logistic growth curve, based on historical data, and indicates a two-fold increase in demand for desalination by 2050, relative to the current installed capacity. The desalination demand estimated was 1.7×10^8 m^3/day, with RO accounting for about 80% of the total capacity. However, these results are constrained by the factors that drove desalination in the past and do not reflect the future global scenarios. Jia et al. (2019) estimate that the annual growth rate in global desalination capacities from 2010 to 2016

has been 9%. A recent forecast by the GWI conservatively project the CAGR from 2020 to 2025 to be about 8% (Weaver *et al.*, 2020).

Discounting the economic factors, the desalination demand for a country would be driven by the level of water stress and the demand for water resources. As the water stress increases, so does the demand for desalination. A logistic curve allows to capture the relationship between desalination demand and water stress: the desalination demand is lower in regions with less water stress and increases more steeply for higher water stress levels. When a region is suffering from extremely high water stress, where fossil water resources are being exploited, desalinated water will be required to meet all of the water demand. The decadal projections for the future water demand and water stress, for 15,006 hydrological basins, were derived from the Aqueduct Water Atlas (Gassert *et al.*, 2013). This approach was first utilised in **Publication I** to determine the global desalination demand for 2030 on a spatial resolution of 0.45° x 0.45°. **Publications III** and **VI** adopt this approach to estimate the desalination requirements for Saudi Arabia and Iran respectively.

The water supply and demand projections provided in the Aqueduct Water Atlas are driven by the climate scenarios used in general circulation models and socioeconomic factors respectively (Gassert *et al.*, 2013; Luck *et al.*, 2015). The climate scenarios considered are Representative Concentration Pathways 8.0 and 4.5 which are also used in IPCC reports. To estimate the increase in water demand, relevant socioeconomic factors such as current sectoral water withdrawals, irrigation efficiency improvements and irrigation area is considered (Luck *et al.*, 2015). However, the key future drivers of water demand change are population, gross domestic product (GDP) and urbanisation. The water demand for thermal power plants are excluded from the future projections using current thermal power plant water demand data from Spang et al. (2014). This is to account for the absence of thermal fossil plants in the overnight scenarios and the elimination of current fossil based thermal plants in the transition scenarios.

To evaluate the effects of irrigation efficiency improvements, as in **Publications V** and **VII**, the approach in **Publication I** was modified to reflect the new water demand and water stress values. Three scenarios with varying degrees of irrigation efficiency improvements were defined. The ‘Base scenario’ is a BAU scenario, the ‘Irrigation Efficiency Push (IEP)’ scenario exhibits intermediate growth in irrigation efficiency, whilst the ‘High Possible Irrigation Efficiency (HPIE)’ scenario is the most optimistic scenario. Figure 6 (a) and (b) highlight the premises for the IEP and HPIE scenarios respectively. In the IEP scenario, the minimum growth rate is 0.3% per year respective to the relative basis, highest growth rate is 1% and dependent on the level of water stress. Once again, using a logistic curve, the higher the water stress of a region, the steeper is the annual improvement in the irrigation efficiency required. The growth rate values were based on the literature by Hansaki et al. (2013) and Wada et al (2014). In the HPIE scenario, the objective is to achieve a beneficial irrigation efficiency of 90% across all existing irrigation sites by 2050. When the beneficial irrigation efficiencies vary, so does the water demand and therefore the water stress of these irrigation sites. The

corresponding desalination demand in the Base, IEP and HPIE scenarios have been evaluated in **Publications V** and **VII**. The logistic equations that define the curves in Figure 6 are described in the publications.

(a)

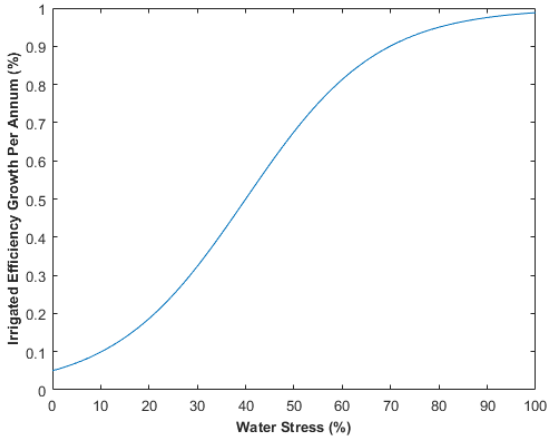

(b)

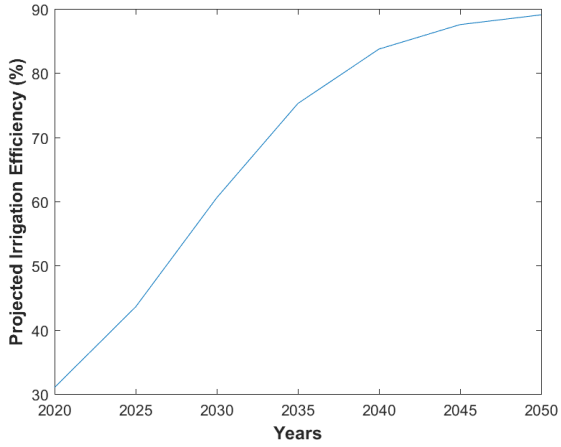

Figure 6 Irrigation efficiency growth per annum assumed for IEP scenario (a), Projected irrigation efficiency for every year in the HPIE scenario (b)

A point to note is that throughout this research only existing irrigation sites for the staple crops of rice, maize and wheat were considered. In the future, there may be more

irrigation sites due to the growing demand for food. As illustrated in Figure 5 there are already irrigation sites of efficiencies greater than 90% in some parts of North America and Europe. The fact that there are irrigation sites with efficiencies greater than 90% highlight the conservative assumption of 90% by 2050 in the HPIE scenario. This notion is further confirmed by companies like Netafim (2018) who advocate for the use of highly efficient drip irrigation systems for the growth of rice, maize and cereals. The irrigation efficiency may be even higher in some places depending on the implementation and use, but a more conservative value was chosen as a global average. Meanwhile, the IEP scenario allows inspection of a scenario where irrigation efficiencies are improved in a more controlled manner.

4.2 Learning curve analysis

As SWRO desalination becomes a crucial part of the global water supply, it is necessary to understand how investment costs for SWRO plants have changed over time and project future cost trends. At the time of carrying out the research for **Publication V**, two key papers have evaluated similar questions with different methods: Loutatidou et al. (2014) define a model that estimates the capital expenditures (capex) of RO plants located in the GCC and Southern Europe based on characteristics of the RO plants. Sood and Smakhtin (2014) established a learning curve to analyse the cost of water desalination, assuming that the capex and operational expenditures (opex) contributed to 40% and 60% of the total cost.

The learning curve concept was first conceived in the aircraft industry by the engineer Wright in 1938 (Nemet, 2006; Junginger *et al.*, 2020). It was observed that as the number of aircrafts constructed increased, the corresponding unit costs decreased. This was due to the 'learning' experiences gained during the construction processes. The learning curve is an extension of the concept of 'learning by doing' and illustrates the relationship between cost reduction and the increase in production output (Nemet, 2006). Since the late 1930s, the formal learning curve concept introduced by Wright, has evolved and been applied in different industries, including the renewable energy sector, to project costs. Kersten et al. (2015) assessed the learning rate of solar PV modules to be about 17% and PV systems to be 16%, using unit cost data from 1976 – 2010. Recent analysis by Breyer et al. (2017) explain that PV plants and battery plants had even higher learning rates of about 20% in the past. The most recent report by the ITRPV (ITRPV, 2018) show that the learning rate of PV modules has been almost 40% since 2006. Similarly, Vartiainen et al. (2020) report that the components of lithium ion battery packs have been experienced a learning rate of 12.5% - 20%.

In **Publication V**, a similar approach using the log-log model, based on the conventional learning curve concept, was used to gauge the relationship between the cumulative SWRO capacity and the capex. The learning rate for SWRO capex was established by analysing a total of 4237 SWRO plants, awarded between 1977 and 2015. All SWRO plants that were online, presumed online, offline, presumed offline or under construction were considered. All contract types were taken into account. The GWI Desal database

provide the data needed to compile the average capex of SWRO plants awarded in every year from 1977 to 2015 (Virgili, 2017). The mean capital expenditures and standard deviation for every year were plotted against the cumulative online capacity on a log-log scale. The historical SWRO capital expenditure trends and the corresponding learning rate can be established from the log-log scale. Based on the learning curve concept, the future SWRO capex are a function of the learning rate, the current and projected SWRO capacities as well as the current capex values. Further details are provided in **Publication V**.

4.3 Energy system analyses

Energy system modelling tools enable researchers to design, in varying degrees of detail, energy systems on a local, national or global scale. The results of such modelling tools provide crucial blueprints for policy makers and energy system planners to transform the current energy system to a 100% RE-based system (Hansen *et al.*, 2019). Hansen et al. (2019) provide an outline of energy system models (ESM) that have been used worldwide to model 100% RE systems for different energy sectors at specific temporal and spatial resolutions.

To identify the RE systems required to power the desalination demand projections in **Publications I, II, III, IV, VI and VII**, and variations of the LUT modelling tool are used (Breyer, Afanasyeva, et al., 2017; Bogdanov et al., 2019). The LUT model is a MOSEK based linear optimisation model, designed in an hourly temporal and 0.45˚ x 0.45˚ spatial resolution. The objective of the model is to design a cost optimized energy system, where the energy demand for every hour is met through a portfolio of different RE technologies. The solar and wind resources, in the high spatial and hourly resolution, have been reprocessed from National Aeronautics and Space Administration (NASA) datasets and account for direct and diffuse solar irradiations, wind speed, roughness length and air temperature (Aghahosseini *et al.*, 2019).

Figure 7 illustrates the energy generation, storage and bridging technologies that comprise the version of the LUT energy systems model used throughout this work. The desalination demand includes that of the thermal and RO technologies. The electricity is generated by solar PV and wind power plants based on the RE resources. The PtG components and battery energy storage complement the electricity generation sources by ensuring cost optimal operation of the desalination plants. The power-to-heat (PtH) is used to generate heat for thermal desalination plants and stored in the thermal energy storage (TES). The hot heat burner (HHB) can be used to burn gas to produce additional heat if required. In addition, the steam turbine (ST) may generate electricity using the heat from the TES. The allocation of the technologies is driven by the total system costs that are a function of the financial costs, technical parameters and RE resource availability. Further details of the functionality of this version model is provided in the publications. Detailed information on the full model can be found in Breyer et al. (2017) and Bogdanov et al. (2019).

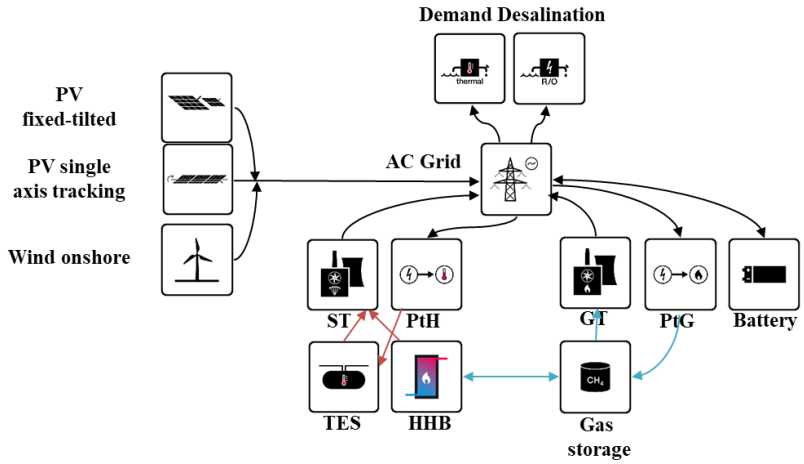

Figure 7 Block diagram of the LUT energy systems model used for analysis of energy systems to power the desalination demand

In **Publication I**, the LUT energy systems model was used to design the RE systems required to meet the energy demand of the SWRO plants for every country with desalination demand in 2030. Utility scale PV and wind onshore were considered as the RE generation technologies, as it is assumed that other renewable options are already in use, but limited in further scaling. Battery and PtG components met the energy storage demands of the system. There were no components for heat generation and storage as only electricity consuming SWRO plants were used. In addition, SWRO plants with hydraulic turbine energy recovery devices were assumed to be available for all regions by 2030. As such, the energy consumption of the SWRO plants were based on the salinity of the feedwater at the nearest coastline. The model also took into account the energy requirements for pumping the water (in the horizontal and vertical direction) from the desalination plant, on the coast, to the node with the demand for the desalinated water. The financial and technical parameters of all RE, desalination system technologies and demand were defined for the year 2030. The cost components like land lease, grid connection and taxes, which vary with country and project, are accounted for under operational expenditures (opex). However, these costs may differ drastically in some instances and would lead to higher opex values.

The levelised cost of electricity (LCOE) and levelised cost of water (LCOW) are key results to analyse the proposed design in **Publication I**. Equation 1 and Equation 2 below summarise the approach to calculate the LCOW and LCOE respectively (Caldera *et al.*, 2016) :

$$LCOW_{desal} =$$

$$\frac{(Capex_{desal} \times crf_{desal} + Capex_{water\ storage} \times crf_{water\ storage}) + opex_{fixed\ desal} + opex_{water\ storage}}{Total\ water\ produced\ in\ a\ year} +$$

$$Opex_{var\ desal} \times SEC \quad \text{1a}$$

$$Opex_{var\ desal} = LCOE \quad \text{1b}$$

$$LCOT_{desal} =$$

$$\frac{(Capex_{hpumps} \times crf_{hpumps} + Capex_{vpumps} \times crf_{vpumps}) + Capex_{pipes} \times crf_{pipes}) + opex_{fixedt}}{Total\ water\ produced\ in\ a\ year} +$$

$$Opex_{vart} \times SEC_t \quad \text{1c}$$

$$LCOW = LCOW_{desal} + LCOT_{desal} \quad \text{1d}$$

Equation 1 Levelised cost of water (LCOW). Here, $\mathbf{capex_{desal}}$ is the capex of the desalination plant in €/(m^3·a) and $\mathbf{crf_{desal}}$ is the annuity factor for desalination plant. Total water produced in a year is in m^3, $\mathbf{opex_{fixeddesal}}$ is the fixed opex of the desalination plant in €/(m^3·a). $\mathbf{opex_{vardesal}}$ is the LCOW levelised cost of electricity and is in €/kWh. **SEC** is the specific energy consumption in kWh/m^3. The product of the **LCOE** and **SEC** is the energy cost of the desalination plant in €/(m^3.a). $\mathbf{capex_{water\ storage}}$ is the capex of water storage and $\mathbf{crf_{water\ storage}}$ is the annuity factor for water storage. $\mathbf{LCOT_{desal}}$ is the levelized cost of water transportation. $\mathbf{capex_{hpumps}}$ is the capex of the horizontal pumps in €/(m^3·a) and $\mathbf{crf_{hpumps}}$ is the annuity factor for horizontal pumps, $\mathbf{capex_{vpumps}}$ is the capex of the vertical pumps in €/(m^3·a) and $\mathbf{crf_{vpumps}}$ is the annuity factor for the vertical pumps. $\mathbf{opex_{fixedt}}$ is the fixed opex of the horizontal and vertical pumps in €/(m^3·a). $\mathbf{opex_{vart}}$ is the **LCOE** and $\mathbf{SEC_t}$ is the total energy consumption for water pumping.

The LCOW is the sum of the $LCOW_{desal}$ and $LCOT_{desal}$.

$$LCOE_r = LCOE_{prim,r} + LCOC_r + LCOS_r + LCOT_r \quad \text{2}$$

Equation 2 Levelised cost of electricity (LCOE) for a region **r**. Here, $\mathbf{LCOE_{prim,r}}$ is the levelised cost of electricity for the primary generation source, $\mathbf{LCOC_r}$ is the levelised cost of curtailment, $\mathbf{LCOS_r}$ is the levelised cost for energy storage in the region and $\mathbf{LCOT_r}$ is the levelised cost of transmission of electricity in the region r. Further details can be found in (Breyer, Bogdanov, *et al.*, 2017; Bogdanov *et al.*, 2019)

To estimate the levelised cost of water transportation (LCOT), the water infrastructure costs were separated into piping and pumping costs in both the horizontal and vertical directions. A detailed breakdown of the costs is provided in **Publication I**. The piping costs are based on a study on the water transfer from the Suez to Negev in Israel (UN ESCWA 2009). The minimum energy needed to lift water in the horizontal and vertical directions, for medium size pumps with an efficiency of 75%, is estimated to be 0.04 kWh/(m^3·hr·100km) and 0.36 kWh/(m^3·hr·100m) respectively. The costs of operating horizontal and vertical pumping stations were obtained from Missimer et al. (2014). The authors provide details of the pumps required to supply desalinated or treated wastewater

to wadi communities in Saudi Arabia. Construction costs assumed are specific to the characteristics of the wadi valley, and costs will differ between regions.

The above described version of the LUT energy systems model was also used in a similar manner for **Publication II**, where a detailed study of RE-based SWRO power plants in Iran was carried out. In the study, concerns were raised about the use of inland seas as a feedwater source for desalinations plants and in particular, the Caspian Sea for Iran. As such, the use of inland seas was blocked and only the Persian Gulf could be used as a feedwater source. This further extended the water transportation distances for the regions with desalination demand in the northern regions of the country, mainly due to the mountainous terrain. The horizontal water pumping distance is taken to be the shortest path from the demand site to the coast where the SWRO desalination plants are located. The highest elevation on the horizontal path is found using a global relief model and considered to be the vertical pumping distance.

In **Publication VI**, the same model was applied to assess the cost of supplying desalinated water from RE-based SWRO plants to irrigation sites in years 2030 and 2050. The financial, technical and demand parameters were used according to the respective year and scenario. The common thread between **Publications I, II** and **VI** is that they are 'overnight' scenarios where the system and costs are projected for the specified year. In contrast, **Publications III, IV** and **VII** call for the design and inspection of energy transition pathways towards achieving RE-based desalination sectors by 2050.

The LUT energy systems transition model builds on the LUT energy systems model and allows to simulate the energy system transition for 5-year time periods for the years 2015−2050 (Breyer, Bogdanov, *et al.*, 2017; Bogdanov *et al.*, 2019). The model takes the 2015 installed power plant capacities, corresponding lifetimes, total electrical energy demand, and optimizes the mix of RE plants needed to be installed to achieve a 100% renewable energy power system by 2050. The optimization for each time period considers the relevant financial and technical status of the renewable energy technologies. Energy transition studies have been carried out for the power sector of different countries using the LUT energy systems transition model (Breyer, Bogdanov, *et al.*, 2017; Bogdanov *et al.*, 2019). In **Publication III**, the energy transition of the desalination, power and industrial gas sectors of Saudi Arabia is carried out. For the transition study, Saudi Arabia is considered as a single node, rather than different nodes in a high spatial resolution as in **Publication I** or **II**. Thus, the spatially weighted average values of the country's solar and wind resources are used, as described in Aghahosseini et al. (2019). Similarly, for water transportation, the weighted average pumping distance and height are calculated based on the distance, height, and desalination demand of the nodes within the country.

The thermal desalination technologies MSF and MED were added specifically for **Publication III** and inspects the role of thermal desalination plants during the energy transition. To meet the new desalination demand, MED stand alone and SWRO plants are used by the model. This is due to the lower thermal and electricity demand of these technologies. MED stand alone plants are installed based on the excess heat during the

transition. Excess heat may be generated from the gas turbines, internal combustion generators, municipal waste incinerators and power-to-gas units. Based on the availability of heat in the system and the cost of required heat generation, the model optimizes the water production from MED stand alone plants. MSF standalone plants are not installed after 2015. This is due to the higher thermal consumption compared to MED stand alone plants. The MSF and MED cogeneration plants are phased out based on the lifetime of the plants. Similarly, the fossil power plants online in 2015, except fossil gas plants, are phased out according to the lifetime. The use of RE sources and natural gas, at an unsubsidised cost, are optimised to meet the increasing electricity demand in the transition. Battery storage and PtG plants are used to complement the electricity generation during the transition.

Publication IV builds on the results of **Publication III** and further inspects the interplay between battery and water storage in the energy transition for Saudi Arabia. A sensitivity analysis is employed to understand how the capex of SWRO plants and battery storage affects the energy transition of Saudi Arabia. The current SWRO capex is reduced at different rates and the impacts on the SWRO full load hours, battery storage output and system costs are analysed. The results for the years 2030 and 2050 for each of the scenarios are compared.

After understanding the necessities for the decarbonization of the Saudi Arabian power, desalination and industrial gas sector, the focus shifts to a global perspective with an emphasis on the desalination sector. In **Publication VII**, the LUT energy systems transitioning model is adapted to study the decarbonization of the global desalination sector through an analysis of 145 regions (Bogdanov *et al.*, 2019). The input data such as the RE resources, water transportation distances and desalination demand values are assigned appropriately to the 145 regions. The methods are similar to those used for **Publication III**, but the study focuses solely on the desalination sector.

5 Results

The following sections present the main insights encountered during the research, through the lens of the Publications.

5.1 Publication I: Local cost of SWRO desalination based on solar PV and wind energy: A global estimate

Using the methods described in chapter 4, the global desalination demand, on a spatial resolution of 0.45° x 0.45°, was estimated as illustrated in Figure 8. The total desalination demand is found to be 2.9 billion m^3/day, with the demand for desalination mostly significant in North America, Middle East, the Indian sub-continent and China. The distribution of the desalination demand reflects the severe water stress being endured by many countries in these regions.

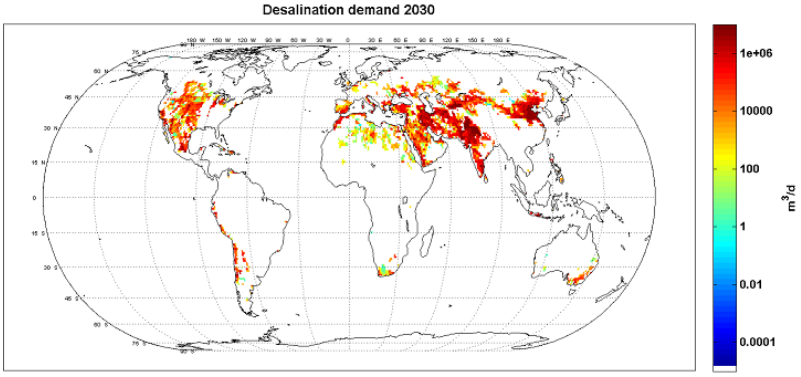

Figure 8 Desalination demand projection for the year 2030

The energy systems required to power the SWRO demand shown in Figure *8* was modelled via the LUT energy systems model. The resulting LCOW range when desalination plants, in 2030, are powered by hybrid PV, wind, battery and PtG plants is found to be between 1.0 €/m^3 – 4.5 €/m^3. The prevalent LCOW range is between 1.0 €/m^3 – 2.0 €/m^3 and is illustrated in Figure 9 (a). The LCOW presented include water transportation costs. On a global scale, the weighted average horizontal and vertical pumping distances from the desalination node to the coastline is estimated to be 150 km and 550 m respectively. In regions like Central Asia, where the pumping distances are significant, the pumping energy costs account for 40% of the final LCOW. Globally, the average pumping electricity cost is about 16% of the LCOW. Hybrid RE power plants are optimal as they offer higher full load hours and therefore allow for better utilisation of the desalination plant capacity. Depending on the terrain, the water transportation costs can contribute significantly to the final LCOW. Therefore, in the near future, SWRO plants powered by renewable energy plants will produce water at similar prices to that of today's conventional SWRO plants.

Another key observation was the significant role of solar PV in the energy systems required for SWRO desalination. Figure 9 (b) illustrates the high share of PV globally, accounting for 84% of the global energy demand, the rest is complemented by wind energy. Solar PV, together with battery energy storage, can meet most of the energy needs of SWRO desalination plants. Battery storage meets 24% of the total energy demand while PtG contributes up to 15%. The latter storage option is mostly prevalent in regions with higher shares of wind generation capacities. The significance of solar PV and battery storage also highlights the fact that regions with high water stress are also regions with abundant solar resources that could be harnessed to produce potable water in a lucrative manner. The PtG seasonal storage substantial reduces curtailment of a fully sustainable energy supply and thus reduces LCOE and LCOW. The resulting LCOW also includes the electricity transmission costs from the desalination plant to the demand node as highlighted in Equation 1. On a global scale, transmission costs accounts for less than 3% or the average LCOW. A complete assessment of the resulting desalination and energy systems are provided in **Publication I** (Caldera *et al.*, 2016).

(a)

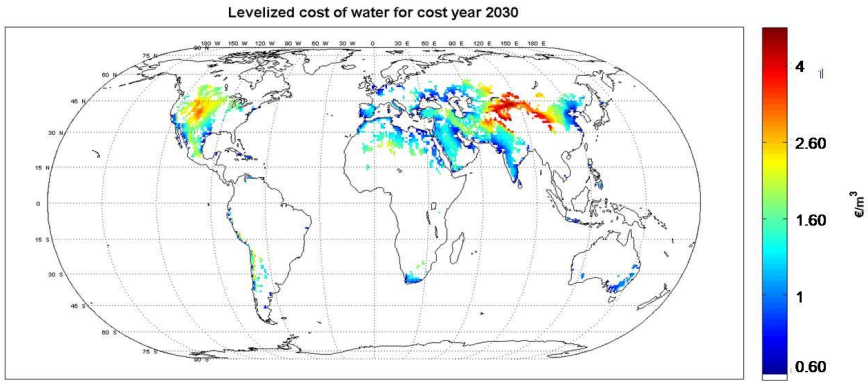

(b)

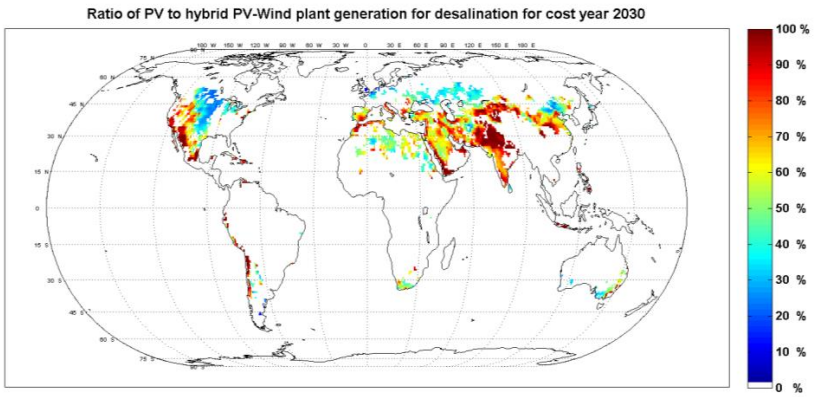

Figure 9 LCOW when 100% RE-based SWRO desalination plants are used (a), Contribution of solar PV to the electricity generation of hybrid PV-Wind plants in 2030 (b)

5.2 Publication II: Securing future water supply for Iran through 100% RE powered desalination

At the time of writing **Publication I**, the water crisis plaguing Iran was gaining attention through various organisations such as the World Resources Institute (Gassert *et al.*, 2013), Middle East Business Intelligence (Middle East Business Intelligence, 2015) and the Heinrich Böll Stiftung (Heinrich Böll Stiftung *et al.*, 2016). The construction of superfluous dams, poor management of existing freshwater resources and climate change are considered to have contributed to the water crisis. To help overcome the current water supply shortage, the Iranian government has approved a plan to desalinate and transfer seawater from the Persian Gulf and Gulf of Oman to the Central Plateau of the country.

In **Publication II**, the 2030 desalination demand for Iran was estimated, as shown in Figure 10 (a), and the corresponding LCOW for only renewable energy powered desalination plants was estimated, as shown in Figure 10 (b). It was found that a combination of solar PV and wind power plants, together with battery storage and PtG, enables the least system costs. The average LCOE of PV and wind for Iran in 2030 was estimated to be 0.03 €/kWh and 0.05 €/kWh. The corresponding LCOE range for the complete system is approximately 0.06 €/kWh – 0.11 €/kWh, including electricity generation, power transmission, storage and curtailment. To provide context, the recent power purchase agreement for 900 MW of the 5 GW solar park in neighbouring Dubai was made at 0.012 €/kWh (Bellini, 2020).

The modelled LCOW range for Iran, including cost of water transportation and storage, is 1.0 €/m^3 – 3.5 €/m^3 for cost assumptions of the year 2030 and will decline further with the cost of system components. The current water production cost, excluding water transportation and storage, of fossil powered SWRO plants in the southern province of Hormozgan is about 0.70 €/m^3 (excluding water transport) (GWI, 2016b). With a 100% renewable energy powered system, the LCOW range for Hormozgan is estimated to be 1.0 €/m^3 - 1.50 €/m^3. The higher LCOW range is attributed to the high water transportation costs in Iran and energy required for water pumping.

(a)

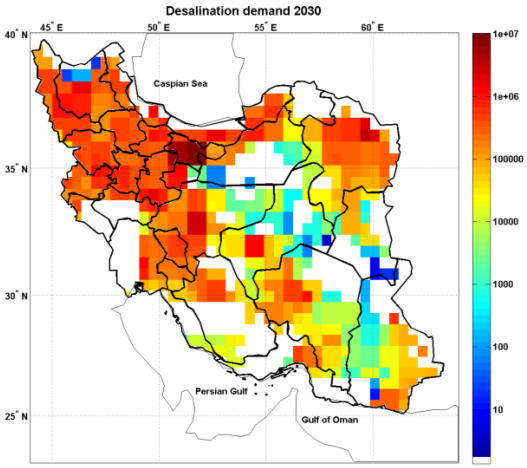

(b)

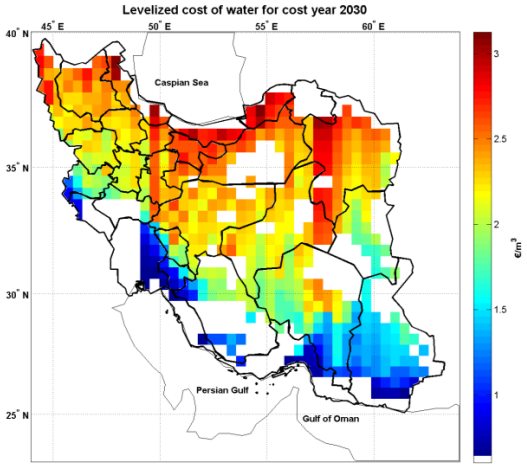

Figure 10 Desalination demand estimated for Iran in 2030 (a), LCOW when using 100% RE powered SWRO systems in Iran. LCOW includes cost of water production and transportation (b)

Thus, our work illustrates how the increasing water demand of Iran can be met through 100% renewable energy powered SWRO plants, at a cost competitive with current fossil powered SWRO plants. In addition, Iran can overcome one of the key issues surrounding desalination: the dependency on fossil fuel and greenhouse gas emissions.

5.3 Publication III: Role of seawater desalination in the management of an integrated water and 100% RE-based power sector in Saudi Arabia

By now, it is understood that RE-based SWRO can be a lucrative solution to produce potable water without the concern of greenhouse emissions. The next objective was to identify the steps that would be required to transition from the current fossil based to a renewable energy based desalination sector. In addition, existing literature suggest that desalination could provide additional flexibility to a renewable energy based system. This hypothesis was put to test by modelling an energy systems transition pathway for the desalination, power and industrial gas sectors of Saudi Arabia in integrated and non-integrated scenarios. In the latter scenario, the energy system transition required is modelled separately for the desalination sector and the power and non-industrial gas sectors. In contrast, in the integrated scenario, the three sectors are run together. By comparing the results of the two scenarios, the impacts of the desalination sector can be observed, if any. The desalination sector included the thermal and SWRO technologies.

The study revealed that the integration of the three sectors resulted in a reduction of the LCOE from 139 €/MWh in 2015 to 39 €/MWh by 2050. In addition, the results showed that a 100% RE system for Saudi Arabia can be achieved by 2040. Figure 11 captures some of the key observations. Figure 11 (a) presents trends in power capacities required to meet the increasing demand. PV single-axis tracking accounts for 409 GW of the 622 GW required by 2050 while battery storage met 44% of the total 2050 electricity demand, and thus bridged the solar resource gap from late afternoon to early morning hours.

(a) (b)

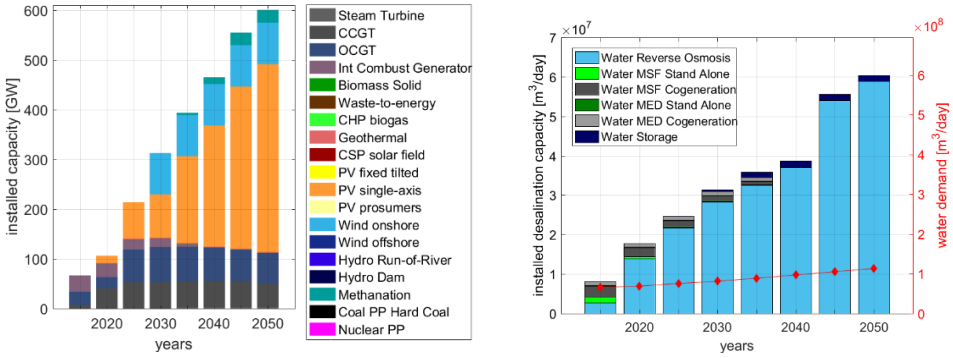

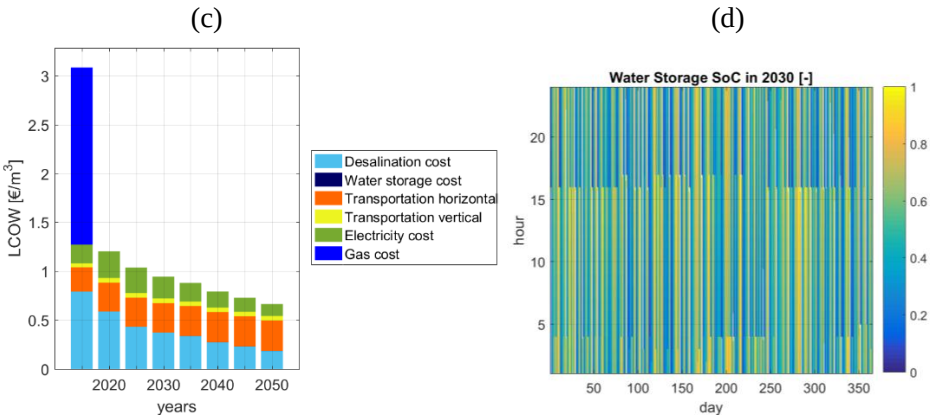

Figure 11 Change in energy system during the transition of Saudi Arabia's desalination, power and industrial sectors (a), Desalination capacity growth to help meet water demand from 2020 to 2050 (b), LCOW variation during the energy transition in Saudi Arabia (c), State of charge of water storage in 2030 (d)

Figure 11 (b) presents the increase in water desalination capacities required to meet the total desalination demand for the country. By 2050, it is expected that there is a total water demand of 112 million m^3/day and almost 52% of the demand is met through SWRO desalination. MED stand alone contributes up to 1% of the total desalination demand. The lower installed capacities of MED stand alone is due to less excess heat available in the energy system. The installation of SWRO and MED stand alone plants are optimised during the transition to deliver the system with least annualised costs. Figure 11 (c) shows the decrease in the weighted average LCOW from 3 €/m^3 in 2015 to 0.66 €/m^3 in 2050. The reduction in LCOW can be attributed to the reducing LCOE during the transition, the elimination of gas costs for thermal desalination by the electrification of the desalination sector, the improved efficiency and decreasing costs of desalination plants. By 2050, transportation costs contribute almost half of the LCOW.

Figure 11 (d) highlights the variation in water storage for the year 2030. Water storage is minimal and is used on a daily basis to optimise the operation of the desalination plants. In 2030, the total water storage capacity was 5 x 10^5 m^3, and as shown in Figure 11 (d) was used later in the day and replenished on days that there is a surplus of water. However, the role of water storage was not as significant as the initial hypothesis, indicating that not much flexibility was offered to the energy system. To quantify the benefits of the integrated scenario, the annualised costs of the systems from 2020 to 2050 were compared. Figure 12 illustrates the annualised system costs for the two scenarios. It was found that the approximate percentage benefit of the integrated scenario, in terms of annualised costs, is between 1% to 3%. The slight flexibility added to the integrated energy system allowed for a 1% decrease in PtG electrolyser capacities, with not much impact on battery storage systems.

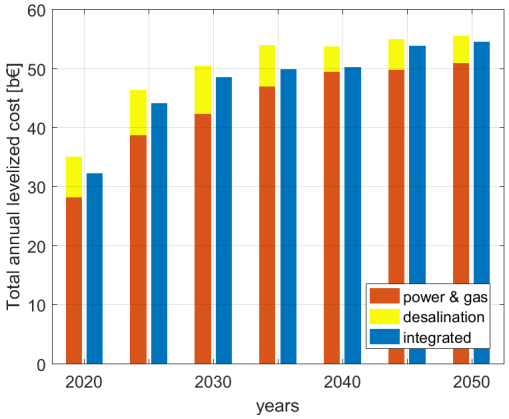

Figure 12 Comparison of annualised costs of the Saudi energy transition in an integrated and non-integrated scenario

The expected observation was a distinct variation in battery storage capacities in the integrated scenario, as it may be economical to store the excess as water and utilize the water when there is insufficient renewable energy in the system. This in turn would lead to a decrease in the requirement for battery storage. The disparity in results paved the way for a detailed study of the interplay between SWRO desalination, water storage and battery storage in the energy transition. The results are presented in **Publication IV**, discussed below, using Saudi Arabia as the case study.

5.4 Publication IV: The role that battery and water storage play in Saudi Arabia's transition to an integrated 100% RE power system

Water storage is a crucial component of Saudi Arabia's plan to achieve water security and the country is reported to be expanding strategic reserves in various cities. Simultaneously, the country's desalination sector is forecasted to grow rapidly, as the available freshwater resources diminish. Therefore, the question of the impacts of desalinated water storage in the Saudi Arabian energy transition is even more pertinent.

To determine the relationship between battery and water storage, the energy transition is first run and then re-run for various SWRO capex levels. The results were obtained for the transition periods 2030 and 2050. This sensitivity analysis was conducted for 100%, 80%, 75%, 50% and 25% of the SWRO capex. The numbers suggested that the energy system preferred to run the SWRO plants at higher full load hours rather than in a flexible manner. In 2030, at 50% of the actual SWRO capex, the full load hours of the SWRO plant only reduced by 3%. At 25% of capex, the full load hours reduced to 5%. In 2050, at 50% and 25% of the SWRO capex, the full load hours reduced by 1% and 3%. At unrealistically low capex values, the SWRO plants were still being run in a baseload manner.

Similarly, at 50% of the SWRO capex, the battery storage output was reduced by 5% in 2030 and 0.6% in 2050. At higher SWRO capex values, there was hardly any change in the full load hours of the SWRO plants or the battery storage output. The observed behaviour can be attributed to the fact that, even with reduction in SWRO capex, the desalination plants are still more capital intensive than solar PV and battery storage. As such, the model, that optimises the energy system based on the annual costs, prefers to run SWRO plants at higher full load hours and use battery storage for flexibility. This explains the low variation in SWRO hours and battery storage output. In addition, the variations are even less in 2050, when the battery and solar PV costs are much lower.

5.5 Publication V: Learning curve for SWRO desalination plants: capital cost trend of the past, present and future

The motivation for this paper came about during the initial research for **Publication I**. While trying to project the SWRO capital costs for 2030, it was noticed that there was a lack of literature on the learning curves of SWRO plants. The intention of **Publication V** is to close this research gap by applying the methods discussed in chapter 4 to 4237 SWRO plants that came online between 1977 and 2015.

Using the log-log model and the relevant data, the learning curve for the time periods from 1977-2015 and 1979-2003 was plotted as shown in Figure 12 (Caldera *et al.*, 2017). The error bars indicate the standard deviation for each time period. The learning rate for 1977-2015 was found to be approximately 15%, implying that when the global cumulative online capacity was doubled, the unit capex of SWRO plants decreased by about 15%. This has never reported before.

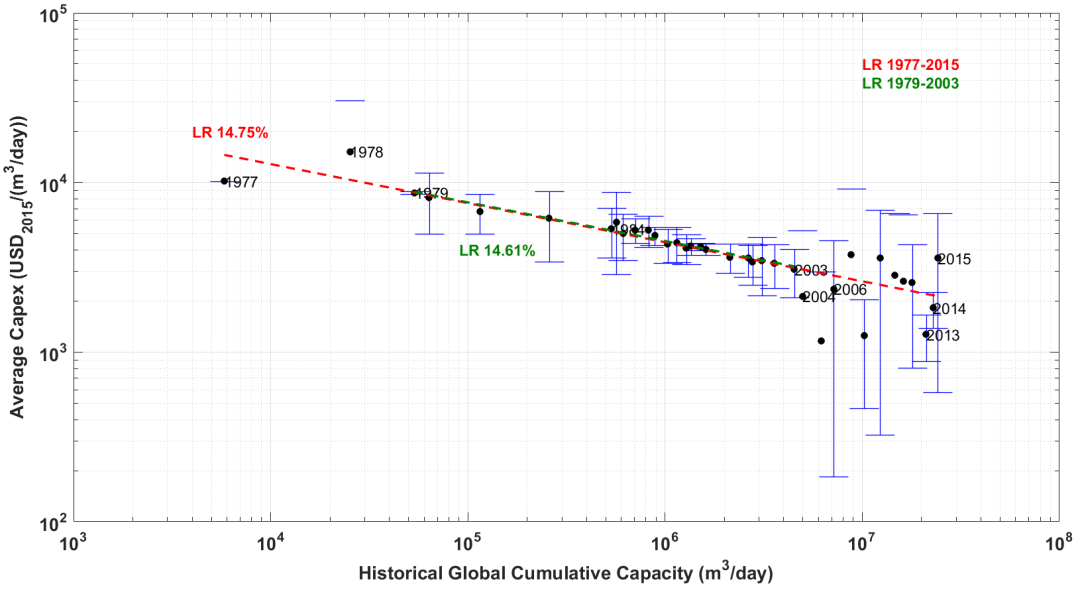

Figure 13 SWRO capex learning curve for 1977 – 2015 and 1979 – 2003

Due to the economy of scale effect, there was a sudden drop in SWRO capex post-2004, deviating from the learning curve. Furthermore, in some years, the average capex increased sharply due to site specific parameters.

By using the 15% learning rate, SWRO capacity annual growth rate and RE costs, it is possible to project the future water production costs.

Table 2 illustrates the SWRO capex trends for the coming years assuming a 15% learning rate, a 10% and 20% increase in annual online capacity from 2022 onwards. As more SWRO capacities are installed globally, spurred on by increasing water demand, improvements in design and construction, the SWRO capex may decrease even more sharply.

Table 2 SWRO capex projections based on the learning rate of 15% and annual growth rates of 10% and 20%

		2015	**2022**	**2030**	**2040**	**2050**
with annual growth rate of 10%						
Global historic cumulative online SWRO capacity	**[mill m^3/day]**	24	34	72	188	487
Capex	**[USD/(m^3/day)]**	2070	1917	1603	1282	1025
with annual growth rate of 20%						
Global historic cumulative online SWRO capacity	**[mill m^3/day]**	24	34	145	899	5567
Capex	**[USD/(m^3/day)]**	2070	1917	1361	888	580

5.6 Publication VI: Assessing the potential for RE powered desalination for the global irrigation sector

Water scarcity poses one of the greatest threats to conventional irrigation systems, a sector whose water demand is continuously growing. As freshwater resources dwindle and become expensive for farmers, SWRO desalination offers reliable water supplies for irrigation of cash crops. However, the consensus is that SWRO desalination is too expensive to irrigate crops such as rice, wheat and maize. The aim of this paper was to analyse what might be the cost of irrigated water if RE-based SWRO plants were used for existing irrigation sites.

Using the methods described in Chapter 3, the new water stress values were projected for the years 2030 and 2050. The average irrigation efficiency was assumed to be 60% in 2030 and 90% in 2050, as opposed to the 33% estimated in 2015. Figure 14 compares the water stress in 2030 under the BAU scenario (Base) and the highest possible irrigation efficiency (HPIE) scenario. Distinct reduction in water stress was found in India, China,

Central Asia, Mediterranean and North America. Nevertheless, regions of high or extremely high stress were observed in central United States and Northeast China. This could be because these sites face higher water demand from the industrial and municipal sectors rather than the irrigation sector.

(a)

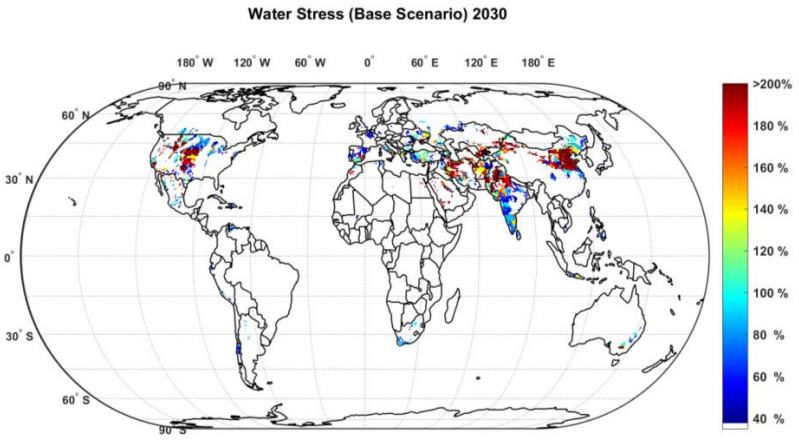

(b)

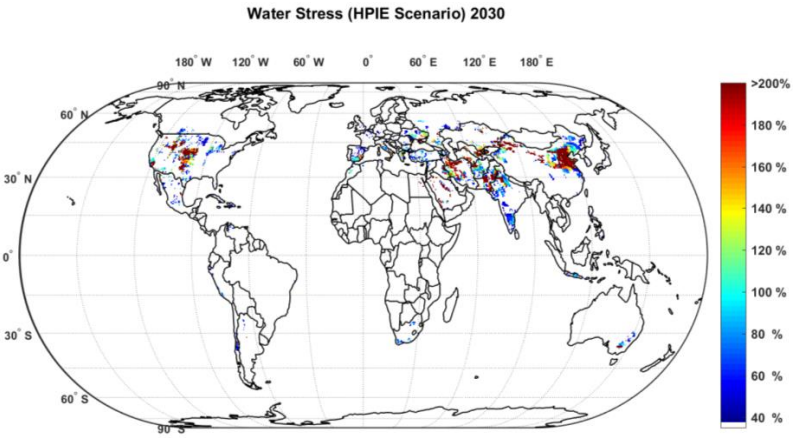

Figure 14 Water stress across existing irrigation sites in 2030 (a) Base scenario and HPIE scenario (b)

The resulting global desalination demand in 2030, in the HPIE scenario is 8.32 x 10^8 m^3/day. The demand decreases further by 25% in 2050, owing to the continuous increase in irrigation efficiency. In 2030, 55% of the demand is concentrated in China, Iran and Pakistan. This share drops to 50% in 2050. Table 3 compares the water withdrawal demand and the desalination demand numbers for the global irrigation sectors in both

scenarios. The water withdrawals increase over time in the HPIE scenario due to the growing demand, but is still less than in the Base scenario. If the irrigation efficiencies are implemented, this would mean less demand for desalination and more freshwater resources for the municipal and industrial sectors.

Table 3 Global Irrigation Water Demand in Base and HPIE scenarios

		Base Scenario 2030	**Base Scenario 2050**	**HPIE Scenario 2030**	**HPIE Scenario 2050**
Water demand for irrigation	m^3/day	$1.10 \cdot 10^{10}$	$1.30 \cdot 10^{10}$	$8.06 \cdot 10^{9}$	$8.32 \cdot 10^{9}$
Desalination demand for irrigation	m^3/day	$2.31 \cdot 10^{9}$	$3.10 \cdot 10^{9}$	$8.32 \cdot 10^{8}$	$6.25 \cdot 10^{8}$

After evaluating the impacts of the increased irrigation efficiency, the cost of supplying desalinated water to the irrigation sites, in the HPIE scenario, was modelled. In 2030, the LCOW range estimated was large, with a minimum of 0.7 €/m^3 and maximum of 6 €/m^3. However, the most common range was 0.7 €/m^3 – 2 €/m^3 with countries like Algeria, Morocco, Israel, Philippines, Venezuela and Italy having to pay the least cost. Countries in Central Asia are found to have a higher water production cost range of 3 €/m^3 – 5.8 €/m^3, which can be attributed to the longer water pumping distances. The global range in 2050 was estimated to be 0.45 €/m^3 – 1.7 €/m^3 reflecting the lower costs of the SWRO and renewable energy power plants in 2050. The corresponding global LCOE range in 2030 and 2050 are estimated to be 0.08 €/kWh – 0.13 €/kWh and 0.05 €/kWh – 0.10 €/kWh respectively.

To contextualise the relevance of these results, the LCOW values of the proposed system were compared with current costs of irrigated freshwater and what farmers are willing to pay. The system would be ideal for many irrigation intensive regions in Australia and North China Plain where farmers are willing to pay no more than 0.6 €/m^3. In addition, the competitive LCOW costs, feasible as early as 2030, include water transportation and become even more attractive as traditional water treatment costs increase.

5.7 Publication VII: Strengthening the global water supply through a decarbonised global desalination sector and improved irrigation systems

The HPIE scenario introduced in **Publication VI** is an optimistic one, where it is envisioned that countries would take swift action to improve irrigation systems and achieve a 90% efficiency by 2050. An objective of **Publication VII** was to identify the impacts if irrigation efficiencies continued in a BAU scenario, or improved at a moderate

rate in an Irrigation Efficiency Push (IEP) scenario. The scenarios are described in detail in chapter 3. The new irrigation water demand projections were added to the corresponding demands of the municipal and industrial sectors. Then, instead of focusing on the irrigation sector, the desalination demand of all three sectors were assessed in the Base, IEP and HPIE scenarios. The country specific desalination demand numbers were collated to the 145 regions listed in chapter 4.

After estimating the desalination water demand under the three scenarios, we modelled the energy transition pathways required to achieve a 100% RE sector across the 145 regions, by 2050. This is in contrast to **Publication VI** where an overnight scenario was modelled to gauge the water production costs in 2030 and 2050. The weighted average pumping distance and height for each of the 145 regions was estimated from the nodal pumping distances and height.

Figure 15 summarises the global desalination demand projections for the Base, IEP and HPIE scenarios. By 2050, in the HPIE scenario the global desalination demand was 1.7 x 10^9 m^3/day - 60% less desalination demand relative to the Base scenario. In the moderate IEP scenario, the desalination demand was estimated to be 3 x 10^9 m^3/ day, a modest decrease of 30% reduction relative to the Base scenario.

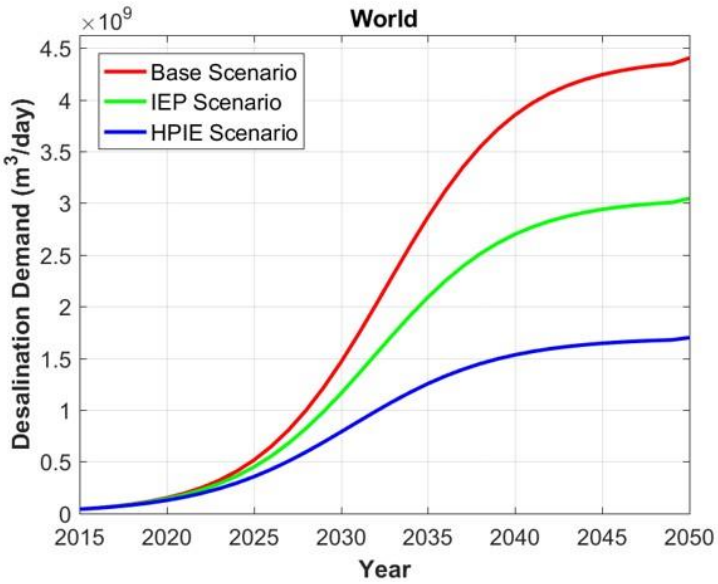

Figure 15 Desalination demand growth in the Base, IEP and HPIE scenarios

Figure 16 (a), (b) and (d) compares the 2050 desalination demand of the 145 regions in the three scenarios. In the three scenarios, India, China, USA, Pakistan and Iran account for between 56% and 62% of the global desalination demand in 2050. Figure 16 (d) and (e) also show the percentage by which the desalination demand changed across the 145

regions in the IEP and HPIE scenarios, relative to the Base scenario. This enables to understand which countries would be most affected by the irrigation efficiency change and to what degree. Globally, the weighted average reduction is about 29% and 48% in the IEP and HPIE scenarios respectively.

(a)

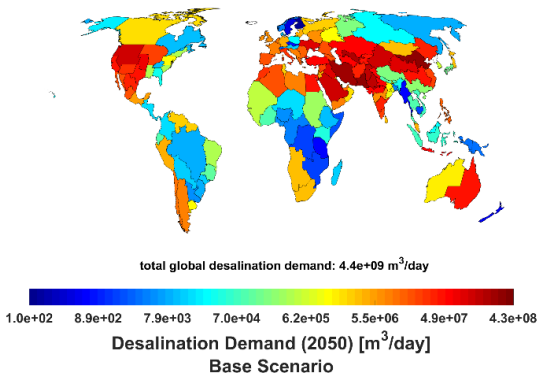

(b)

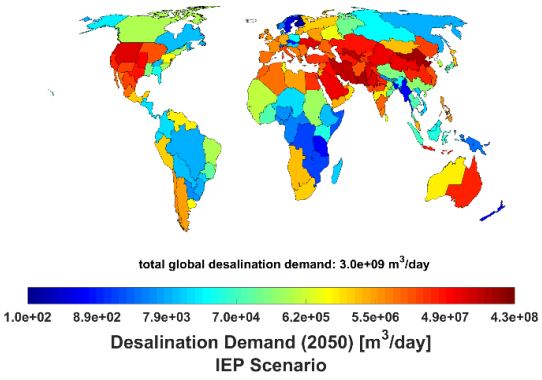

(c)

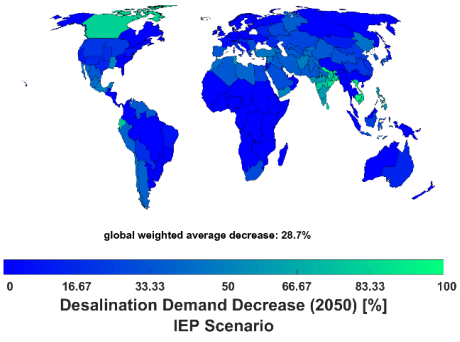

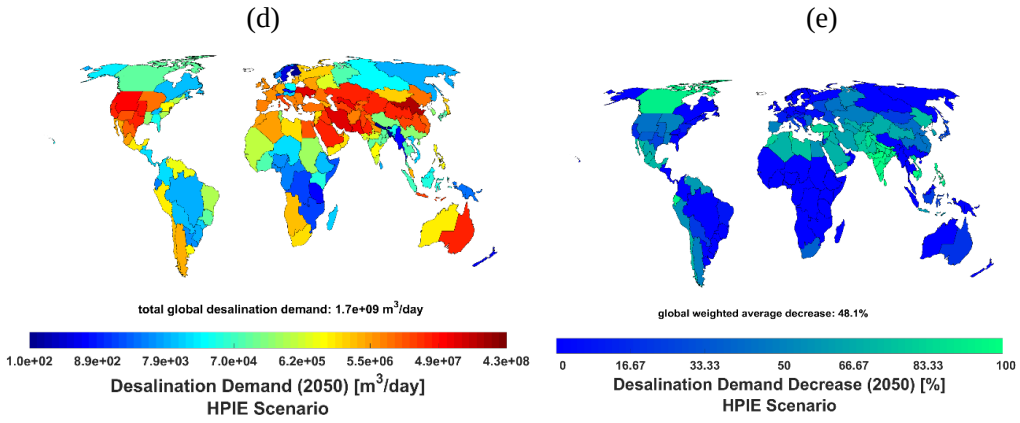

Figure 16 Desalination demand in 2050 in the Base scenario (a), IEP scenario (b), demand decrease in percent in the IEP scenario (c), desalination demand in 2050 in the HPIE scenario (d), demand decrease in percent in the HPIE scenario (e).

Decarbonising the desalination sector by 2050, will result in the global average LCOW decreasing from about 2.4 €/m^3 in 2015, considering unsubsidised fossil fuel costs, to approximately 1.05 €/m^3 by 2050. The corresponding LCOE decreases from 180 €/MWh to approximately 50 €/MWh across the three scenarios. By 2050, the levelised cost of electricity from the primary generation sources and energy storage account for almost 95% of the final LCOE. Transmission and curtailment costs make up the remainder of the LCOE.

Most regions will have an LCOW in the cost range of 0.32 €/m^3 – 1.66 €/m^3, including the costs of water transportation from the coast to the desalination demand site. Figure 17 (a) illustrates the weighted average LCOW for the 145 regions in 2050, under the moderate IEP scenario. The Base and HPIE scenarios also project a similar LCOW range by 2050. In contrast, the average municipal water price is projected to increase and by 2050, lie between 1.2 USD/m^3 - 1.4 USD/m^3 or 0.9 €/m^3 - 1.0 €/m^3, based on a 1.3 USD to 1 € exchange rate. The results show that a decarbonised desalination sector will enable water costs competitive with the municipal water prices, across all the major regions. The main energy source is solar PV as shown in Figure 17 (b). The globally weighted average solar PV and wind generation shares are about 78% and 22% respectively. Globally, the installed capacities of solar PV required, in a moderate desalination demand scenario, are 3144 GW and battery storage output meets 42% of the electricity demand. The regions with high wind generation shares are also regions with relatively lower desalination demand. Further details on the total costs of the different systems and scenarios are provided in **Publication VII**.

(a)

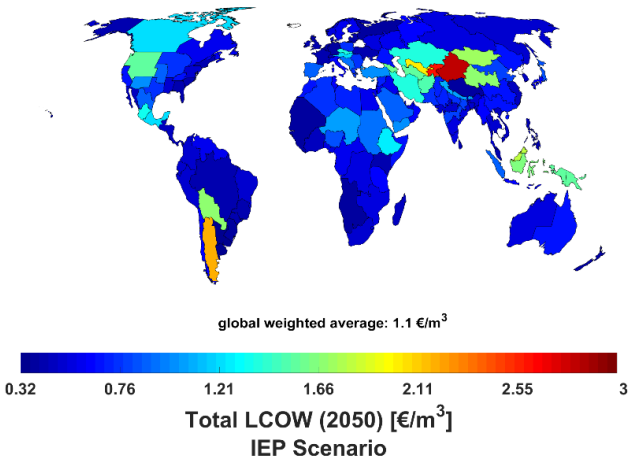

(b)

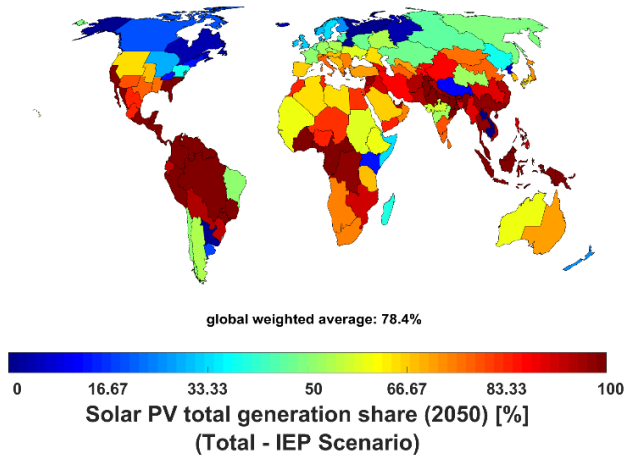

Figure 17 Weighted average LCOW for the 145 regions in 2050 , in the IEP scenario (a) , share of solar PV in the renewable energy generation mix by 2050 , in the IEP scenario (b)

6 Discussion

6.1 General discussion of presented results in publications

The desalination demand estimated for 2030, in **Publication I**, is approximately 25 times more than the 2015 installed capacity of 89.4 million m^3/day. The water stress situation is projected to worsen, especially in parts of North America, North Africa, Middle East and Southern Asia. These results indicate that significant investments are required to ensure that the water demand is met in all parts of the world in the years to come. The total capex of the proposed system to meet the 2030 global desalination demand is estimated to be 9,790 b€, with annualised costs of 1,230 b€, for a WACC of 7%. However, the results also show that by coupling RE power plants and SWRO plants, we obtain potable water within the cost range of 0.59 €/m^3 – 2.81 €/m^3. The LCOW range includes the cost of water transportation, which can play a significant role as the demand lies further away from the coast. The technical and financial assumptions of all technologies used in **Publication I** are for the year 2030 based on trends observed until 2015. The ITRPV report (2018) estimate the current system price of utility scale fixed-titled PV systems to be 680 USD/kW, which is equivalent to 524 €/kW assuming an exchange rate of 1.3 USD to 1 €. In our study, we assumed system costs of 550 €/kW for fixed-tilted PV and 620 €/kW for single-axis tracking PV to be achieved by 2030. Similarly, BloombergNEF (2019) explains that current battery pack prices are already at 156 USD/kWh or 120 €/kWh. In **Publication I**, we assumed a cost of 150 €/kWh. In addition, solar PV is found to contribute up to 82% of the total energy demand, while battery storage is used almost daily and meets 24% of the total energy demand. Therefore, the LCOW range calculated for 2030 in **Publication I** can be considered conservative and an overestimate of the actual LCOW. The costs that vary with the project type and geography, such as land rent and project costs, are accounted for under the opex costs. According to Vartiainen et al. (2020), for utility scale PV, the opex costs are on average about 2% of the capex, and may differ drastically for certain projects. However, the authors conducted a sensitivity analysis on the PV LCOE for different parameters and noticed that an increase of 50% in the opex results in a 14% increase in the PV LCOE. Thus, the analysis highlights the fact that the opex does not have a significant impact on the PV LCOE.

A report by Fichtner (2011) on the desalination outlook for the MENA region compiled the average water prices of desalination projects between 2003 and 2010. The range varied and for conventional SWRO plants lay between 0.4 €/m^3 to 1.9 €/m^3, excluding the transportation costs. In some cases, the LCOW is much lower due to the highly subsidized electricity or fuel costs. For instance, Fthenakis et al. (2016) explain that Saudi Arabia utilizes more than 1.5 billion barrels of oil per day for the desalination sector, while the liquid fuels and natural gas are purchased by local power producers at 3% and 6% of the market price respectively. Based on the PV costs in 2015, Fthenakis et al. (2016) finds that if the unsubsidized cost of electricity was used in Saudi Arabia, grid electricity would cost 0.21 USD/kWh as opposed to the 0.09 USD/kWh of single-axis

tracking PV. Therefore, without subsidies, the cost of water production, which is dependent on the cost of electricity or fuel, would be much higher. An article by the Smart Water Magazine (2019a) estimates the water production costs to be between 0.4 €/m^3 to 1.2 €/m^3 and shares the view that lower costs are found in countries with cheaper electricity costs. These facts suggest that the 100% RE-based SWRO desalination system determined in **Publication I** would indeed allow countries to produce potable water at costs less than that of conventional fossil power plants. The results of **Publication II** provide further evidence of the feasibility of 100% RE-based SWRO desalination for the water stressed country of Iran. Conventional SWRO plants are reported to currently produce water at an LCOW of 0.70 €/m^3, excluding water transportation. We find that potable water can be produced and transported to the coastal regions of Iran at a cost of 1.0 €/m^3 using 100% renewable energy. For further inland regions like Zahedan, where people are dependent on an increasingly saline and receding groundwater levels (Lashkaripour *et al.*, 2005). RE-based SWRO systems can provide water at costs of between 1.0 €/m^3 - 1.5 €/m^3. More mountainous regions in the North West and East, have steeper transportation costs, pushing the LCOW to between 2 €/m^3 – 3 €/m^3. The water transportation costs may be optimized by using existing infrastructure such as roads and electrical grid lines to determine the pumping distances. According to Lashkaripour and Zivdar (2005), in Zahedan, 50% of the drinking water is currently supplied by water tankers bringing water from a city 100 km away. The government has plans to transfer water, through a 193 km long pipeline, from a reservoir that is being fed by rivers originating in the neighbouring Hendokosh mountains in Afghanistan. The authors voice concern over the reliability of this project due to the instability of the region. Lamei et al. (2008) compared the costs of supplying freshwater to tourist resorts in Egypt through RO desalination and long-distance piping. The results showed that after a certain distance and flow capacity, it was economically sound to use RO desalination as opposed to long-distance piping. This study highlights the significance of water transportation costs. Our results show that Zahedan can in fact be provided with a steady and reliable supply of water through 100% RE-based SWRO plants located along the Persian Gulf.

In **Publication III**, crucial aspects of the 100% RE-based desalination systems discussed previously were evaluated and addressed: how to achieve the proposed system from the current fossil based desalination sector and can desalination be used to improve flexibility in a system with high shares of renewable energy. Saudi Arabia makes for an interesting case study due to the large desalination sector in the country, the local consumption of highly subsidized fossil fuels, the growing water and electricity demand as well as the government's vision to steer the country away from using fossil fuels locally. In addition, Saudi Arabia leads the global production and export of petroleum products and during the time period 2010 – 2013, the country's oil revenues are reported to have contributed up to 91% of the national income (Albassam, 2015).

In the transition study for Saudi Arabia, the electricity and desalination demand for Saudi Arabia, from 2015 to 2050, were estimated and the LUT Energy System model used to find the least cost energy transition path. In the transition, the model does not allow installation of any fossil based thermal plants after 2015 and existing plants are phased

out based on lifetime. Two scenarios, non-integrated and the integrated energy transitions, are modelled to assess the benefits of integration. The LCOE decreases from 139 €/MWh in 2015 to 38 €/MWh by 2050 and a 100% RE system is in fact achieved by 2040. Single-axis tracking PV and battery storage form the backbone of the electricity supply by 2050, the latter contributing 368 GW out of the total 480 GW of installed capacity and the former meeting 48% of the total electricity demand.

The integrated scenario provides a slight 2 - 4% decrease in the annualised costs of the transition, compared to the non-integrated scenario. Integration provides flexibility to the energy system through better utilisation of the hourly produced renewable energy and therefore less storage in the form of PtG capacities. The work also highlighted that water storage is not relied upon to improve the flexibility of the system and contribute to less than 1% of the total desalination demand in 2050. This contradicts our initial hypothesis and the insights of other researchers. For instance, Al-Nory and El-Beltagy (2014) determined that using SWRO desalination as a deferrable load in an energy system with high shares of renewable energy will result in a 12% reduction in costs. Heihsel et al. (2019) use 100% RE powered SWRO desalination to augment water reservoirs in the Murray Darling Basin in Australia. The authors find that using the SWRO desalination plants to shift the load reduced the cost of electricity by 43% and the total annualized costs by 35% relative to the no-shift scenario. However, in these discussed studies, no energy storage is considered to optimize the energy system.

In **Publication IV**, we focus on the interplay between battery and water storage in the Saudi Arabian energy transition studied previously. The results show that battery storage and solar PV offer a more cost-effective flexibility solution to the energy system as opposed to the capex intensive SWRO plants. The energy system prefers to run the SWRO plants in a baseload manner and optimise with the combination of battery storage and solar PV. In order to use the SWRO plants as a deferable load resource, Atia and Fthenakis (2019) investigated several scenarios using an active salinity control. In this proposed concept, the salinity of the feedwater is increased via blending during periods of high electricity supply. During periods of low electricity supply, the salinity is decreased. This way the permeate output can still be kept the same.

The results of **Publication IV** also provide fundamental insights into renewable energy systems: It is cost effective for any relatively high capex energy conversion technology in the system to operate in baseload mode, when low cost PV and battery can offer the required flexibility. Recent research (Breyer *et al.*, 2019; Fasihi *et al.*, 2019) highlight similar behaviour with direct air capture (DAC) units that provide least cost CO_2 capture when operated at high full load hours.

For the publications that have been discussed, the capex projections of SWRO plants were based on the findings of Loutatidou et al. (2014). The authors use a linear regression model to determine the relationship between the RO capex and factors such as the plant capacity, location of plant, type of plant and contract awarded year. Based on the correlation, a quantitative model to estimate the capex of RO plants is established. The

study then continues to use the quantitative model to forecast the capex of SWRO plants in the GCC region, for the time period from 2014 - 2030. In **Publication V**, the tried and tested learning curve approach based on the concept of 'learning by doing' was used to analyse the capex trends of 4237 SWRO plants between the period 1977 – 2015. The average learning rate for the time period was 15% indicating that as the global cumulative SWRO capacity doubled, the capex reduced by 15%. Due to the economy of scale effect, there was a sudden drop in SWRO capex post-2004, deviating from the learning curve. Furthermore, in some years, the average capex increased sharply due to site specific parameters. Since the publication of our research, Mayor (2019) has conducted a study on the learning rates of the main desalination technologies and observed a similar learning rate of 15% for SWRO plants.

It has to be noted that the costs of SWRO plants are based on the data provided by GWI Desal Database (Loutatidou *et al.*, 2014) and do not account for the land costs. Papapetrou et al. (2017) explain that land costs for desalination plants are not generally reported and can be assumed to be about 2% of the construction costs. Construction costs generally account for about half of the total SWRO capex, implying that land costs are 1% of the SWRO capex (World Bank, 2019). In regions of very high real estate costs such as Israel, it is reported that land costs are managed by the government (World Bank, 2019).

The results so far showed us that desalination powered by renewable energy can indeed be a reliable source of water supply for many regions of the world. However, the desalination demand projected is much higher than the current global installed capacity. This was due to the consideration of desalination for the irrigation sector which currently accounts for 70% of the total water withdrawals. While many of the world's breadbaskets are in water stressed regions, desalinated water is considered too expensive and only used for cash crops such as vegetables, fruits and flowers (Burn *et al.*, 2015). It has to be noted that water withdrawals for the irrigation sector are exacerbated by low water use efficiency (Jägermeyr *et al.*, 2015). In **Publication VI**, emphasis was placed on assessing if, based on our earlier work on 100% RE-based SWRO plants, desalinated water was still expensive for irrigating important crops like rice, maize and wheat. The desalination demand was estimated for a scenario where the irrigation efficiency across all sites was increased such that by 2050, all sites would have an efficiency of 90% by 2050. Based on the assumptions made, it was found that in 2030, the LCOW for most irrigation sites in water stressed regions would be in the range 0.7 €/m^3 – 2 €/m^3. In 2050, this range would decrease slightly to 0.45 €/m^3 – 1.7 €/m^3. The LCOW range also includes pumping water from the nearest coastline to the site of irrigation. Most irrigation sites are located further away from the coastline and based on the results of **Publication VI**, the weighted average horizontal and vertical pumping distance are about 750 km & 1500 m respectively. Our results show that competitive costs can be achieved by 100% SWRO desalination in Australia where farmers are not willing to pay no more than 0.68 €/m^3. The cost range estimated in **Publication VI** include remineralisation of the SWRO permeate with magnesium based on data from Ben-Gal et al. (2009). However, further treatment to the permeate may be required to achieve the right water quality parameters such as the sodium absorption ratio and boron concentration. Desalination also strips other important

elements such as calcium and sulphur from the seawater. Post-treatment strategies depend on the crop types and soil conditions and incur an additional cost to the desalinated water. At desalination plants that currently provide water for irrigation, different techniques are used such as blending the permeate with other water resources, using a partial second RO pass or an ion exchange resin (Quist-Jensen *et al.*, 2015). Gao et al. (2017) explains the inevitable increase in cost of conventional water supplies due to diminishing surface water resource, declining groundwater levels, seawater intrusion and pollution. As such, SWRO desalination becomes a more attractive option for meeting the demands of the irrigation sector. In **Publication VII**, the role that renewable energy-based desalination, in conjunction with improvements in water use efficiency in the irrigation sector, can play towards securing future global water supplies is analysed. It is found that the global desalination demand by 2050 can be reduced by as much as 30% and 60%, depending on the irrigation efficiency growth rate. India, China, USA, Pakistan and Iran account for between 56% to 62% of the global desalination demand. Decarbonising the desalination sector by 2050, will result in global average levelised cost of water decreasing from about 2.4 €/m^3 in 2015, considering unsubsidised fossil fuel costs, to approximately 1.05 €/m^3 by 2050, with most regions in the cost range of 0.32 €/m^3 – 1.66 €/m^3. Low-cost renewable electricity, in particular solar photovoltaics and battery storage, is the key driver to maintain global clean water supply supported by measures to increase irrigation efficiency so that major disruptions due to the arising clean water crisis can be avoided and United Nations Sustainable Development Goals are supported.

The results of the publications indicate that solar PV and battery storage play a crucial role in extending the role of desalination in water stressed regions. To understand the impacts of the capex of RE systems on the LCOW, a sensitivity analysis was conducted on the results of **Publication VII**. The results of Saudi Arabia, for the Base scenario, was chosen as a case study. For the sensitivity analysis, the PV capex was increased by 25% in several steps, for the time periods from 2020 to 2050. Table 4 captures the impacts of PV capex variation on the LCOE and LCOW in 2050. The initial 2050 results of **Publication VII** are based on PV fixed tilted, single-axis tracking and battery storage capex values of 246 €/kW, 271 €/kW and 75 €/kWh respectively (Vartiainen *et al.*, 2017, 2020). The battery capex was also changed accordingly while keeping the original PV capex values. Table 5 illustrates the impacts of battery capex increase.

Table 4 Impacts of increasing PV capex by 25% on the LCOE and LCOW of Saudi Arabia. Results are shown for the year 2050. Bold capex values are the original assumption in **Publication VII**.

		2050 fixed-tilted & single-axis tracking PV capex €/kWp			
		246 & 271	308 & 338.75 (+ 25%)	369 & 406.5 (+ 50%)	431 & 474 (+ 75%)
Average LCOE	€/kWh	54.7	57.4	60	62.6
Average LCOW	€/m^3	0.880	0.882	0.896	0.90

Table 5 Impacts of increasing battery capex by 25% on the LCOE and LCOW of Saudi Arabia. Results are shown for the year 2050. Bold capex value is the original assumption in **Publication VII**.

		2050 battery capex €/kWh			
		75	93.75 (+ 25%)	112.5 (+ 50%)	131 (+ 75%)
Average LCOE	€/kWh	54.7	57.5	60.3	63.1
Average LCOW	€/m^3	0.880	0.888	0.897	0.905

The new PV and battery capex values resulted in a significant increase in the average LCOE of the country. However, the changes in the LCOW do not reflect the increase in LCOE – a maximum increase of 2% is observed for a 75% increase in PV capex. This may be attributed to the overall composition of the LCOW. About 50% of the 2050 LCOW is made up of water transportation costs, excluding electricity for pumping. The total electricity contribution to the LCOW is estimated to be around 20%. The remaining costs are due to the cost of desalination plants. These values also reflect the Saudi Arabian and global LCOW breakdowns illustrated in Figure 11 (c) and **Publication VII** respectively.

As the analysis above shows, changes in the PV and battery capex do not have a significant impact on the final LCOW.

6.2 Policy implications

From the outset, the intention of the research was to illuminate the untapped potential of 100% RE-based desalination systems, more specifically the SWRO desalination technology. Small-scale solar desalination has been discussed since the 1970s, with RE-based large-scale plants being considered for the current market. However, Water International (2019a) describes the coupling of 100% RE with desalination as more an engagement due to the lack of the desalination industry to fully commit to RE sources. In our research, we place 100% RE-based desalination in relevant context for policy makers so that they may start to visualize using these systems to abate the global water crisis.

The recent report by the World Bank (2019) on the role of desalination aims to guide policy makers with pertinent questions regarding the use of desalination as an alternative water supply solution. While the report projects a shift towards RE-based desalination, the authors posit that it is not currently possible due to the high costs of energy storage. However, the authors also acknowledge that due to the dropping costs, RE-based desalination will become competitive within a decade. The Global Clean Water Desalination Alliance (2015), launched at COP21 in Paris, pursue a vision of reducing CO_2 emissions from existing and new desalination plants worldwide.

In this research, we have assessed the potential desalination markets worldwide based on the physical water stress factor. This study was first done in **Publication I**, where desalination demand was quantified for all countries for the year 2030. The global desalination market was estimated to be 2.4 billion m^3/day. In **Publication VII**, we estimated the market to grow to 4.4 billion m^3/day by 2050 in a BAU scenario. As of 2015, Saudi Arabia was the largest desalination market with 18% of the cumulative 89 million m^3/day installed capacity. However, in 2050, we estimate the top 5 desalination markets to be China, Pakistan, India, USA and Iran accounting for 19%, 15%, 11%, 10% and 7% respectively of the desalination demand. In contrast, in 2015, the countries with the largest desalination market shares after Saudi Arabia, were United Arab Emirates and Qatar (Virgili, 2017).

After improvements in irrigation efficiency, the global desalination demand decreases by 30% and 60% in the IEP and HPIE scenarios respectively. However, the countries with the top 5 desalination markets continue to be the same, although with different shares. These results show that even after improving water use efficiency in the irrigation sector, there is still substantial demand from the industrial and municipal sectors, resulting in a large desalination demand. Furthermore, the 60% decrease in the desalination demand in the HPIE scenario, relative to the Base scenario, highlights the fact that most of the world's irrigation sites lie in water scarce regions. The total capital investments required for the global transition towards achieving 100% RE-based desalination in the Base, IEP and HPE are estimated to be 15,185 b€, 10,352 b€ and 5766 b€ respectively. To put it into context, the International Monetary Fund (Coady *et al.*, 2019) report that the world spends 4.7 trillion USD (3.6 trillion €) on direct and indirect subsidies for coal, gas and

oil use. China and USA were found to be the largest subsidisers spending 1.4 trillion USD (1.1 trillion €) and 699 bUSD (538 b€) in 2015 respectively.

Research by Jones et al. (2019) has brought attention to the issues of large quantities of concentrated brine from the desalination sector being recklessly discharged into the marine environment. This results in the pollution of coastal waters and damage sensitive marine life. A recent article in the Guardian (2020) highlights this issue in a town on the edge of the Atacama desert in Chile, that relies heavily on desalinated water. Fishermen claim that the effluent from desalination plants have been killing the marine life and endangering their sources of income. To minimise the impact on the environment, more complex outfall infrastructure is required, leading to an increase in the final project costs. Jones et al. (2019) recognise the vital role of desalination in the future global water supply and recommend the use of brine discharge for economic gains. The alternatives to discharging the brine maybe the use of concentrated brine for commercial salt production and recovery of precious metals like lithium (Drioli *et al.*, 2015; Jones *et al.*, 2019). Davies et al. (2018) also present a case for utilising the magnesium chloride in the concentrated brine to emulate the natural ocean liming process, thereby contributing to the removal of CO_2 from the atmosphere. The authors claim that if renewable energy is used, the SWRO plant can behave as a negative emissions technology and deserve further investigation.

6.3 Limitations of the current research

Through the course of this research there have been several assumptions or simplifications made to comprehend the role of 100% RE-based SWRO in securing our current and future global water supplies. The resulting limitations have been outlined in the articles and pose as further points of research. The main limitations of the research can be summarized as below:

1. The inability to predict water availability and water withdrawals in a high spatial resolution against the backdrop of the changing climate. This affects the projection of the desalination demand. In August 2019, the Aqueduct Water Atlas was updated and enhanced with more granular and higher resolution data. For future work, it might make sense to consider this updated data set that will provide better insights into the current situation of the world's hydrological basins.

2. The water demand for cooling of the global power plant fleet in 2015 was recently estimated by Lohrmann et al. (2019), who also determined the corresponding water demand during the global energy transition towards a 100% RE-based energy sector by 2050. The presented data may be used to more accurately account for the desalination water demands of the power sector during the energy transition.

3. Optimising the water transportation paths for desalination demand sites by considering existing infrastructure such as roads and grids, as well as the sharing of infrastructure for different sites. This idea has been discussed by Herrera Leon et al.(2019) for the mining industry in Chile where some mining sites have to convey water over altitudes of 3000 m above sea level. Such detailed studies can be done on a country level to optimize the water transportation pathways and arrive at the least cost water supply options for the water stressed regions. In addition, existing literature (Lamei *et al.*, 2008) makes reference to 1993 water transportation costs as current costs are usually not disclosed by companies. It would therefore make sense to determine and use the updated infrastructure costs.

4. When assessing a country's ability to use RE-based SWRO to augment local water supplies, it is also necessary to consider the country's policy and institutional factors such as transboundary issues. For instance, the State of Palestine relies on desalinated water imports from Israel, which is impacted by the political relationship between the two regions (World Bank, 2018). Similarly, Central Asian countries such as Tajikistan and Uzbekistan have high levels of water stress but would require desalinated seawater to be pumped through neighbouring countries. Meanwhile, in Spain, changing political views on the use of desalination or water transfer projects to best tackle the water scarcity issues in the country has greatly affected the national water policy (Zarzo *et al.*, 2013). These are aspects that should be considered when implementing desalination plants for a country.

5. In **Publications III** and **IV**, the energy transition for Saudi Arabia was simplified to a single node and the country weighted average of the corresponding input data considered. This was because of the significant computational capacity necessary to implement an energy transition from 2015 to 2050, in an hourly resolution and spatial resolution of 0.45° x 0.45°. Similarly, in **Publication VII**, the world was simplified to 145 nodes as described in chapter 4. This allows us to capture the global results, but at the cost of granular data. Country specific studies, on a high nodal resolution, will allow to capture more detailed results.

6. The use of geothermal heat for thermal desalination technologies is not considered during the transition. In some countries, this may prove to be a cost-effective energy supply for MED desalination and warrant further inspection. Other scenarios of interest are the use of CSP plants for hybrid configurations of thermal and RO desalination technologies or the integration of process waste heat with thermal processes like membrane distillation.

7. In order to complete the research in **Publications VI** and **VII**, a further study on the investments required to upgrade the irrigation infrastructure across the regions is necessary. This would help generate a comprehensive understanding of the investments needed and the most attractive pathways for regions to secure water

supply with efficient irrigation sectors. In addition, in **Publications VI** and **VII**, the beneficial irrigation efficiencies are considered due to the availability of the global estimates. However, these values do not account for water withdrawals that may be reused from the basin as a least cost water supply option and a higher water savings potential. This would entail further research into the irrigation efficiencies across existing sites.

8. When designing desalination plants for irrigation, the quality of water required for the crops being grown should be considered and the most cost-effective way to achieve this quality determined. To overcome the drawbacks and minimise the costs of using SWRO for irrigation water, several alternatives are being investigated. For instance, Shaffer et al. (2012) propose the integration of forward osmosis and seawater reverse osmosis which reduces the boron and chloride concentration in the permeate and consequently reduce the energy required for post-treatment. Other alternatives being explored are RE-based electrodialysis, membrane distillation and hybrid combinations with SWRO (Quist-Jensen *et al.*, 2015).

7 Conclusion

This thesis introduces and describes the ways in which 100% RE-based SWRO desalination can be used to help overcome the world's water issues. Concerns within the desalination industry about switching to solely RE sources were tackled, and new ways of using desalination with better water management added. The results of this thesis clearly show that desalination demand across many regions will increase and adopting 100% RE-based desalination can help assuage global water stress. Ultimately, by addressing the issues of water stress, water demand management in the irrigation sector, the transition to RE resources, the research establishes pathways that could achieve the United Nations SDGs 2, 6 and 7.

The global desalination demand was estimated for the time period from 2020 to 2050, in 5-year time steps. The decadal water stress and total water demand projections were used to determine the desalination demand for 15,006 hydrological basins, at a spatial resolution of 0.45° x 0.45°. By 2050, the global desalination demand is estimated to be 4.4 x 10^9 m^3/day for the municipal, irrigation and industrial sectors, excluding thermal power plants - an almost 49-fold increase from the online capacity in 2015. This projection assumes that there is no significant improvement in the water use efficiency of the irrigation sector, the sector responsible for 70% of the global water withdrawals. The estimate of the global beneficial irrigation efficiency is reported to be 33%, with even dismal irrigation systems being used in Pakistan and India, the breadbaskets of the world. In this thesis, scenarios were established where the efficiency of existing irrigation sites were increased under different conditions. In the most optimistic scenario, the desalination demand in 2050 was 1.7 x 10^9 m^3/day. In the moderate scenario, the desalination demand in 2050 fell to 3 x 10^9 m^3/day. The impacts of the improved water use efficiency on the global irrigation sites could be observed and the subsequent influence on the demand for desalination.

In addition to assessing the potential for desalination, the costs of running an entirely RE-based global desalination sector was analysed. The initial overnight study showed that it was indeed possible to run 100% RE-based SWRO desalination at costs competitive with the current fossil based desalination sector. This led to further work on understanding the transition pathway that can allow countries to achieve an entirely RE-based industry by 2050. The findings show that the key RE resources that will drive the desalination sector are solar PV and battery energy storage. This shows that most regions with water stress are also those with plentiful solar resources. By taking advantage of these RE resources, a global LCOW range of 0.32 €/m^3 – 1.66 €/m^3 can be achieved by 2050 through 100% RE-based desalination. These costs are competitive with the conventional cost of water desalination, as well as the projected costs of traditional water treatment methods in many parts of the world. As surface water diminish, groundwater levels decline, mountain glaciers retreat and pollution and salinization threaten available resources, traditional water collection methods become threatened and expensive.

The role of SWRO desalination and water storage in energy systems with high shares of RE was also analysed. The results were contrary to the initial idea that water storage can provide much flexibility to the energy system through better management of excess energy generation and demand. It was observed that it is preferable to run the expensive SWRO plants in baseload operation for total energy system cost reasons. Flexibility to the energy system can be provided at a lower cost by solar PV and battery storage than by SWRO plants and water storage. costs. The SWRO capex has to be reduced by 50% to achieve a reduction of 1% in SWRO FLH and a 2.1% in the annualised energy system costs. Such a reduction in SWRO capex is not feasible in the foreseeable future and does not anyway add flexibility to the energy system.

To estimate the costs of producing water from SWRO desalination plants, it was necessary to understand the historical SWRO capex trends and establish the learning rate for SWRO desalination plants. This was done by analysing 4237 SWRO plants that came online from 1977 – 2015 using the learning curve model. It was found that SWRO capex has decreased by 15% for every doubling of cumulative online SWRO capacity. This implies a learning rate of 15% for SWRO plants. Deviations from the learning curve were observed in the last decade and can be explained by the economy of scale effect and site-specific features. Using the learning rate presented and future growth rates for SWRO desalination, the SWRO capex can be estimated in future studies.

Slowly, but surely, there is an increasing acknowledgement of the feasibility for an almost 100% RE-based desalination. This can be observed in recent literature by Heihsel et al. (2019) and Atia and Fthenakis (2019) where such desalination systems are considered conducive for water supply. These studies consider either battery storage or elevated seawater reservoirs to provide the energy storage required to optimize the operation of the SWRO plants. The results of this work fill in several gaps wihthin the concept of 100% RE-based desalination and help policy makers visualize 100% RE-based desalination in the water supply repertoire. In addition, the results of the research present points of discussion that warrant further research to fully exploit the benefits of 100% RE-based desalination.

References

Aghahosseini, A., Bogdanov, D., Barbosa, L. S. N. S. and Breyer, C. (2019) 'Analysing the feasibility of powering the Americas with renewable energy and inter-regional grid interconnections by 2030', *Renewable and Sustainable Energy Reviews*, 105, pp. 187–205. doi: 10.1016/j.rser.2019.01.046.

Al-Karaghouli, A. and Kazmerski, L. L. (2013) 'Energy consumption and water production cost of conventional and renewable-energy-powered desalination processes', *Renewable and Sustainable Energy Reviews*, 24, pp. 343–356. doi: 10.1016/j.rser.2012.12.064.

Al-Nory, M. and El-Beltagy, M. (2014) 'An energy management approach for renewable energy integration with power generation and water desalination', *Renewable Energy*, 72, pp. 377–385. doi: 10.1016/j.renene.2014.07.032.

Albassam, B. A. (2015) 'Economic diversification in Saudi Arabia: Myth or reality?', *Resources Policy*, 44, pp. 112–117. doi: 10.1016/j.resourpol.2015.02.005.

Ashraf, B., Aghakouchak, A., Alizadeh, A., Mousavi Baygi, M., Moftakhari, H. R., Mirchi, A., Anjileli, H. and Madani, K. (2017) 'Quantifying Anthropogenic Stress on Groundwater Resources', *Scientific Reports*, 7(1). doi: 10.1038/s41598-017-12877-4.

Atia, A. A. and Fthenakis, V. (2019) 'Active-salinity-control reverse osmosis desalination as a flexible load resource', *Desalination*, 468(114062), pp. 1–14. doi: 10.1016/j.desal.2019.07.002.

BBC News (2018) 'The 11 cities most likely to run out of drinking water - like Cape Town'. London, United Kingdom. Available at: https://www.bbc.com/news/world-42982959 (Accessed: 13 November 2019).

Bellini, E. (2019) 'Global cumulative PV capacity tops 480 GW, IRENA says'. Berlin, Germany: PV Magazine. Available at: https://www.pv-magazine.com/2019/04/02/global-cumulative-pv-capacity-tops-480-gw-irena-says/ (Accessed: 5 January 2020).

Bellini, E. (2020) 'The 900 MW fifth phase of 5 GW solar park moves forward in Dubai'. Berlin, Germany. Available at: https://www.pv-magazine.com/2020/04/30/fifth-900-mw-phase-of-5-gw-solar-park-moves-forward-in-dubai/ (Accessed: 18 September 2020).

Ben-Gal, A., Yermiyahu, U. and Cohen, S. (2009) 'Fertilization and Blending Alternatives for Irrigation with Desalinated Water', *Journal of Environmental Quality*, 38(2), pp. 529–536. doi: 10.2134/jeq2008.0199.

BloombergNEF (2019) 'Battery Pack Prices Fall As Market Ramps Up With Market Average At $156/kWh In 2019'. NewYork, USA. Available at:

https://about.bnef.com/blog/battery-pack-prices-fall-as-market-ramps-up-with-market-average-at-156-kwh-in-2019/ (Accessed: 5 January 2020).

Bogdanov, D., Farfan, J., Sadovskaia, K., Aghahosseini, A., Child, M., Gulagi, A., Oyewo, A. S., de Souza Noel Simas Barbosa, L. and Breyer, C. (2019) 'Radical transformation pathway towards sustainable electricity via evolutionary steps', *Nature Communications*, 10(1), pp. 1–16. doi: 10.1038/s41467-019-08855-1.

Boretti, A. and Rosa, L. (2019) 'Reassessing the projections of the World Water Development Report', *npj Clean Water*, 2(1). doi: 10.1038/s41545-019-0039-9.

Breyer, C., Afanasyeva, S., Brakemeier, D., Engelhard, M., Giuliano, S., Puppe, M., Schenk, H., Hirsch, T. and Moser, M. (2017) 'Assessment of mid-term growth assumptions and learning rates for comparative studies of CSP and hybrid PV-battery power plants', in *AIP Conference Proceedings*, p. 110006. doi: 10.1063/1.4984535.

Breyer, C., Bogdanov, D., Gulagi, A., Aghahosseini, A., Barbosa, L. S. N. S., Koskinen, O., Barasa, M., Caldera, U., Afanasyeva, S., Child, M., Farfan, J. and Vainikka, P. (2017) 'On the role of solar photovoltaics in global energy transition scenarios', *Progress in Photovoltaics: Research and Applications*, 25(8), pp. 727–745. doi: 10.1002/pip.2885.

Breyer, C., Fasihi, M., Bajamundi, C. and Creutzig, F. (2019) 'Direct Air Capture of CO2: A Key Technology for Ambitious Climate Change Mitigation', *Joule*, pp. 2053–2057. doi: 10.1016/j.joule.2019.08.010.

Burek, P., Satoh, Y., Fischer, G., Kahil, T., Jimenez, L. N., Scherzer, A., Tramberend, S., Wada, Y., Eisner, S., Flörke, M., Hanasaki, N., Magnusziewski, P., Cosgrove, W. and Wiberg, D. (2016) *Final Report Water Futures and Solution Fast Track Initiative*. Vienna, Austria.

Burn, S., Hoang, M., Zarzo, D., Olewniak, F., Campos, E., Bolto, B. and Barron, O. (2015) 'Desalination techniques - A review of the opportunities for desalination in agriculture', *Desalination*, 364, pp. 2–16. doi: 10.1016/j.desal.2015.01.041.

Caldera, U., Bogdanov, D. and Breyer, C. (2016) 'Local cost of seawater RO desalination based on solar PV and wind energy: A global estimate', *Desalination*, 385. doi: 10.1016/j.desal.2016.02.004.

Caldera, U. and Breyer, C. (2017) 'Learning Curve for Seawater Reverse Osmosis Desalination Plants: Capital Cost Trend of the Past, Present, and Future', *Water Resources Research*, 53(12), pp. 10523–10538. doi: 10.1002/2017WR021402.

Circle of Blue (2019) *Experts Name the Top 19 Solutions to the Global Freshwater Crisis*. Michigan, USA.

City Lab (2019) 'Looking Back on Cape Town's Drought and "Day Zero"'. Available at:

https://www.citylab.com/environment/2019/04/cape-town-water-conservation-south-africa-drought/587011/ (Accessed: 13 November 2019).

Coady, D., Parry, I., Le, N.-P. and Shang, B. (2019) *Global Fossil Fuel Subsidies Remain Large: An Update Based on Country-Level Estimates*, *IMF Working Papers*. doi: 10.5089/9781484393178.001.

Cornejo, P. K., Santana, M. V. E., Hokanson, D. R., Mihelcic, J. R. and Zhang, Q. (2014) 'Carbon footprint of water reuse and desalination: A review of greenhouse gas emissions and estimation tools', *Journal of Water Reuse and Desalination*, 4(4), pp. 238–252. doi: 10.2166/wrd.2014.058.

Davies, P. A., Yuan, Q. and De Richter, R. (2018) 'Desalination as a negative emissions technology', *Environmental Science: Water Research and Technology*, 4(6), pp. 839–850. doi: 10.1039/c7ew00502d.

Demirbas, A., Hashem, A. A. and Bakhsh, A. A. (2017) 'The cost analysis of electric power generation in Saudi Arabia', *Energy Sources, Part B: Economics, Planning, and Policy*, 12(6), pp. 591–596. doi: 10.1080/15567249.2016.1248874.

Döll, P., Hoffmann-Dobrev, H., Portmann, F. T., Siebert, S., Eicker, A., Rodell, M., Strassberg, G. and Scanlon, B. R. (2012) 'Impact of water withdrawals from groundwater and surface water on continental water storage variations', *Journal of Geodynamics*, 59–60, pp. 143–156. doi: 10.1016/j.jog.2011.05.001.

Drioli, E., Ali, A., Macedonio, F. and Quist-Jensen, C. (2015) 'Minerals , Energy and Water from the Sea : A New Strategy for Zero Liquid Discharge in Desalination', *JSM Environmental Science & Ecology*, 3, pp. 1018–1022.

Elimelech, M. and Phillip, W. A. (2011) 'The future of seawater desalination: Energy, technology, and the environment', *Science*, 333(6043), pp. 712–717. doi: 10.1126/science.1200488.

FAO - Food and Agricultural Organisation of the United Nations (no date) 'Water charging in irrigated agriculture'. Rome, Italy. Available at: http://www.fao.org/3/y5690e/y5690e0b.htm (Accessed: 8 January 2020).

FAO - Food and Agricutural Organisation of the United Nations (2010) *Disambiguation of water statistics*. Rome, Italy. Available at: http://www.fao.org/3/a-bc816e.pdf (Accessed: 12 November 2019).

FAO - Food and Agricutural Organisation of the United Nations (2016) 'AQUASTAT - FAO's Information System on Water and Agriculture'. Rome, Itatly. Available at: http://www.fao.org/nr/water/aquastat/didyouknow/index2.stm (Accessed: 12 November 2019).

FAO - Food and Agricutural Organisation of the United Nations (no date) ‘Concepts And Definitions’. Rome, Italy. Available at: http://www.fao.org/3/y4473e/y4473e06.htm (Accessed: 13 November 2019).

Fasihi, M., Efimova, O. and Breyer, C. (2019) ‘Techno-economic assessment of CO 2 direct air capture plants’, *Journal of Cleaner Production*, 224, pp. 957–980. doi: 10.1016/j.jclepro.2019.03.086.

Financial Tribune (2018) ‘Desalination Plant Starts Operation in Iran’s Bandar Abbas’. Tehran, Iran. Available at: https://financialtribune.com/articles/energy/95532/desalination-plant-starts-operation-in-irans-bandar-abbas (Accessed: 7 January 2020).

Foltz, R. C. (2002) ‘Iran’s water crisis: Cultural, political, and ethical dimensions’, *Journal of Agricultural and Environmental Ethics*, 15(4), pp. 357–380. doi: 10.1023/A:1021268621490.

Fthenakis, V., Atia, A. A., Morin, O., Bkayrat, R. and Sinha, P. (2016) ‘New prospects for PV powered water desalination plants: Case studies in Saudi Arabia’, *Progress in Photovoltaics: Research and Applications*, 24(4), pp. 543–550. doi: 10.1002/pip.2572.

Fulya, V. (2011) *MENA Regional Water Outlook: Part II Desalination Using Renewable Energy*, *Fichtner*. Stuttgart, Germany. doi: 6543P07/FICHT-7109954-v2.

Gao, L., Yoshikawa, S., Iseri, Y., Fujimori, S. and Kanae, S. (2017) ‘An economic assessment of the global potential for seawater desalination to 2050’, *Water (Switzerland)*, 9(10). doi: 10.3390/w9100763.

Gassert, F., Landis, R. M., Luck, M., Reig, P. and Shiao, T. (2013) *Aqueduct global maps 2.0*. Washington D.C, USA. Available at: http://pdf.wri.org/aqueduct_metadata_global.pdf%5Cnhttp://www.thecityfix.comwww.thecityfix.com/sites/default/files/resources/aqueduct_metadata_global.pdf.

Ghaffour, N., Missimer, T. M. and Amy, G. L. (2013) ‘Technical review and evaluation of the economics of water desalination: Current and future challenges for better water supply sustainability’, *Desalination*, 309(2013), pp. 197–207. doi: 10.1016/j.desal.2012.10.015.

Gleeson, T., Wada, Y., Bierkens, M. F. P. and Van Beek, L. P. H. (2012) ‘Water balance of global aquifers revealed by groundwater footprint’, *Nature*, 488(7410), pp. 197–200. doi: 10.1038/nature11295.

Global Clean Water Desalination Alliance (2015) *H2O minus CO2. Concept Paper*. Abu Dhabi, UAE. Available at: http://www.diplomatie.gouv.fr/fr/IMG/pdf/global_water_desalination_alliance_1dec2015_cle8d61cb.pdf.

de Graaf, I. E. M., van Beek, L. P. H., Wada, Y. and Bierkens, M. F. P. (2014) 'Dynamic attribution of global water demand to surface water and groundwater resources: Effects of abstractions and return flows on river discharges', *Advances in Water Resources*, 64, pp. 21–33. doi: 10.1016/j.advwatres.2013.12.002.

de Graaf, I. E. M., Gleeson, T., (Rens) van Beek, L. P. H., Sutanudjaja, E. H. and Bierkens, M. F. P. (2019) 'Environmental flow limits to global groundwater pumping', *Nature*. Springer Science and Business Media LLC, 574(7776), pp. 90–94. doi: 10.1038/s41586-019-1594-4.

Guardian (2016) 'A grand but faulty vision for Iran's water problems'. London, United Kingdom. Available at: https://www.theguardian.com/world/2016/may/09/iran-desalination-water (Accessed: 7 January 2020).

Gulf News (2017) 'Solar energy to power Dubai desalination plants'. Dubai, UAE. Available at: https://gulfnews.com/uae/government/solar-energy-to-power-dubai-desalination-plants-1.1978217 (Accessed: 6 January 2020).

GWI - Global Water Intelligence (2016a) 'Country Profile - Saudi Arabia'. Oxford, United Kingdom. Available at: https://www.desaldata.com/countries/31 (Accessed: 7 January 2020).

GWI - Global Water Intelligence (2016b) 'DesalData: Iran Country Profile'. Oxford, United Kingdom. Available at: www.desaldata.com/countries/67 (Accessed: 7 January 2020).

Haegel, N. M., Atwater, H., Barnes, T., Breyer, C., Burrell, A., Chiang, Y.-M., De Wolf, S., Dimmler, B., Feldman, D., Glunz, S., Goldschmidt, J. C., Hochschild, D., Inzunza, R., Kaizuka, I., Kroposki, B., *et al.* (2019) 'Terawatt-scale photovoltaics: Transform global energy', *Science*, 364(6443), pp. 836–838. doi: 10.1126/science.aaw1845.

Hanasaki, N., Fujimori, S., Yamamoto, T., Yoshikawa, S., Masaki, Y., Hijioka, Y., Kainuma, M., Kanamori, Y., Masui, T., Takahashi, K. and Kanae, S. (2013) 'A global water scarcity assessment under Shared Socio-economic Pathways - Part 1: Water use', *Hydrology and Earth System Sciences*, 17(7), pp. 2375–2391. doi: 10.5194/hess-17-2375-2013.

Hansen, K., Breyer, C. and Lund, H. (2019) 'Status and perspectives on 100% renewable energy systems', *Energy*, 175, pp. 471–480. doi: 10.1016/j.energy.2019.03.092.

Heihsel, M., Ali, S. M. H., Kirchherr, J. and Lenzen, M. (2019) 'Renewable-powered desalination as an optimisation pathway for renewable energy systems: The case of Australia's Murray-Darling Basin', *Environmental Research Letters*, 14(124054).

Heinrich Böll Stiftung and Small Media (2016) *Paradise Lost? Developing solutions to Irans environmental crisis*. Berlin, Germany London, United Kingdom. doi:

10.1093/nq/s1-VI.152.293-d.

Herrera-León, S., Lucay, F. A., Cisternas, L. A. and Kraslawski, A. (2019) 'Applying a multi-objective optimization approach in designing water supply systems for mining industries. The case of Chile', *Journal of Cleaner Production*, 210, pp. 994–1004. doi: 10.1016/j.jclepro.2018.11.081.

Hutchins, M. (2020) 'Egypt evaluating solar desalinators – pv magazine International'. Berlin, Germany. Available at: https://www.pv-magazine.com/2020/03/05/egypt-evaluating-solar-desalinators/ (Accessed: 6 March 2020).

Immerzeel, W. W., Lutz, A. F., Andrade, M., Bahl, A., Biemans, H., Bolch, T., Hyde, S., Brumby, S., Davies, B. J., Elmore, A. C., Emmer, A., Feng, M., Fernández, A., Haritashya, U., Kargel, J. S., *et al.* (2019) 'Importance and vulnerability of the world's water towers', *Nature*. doi: 10.1038/s41586-019-1822-y.

Intergovernmental Panel on Climate Change (2018) *An IPCC special report on the impacts of global warming of 1.5°C above pre-industrial levels and related global greenhouse gas emission pathways, in the context of strengthening the global response to the threat of climate change, sustainable development,*. Geneva, Switzerland. Available at: www.environmentalgraphiti.org.

International Technology Roadmap for Photovoltaic (2018) *Results 2017 including maturity report 2018*. Frankfurt am Main, Germany. Available at: http://www.ncbi.nlm.nih.gov/pubmed/14945410.

Jägermeyr, J., Gerten, D., Heinke, J., Schaphoff, S., Kummu, M. and Lucht, W. (2015) 'Water savings potentials of irrigation systems: Global simulation of processes and linkages', *Hydrology and Earth System Sciences*, 19(7), pp. 3073–3091. doi: 10.5194/hess-19-3073-2015.

Jansen, J. (2019) *Global battery storage pipeline reaches 15 GW*. Berlin: PV Magazine. Available at: https://www.pv-magazine.com/2019/03/04/global-battery-storage-pipeline-reaches-15-gw/ (Accessed: 5 January 2020).

Jia, X., Klemeš, J. J., Varbanov, P. S. and Alwi, S. R. W. (2019) 'Analyzing the energy consumption, GHG emission, and cost of seawater desalination in China', *Energies*, 12(3), pp. 1–16. doi: 10.3390/en12030463.

Jones, E., Qadir, M., van Vliet, M. T. H., Smakhtin, V. and Kang, S. mu (2019) 'The state of desalination and brine production: A global outlook', *Science of the Total Environment*, 657, pp. 1343–1356. doi: 10.1016/j.scitotenv.2018.12.076.

Joodaki, G., Wahr, J. and Swenson, S. (2014) 'Estimating the human contribution to groundwater depletion in the Middle East, from GRACE data, land surface models, and well observations', *Water Resources Research*, 50(3), pp. 2679–2692. doi:

10.1002/2013WR014633.

Junginger, M. and Louwen, A. (2020) *Technological learning in the transition to a low-carbon energy system conceptual issues, empirical findings, and use in energy modeling*. Massachusetts, USA: Academic Press.

Karbassi, A., Bidhendi, G. N., Pejman, A. and Bidhendi, M. E. (2010) 'Environmental impacts of desalination on the ecology of Lake Urmia', *Journal of Great Lakes Research*, 36(3), pp. 419–424. doi: 10.1016/j.jglr.2010.06.004.

Kersten, F., Görig, M. A., Breyer, C., Müller, J. W. and Wawer, P. (2015) 'PV-Learning Curves : Past and Future Drivers of Cost Reduction', in. Hamburg, Germany.

Kucera, J. (2014) *Desalination : Water from Water*. Edited by J. Kucera. Massachusetts, USA: Scrivener Publishing.

Kummu, M., Guillaume, J. H. A., De Moel, H., Eisner, S., Flörke, M., Porkka, M., Siebert, S., Veldkamp, T. I. E. and Ward, P. J. (2016) 'The world's road to water scarcity: Shortage and stress in the 20th century and pathways towards sustainability', *Scientific Reports*. Nature Publishing Group, 6(May), pp. 1–16. doi: 10.1038/srep38495.

Lamei, A., van der Zaag, P. and von Münch, E. (2008) 'Basic cost equations to estimate unit production costs for RO desalination and long-distance piping to supply water to tourism-dominated arid coastal regions of Egypt', *Desalination*, 225(1–3), pp. 1–12. doi: 10.1016/j.desal.2007.08.003.

Lashkaripour, G. R. and Zivdar, M. (2005) 'Desalination of brackish groundwater in Zahedan city in Iran', *Desalination*, 177(1–3), pp. 1–5. doi: 10.1016/j.desal.2004.12.002.

Liemberger, R. and Wyatt, A. (2019) 'Quantifying the global non-revenue water problem', *Water Science and Technology: Water Supply*, 19(3), pp. 831–837. doi: 10.2166/ws.2018.129.

Lohrmann, A., Farfan, J., Caldera, U., Lohrmann, C. and Breyer, C. (2019) 'Global scenarios for significant water use reduction in thermal power plants based on cooling water demand estimation using satellite imagery', *Nature Energy*, 4(12), pp. 1040–1048. doi: 10.1038/s41560-019-0501-4.

Loutatidou, S., Chalermthai, B., Marpu, P. R. and Arafat, H. A. (2014) 'Capital cost estimation of RO plants: GCC countries versus southern Europe', *Desalination*, 347(August), pp. 103–111. doi: 10.1016/j.desal.2014.05.033.

Luck, M., Landis, M. and Gassert, F. (2015) *Aqueduct Water Stress Projections: Decadal projections of water supply and demand using CMIP5 GCMs.* Washington D.C, USA. Available at: wri.org/publication/aqueduct-water-stress-projections.

Luo, X., Wang, J., Dooner, M. and Clarke, J. (2015) 'Overview of current development in electrical energy storage technologies and the application potential in power system operation', *Applied Energy*, 137, pp. 511–536. doi: 10.1016/j.apenergy.2014.09.081.

Madani, K. (2014) 'Water management in Iran: what is causing the looming crisis?', *Journal of Environmental Studies and Sciences*, 4(4), pp. 315–328. doi: 10.1007/s13412-014-0182-z.

Mayor, B. (2019) 'Growth patterns in mature desalination technologies and analogies with the energy field', *Desalination*, 457(May 2018), pp. 75–84. doi: 10.1016/j.desal.2019.01.029.

Mekonnen, M. M. and Hoekstra, A. Y. (2016) 'Sustainability: Four billion people facing severe water scarcity', *Science Advances*, 2(2), pp. 1–7. doi: 10.1126/sciadv.1500323.

Middle East Business Intelligence (2015) 'Tehran's dwindling water supplies'. Dubai, UAE. Available at: https://www.meed.com/tehrans-dwindling-water-supplies/ (Accessed: 9 January 2020).

Missimer, T. M., Maliva, R. G., Ghaffour, N., Leiknes, T. O. and Amy, G. L. (2014) 'Managed aquifer recharge (MAR) economics for wastewater reuse in low population wadi communities, Kingdom of Saudi Arabia', *Water (Switzerland)*, 6(8), pp. 2322–2338. doi: 10.3390/w6082322.

Mito, M. T., Ma, X., Albuflasa, H. and Davies, P. A. (2019) 'Reverse osmosis (RO) membrane desalination driven by wind and solar photovoltaic (PV) energy: State of the art and challenges for large-scale implementation', *Renewable and Sustainable Energy Reviews*, 112, pp. 669–685. doi: 10.1016/j.rser.2019.06.008.

Nemet, G. F. (2006) 'Beyond the learning curve: factors influencing cost reductions in photovoltaics', *Energy Policy*, 34(17), pp. 3218–3232. doi: 10.1016/j.enpol.2005.06.020.

Netafim (2018) 'Increase Rice Yield Using Drip Irrigation'. Hatzerim, Israel. Available at: https://www.netafim.com/en/crop-knowledge/rice/ (Accessed: 8 January 2020).

Papapetrou, M., Cipollina, A., La Commare, U., Micale, G., Zaragoza, G. and Kosmadakis, G. (2017) 'Assessment of methodologies and data used to calculate desalination costs', *Desalination*. Elsevier, 419(June), pp. 8–19. doi: 10.1016/j.desal.2017.05.038.

Parry, J., Osman, H., Terton, A., Asad, S. and Ahmed, T. (2016) *The Vulnerability of Pakistan's Water Sector To the Impact of Climate Change : Identification of Gaps and Recommendations for Action*. Islamabad, Pakistan. Available at: https://www.undp.org/content/dam/pakistan/docs/Environment & Climate Change/Report.pdf.

Pearce, F. (2018) *When the Rivers Run Dry, Fully Revised and Updated Edition: Water - The Defining Crisis of the Twenty-First Centur*. Boston, Massachusetts: Beacon Press.

Quist-Jensen, C. A., Macedonio, F. and Drioli, E. (2015) 'Membrane technology for water production in agriculture: Desalination and wastewater reuse', *Desalination*. Elsevier B.V., 364, pp. 17–32. doi: 10.1016/j.desal.2015.03.001.

Semiat, R. (2008) 'Energy issues in desalination processes', *Environmental Science and Technology*, 42(22), pp. 8193–8201. doi: 10.1021/es801330u.

Shaffer, D. L., Yip, N. Y., Gilron, J. and Elimelech, M. (2012) 'Seawater desalination for agriculture by integrated forward and reverse osmosis: Improved product water quality for potentially less energy', *Journal of Membrane Science*. Elsevier, 415–416, pp. 1–8. doi: 10.1016/j.memsci.2012.05.016.

Shrestha, E., Ahmad, S., Johnson, W., Shrestha, P. and Batista, J. R. (2011) 'Carbon footprint of water conveyance versus desalination as alternatives to expand water supply', *Desalination*, 280, pp. 33–43. doi: 10.1016/j.desal.2011.06.062.

Smart Water Magazine (2019a) 'The evolution of rates in desalination (Part I)'. Available at: https://smartwatermagazine.com/blogs/carlos-cosin/evolution-rates-desalination-part-i (Accessed: 6 January 2020).

Smart Water Magazine (2019b) 'Toray to supply SWRO membranes to Shoaibah 4 and Shoaibah 3 expansion projects'. Available at: https://smartwatermagazine.com/news/toray/toray-supply-swro-membranes-shoaibah-4-and-shoaibah-3-expansion-projects (Accessed: 10 January 2020).

Sood, A. and Smakhtin, V. (2014) 'Can desalination and clean energy combined help to alleviate global water scarcity?', *Journal of the American Water Resources Association*, 50(5), pp. 1111–1123. doi: 10.1111/jawr.12174.

Spang, E. S., Moomaw, W. R., Gallagher, K. S., Kirshen, P. H. and Marks, D. H. (2014) 'The water consumption of energy production: An international comparison', *Environmental Research Letters*, 9(10). doi: 10.1088/1748-9326/9/10/105002.

Steduto, P., Schultz, B., Unver, O., Ota, S., Vallee, D., Kulkarni, S. and Dagnino-Johns Garcia, M. (2018) 'Food Security by Optimal Use of Water: Synthesis of the 6th and 7th World Water Forums and Developments since Then', *Irrigation and Drainage*, 67(3), pp. 327–344. doi: 10.1002/ird.2215.

The Guardian (2020) '"The salt they pump back in kills everything": is the cost of Chile's fresh water too high?' London, United Kingdom. Available at: https://www.theguardian.com/cities/2020/jan/02/the-salt-they-pump-back-in-kills-everything-is-the-cost-of-chiles-fresh-water-too-high?CMP=twt_a-environment_b-gdneco&fbclid=IwAR1BtGENa_v075TVvzTgYtdp72OgmSqMz90qyYBSxV46nI_Ul

YpY8lPtjhI (Accessed: 10 January 2020).

UNEP - United Nations Environment Programme (2002) *Vital Water Graphics. An Overview of the State of the World's Fresh and Marine Waters*. Nairobi, Kenya. Available at: www.unep.org/vitalwater. (Accessed: 13 November 2019).

UNEP - United Nations Environment Programme (2014) *Sand, rarer than one thinks*. Paris. Available at: https://wedocs.unep.org/bitstream/handle/20.500.11822/8665/GEAS_Mar2014_Sand_Mining.pdf?sequence=3&isAllowed=y.

United Nations. Economic and Social Commission for Western Asia. (2009) 'Role of desalination in addressing water scarcity'. New York, USA, p. 46.

United Nations (no date) *Sustainable Development Goals Knowledge Platform*. Available at: https://sustainabledevelopment.un.org/sdg6 (Accessed: 3 January 2020).

UNWWAP - United Nations World Water Assessment Porgramme (2019) *The United Nations World Water Development Report 2019: Leavning No One Behind*. Paris, France.

UNWWAP - United Nations World Water Assessment Programme (2014) *The United Nations World Water Development Report 2014: Water and Energy*. Paris, France. Available at: http://www.unwater.org/publications (Accessed: 13 November 2019).

UNWWAP - United Nations World Water Assessment Programme (2015) *The United Nations World Water Development Report 2015: Water for a Sustainable World. Paris, UNESCO.* Paris, France: UNESCO. Available at: http://unesdoc.unesco.org/images/0023/002318/231823E.pdf.

UNWWAP - United Nations World Water Assessment Programme (2018) *The United Nations World Water Development Report 2018: Nature-based solutions for water: Development Report*. Paris, France.

Vartiainen, E., Masson, G. and Breyer, C. (2017) 'The True competitiveness of Solar PV - A European case study', p. 27.

Vartiainen, E., Masson, G., Breyer, C., Moser, D. and Román Medina, E. (2020) 'Impact of weighted average cost of capital, capital expenditure, and other parameters on future utility-scale PV levelised cost of electricity', *Progress in Photovoltaics: Research and Applications*, (July), pp. 1–15. doi: 10.1002/pip.3189.

Virgili, F. (2017) 'Q2 2017 Market Update'. Oxford, United Kingdom: Global Water Intelligence. Available at: https://www.desaldata.com/customers/sign_in (Accessed: 4 January 2020).

Voutchkov, N. (2013) *Desalination Engineering: Planning and Design*. New York, USA:

McGraw Hill Education. Available at: https://www.amazon.com/Desalination-Engineering-Planning-Nikolay-Voutchkov/dp/0071777156.

Wada, Y., Van Beek, L. P. H. and Bierkens, M. F. P. (2012) 'Nonsustainable groundwater sustaining irrigation: A global assessment', *Water Resources Research*, 48(1). doi: 10.1029/2011WR010562.

Wada, Y., Gleeson, T. and Esnault, L. (2014) 'Wedge approach to water stress', *Nature Geoscience*, 7(9), pp. 615–617. doi: 10.1038/ngeo2241.

Water Technology (2019) 'Growth expected for global water desalination market from 2018 to 2025'. Wisconsin, USA. Available at: https://www.watertechonline.com/water-reuse/article/15550726/growth-expected-for-global-water-desalination-market-from-2018-to-2025 (Accessed: 4 January 2020).

Water Technology (no date) 'Al Khafji Solar Saline Water Reverse Osmosis (Solar SWRO) Desalination Plant'. Wisconsin, USA. Available at: https://www.water-technology.net/projects/al-khafji-solar-saline-water-reverse-osmosis-solar-swro-desalination-plant/ (Accessed: 6 January 2020).

Water World (2019a) 'Desalination + Renewables: A long engagement without the wedding?' Available at: https://www.waterworld.com/international/desalination/article/16201273/desalination-renewables-a-long-engagement-without-the-wedding (Accessed: 6 January 2020).

Water World (2019b) 'Emirates Water Electricity Company, ACWA Power finalize deal for world's largest RO desal project'. Available at: https://www.waterworld.com/international/desalination/article/14039734/emirates-water-electricity-company-acwa-power-finalize-deal-for-worlds-largest-ro-desal-project (Accessed: 6 January 2020).

Weaver, R. and Birch, H. (2020) 'GWI DesalData Market Assessment Webinar: Desalination Market Update'. Oxo.

Welch, C. (2018) *Why Cape Town Is Running Out of Water, and the Cities That Are Next*. Available at: https://www.nationalgeographic.com/news/2018/02/cape-town-running-out-of-water-drought-taps-shutoff-other-cities/ (Accessed: 13 November 2019).

World Bank (2018) *Securing Water for Development in West Bank and Gaza*, *Securing Water for Development in West Bank and Gaza*. Washington D.C, USA. doi: 10.1596/30252.

World Bank (2019) *The Role of Desalination in an Increasingly Water-Scarce World*. Washington, D.C, USA. doi: 10.1596/31416.

World Economic Forum (no date) *We're helping to close the gap between global water*

demand and supply. Available at: https://www.weforum.org/our-impact/closing-the-water-gap (Accessed: 13 November 2019).

World Energy Council (2019) *Energy Storage Monitor. Latest Trends In Energy Storage*. London, United Kingdom.

WRI - World Resources Institute (2018) '3 Things Cities Can Learn from Cape Town's Impending "Day Zero" Water Shut-Off'. Washington D.C, USA. Available at: https://www.wri.org/blog/2018/02/3-things-cities-can-learn-cape-towns-impending-day-zero-water-shut (Accessed: 13 November 2019).

WRI - World Resources Institute (2019a) '17 Countries, Home to One-Quarter of the World's Population, Face Extremely High Water Stress'. Washington D.C, USA. Available at: https://www.wri.org/blog/2019/08/17-countries-home-one-quarter-world-population-face-extremely-high-water-stress (Accessed: 13 November 2019).

WRI - World Resources Institute (2019b) 'How Does a Flood-prone City Run Out of Water? Inside Chennai's "Day Zero" Crisis'. Washington D.C, USA. Available at: https://www.wri.org/blog/2019/06/how-does-flood-prone-city-run-out-water-inside-chennai-day-zero-crisis (Accessed: 13 November 2019).

WWF - World Wildlife Fund Germany (2019) *DROUGHT RISK The Global Thirst for Water in the Era of Climate Crisis*. Berlin, Germany. Available at: www.studioazola.com.

Zarzo, D., Campos, E. and Terrero, P. (2013) 'Spanish experience in desalination for agriculture', *Desalination and Water Treatment*, 51(1–3), pp. 53–66. doi: 10.1080/19443994.2012.708155.

Publication I

Caldera, U., Bogdanov, D., and Breyer, C.
Local cost of SWRO desalination based on solar PV and wind energy: A global estimate

Reprinted with permission from
Desalination
Vol. 385, pp. 207-216, 2016

Desalination 385 (2016) 207–216

Contents lists available at ScienceDirect

Desalination

journal homepage: www.elsevier.com/locate/desal

Local cost of seawater RO desalination based on solar PV and wind energy: A global estimate

Upeksha Caldera [a,*], Dmitrii Bogdanov [b], Christian Breyer [b]

[a] Technische Universität Berlin, 10623 Berlin, Germany
[b] Lappeenranta University of Technology, Skinnarilankatu 34, 53850 Lappeenranta, Finland

HIGHLIGHTS

- Seawater reverse osmosis (SWRO) plants can be powered solely with renewable energy.
- Single-axis, fixed-tilted PV and wind energy offer optimal renewable energy systems globally.
- Batteries and power-to-gas provide the optimal energy storage solution.
- 2030 global water costs for the proposed system lie between 0.59 €/m^3–2.81 €/m^3.
- Costs include water production, transportation to water demand site and storage.

ARTICLE INFO

Article history:
Received 5 October 2015
Received in revised form 9 January 2016
Accepted 4 February 2016
Available online 10 March 2016

Keywords:
Seawater reverse osmosis desalination
Economics
Hybrid PV–wind power plants
Power-to-gas
Levelised cost of water

ABSTRACT

This study demonstrates how seawater reverse osmosis (SWRO) plants, necessary to meet increasing future global water demand, can be powered solely through renewable energy. Hybrid PV–wind–battery and power-to-gas (PtG) power plants allow for optimal utilisation of the installed desalination capacity, resulting in water production costs competitive with that of existing fossil fuel powered SWRO plants. In this paper, we provide a global estimate of the water production cost for the 2030 desalination demand with renewable electricity generation costs for 2030 for an optimised local system configuration based on an hourly temporal and 0.45° × 0.45° spatial resolution. The SWRO desalination capacity required to meet the 2030 global water demand is estimated to about 2374 million m^3/day. The levelised cost of water (LCOW), which includes water production, electricity, water transportation and water storage costs, for regions of desalination demand in 2030, is found to lie between 0.59 €/m^3–2.81 €/m^3, depending on renewable resource availability and cost of water transport to demand sites. The global system required to meet the 2030 global water demand is estimated to cost 9790 billion € of initial investments. It is possible to overcome the water supply limitations in a sustainable and financially competitive way.

1. Introduction

It is estimated that there are 200,000 km^3 of renewable fresh water resources for all life on Earth (UNEP) [1]. The demand for this finite renewable resource is projected to increase due to the needs of the agricultural, industrial and municipal sectors. The United Nations World Water Assessment Programme (WWAP) estimates that by 2030, in a business as usual scenario, only 60% of the global water demand can be met [2]. The OECD expects that, in a business as usual scenario, by 2050, the global fresh water withdrawals will increase by 55%. Consequently, by the end of this period, 40% of the global population will be living in water-stressed regions. In particular, this will be evident in North and South Africa, and Central and South Asia [3].

In addition to the rapidly increasing water demand, climate change and water pollution will further limit the availability of fresh water. As water becomes a critical resource, there is a global drive to better manage and augment the existing fresh water supply [2].

Seawater desalination is growing as an alternative fresh water resource. The Global Water Intelligence (GWI) reports that in 2012, the installed global desalination capacity was increasing by 55% a year [4]. As of 2013, 150 countries have taken up desalination to augment the fresh water supply. This resulted in a global installed capacity of 80 million m^3 of fresh water a day [5].

Desalination has high specific energy consumption (SEC), compared to traditional water treatment methods. Grubert et al. [6] suggest that the typical energy usage for the treatment of surface fresh water is about 0.06 kWh/m^3. In contrast, the energy usage for seawater desalination is of the range 3.6–4.5 kWh/m^3. Ghaffour et al. [4] explain that, depending on the desalination technology, the total SEC can range between 0.5–16 kWh/m^3. Desalination technologies are broadly classified

* Corresponding author.
E-mail addresses: upeksha.caldera@gmail.com (U. Caldera), dmitrii.bogdanov@lut.fi (D. Bogdanov), christian.breyer@lut.fi (C. Breyer).

http://dx.doi.org/10.1016/j.desal.2016.02.004
0011-9164/

as thermal or membrane processes. Thermal processes utilise thermal energy and electrical energy. The thermal energy required is approximately of the range 4–12 kWh/m^3 and electrical energy of the range 1.5–4 kWh/m^3. Thus, the total energy required is of the range 9–16 kWh/m^3. Membrane processes utilise only electrical energy to produce the same amount of fresh water and is of the range 0.5–4 kWh/m^3. Membrane processes avoid the evaporation of the seawater leading to lower SEC than thermal processes.

Burn et al. [7] notes that by 2013, the membrane process reverse osmosis (RO) accounted for 65% of the total global installed desalination capacity. In addition, 59% of the installed global desalination capacity used seawater as the feed water type. Ghaffour et al. [4] explain that seawater RO (SWRO) will continue to remain the dominant desalination technology, owing to the lower costs, energy consumption and technological improvements.

Lienhard and Jameel [8] write that, as desalination becomes a staple water technology, there is ongoing concern about the energy consumption of the plants. This has driven research towards more energy efficient and cost-effective solutions. Reflecting similar concerns, Latorre et al. [9] explain that due to the unpredictable costs and availability of fossil fuels, there is increasing interest in the use of renewable energy to power desalination plants. This will make desalination accessible to regions with scant fossil fuel resources and high water scarcity.

Current concerns with the use of renewable energy systems plants are the intermittency and energy storage requirements. Mentis et al. [10] analysed the case for using completely renewable energy powered desalination units in the South Aegean Islands. Instead, it was decided to opt for PV–wind hybrid power plant and grid electricity to meet the energy demand of the desalination units. Novosel et al. [11] presented the case for using PV and wind energy for desalination in Jordan. Brine operated pump storage was used to allow for higher penetration of renewable energy. However, fossil fuel backup is necessary for optimal utilisation of the desalination plants.

The objective of our work was to determine if it is viable to meet the 2030 global water demand, with SWRO desalination powered solely with renewable energy. This was done by estimating the unit cost of water production (€/m^3) or the levelised cost of water (LCOW) for renewable energy powered SWRO plants in 2030 and comparing it with costs of existing fossil-powered SWRO desalination plants. Fig. 1 presents the SWRO desalination system envisaged in this work.

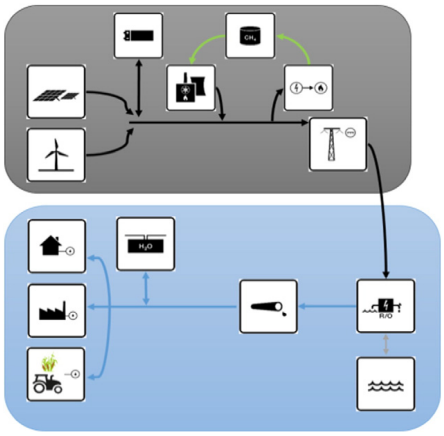

Fig. 1. The final desalination system. SWRO desalination plants are powered by hybrid renewable energy power plants being cost optimised by storage. High voltage DC cables transport power to the desalination plants on the coast. The water produced is transported to meet the demands of the municipal, industrial and agricultural sectors. Water storage at the site of demand ensures constant water supply.

2. Methodology

2.1. Overview

The key aim in this work is to determine the LCOW for the system presented in Fig. 1 for the regions of desalination demand in 2030. For our analysis, a 2030 future scenario without thermal power plants was assumed. More and more researchers take this shift to power seriously into account [12–17] and as a consequence the share of thermal power plants can be expected to decrease due to economic and environmental reasons. Therefore, the results of this work are for the 2030 optimistic scenario, discussed in the IPCC 5th assessment report [18, 19].

Breyer et al. [20], based on Sort et al. [21], describe the approach to calculate the levelised cost of electricity (LCOE) of PV plants and fossil fired power plants. This approach can be adapted to calculate the unit production cost of water at the site of the desalination plant and the water transportation to the region of desalination demand as shown in Eqs. (1a) to (1h).

$$LCOW_{desal} = \frac{(Capex_{desal} \times crf_{desal} + Capex_{water\ storage} \times crf_{water\ storage}) + opex_{fixed}}{Total\ water\ produced\ in\ a\ year} + Opex_{var\ desal} \times SEC \quad (1a)$$

$$Opex_{fixed} = Opex_{fixed\ desal} + Opex_{water\ storage} \quad (1b)$$

$$Opex_{var\ desal} = LCOE \quad (1c)$$

$$crf = \frac{WACC \times (1 + WACC)^N}{(1 + WACC)^N - 1} \quad (1d)$$

$$WACC = \frac{E}{E+D} \times k_E + \frac{D}{E+D} \times k_D \quad (1e)$$

$$LCOT_{desal} = \frac{(Capex_{hpumps} \times crf_{hpumps} + Capex_{vpumps} \times crf_{vpumps}) + Capex_{pipes} \times crf_{pipes}) + opex_{fixedt}}{Total\ water\ produced\ in\ a\ year} + Opex_{vart} \times SEC_t \quad (1f)$$

$$opex_{fixedt} = opex_{fixed\ pumps} + opex_{fixed\ pipes} \quad (1g)$$

$$opex_{vart} = LCOE \quad (1h)$$

$$LCOW = LCOW_{desal} + LCOT_{desal} \quad (1i)$$

Eqs. (1a) to (1h): Levelised cost of water (LCOW) for regions with desalination demand in 2030. Here, $capex_{desal}$ is the capex of the desalination plant in €/m^3, $capex_{water\ storage}$ is the capex of water storage tank at demand site in €/m^3, crf_{desal} is the annuity factor for desalination plant, and $crf_{water\ storage}$ is the annuity factor for water storage. *Total water produced in a year* is in m^3, $opex_{fixed\ desal}$ is the fixed opex of the desalination plant in €/m^3, $opex_{water\ storage}$ is the opex of the water storage tank in €/m^3, and $opex_{var\ desal}$ is the variable opex of the desalination plant. The variable opex is equal to the levelised cost of electricity (LCOE) of the plant and is in €/kWh. *SEC* is the specific energy consumption in kWh/m^3. The product of the *LCOE* and *SEC* is the energy cost of the desalination plant in €/m^3.

WACC is the weighted average cost of capital, *N* is the lifetime of the desalination plant or the water storage, *E* is the equity in €, *D* is the debt in €, k_E is return on equity, and k_D is the cost of debt.

$LCOT_{desal}$ is the levelised cost of power transmission for the electricity for desalination, $capex_{hpumps}$ is the capex of the horizontal pumps,

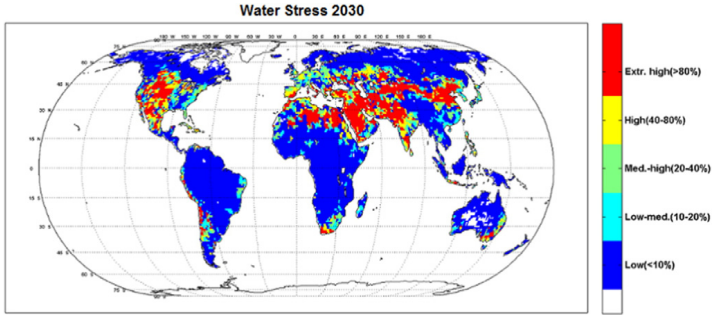

Fig. 2. Projected water stress for the 2030 optimistic scenario. The water stress is the ratio of the total water demand in the region to the annual renewable water resources available in that region [18].

crf_{hpumps} is the annuity factor for the horizontal pumps, $capex_{vpumps}$ is the capex of the vertical pumps, crf_{vpumps} is the annuity factor for the vertical pumps, $capex_{pipes}$ is the capex for the vertical and horizontal pipes, $opex_{fixedt}$ is the fixed operational expenditures of the pipes and pumps, $opex_{fixed\ pumps}$ is the fixed operational expenditures of the horizontal and vertical pumps, $opex_{fixed\ pipes}$ is the fixed operational expenditures of the horizontal and vertical pipes, $opex_{vart}$ is equal to the $LCOE$, SEC_t is the specific energy consumption of the pumps in kWh/m^3, and $LCOW$ is the resulting levelised cost of water in €/m^3.

Breyer et al. [15] describe the approach to calculate the LCOE for a region as summarised in Eq. (2).

$$LCOE_r = LCOE_{prim,r} + LCOC_r + LCOS_r + LCOT_r \quad (2)$$

Eq. (2): Levelised cost of electricity for a region. Here, $LCOE_{prim,r}$ is the levelised cost of electricity for primary a generation source, $LCOC_r$ is the levelised cost of curtailment, $LCOS_r$ is the levelised cost for energy storage in the region and $LCOT_r$ is the levelised cost of transmission of electricity in the region r.

2.2. Model and input data

The energy model, used and further developed at LUT (based on previous results at the Reiner Lemoine Institut), is used to determine the global LCOE and LCOW [14, 15]. The model allows for the design of different energy systems and can be modified to model local, national or global energy systems. The energy model is based on the linear optimisation method with interior point optimisation and designed in an hourly temporal and 0.45° × 0.45° spatial resolution.

To determine the LCOW based on (1a) to (1h), the following are the data parameters utilised by the model:

1. Regions with high or extremely high water stress in 2030. That is, regions where more than 40% of the renewable water resources are being withdrawn. Fig. 2 illustrates the regions in a global water stress map for the 2030 optimistic scenario. The water stress data for baseline and future scenarios are provided by the World Resources Institute (WRI) Water Atlas [18].
2. Total water demand in the regions with higher or extremely high water stress in 2030. The total water demand is the sum of the water withdrawals for agriculture, domestic use and industry. It is assumed that a future scenario does not include thermal power plants and therefore the water withdrawal of thermal power plants is excluded. This results in a reduction of the total global water demand [22]. The Water Atlas provides the water demand increase factors from the 2010 water demand for all future scenarios, including the 2030 optimistic scenario. The total water demand in 2010 was obtained from the FAO Aquastat database [23]. These data in conjunction with the water demand increase factor were used to calculate the total water demand for a region in 2030.
3. The desalination demand is calculated based on a logistic function of the total water demand and the water stress level. A logistic function allows to express the variation in increase in desalination demand

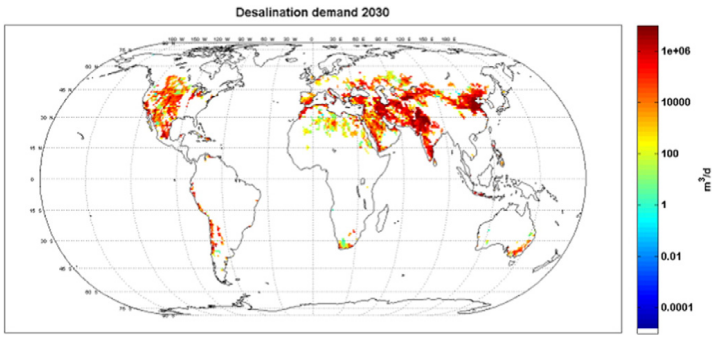

Fig. 3. Desalination demand for the optimistic scenario 2030. The desalination demand is calculated as per Eqs. (3a) to (3e), based on ref. [18, 19, 23] and projected on a mesh of 0.45° × 0.45° for further calculation.

Table 1
Key assumptions for the SWRO plant, water storage, and water transportation in the model for 2030 [28–33].

SWRO desalination system		
Capacity	m^3/a	Equal to desalination demand of region
Capex	€/(m^3·a)	2.23
Fixed Opex	€/(m^3·a)	4% of Capex
Full load hours	hrs	System optimum
Energy consumption	kWh/m^3	Calculated for desalination site. Approximate range is 2.80–3.30. See Fig. 4
Lifetime	yrs	30
Water storage		
Capex	€/m^3	65
Fixed Opex	€/(m^3)	2% of Capex
Lifetime	yrs	30
Horizontal pumping and piping		
Horizontal pipes Capex	€/(m^3·a·km)	0.053
Horizontal pipes Fixed Opex	€/(m^3·a·100 km)	0.023
Horizontal pump Capex	€/(m^3·h·km)	19.23
Horizontal pump Fixed Opex	€/(m^3·h·km)	2% of Capex
Energy consumption	kWh/(m^3·h·100 km)	0.04
Lifetime	yrs	30
Vertical pumping and piping		
Vertical pipes Capex	€/(m^3·a·km)	0.053
Vertical pipes Fixed Opex	€/(m^3·a·100 km)	0.023
Vertical pump Capex	€/(m^3·h·m)	15.40
Vertical pump Fixed Opex	€/(m^3·h·m)	2% of Capex
Energy consumption	kWh/(m^3·h·100 m)	0.36
Lifetime	yrs	30

with the increase in water stress. This is explained in Eqs. (3a) to (3e). The resulting global desalination demand is presented in Fig. 3. The desalination demand for a region is equal to the required installed SWRO capacity for the region.

4. Water transportation costs, for the horizontal and vertical distance, from the desalination plant to the demand site. These costs are comprised of the pumping and piping capex and opex costs.
5. Energy consumption of SWRO plants, based on location, and the energy costs for water transportation. This provides the energy required to meet the desalination demand in a region.
6. Solar irradiation and wind energy data for the year 2005 as a reference in hourly temporal and 0.45° × 0.45° spatial resolution as described in more detail in Breyer et al. [15].
7. Hybrid renewable power plant costs for 2030. These costs are comprised of single-axis tracking PV, fixed-tilted PV, wind, batteries and power-to-gas (PtG) power plant capex and opex costs. SWRO desalination plant capex and opex values for 2030, including water storage costs at the desalination site. More information on the PtG technology can be found in Sterner [24], Lehner [25] and Götz et al. [26].

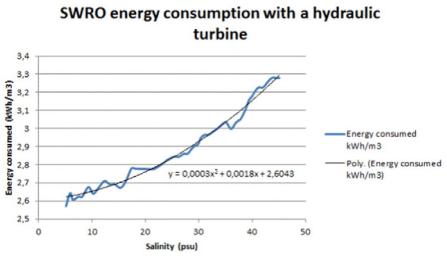

Fig. 4. SWRO energy consumption with a hydraulic turbine [33].

Table 2
Costs and technical assumptions for PV, wind, battery and PtG hybrid power plants in 2030 [15, 36, 37].

Fixed-tilted PV plant		
Capex	€/kW	550
Opex	€/(kW·a)	1.5% of Capex
Lifetime	yrs	35
Single-axis tracking PV plant		
Capex	€/kW	620
Opex	€/(kW·a)	1.5% of Capex
Lifetime`	yrs	35
Wind plant		
Capex	€/kW	1000
Opex	€/(kW·a)	2% of Capex
Lifetime	yrs	25
Batteries		
Capex	€/kWh	150
Fixed Opex	€/(kWh·a)	10
Lifetime	yrs	15
Efficiency	%	90
PtG		
Water electrolysis Capex	€/kW_{H2}	380
Water electrolysis Fixed Opex	€/(kW_{H2}·a)	13
Efficiency	%	84
Lifetime	yrs	30
CO_2 scrubbing Capex	€/kW_{SNG}	356
CO_2 scrubbing Opex	€/(kW_{SNG}·a)	14.24
Efficiency	%	78
Lifetime	yrs	30
Methanation Capex	€/kW_{SNG}	234
Methanation Opex	€/(kW_{SNG}·a)	5
Efficiency	%	77
Lifetime	yrs	30
Gas storage	€/kWh	0.05
Efficiency	%	100
Lifetime	yrs	50

Based on the above parameters, the model compares the use of different hybrid renewable energy power plant combinations. The least cost system that meets the 2030 desalination demand of regions with water scarcity is the optimal system.

$$\text{If } 40\% < WS < 50\% : \text{desalination demand} = (WS - 40\%) \times \frac{\text{Total water demand}}{WS} \times \text{logistic}(40\%) \quad (3a)$$

$$\text{If } 50\% < WS < 60\% : \text{desalination demand} = (WS - 50\%) \times \frac{\text{Total water demand}}{WS} \times \text{logistic}(50\%) \quad (3b)$$

$$\text{If } 60\% < WS < 70\% : \text{desalination demand} = (WS - 60\%) \times \frac{\text{Total water demand}}{WS} \times \text{logistic}(60\%) \quad (3c)$$

$$\text{If } 70\% < WS < 80\% : \text{desalination demand} = (WS - 70\%) \times \frac{\text{Total water demand}}{WS} \times \text{logistic}(70\%) \quad (3d)$$

$$\text{If } WS > 80\% : \text{desalination demand} = (WS - 80\%) \times \frac{\text{Total water demand}}{WS} \quad (3e)$$

Eqs. (3a) to (3e): Desalination demand for a region based on 2030 optimistic scenario [18, 19, 23]. Here, *WS* is the water stress for a region based on the 2030 optimistic scenario, *Total water demand* is the total water demand for the region based on 2030 optimistic scenario, excluding thermal power plants.

2.3. Technical and financial assumptions

Table 1 presents the key assumptions used for the model for the SWRO desalination plant, water storage at the desalination demand site and water transportation from the desalination site to the demand site. For the purpose of our work, SWRO plants with hydraulic turbine energy recovery devices (ERD) are considered [27]. Water storage of a minimum of 7 days at the desalination site is assumed. A weighted average cost of capital (WACC) of 7% is considered. Where specific data of the opex is not available, it is assumed to be 2% of the capex.

The SEC of SWRO desalination plants vary with the salinity, temperature of feedwater and the type of energy recovery device used [34]. The minimum SEC variation for SWRO plants with hydraulic turbine ERDs is represented in Fig. 4.

The second order polynomial $y = 0.0003x^2 + 0.0018x + 2.6049$, where x is the salinity in Practical Salinity Unit (PSU), represents the trend line. The salinity, x, of the feed water can be found for a specific region from the NCEI World Ocean Database [35]. Therefore, the minimum SEC for SWRO plants with hydraulic turbine ERDs, located in different regions, can be calculated.

Table 2 presents the cost and technical parameters for the renewable energy power plants used for the simulation. A WACC of 7% is considered. Where specific data of the opex is not available, it is assumed to be 2% of the capex. The high voltage direct current (HVDC) transmission grid is assumed to have a power loss of 1.6% per 1000 km as explained by Bogdanov and Breyer [36].

3. Results

The model's results show that the least cost system to meet the 2030 desalination demand is comprised of a combination of fixed-tilted PV, single-axis tracking PV, wind energy plants, batteries and PtG power plants. This energy system allows for a 10% reduction in the global average LCOW compared to the energy system without PtG power plants. The use of batteries and PtG enable higher full load hours of the renewable energy plant and therefore, better utilisation of the installed SWRO capacity. This results in lower LCOW.

The figures that follow present an overview of the energy system, desalination system and the resulting global LCOW.

Fig. 5 (top) presents the required installed capacities of hybrid PV–wind power plants to meet a region's 2030 global desalination demand. A region is defined as an area of 50 km × 50 km (exactly 0.45° × 0.45° in units of latitude and longitude). Fig. 5 (bottom) presents the contribution of PV to the PV–wind hybrid power plant energy generation.

PV power plants provide up to 82% of the total global energy demand with single-axis tracking accounting for 70% of this supplied energy. The higher contribution of PV power plants is attributed to the fact that there is higher desalination demand, and thus higher SWRO capacity, in regions where PV is more favourable than wind. Based on Fig. 5 (top) the global installed capacities of fixed-tilted PV, single-axis tracking PV, wind power plants required are approximately 1040 GW, 1960 GW and 550 GW, respectively.

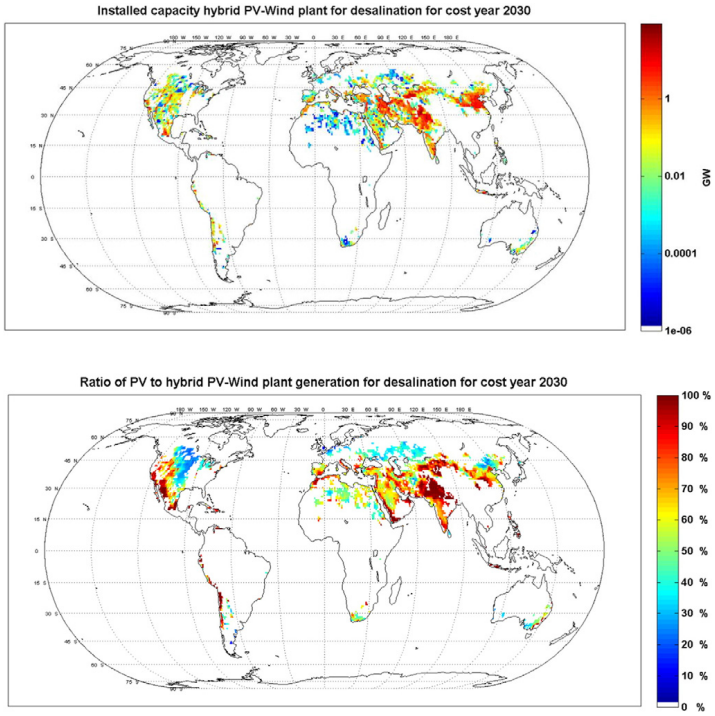

Fig. 5. Top: Installed hybrid PV–wind power plant capacity for the 2030 desalination demand. Bottom: Contribution of PV to the PV–wind generation for the 2030 desalination demand.

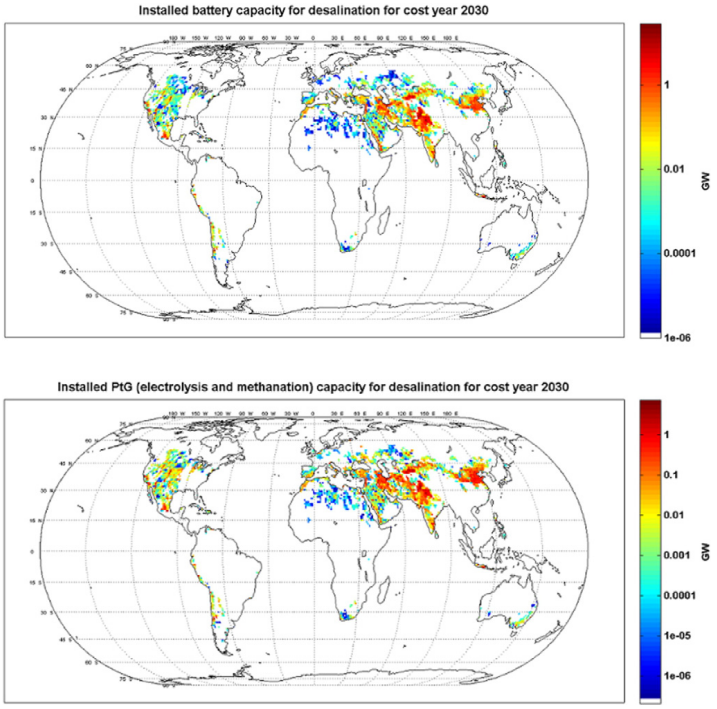

Fig. 6. Top: Installed battery capacity required for the 2030 desalination demand. Bottom: Installed PtG capacity required for the 2030 desalination demand.

Fig. 6 (top) and (bottom) shows the additional required capacities of batteries and PtG power plants. Batteries and PtG plants allow high full load hours (FLH) and therefore, better utilisation of the desalination capacity.

The required installed battery capacity is approximately 5480 GWh. These batteries are cycled almost every day reaching about 350 cycles per day and therefore providing up to 24% of the total global energy demand for the desalination demand. PtG contributes up to 15% of the total global energy demand with a required installed capacity of approximately 300GW. The results in Fig. 7 (top) show the optimal water storage required to obtain the lowest LCOW in all regions. The value ranges between 7–8 days. This can be explained through Fig. 7 (bottom). The figure illustrates the excess energy generated by the complete system. In the global average, the excess energy is about 6% of the total generated electricity.

The LCOE of the complete system to meet the 2030 desalination demand is presented in Fig. 8 (top). The LCOE of the system ranges from 0.06 €/kWh–0.13 €/kWh. The prevalent LCOE range is 0.09 €/kWh–0.12 €/kWh. Fig. 8 (center) presents the resulting global LCOW. The final LCOW range is between 0.59 €/m^3–2.81 €/m^3, mostly prevalent between 0.70 €/m^3–2.00 €/m^3.

Fig. 8 (bottom) explains the significance of the water transportation costs to the LCOW. The energy required for water pumping, and therefore the pumping electricity costs, are significant in regions where the demand site is distant from the desalination site. This includes both the vertical and horizontal distances. In regions like Central Asia, the LCOW can contribute up to 40% towards the LCOW. The corresponding LCOW in this region is approximately 3 €/m^3–4 €/m^3. Globally, the average pumping electricity cost contribution to the LCOW is about 17% and the total Opex contribution to the LCOW is approximately 39%.

To conclude, Fig. 9 illustrates the cost contribution to the final LCOW. Fig. 9 (top) highlights the contribution of the total system Capex to the LCOW for regions with desalination demand in 2030. The Capex contributes between 50–80% to the final LCOW. The average global Capex contribution to the LCOW is approximately 62%.

Fig. 9 (bottom) illustrates the contribution that PtG has to the reduction of the LCOW. The reduction in LCOW of about 10% in the global average is brought about by the PtG storage capacities. The required PV, wind and battery capacities are reduced by 24%, 14% and 33%, respectively.

4. Discussion

The global LCOW range when desalination plants, in 2030, are powered by hybrid PV, wind, battery and PtG plants is found to be

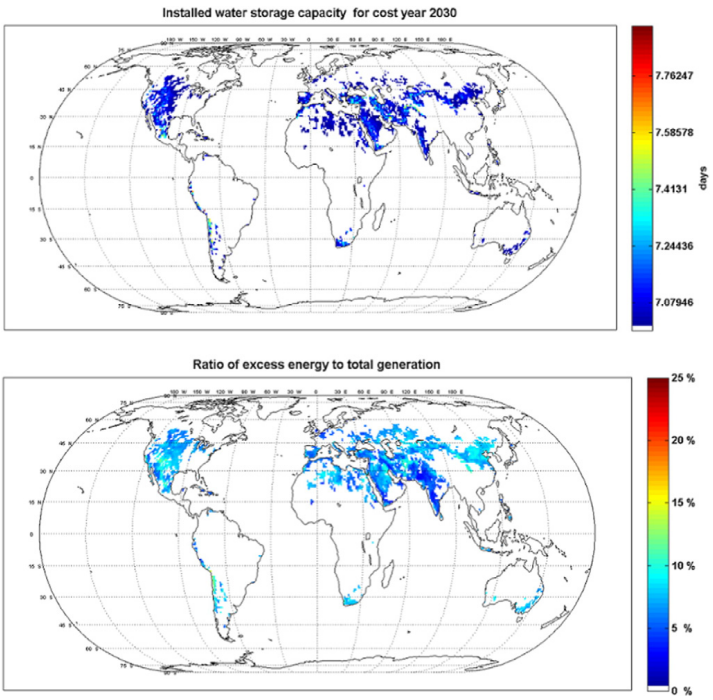

Fig. 7. Top: Optimal water storage capacity needed for the 2030 system. Bottom: Ratio of the excess energy to the total energy generated for the 2030 system.

between 0.59 €/m^3–2.81 €/m^3. The prevalent LCOW range is between 0.70 €/m^3–2.00 €/m^3.

Fichtner [38] presented water production costs for fossil powered SWRO desalination plants, located in different regions. The costs range approximately between 0.60 €/m^3–1.90 €/m^3. The higher LCOW range of the model can be attributed to the high water transportation costs, as shown in Fig. 8 (bottom). The costs presented by Fichtner do not include water transportation costs. The electricity costs for water pumping, in both horizontal and vertical distance, can make a substantial contribution to the final water production cost. On average, globally, electricity for pumping contributes up to 17% towards the final LCOW.

The results show that it is indeed possible to meet the increasing water global demand with SWRO desalination plants powered by hybrid renewable energy power plants. In the near future the production cost of water from the hybrid system will be competitive with the cost of fossil powered SWRO plants today. This will be driven by the increase in desalination demand and the decrease in PV and storage costs due to learning curve effects.

The energy model utilised optimises the cost of the system for the different components of the hybrid power plant and their relative configuration. The total Capex of the above system to meet the 2030 global desalination demand is estimated to be 9790 billion €, with annualised costs of 1230 billion €. This is for a WACC of 7%. The 2030 global desalination demand, for an optimistic scenario, is found to be about 2374 million m^3/day. The average global excess energy generated is minimised to 6% through the use of battery and PtG storage. Table 3 summarises key aspects of the necessary global system.

5. Conclusions

An energy model is used to estimate the viability of meeting the 2030 global water demand, based on the optimistic scenario, solely with SWRO plants powered by renewable energy. Hybrid renewable energy power plants are used as they offer higher full load hours and therefore allow for better utilisation of the desalination plant capacity. The 2030 costs for different renewable energy technologies are used.

The least cost system is found to be a combination of fixed-tilt PV, single-axis tracking PV, wind energy, batteries and PtG power plants. The LCOW range is predominantly between 0.70 €/m^3–2.00 €/m^3.The current LCOW range of fossil powered SWRO plants, excluding water transportation, is between 0.60 €/m^3–1.90 €/m^3. Therefore, in the near future, SWRO plants powered by renewable energy will produce water at similar prices to that of today's fossil plants. Furthermore, depending on the terrain, the water transportation costs can contribute significantly to the final LCOW.

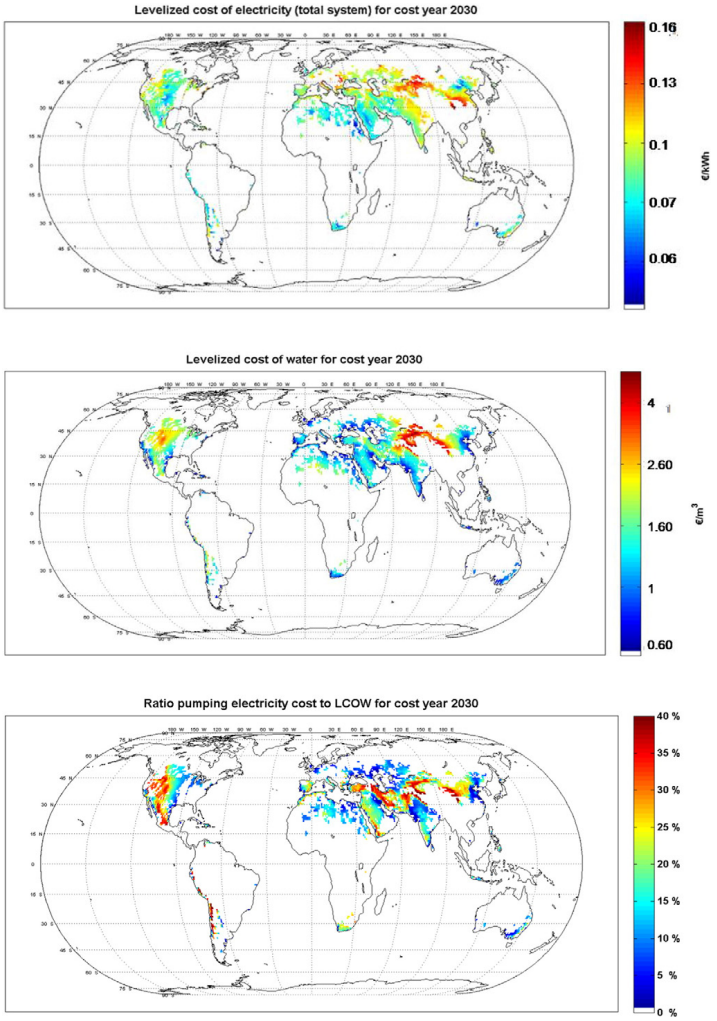

Fig. 8. Top: LCOE of the complete system for 2030 system. Center: LCOW of the complete system for 2030 system. Bottom: Pumping electricity cost contribution to the LCOW for the 2030 system.

It has to be noted that there are gaps in the data assumptions used for this research work. These gaps can be summarised as below:

1. No well-defined learning curve for SWRO desalination plants. This makes it difficult to project the future SWRO costs.
2. Lacking updated water transportation costs. Recent literature makes reference to 1993 water transportation costs.
3. Need of a more accurate model of the future water stress and demand. For instance, water stress should take into account the impact of climate change. Water demand should consider the complete removal of thermal power plants.

By filling in the data gaps, a more accurate model of the future global water scenario and water production costs can be built. This will enable us to better understand the potential role for SWRO desalination and renewable energy systems in meeting the water supply challenges of the decades to come.

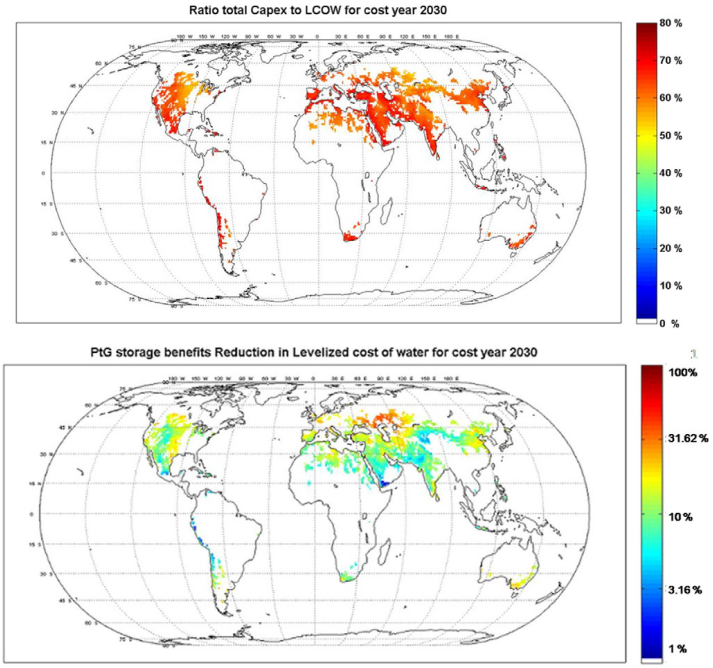

Fig. 9. Top: Total system Capex contribution to the final LCOW. Bottom: Contribution of PtG the reduction of the LCOW.

Nomenclature

a	annum
Capex	capital expenditures
crf	capital recovery factor
LCOE	levelised cost of electricity
LCOW	levelised cost of water
Opex	operating and maintenance expenditures
PtG	power-to-gas
PV	photovoltaic
SEC	specific energy consumption
SNG	synthetic natural gas
SWRO	seawater reverse osmosis
WACC	weighted average cost of capital
WS	water stress

Table 3
Summary of the key technical and cost data for the 2030 global system.

		2030 global system
SWRO total global desalination demand per day	m^3/day	2374 million
Installed PV capacity	GW	2996
Fixed-tilted PV	GW	1036
Single-axis tracking PV	GW	1960
Installed wind capacity	GW	550
Installed battery capacity	TWh	1930
Installed PtG capacity	GW	300
Average global excess energy generated	%	6
Total Capex	bn€	9790
Annualised costs	bn€	1230
LCOW range	€/m^3	0.60–2.80
Prevalent LCOW range	€/m^3	0.70–2.00

Acknowledgements

The LUT authors gratefully acknowledge the public financing of Tekes, the Finnish Funding Agency for Innovation, for the 'Neo-Carbon Energy' project under the number 40101/14. We also thank Thomas Dittrich for helping to initiate this research work and Michael Child for proofreading.

References

[1] United Nations Environment Programme, Vital Water Graphics — An Overview of the State of the World's Fresh and Marine Waters, second ed. UNEP, Nairobi, Kenya, 2008.
[2] United Nations World Water Assessment Programme, The United Nations World Water Development Report 2015: Water for a Sustainable World, WWAP, Paris, UNESCO, 2015.
[3] United Nations World Water Assessment Programme, The United Nations World Water Development Report 2014: Water and Energy, WWAP, Paris, UNESCO, 2014.
[4] N. Ghaffour, M.T. Missimer, L.G. Amy, Technical review and evaluation of the economics of water desalination: current and future challenges for better water supply sustainability, Desalination 309 (2013) 197–207.
[5] International Desalination Association, Desalination by the numbers, International Desalination Association, [accessed: May 1, 2015], http://idadesal.org/desalination-101/desalination-by-the-numbers/
[6] A.E. Grubert, A.S. Stillwell, M.E. Webber, Where does solar-aided seawater desalination make sense? A method for identifying suitable sites, Desalination 339 (2014) 10–17.
[7] S. Burn, M. Hoang, D. Zarzo, F. Olewniak, E. Campos, Desalination techniques — a review of the opportunities for desalination in agriculture, Desalination 364 (2015) 2–16.
[8] J.H.V. Lienhard, A.L. Jameel, Foreword for special issue: energy and desalination, Desalination 366 (2015) 1.
[9] F.J.G. Latorre, S.O.P. Báez, A.G. Gotor, Energy performance of a reverse osmosis desalination plant operating with variable pressure and flow, Desalination 366 (2015) 146–153.

[10] D. Mentis, G. Karalis, A. Zervos, M. Howells, C. Taliotis, M. Bazilian, H. Rogner, Desalination using renewable energy sources on the arid islands of the South Aegean Sea, Energy 94 (2016) 262–272.
[11] T. Novosel, B. Cosic, T. Puksec, G. Krajacic, N. Duic, B.V. Mathiesen, H. Lund, M. Mustafa, Integration of renewables and reverse osmosis desalination — case study for the Jordanian energy system with a high share of wind and photovoltaics, *Energy* (2015) in press.
[12] A. Palzer, H.-M. Henning, A comprehensive model for the German electricity and heat sector in a future energy system with a dominant contribution from renewable energy technologies — part II: results, Renew. Sust. Energ. Rev. 30 (2014) 1019–1034.
[13] D. Connolly, V. Mathiesen, A technical and economic analysis of one potential pathway to a 100% renewable energy system, Int. J. Sustain. Energy Plann. Manage. 1 (2014) 7–28.
[14] G. Pleßmann, M. Erdmann, M. Hlusiak, Ch. Breyer, Global energy storage demand for a 100% renewable electricity supply, Energy Procedia 46 (2014) 22–31.
[15] Ch. Breyer, D. Bogdanov, K. Komoto, T. Ehara, J. Song, N. Enebish, North-east Asian super grid: renewable energy mix and economics, Jpn. J. Appl. Phys. 54 (2015) 08KJ01.
[16] M.Z. Jacobson, M.A. Delucchi, G. Bazouin, Z.A.F. Bauer, C.C. Heavey, E. Fisher, S.B. Morris, D.J.Y. Piekutowski, T.A. Vencilla, T.W. Yeskoo, 100% clean and renewable wind, water, and sunlight (WWS) all-sector energy roadmaps for the 50 United States, Energy Environ. Sci. 8 (2015) 2093–2117.
[17] Greenpeace International, Energy [r]evolution — a sustainable world energy outlook 2015, Amsterdam, A Report Commonly Published with GWEC and SPE, 2015.
[18] M. Luck, M. Landis, F. Gassert, Aqueduct Water Stress Projections: Decadal Projections of Water Supply and Demand Using CMIP5 GCMs, World Resources Institute, Washington DC, 2015 ([accessed: September 9, 2015], http://www.wri.org/sites/default/files/aqueduct-water-stress-projections-technical-note.pdf).
[19] [IPCC] — Intergovernmental Panel on Climate Change, Climate Change 2015: Synthesis Report — Summary for Policymakers, IPCC, Geneva, 2014 ([accessed: September 9, 2015], www.ipcc.ch).
[20] Ch. Breyer, M. Görig, A.-K. Gerlach, J. Schmid, Economics of hybrid PV–fossil power plants, Proceedings of the 26th European Photovoltaic Solar Energy Conference, Hamburg, 2011 (September 5–9).
[21] W. Short, D.J. Packey, T. Holt, A Manual for the Economic Evaluation of Energy Efficiency and Renewable Energy Technologies, NREL, NREL/TP-462-5173, Golden, 1995.
[22] J. Macknick, R. Newmark, G. Heath, C.K. Hallett, Operational water consumption and withdrawal factors for electricity generating technologies: a review of existing literature, Environ. Res. Lett. 7 (2012) 045802.
[23] Food and Agricultural Organisation of the United Nations, AQUASTAT database, FAO, 2015 [accessed April 6, 2015] http://www.fao.org/nr/water/aquastat/data/query/index.html?lang=en.
[24] M. Sterner, Bioenergy and renewable power methane in integrated 100% renewable energy systemsPhD thesis Faculty of Electrical Engineering and Computer Science, University of Kassel, 2009.
[25] M. Lehner, R. Tichler, H. Steinmüller, M. Koppe, Power-to-Gas: Technology and Business Models, Springer, Heidelberg, 2014.
[26] M. Götz, J. Lefebvre, F. Mörs, A. McDaniel Koch, F. Graf, S. Bajohr, R. Reimert, T. Kolb, Renewable power-to-gas: a technological and economic review, Renew. Energy (2015) (in press).
[27] G.V. Gude, Energy consumption and recovery in reverse osmosis, Desalin. Water Treat. 36 (2011) 239-26.
[28] S. Loutatidou, B. Chalermthai, P.R. Marpu, H. Arafat, Capital cost estimation of RO plants: GCC countries versus southern Europe, Desalination 347 (2014) 103–111.
[29] A. Lamei, P. Zaag van der, E. Münch von, Basic cost equations to estimate unit productivity costs for RO desalination and long-distance piping to supply water to tourism-dominated arid coastal regions of Egypt, Desalination 225 (2008) 1–12.
[30] M. Al-Nory, M. El-Beltagy, An energy management approach for renewable energy integration with power generation and water desalination, Renew. Energy 72 (2014) 377–385.
[31] Government of Newfoundland & Labrador Department of Environment and Conservation Water Resources Management Division, Evaluation of potable water storage tanks in Newfoundland and Labrador and their effect on drinking water quality, 2011 [accessed: June 15, 2015] http://www.env.gov.nl.ca/env/waterres/reports/drinking_water/Tank_Report_July_12_2011.pdf.
[32] Economic & Social Commission for Western Asia, Role of desalination in addressing water scarcity, ESCWA, viewed 15th June 2015, http://www.escwa.un.org/information/publications/edit/upload/sdpd-09-4.pdf2009.
[33] M.T. Missimer, G,.R. Maliva, N. Ghaffour, T. Leiknes, G.L. Amy, Managed aquifer recharge (MAR) economics for wastewater reuse in low population Wadi Communities, Kingdom of Saudi Arabia, Water 6 (2014) 2322–2338.
[34] A. Al-Zahrani, J. Orfi, Z. Al-Suhaibani, B. Salim, H. Al-Ansary, Thermodynamic analysis of a reverse osmosis desalination unit with energy recovery system, Proceedia Eng. 33 (2012) 404–414.
[35] National Center for Environmental Information, World Ocean Atlas 2013. NCEI, 2013 [accessed: June 15, 2015] https://www.nodc.noaa.gov/OC5/woa13/woa13data.html.
[36] D. Bogdanov, Ch. Breyer, North-east asian super grid for 100% Renewable energy power supply: distributed small-scale and centralized large-scale solar PV as a major energy source, 31st EU PVSEC, 2015http://dx.doi.org/10.4229/31stEUPVSEC2015-7DO.14.6 (Hamburg).
[37] F. Kersten, R. Doll, A. Kux, D.M. Huljić, M.A. Görig, Ch. Breyer, J. Müller, P. Wawer, PV-learning curves: past and future drivers of cost reduction, 26th EU PVSEC, 2011http://dx.doi.org/10.4229/26thEUPVSEC2011-6CV.1.63 Hamburg, September 5–9.
[38] Fichtner, MENA Regional Water Outlook. Part 2. Desalination Using Renewable Energy Final Report, 2011.

Publication II

Caldera, U., Bogdanov, D., Fasihi M., Aghahosseini A. and Breyer, C.
Securing future water supply for Iran through 100% renewable energy powered desalination

Reprinted with permission from
International Journal of Sustainable Energy Planning and Management
Vol. 23, pp. 39-54, 2019

International Journal of Sustainable Energy Planning and Management Vol. 23 2019 39–54

International Journal of
Sustainable Energy Planning and Management

Securing future water supply for Iran through 100% renewable energy powered desalination

Upeksha Caldera*, Dmitrii Bogdanov, Mahdi Fasihi, Arman Aghahosseini and Christian Breyer

LUT University, Yliopistonkatu 34, 53850 Lappeenranta, Finland

ABSTRACT

Iran is the 17th most populated country in the world with several regions facing high or extremely high water stress. It is estimated that half the population live in regions with 30% of Iran's freshwater resources. The combination of climate change, increasing water demand and mismanagement of water resources is forecasted to worsen the situation. This paper shows how the future water demand of Iran can be secured through seawater reverse osmosis (SWRO) desalination plants powered by 100% renewable energy systems (RES), at a cost level competitive with that of current SWRO plants powered by fossil plants in Iran. The optimal hybrid RES for Iran is found to be a combination of solar photovoltaics (PV) fixed-tilted, PV single-axis tracking, Wind, Battery and Power-to-Gas (PtG) plants. The levelised cost of water (LCOW) is found to lie between 1.0 €/m^3 and 3.5 €/m^3, depending on renewable resource availability and water transportation costs.

Keywords:

Levelised cost of water:
Fossil fuel independency;
Seawater reverse osmosis;
Iran;
Hybrid renewable energy systems

URL: http://doi.org/10.5278/ijsepm.3305

1. Introduction

Iran is ranked in the top 10 water stressed countries globally, with the industrial, agricultural and domestic sectors in the country facing high to extremely high water stress [1]. High water stress implies that greater than 40% of the renewable water resources available is being withdrawn, indicating the use of fossil groundwater. Gleeson et al. [2] show that the area of the Persian aquifer required to sustain the current groundwater withdrawals and dependent ecosystems is 10–20 times larger than the actual area of the Persian aquifer. A study by Joodaki et al. [3] on groundwater in the Middle East found that from 2003 to 2012, Iran suffered the largest groundwater depletion at a rate of 25 ± 3 Gt per year. The reduction is attributed to both climate change and increasing water withdrawals.

The World Resources Institute (WRI) projects that even in an optimistic scenario, as explained in the Intergovernmental Panel on Climate Change 5th assessment report, Iran will continue to rank in the top 15 water stressed countries [1]. At present, the annual renewable water resources per capita in Iran is less than 1700 m^3 and is expected to decrease to 800 m^3 by 2021. The water crisis threshold is 1000 m^3 of annual renewable water resource per capita [4]. A joint report by the Heinrich Böll Foundation and Small Media [5] has identified the water crisis to pose the greatest threat to Iran in the coming decades, with the potential to render vast areas of the country uninhabitable.

Alipour et al. [6] suggest that over-extraction of groundwater resources in the Greater Tehran area of Iran, has led to land subsidence at the rate of several centimeters a year. Land subsidence results in damage to buildings, roads and infrastructure contributing towards economic losses. In addition, the water shortage has rendered lakes and wetlands across the country dry. It is

*Corresponding author-e-mail: upeksha.caldera@lut.fi

Nomenclature

a	annum
b€	billion Euro
CAGR	compound annual growth rate
crf	capital recovery factor
D	debt
E	equity
FLH	full load hours
GWI	Global Water Intelligence
HVDC	High Voltage Direct Current
LCOE	levelised cost of electricity
LCOC	levelised cost of curtailment
LCOS	levelised cost of storage
LCOT	levelised cost of water transportation
LCOW	levelised cost of water
PtG	power-to-gas
PV	photovoltaic
SEC	specific energy consumption
SNG	synthetic natural gas
SWRO	seawater reverse osmosis
WACC	weighted average cost of capital

also argued that over extraction of water and diversion of the rivers that feed the lakes in Iran is the main contributor to the diminishing lakes in the country. The report by Heinrich Böll Foundation and Small Media [5] reasons these to be causes for the shrinking Lake Urmia and Lake Houman.

Madani [7] explains that Iran receives an average annual rainfall of 250 mm, less than 1/3rd of the global average. The precipitation is distributed unevenly across the country, with 25% of the country receiving 75% of the precipitation, more specifically, the Northern and Western regions. In addition, 75% of the precipitation occurs during the winter period, when not required by the agricultural sector. This high variability in rainfall, both in a spatial and temporal resolution, has sustained Iran's reliance on dams and reservoirs to regulate water flows. As of 2016, Iran had 171 dams with a total storage capacity of 4907 bn m^3 from which only 60% was full [8].

Various sources mention that the government's response to the water shortage has been the construction of more dams [4, 7, 9]. Madani [7] argues that dams worsen the water crisis by blocking water flow to lakes, degrading water quality, destroying ecosystems and encouraging downstream development under the impressions of water availability. Similar arguments are expressed by Foltz [9] and Tahbaz [10]. Madani [7] reasons that the main factors that have contributed to Iran's water crisis are population growth, mismatch between population distribution and available water resources, promotion of unsustainable agriculture practices and poor management of water resources. In addition, Gorjian and Ghobadian [4] and Tahbaz [10] highlight the impact of climate change and the resulting droughts and floods on the water resources in Iran.

The Heinrich Böll Foundation and Small Media [5] discuss water demand management and increase in efficiency in the agricultural sector as some of the most effective ways of overcoming water stress in Iran. According to GWI [11], the Iranian government is looking to secure water availability through water efficiency, water reuse particularly for irrigation and the increased use of seawater desalination. In November 2015, the Iranian Energy Minister announced project plans to desalinate and transfer drinking water from the Persian Gulf and the Sea of Oman to 47 million people located within the 16 central provinces of the country [12]. A report by The Iran Project explains that construction of the project has already started and is being called the largest water transfer project in the Middle East [13]. Collins [14] provide another example of a desalination facility being built in Bandar Abbas to provide desalinated water to an iron ore mine 300 km inland and at an elevation of 1700 m. This will further be expanded to provide water to a copper mine at 2700 m altitude. The first phase of the project, constructing a 100,000 m^3/day SWRO plant in Bandar Abbas, is reported to have been completed in 2018 and supplying water to the region [15].

The installed desalination capacity in Iran, as of 2015, is estimated to be 809,607 m^3/day, out of which 21.6% is seawater reverse osmosis (SWRO) [11]. Approximately, 62% of the desalinated water is used by the industrial sector and the remaining 38% to meet the domestic demand. According to Gude [16], Iran is ranked as one of the top 20 countries with the largest desalination market in recent years. Currently, the desalination plants for domestic demand are situated in the southern provinces of Hormozghan as well as Sistan and Baluchestan.

The growth of seawater desalination as an alternative water resource has raised concerns about the high energy consumption of desalination and the dependence of the industry on fossil fuels [4, 17–22]. Therefore, despite helping to meet the water demand of society, the

desalination industry also further contributes to climate change, only exacerbating water stress situations globally. Razmjoo et al. [23] studied different energy sustainability indicators for a group of countries, including Iran. It was found that Iran ranked the least in terms of environmental and social aspects, highlighting the high shares of fossil fuel used in the country.

Connolly and Mathiesen [24] discuss the risks associated with the current fossil based energy system and analyse the feasibility of achieving 100% renewable energy systems across different sectors for the case of Ireland. With the increasing threat of runaway climate change, various literature and reports address the aspects of 100% renewable energy based systems on a local and global scale [25]. The adoption of renewable energy to power the desalination sector has also been explored. Østergaard et al. [26] investigated the impacts of running desalination plants with increasing wind capacities on the Jordanian energy system, considering the large demand for desalination in Jordan. In addition to increasing the penetration of renewable energy in the system, the study also investigated the flexibility options that different desalination technologies may provide to the energy system. The main concerns with renewable energy power plants are their intermittency and need for energy storage [20–22, 27]. In Caldera et al. [27], it was shown that the global water demand of 2030 can be met by SWRO plants powered by 100% hybrid renewable energy power plants at a cost level competitive with that of fossil powered SWRO plants today. The hybrid power plants were comprised of solar photovoltaic (PV), wind energy, battery and Power-to-Gas (PtG) plants and allowed for the optimal utilisation of the installed desalination capacity.

This paper focuses on the water stress in Iran and assesses the techno-economic feasibility of alleviating the country's water crisis through 100% renewable powered SWRO systems by 2030. The proposed research will enable Iran to produce water for the country without concern of fossil fuel consumption and, consequently, greenhouse gas emissions. The system envisaged to meet the future water demand of Iran is presented in Figure 1.

SWRO desalination plants along the coastline are powered by hybrid renewable energy power plants being cost optimized by storage. High voltage direct current (HVDC) power lines transport power to the desalination plants on the coast of the Persian Gulf and the Gulf of Oman. The water produced is transported to meet the demands of the domestic, industrial and agricultural sectors throughout the country. Water storage at the desalination plant site ensures reliable water supply.

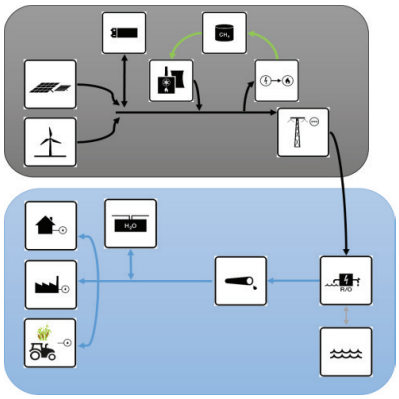

Figure 1: The desalination system proposed to meet the future water demand of Iran. The different components are the renewable energy power plant configuration (top panel), water demand of the municipal, industrial and agricultural sectors (bottom panel) and SWRO plants located on the coast line (bottom panel)

2. Methodology

2.1. Overview

The feasibility of a 100% renewable energy powered SWRO desalination system for Iran can be determined by comparing the water production costs of the system with that of fossil powered SWRO plants in operation today. In this study, the system, illustrated in Figure 1, is analysed for the 2030 optimistic scenario in Iran. In addition, it is assumed that there are no thermal power plants using fossil fuels in the future scenario for Iran, in alignment with the COP21 agreement to achieve a net zero greenhouse gas emission system. The feasibility of a 100% renewable energy based power system in Iran has already been illustrated by Aghahosseini et al. [28] and Ghorbani et al. [29, 30]. The assumption of no fossil fuel based plants is further validated by recent literature that discuss the transition to 100% renewable energy power systems of different countries and regions [25, 31–33]. Thus, the 2030 total water demand of the agricultural, domestic and industrial sectors, excluding that of thermal power plants in Iran, is considered.

The unit production cost of water (€/m^3) or the levelised cost of water (LCOW) is calculated as discussed in [27]. The LCOW includes the unit production cost of water at the site of the desalination plant, electricity costs, water storage at the site of demand and the water transportation to the region of desalination demand. Equation 1 summarizes the approach used to calculate the LCOW.

$$LCOW_{desal} = \frac{Capex_{desal} \times crf_{desal} + opex_{fixed\ desal}}{Total\ water\ produced\ in\ a\ year} + (LCOE_r \times SEC) \quad (1)$$

Equation 1: Levelised cost of water (LCOW). Here, $\boldsymbol{Capex_{desal}}$ is the CAPEX of the desalination plant in €/(m^3·a) and $\boldsymbol{crf_{desal}}$ is the annuity factor for desalination plant. Total water produced in a year is in m^3, $\boldsymbol{Opex_{fixeddesal}}$ is the fixed OPEX of the desalination plant in €/(m^3·a), $\boldsymbol{LCOE_r}$ is the levelised cost of electricity and is in €/kWh. SEC is the specific energy consumption in kWh/m^3. The product of the LCOE and SEC is the energy cost of the desalination plant in €/(m^3 a).

The approach to calculate the LCOE for a region as summarised in Equation 2.

$$LCOE_r = LCOE_{prim,r} + LCOC_r + LCOS_r + LCOT_r \quad (2)$$

Equation 2**:** Levelised cost of electricity for a region. Here, $LCOE_{prim,\ r}$ is the levelised cost of electricity for a primary generation source, $LCOC_r$ is the levelised cost of curtailment, $LCOS_r$ is the levelised cost for energy storage in the region and $LCOT_r$ is the levelised cost of transmission of electricity in the region *r*.

To project the SWRO CAPEX, a learning rate of 15%, presented in the maiden paper on learning curves [34] for SWRO CAPEX, was used. The research by Caldera and Breyer [34] demonstrates, that when the historic global cumulative online SWRO capacity doubled, the SWRO CAPEX decreased by 15%. In addition to the 15% learning rate, a cumulative annual growth rate (CAGR) of 35% was assumed to meet the global desalination demand by 2030.

2.2. Model and Input Data

The LUT energy system model used for the global study of the LCOW in [27], is utilised for the Iran specific study. The model determines the LCOW for regions with high or greater water stress in Iran, based on Equation 1. The energy system model allows determination of the optimal renewable energy mix required, at an hourly temporal resolution and a spatial resolution of 0.45° × 0.45°. The optimal renewable energy mix, based on the energy and desalination sector constraints defined in [28] and [31], allows for the least cost of electricity (LCOE). The objective of the target function is to minimise the total annual costs of the energy and desalination sectors and is described in Equation 2.

$$min \left(\begin{array}{l} \sum_{t=1}^{tech} (CAPEX_t \times crf_t + OPEXfix_t) \times instCap_t + OPEXvar_t \times E_{gen,t} \\ + rampCost_t \times totRamp_t + \sum_{dt=1}^{desal\ tech} (CAPEX_{dt} crf_{dt} + OPEXfix_{dt}) \\ \times instCap_{dt} + \sum_{dd=1}^{desal\ distance} (CAPEX_{dd} \times crf_{dd} + OPEXfix_{dd}) \times distance_{dd} \end{array} \right)$$

Equation 2: Target function. Here, *t* is tech and includes storage and transmission technologies, $CAPEX_t$ is capital expenditures for technology *t*, is capital recovery factor for technology *t*, $OPEXfix_t$ is fixed operational expenditures for technology *t*, $OPEXvar_t$ is variable operational expenditures for technology *t*, $instCap_t$ is installed capacity in the country for technology *t*, $Egen_t$ is annual electricity generation by technology *t*, $rampCost_t$ is cost of ramping of technology *t* and $totRamp_t$ is sum of power ramping values during the year for the technology *t*. *dt* represents the desalination components of SWRO plants and water storage. *dd* represents the horizontal and vertical water pumping distances.

As details of how the model works and the required input data are provided in [28] and [31], the following sections present an overview of the input data required specific to Iran:

1. Regions in Iran with high or extremely high water stress in the 2030 optimistic scenario are considered. The WRI Aqueduct Atlas estimates the water supply and water demand values for 15,006 global water catchments, thus not covering all catchments in a country [35]. For the study of Iran, the water stress data from WRI was compared with a detailed map of renewable water resources in Iran.
2. Figure 2 represents the average renewable water resource, based on 1990 – 2002 data, per capita for all basins in Iran [36]. The lower resolution data from WRI suggest high water stress for the northern and western parts of Iran by 2030 [35]. This contradicts the current high renewable water availability in these regions as shown in Figure 2. Due to the lack of high-resolution water stress data for Iran, it was decided to

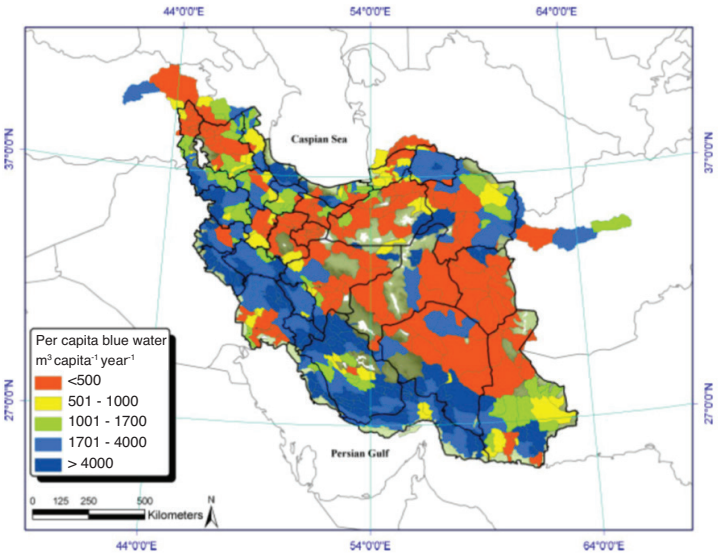

Figure 2: Renewable water resource availability per capita per year for Iran based on 1990 – 2002 water resource data. Water scarcity threshold is 1000 m3 per capita per year. Reproduced with permission from the original publisher [36]

reduce the future water stress in the northern and western parts of the country to low – medium water stress level. This ensures that desalination demand is not considered in the model for these regions. The water demand will increase in 2030. However, the water stress will not be high due to the high renewable water availability. In contrast, the water stress in the central and southern regions of the country deteriorate further, with a high desalination demand. The resulting map is presented in Figure 3. Despite being an optimistic scenario, there are large regions of the country where renewable water resources are scarce and fossil water is used.

3. The total water demand for regions in 2030 with high or extremely high water stress are also considered. To determine the total water demand, the change in water demand factor for 2030, provided by the WRI, were used. This factor estimates the increase in the water demand, from the currently reported water withdrawals, for nodes within the relevant water catchments by 2030. The total water demand for the country is the sum of the water demand across all the nodes in the country and estimated to be about 345 million m^3/day. In contrast, in 2005, the total water consumption of Iran was approximately 246 million m^3/day.
4. The desalination demand is calculated based on a logistic function of the total water demand and the water stress level. The resulting desalination demand or the required SWRO capacity per region is presented in Figure 4. The total required desalination capacity by 2030, to meet the water demands of agricultural, industrial and municipal sectors, is found to be 199 million m^3/day.
5. In this study, only the Gulf of Oman and the Persian Gulf are considered as sources of seawater to satiate Iran's desalination demand. The Caspian Sea is excluded due to environmental concerns with the use of saline lakes as feed water for large desalination capacities [37]. In addition, Mirchi and Madani [38] discuss the environmental disasters such as deforestation and biodiversity loss in the surrounding region as a result of transferring water from the Caspian

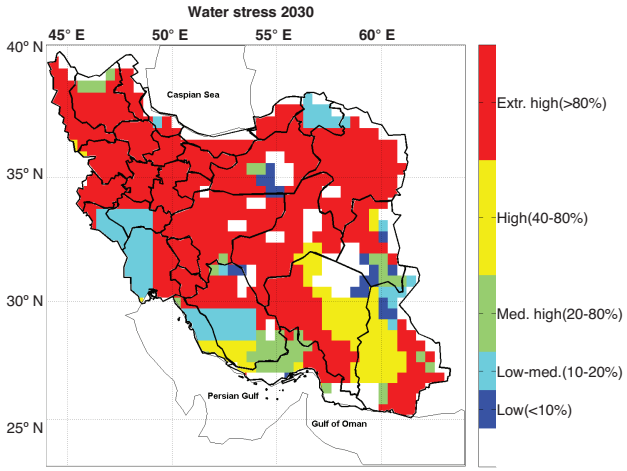

Figure 3: Projected water stress for the 2030 optimistic scenario in Iran. The water stress is the ratio of the total water demand in the region to the annual renewable water resources available in that region. The white regions represent those regions that are arid, have low water or have no available data. The water stress in the northern and western parts of the country were reduced as per Figure 2

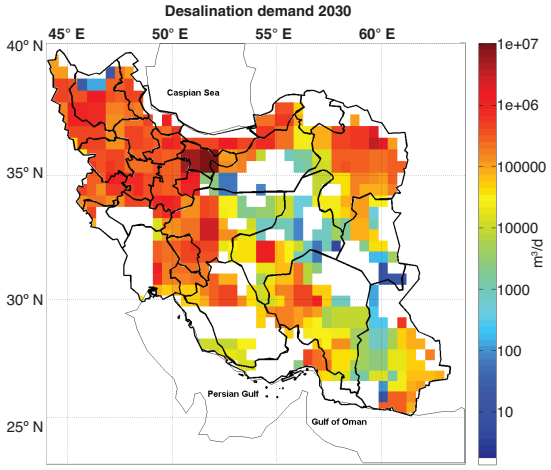

Figure 4: Desalination demand for the 2030 optimistic scenario in Iran. This includes the water demand of the agricultural, domestic and industrial sectors, excluding thermal power plants [39, 42, 46–48]

Sea. The 2030 total desalination demand of Iran is estimated to be about 247 million m^3/day. As mentioned earlier, the total water demand, and consequently the desalination water demand, for Iran excludes the water demand for the power sector. For the Iranian model, the fresh water consumption of thermal power plants was obtained from Spang et al. [39].

6. The SWRO desalination system, water transportation costs, energy consumption and hybrid renewable power plant component costs for 2030 are provided in Table 1. All detailed numbers can be found in [27]. The SWRO CAPEX for 2030 has been found based on the 15% learning rate [34] and a CAGR of 35%. This growth rate would enable to meet the global desalination demand of 2030. In addition, CAPEX of the PV power plant components have been updated as per recent literature and reports [40, 41].
7. The model optimizes the location of the SWRO desalination plants based on the distance between the desalination and demand node. In addition, the highest elevation on the optimal path is found using the ETOPO1 global relief model [42] and considered for the water transportation infrastructure. Future work on water pumping routes may consider the availability of existing infrastructure for water pumping such as electrical grids and roads.
8. Solar irradiation and wind energy data for Iran, for the year 2005 are used as a reference in hourly temporal and 0.45° x 0.45° spatial resolution. The global historical solar and wind data were obtained from NASA datasets [43, 44]

Table 1: Key assumptions for the SWRO desalination plant, water storage, water transportation and hybrid renewable energy components in the model for 2030 [27, 31, 34, 42, 46]. A WACC of 7% is considered. The HVDC transmission grid is assumed to have a power loss of 1.6% per 1000 km. Water storage of a minimum of 7 days at the demand site is assumed.

SWRO Desalination System		
Capacity	m^3/a	equal to desalination demand of 0.45°x0.45° spatially resolved region
CAPEX	€/(m^3·a)	1.90
$OPEX_{fixed}$	€/(m^3·a)	4% of CAPEX
Full load hours	hrs	system optimum
Energy consumption	kWh/m^3	Calculated for desalination site. Approximate range is 2.80 – 3.30, depending on salinity of feed water
Water Storage		
CAPEX	€/m^3	65
Water Transportation		
Pipes CAPEX	€/(m^3·a·km)	0.053
Horizontal pump CAPEX	€/(m^3·hr·km)	19.23
Horizontal pump energy consumption	kWh/(m^3·hr·100km)	0.04
Vertical pump CAPEX	€/(m^3·hr·m)	15.40
Vertical pump energy consumption	kWh/(m^3·hr·100m)	0.36
Hybrid Renewable Energy Power Plant CAPEX		
PV fixed-tilted plant	€/kW	390
PV single-axis tracking plant	€/kW	429
Wind plant	€/kW	1000
Batteries	€/kWh	150
PtG	€/kW	Water electrolysis : 380 CO_2 Direct Air Capture : 356 Methanation : 234
Gas storage	€/kWh	0.05

in a 1° x 1° spatial resolution and temporal resolution of 3 h for a 22 year period. The data was reprocessed by the German Aerospace center to a 0.45° x 0.45° spatial resolution [45].

Based on the above parameters, the model compares the use of different hybrid renewable energy power plant combinations. The least cost system that meets the 2030 desalination demand of Iran is considered to be the optimal system.

3. Results: An Optimal System Design for Iran

The model was used to analyse four different combinations of hybrid renewable energy plants to power the 2030 SWRO desalination capacity for Iran:

1. PV fixed-tilted, Wind, Batteries
2. PV fixed-tilted, Wind, Batteries, PtG
3. PV single-axis tracking, PV fixed-tilted, Wind, Batteries
4. PV single-axis tracking, PV fixed-tilted, Wind, Batteries, PtG

It was found that a combination of PV, Wind, Batteries and PtG power plants offers the least cost solution for Iran. The figures that follow present and discuss the optimal energy and SWRO desalination system for Iran.

Figure 5 (a) illustrates the PV fixed-tilted and single-axis tracking capacities required per region. A region is defined as an area of 50 km x 50 km (exactly 0.45° x 0.45° in units of latitude and longitude). A total of approximately 201 GW of PV fixed-tilted and 360 GW of PV single-axis tracking power plants are required. Figure 5 (b) shows that there is a higher contribution from PV to the hybrid PV-Wind power plants in most regions. On average 82% of the energy generated by the hybrid PV-Wind power plants is provided by PV power plants. Figure 5 (c) shows the total full load hours (FLH) provided by the hybrid PV-Wind power plants. Higher FLH allow for optimal utilisation of the desalination capacity and therefore lower LCOW. However, to allow for the optimal FLH of the SWRO desalination plants, batteries and PtG power plants

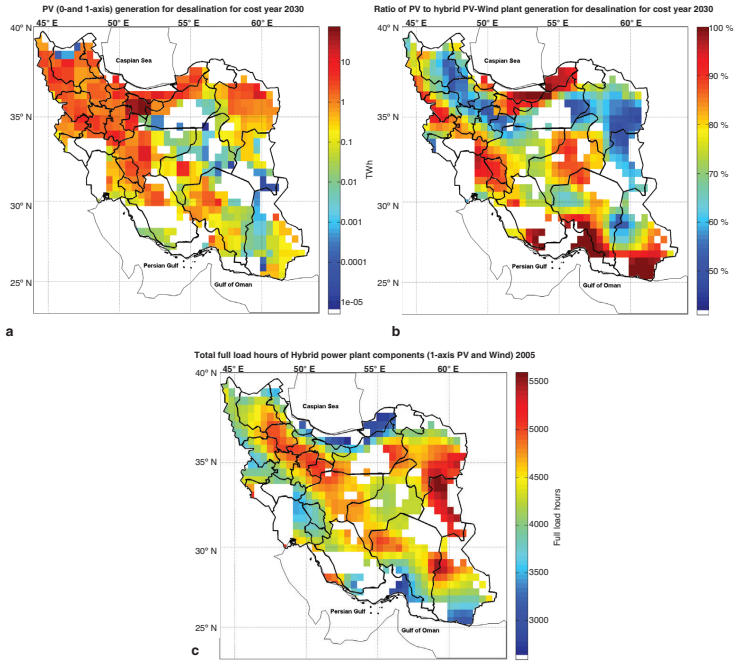

Figure 5: (a) Installed PV capacities required Installed PV capacities required for the 2030 SWRO capacity (b) Contribution of PV to the installed capacities of the hybrid PV-Wind Power Plant (c) Total full load hours provided by the hybrid power plant

have to be used. The required battery, PtG and water storage capacities at the demand site are presented in Figure 6.

The required battery capacity is almost 360 TWh and provides up to 22% of the total energy demand. The batteries have to be charged almost daily with up to 315 cycles per year in some regions. The total electrolyser capacity required for Iran is 91 GW_{el}. The storage capacity required for the produced synthetic natural gas (SNG) is 103 TWh_{th}. The PtG plants provide up to 15% of the total energy demand and decreases the excess energy of the system by 75%. As a result, the total required PV capacity is reduced by 20%, wind capacity is increased by 17% due to a good match with the PtG requirements, battery storage capacity is reduced by 23% and total water storage capacity is decreased by 51%.

Figure 6 (c) presents the ratio of the excess energy to the total energy generated by the system. In most regions, this value is between 5% and 7%.

The resulting LCOE of the complete energy system, taking into account losses in the transmission lines, and the final LCOW for the regions with desalination demand is presented in Figure 7. Figure 7 (a) shows that the 2030 LCOE range for the complete system in Iran is approximately 0.06 €/kWh – 0.11 €/kWh, including electricity generation, power transmission, storage and curtailment. Higher LCOE values are prevalent in the northern regions of Iran. This is attributed to the increased battery and PtG storage requirements in these regions. The resulting LCOW, presented in Figure 7 (b), is of the range 1.0 €/m^3 – 3.0 €/m^3, most prevalent being the 1 €/m^3 – 2.5 €/m^3 range. In comparison, the global LCOW range is mostly between 0.70 €/m^3 and 2.00 €/m^3 [27].

The higher LCOW than the global average can be attributed to the large water pumping distances, both vertical and horizontal, necessary in Iran. As illustrated in Figure 7 (b) the LCOW increases further away from the coast line due to the longer distance and larger elevation. Figure 8 (a) presents the contribution of the energy used for water pumping to the LCOW, which is

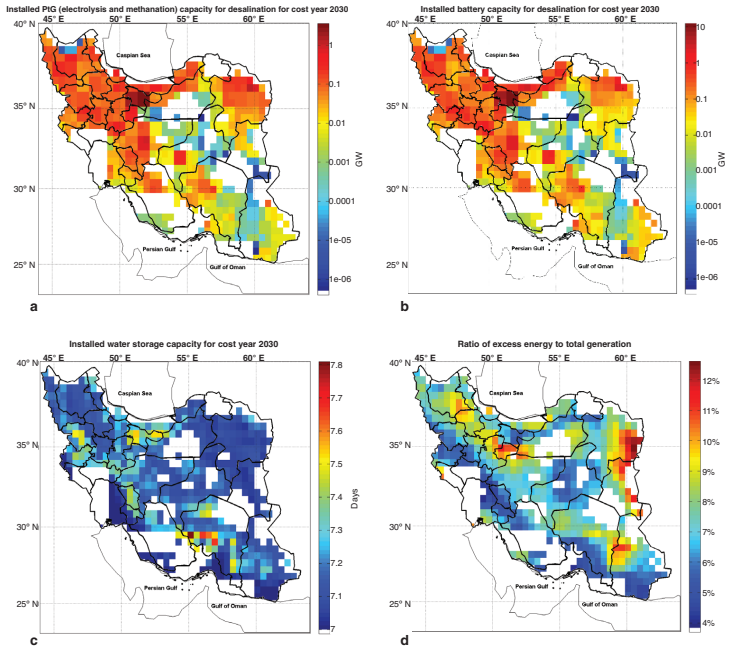

Figure 6: (a) Installed battery capacity required for the 2030 SWRO capacity (b) Installed PtG capacity required for the 2030 SWRO capacity (c) Optimal water storage capacity required for regions with desalination demand in 2030 (d) Ratio of excess energy to total energy generation of the system in 2030

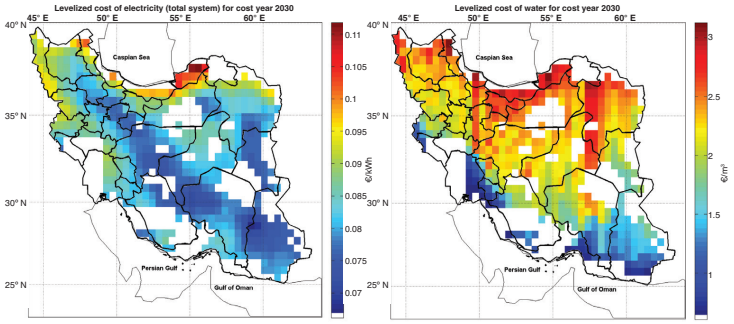

Figure 7: (a) LCOE range for a complete system in Iran for the year 2030 (b) LCOW range for a complete system in Iran for the year 2030

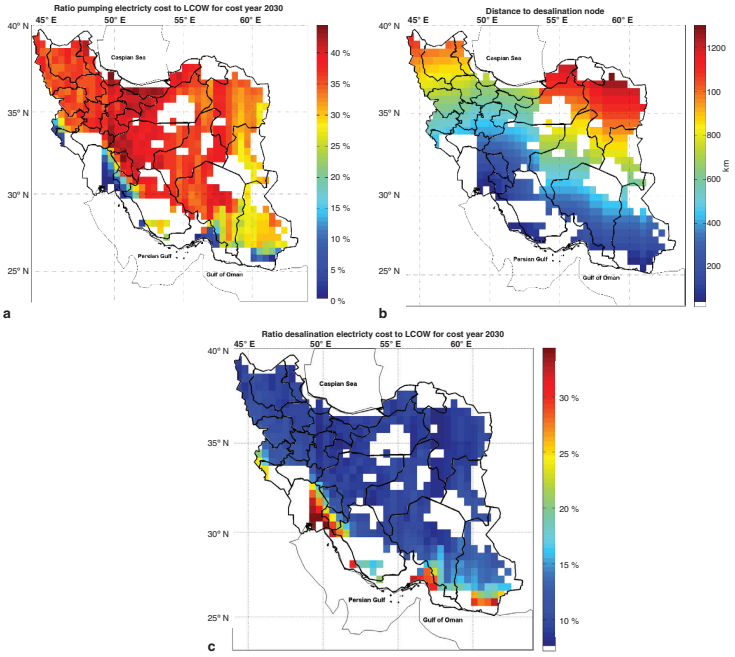

Figure 8: (a) Contribution of the pumping electricity cost to the LCOW in Iran for the year 2030 (b) Distance from desalinated water demand regions to the desalination node (c) Contribution of desalination electricity cost to the LCOW in Iran for the year 2030

approximately 38% in Iran. In contrast, the global average is 16% [24]. Figure 8 (b) presents the optimal distance, determined by the model, between the desalination demand region and the desalination node. It can be observed that as the distance from the desalination nodes increases, the contribution of the pumping electricity costs increases. There are some regions in the eastern part of Iran that have larger distances from the desalina-

tion node than in the west, but the contribution of pumping electricity cost is lower. This may be due to the fact that the north eastern regions of the country have a lower elevation than the north western region. Thus, the resulting electricity required for vertical pumping, and ultimately the total electricity required for pumping, is lower in the north eastern regions than in the north western regions. Figure 8 (bottom) shows the contribution of the electricity for SWRO desalination to the final LCOW. On average the contribution is approximately 10% towards the LCOW. For desalination demand nodes along the coast line, the electricity demand for pumping is low. Thus, the contribution of electricity for the desalination plants to the final LCOW is higher in the nodes along the coast line.

The CAPEX of the total system contributes on average 64% to the final LCOW of the system. The total system CAPEX refers to the sum of the CAPEX of the PV, Wind, Battery, PtG, power lines, water storage, desalination plants and the piping system.

Figure 9 (a) presents the contribution of the CAPEX towards the LCOW.

Figure 9 (b) represents the spread of the capital costs of the 2030 system for Iran. The largest contribution is from the vertical transportation infrastructure, 25%, followed by the single-axis tracking PV plants with a

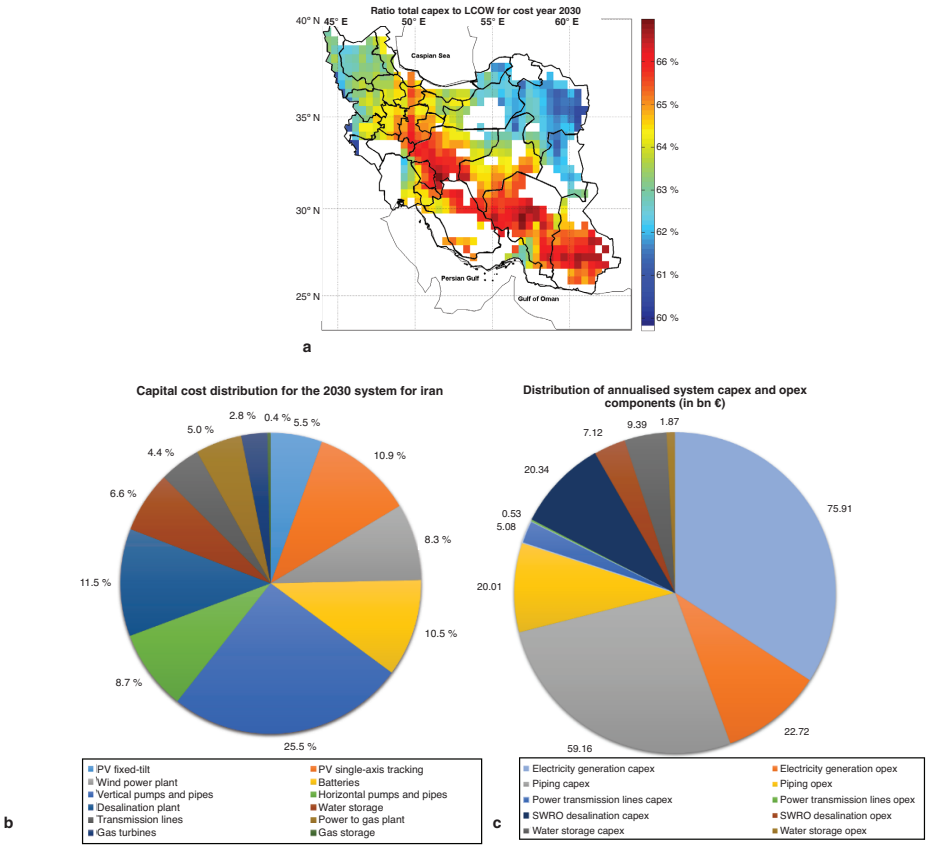

Figure 9: Contribution of the CAPEX to the final LCOW (b) Distribution of the 2030 system capital cost (c) Distribution of annualised system CAPEX and OPEX components (in b) of the proposed 2030 system for Iran

cost contribution of 11%. The desalination plants is the fourth largest contributor with 10% of the total costs. Batteries contribute a slightly higher percentage with 12% of the total costs. The higher contribution of the single-axis tracking PV and batteries can be attributed to the energy requirements for water transportation.

Figure 9 (c) presents the distribution of the annualised CAPEX and OPEX for all the system components. The annualised CAPEX cost for the solution for Iran by 2030 is estimated to be approximately 170 b€ and OPEX cost of 52 b€. The hybrid PV-Wind power plants, together with the batteries and PtG, account for the largest annualised CAPEX of 75 b€. This is followed by the water transportation infrastructure and the desalination plants, with annualised CAPEX of 59 b€ and 20 b€, respectively.

4. Discussion

The LCOW range for Iran when SWRO desalination plants, in 2030, are powered by hybrid PV-Wind-Battery-PtG plants is found to be between 1.0 €/m^3 and 3.0 €/m^3. The prevalent LCOW range is between 1.0 €/m^3 and 2.5 €/m^3. The corresponding LCOE range for Iran is 0.06 €/kWh and 0.11 €/kWh, mostly prevalent between 0.06 €/kWh and 0.09 €/kWh.

GWI [11] provides water production costs for fossil powered SWRO desalination plants, located in southern province of Hormozgan. The water production cost alone is approximately 0.70 €/m^3. In Figure 7 (b), the LCOW, including the water transportation and storage costs, for this region is approximately 1.0 €/m^3 -1.50 €/m^3. The higher LCOW range of the model can be attributed to the high water transportation costs and energy required for water pumping, as shown in Figure 8 (a). The cost provided by DesalData only reflects the water production cost at the desalination plant.

The results show that it is possible to meet the increasing water demand of Iran with SWRO desalination plants, located solely along the southern coast line, powered by hybrid renewable energy power plants. In the near future the production cost of clean water from the hybrid system will be competitive with the cost of fossil powered SWRO plants today. As mentioned in Caldera et al. [27] this will be driven by the increase in global desalination demand and the continued decrease in solar PV and storage costs due to learning curve effects. However, the final LCOW may be high due to the requirements of the transportation infrastructure.

Table 2: Summary of the key technical and cost data for the 2030 optimal system design for Iran

		2030 optimal system for Iran
SWRO total desalination demand per day	**m^3/ day**	**199 mill**
PV capacity installed	GWp	561
PV fixed-tilted	GWp	201
PV single-axis tracking	GWp	360
Wind capacity installed	GW	117
Battery capacity installed	TWh	360
PtG electrolyser capacity installed	GW_{el}	91
Average excess energy curtailed	%	7
Total CAPEX	b€	1420
Annualised costs	b€	222
LCOW range	€/m^3	1.0 – 3.0
Prevalent LCOW range	€/m^3	1.0 – 2.5

Table 2 summarises the key technical and financial aspects of the system proposed for Iran for 2030. The costs are for a WACC of 7%.

Water management and increase in water efficiency in different sectors are paramount to enabling Iran overcome the water crisis. However, for regions where there is high water demand but inadequate surface or groundwater available, transport of desalinated water, powered through renewable energy, from the Persian Gulf and Gulf of Oman is the next best alternative. Marjanizadeh et al. [49] evaluates the impacts of different policies and trends on the Karkheh river basin. It was found that in a scenario where agricultural, livelihood and environmental demands were addressed, wheat self-sufficiency of the country could not be satisfied. In such scenarios, seawater desalination can supplement the sustainable use of renewable water resources. Gohari et al. [50] evaluates the impact of inter-basin water transfer as a solution to the water scarcity. The study was done for the Zayandeh-Rud River Basin, one of the most important and water stressed river basins in Central Iran. The results showed that water transfer solutions are inadequate and provide misconceptions of water availability in a river basin. Gohari et al. [50] stressed the need for improvement of irrigation efficiency, cultivation of water-efficient crops and water demand management to overcome future water scarcity issues. As illustrated in this research, renewable energy powered seawater desalination can aid to relieve the water stress in this river basin. The potential for desalination to aid

in alleviating water scarcity, in conjunction with other water management tools and policies, has also been discussed by Zetland [51].

Despite the role that renewable energy based desalination can play in meeting Iran's water demand, the negative environmental impacts of the discharged brine from the desalination plants have to be considered. The recent paper by Jones et al. [52] highlights the fact that the Gulf countries, such as UAE, Qatar and Kuwait, account for more than half of the world's brine discharge. Therefore, the rise of the desalination sector in Iran will contribute to the brine discharged, further threatening the ecology of the Gulf. Countries such as USA and Australia have adopted strategies like mixing brine with alternative water sources (treated waste water or water used for power plants) before discharge and the use of pressurized nozzles to spray the brine to prevent the brine settling [34]. Jones et al. [52] also discuss these concepts and the idea of harvesting scarce metals such as lithium from the brine. While the latter concept is only in its infancy, the ability to obtain precious metals from desalination brine at reasonable costs would create new economic opportunities.

Meanwhile various researchers have already analyzed the glaring potential for Iran to adopt renewable energy technologies and set up an effective energy strategy for the country. Saleki [53] investigated the potential for solar PV and wind power integration in Tehran to power the city's residential and commercial sectors. The results indicate that solar PV currently offers the most lucrative solution for small-scale projects. Aghahosseini et al. [28] have analysed a 100% renewable energy system for the power, desalination and industrial synthetic natural gas (SNG) production in Iran by the year 2030. The integrated scenario accounts for the power sector electricity demand as well as that of SWRO desalination and industrial SNG production in Iran. It is concluded that the additional flexibility offered by the desalination system and the industrial gas demand sector reduces the specific energy system LCOE. Further expanding on this research, Ghorbani et al. [29, 30] present a least-cost energy transition pathway for Iran, from the current fossil-based power system to a 100% renewable energy based system by 2050. The work takes into account the existing fossil based power plants in Iran and discontinues the plants based on the lifetimes. The 2050 levelised cost of electricity and the levelised cost of water respectively is about 41 €/MWh and 0.77 €/m^3. The combination of solar PV and battery storage provides the most lucrative solution to meet Iran's electricity demands. Thus, this research presents a blueprint for Iran's energy transition.

5. Conclusions

An energy model was used to estimate the viability of meeting the 2030 Iranian water demand, based on the optimistic scenario, with SWRO plants powered by renewable energy. Hybrid renewable energy power plants offer higher full load hours and therefore allow for better utilization of the desalination plant capacity. The 2030 costs for SWRO desalination and different renewable energy technologies were used.

The total desalination demand of Iran by 2030 is estimated to be 199 million m^3/day. The least cost system is found to be a combination of PV fixed-tilted, PV single-axis tracking, wind energy, battery and PtG power plants. The LCOW range is predominantly between 1.0 €/m^3 and 2.50 €/m^3. The current LCOW of fossil powered SWRO plants, excluding water transportation, in Iran is around 0.70 €/m^3, compared to about 1.0 €/m^3 based on 100% renewable energy along the coastlines and including transportation cost. The vertical transport infrastructure has the highest contribution to the final LCOW.

The work shows that in the near future, SWRO plants powered by renewable energy will produce water at similar prices to that of today's fossil powered plants in Iran. Depending on the terrain, the water transportation costs can contribute significantly to the final LCOW.

However, there are gaps in the research data, specific for Iran. These can be summarised as below:

1. Lacking updated water transportation costs, specifically for Iran accounting for factors like the local soil condition and infrastructure availability (like roads and electrical grid).
2. Modelling desalination demand needs of Iran after water management strategies are implemented. This is in particular for the agricultural sector of Iran that currently accounts for 90% of the country's water demand. Future water demand should also consider the complete removal of fossil fuel powered thermal power plants. These strategies further reduce the desalination demand of the country. By filling in the data gaps, a more accurate model of the future Iranian water scenario and water production costs can be built. This will enable a better understanding of the potential role for SWRO desalination and renewable energy systems in meeting the water supply challenges of Iran in the decades to come.

Acknowledgements:

The LUT authors gratefully acknowledge the scholarship offered by the Reiner Lemoine Foundation, public financing of Tekes, the Finnish Funding Agency for Innovation, for the 'Neo-Carbon Energy' project under the number 40101/14. We also thank Michael Child for proofreading and Narges Ghorbani for suggestion of articles relevant to the water crisis in Iran. The authors acknowledge that all data used in this study is available in the references cited.

References

[1] Luo T, Young R, Reig P, Aqueduct Projected Water Stress Country Rankings. Technical Note. Washington, D.C.: World Resources Institute, August 2015. https://www.wri.org/publication/aqueduct-projected-water-stress-country-rankings

[2] Gleeson T, Wada Y, Bierkens M F P, van Beek L P H, Water Balance of Global Aquifers Revealed by Groundwater Footprint, Nature, 488 (7410) (2012) pages 197–200. https://doi.org/10.1038/nature11295

[3] Joodaki G, Wahr J, Swenson S, Estimating the human contribution to groundwater depletion in the Middle East, from GRACE data, land surface models, and well observations, Water Resources Research, 50 (3) (2014) pages 2679–2692, https://doi.org/10.1002/2013WR014633

[4] Gorjian S, Ghobadian B, Solar Desalination: A sustainable solution to the water crisis in Iran, Renewable and Sustainable Energy Reviews, 48 (2015) pages 571–584, https://doi.org/10.1016/j.rser.2015.04.009

[5] Heinrich Böll Stiftung, Small Media, Paradise Lost? Developing solutions to Irans environmental crisis, Berlin, Germany, London, United Kingdom, 2016. https://smallmedia.org.uk/work/paradise-lost-irans-environmental-crisis

[6] Alipour S, Motgah M, Sharifi M A, Walter T R, InSAR Time Series investigation of Land Subsidence due to Groundwater Overex ploitation in Tehran, Iran. *Second Workshop on Use of Remote Sensing Techniques for Monitoring Volcanoes and Seismogenic Areas,* Naples, 2008, pages. 1–5, http://www.volcanotectonics.de/reprints/Alipour_IEEE2008.pdf

[7] Madani K, Water management in Iran: what is causing the looming crisis? Journal of Environmental Studies Science, 4 (4) (2014) pages 315–328, https://doi.org/10.1007/s13412–014–0182–z

[8] Asr Iran News and Analysis Website, Latest statistics on the status of dams in Iran, Tehran, 2017, https://goo.gl/ihdBTT

[9] Foltz R C, Iran's water crisis: Cultural, Political and Ethical dimensions. In: Journal of Agricultural and Environmental Ethics, 15 (4) (2002) pages 357–380, https://link.springer.com/article/10.1023/A:1021268621490

[10] Tahbaz M, Environmental challenges in Today's Iran, Iranian Studies, 49 (6) (2016), pages 943–961, https://doi.org/10.1080/00210862.2016.1241624

[11] [GWI] - Global Water Intelligence, DesalData: Iran Country Profile, Oxford, United Kingdom, 2016, www.desaldata.com/countries/67

[12] Tasnim News Agency, Iran to supply drinking water to 16 provinces through desalination: Minister, Tehran, Iran, 2015, http://www.tasnimnews.com/en/news/2015/11/03/906669/iran-to-supply-drinking-water-to-16-provinces-through-desalination-minister.

[13] The Iran Project, Iran diverting water from Gulf of Oman inwards, Qom, Iran, 2017, http://theiranproject.com/blog/2017/03/23/iran-diverting-water-gulf-oman-inwards/

[14] Collins G, Iran's looming water bankruptcy, Center for Energy Studies, Rice University's Baker Institute for Public Policy, Houston, 2017, https://www.bakerinstitute.org/research/irans-looming-water-bankruptcy/

[15] Financial Tribune, Desalination Plant Starts Operation in Iran's Bandar Abbas, Tehran, Iran, 2018, https://financialtribune.com/articles/energy/95532/desalination-plant-starts-operation-in-irans-bandar-abbas

[16] Gude V G, Desalination and sustainability – An appraisal and current perspective, Water Research, 89 (2016) pages 87-106, https://doi.org/10.1016/j.watres.2015.11.012

[17] Burn S, Hoang M, Zarzo D, Olewniak F, Campos E, Desalination techniques – A review of the opportunities for desalination in agriculture, Desalination, 364 (2015) pages 2-16, https://doi.org/10.1016/j.desal.2015.01.041

[18] Ghaffour N, Missimer M T, Amy L G, Technical review and evaluation of the economics of water desalination: Current and future challenges for better water supply sustainability, Desalination, 309 (2013) pages 197-207, https://doi.org/10.1016/j.desal.2012.10.015

[19] Grubert A E, Stillwell A S, Webber M E, Where does solar-aided seawater desalination make sense? A method for identifying suitable sites. Desalination, 339 (2014) pages 10–17, https://doi.org/10.1016/j.desal.2014.02.004

[20] Lienhard J H V, Jameel A L, Foreword for Special Issue: Energy and Desalination, Desalination, 366 (2015) page 1, http://dx.doi.org/10.1016/j.desal.2015.04.004

[21] Mentis D, Karalis G, Zervos A, Howells M, Taliotis C, Bazilian M, Rogner H, Desalination using renewable energy sources on the arid islands of the South Aegean Sea, Energy, 94 (2016) pages 262–272, https://doi.org/10.1016/j.energy.2015.11.003

[22] Novosel T, Cosic B, Puksec T, Krajacic G, Duic N, Mathiesen B V, Lund H, Mustafa M, Integration of renewables and reverse osmosis desalination – Case study for the Jordanian energy system with a high share of wind and photovoltaics, Energy, 92 (2015) pages 270–278, https://doi.org/10.1016/j.energy.2015.06.057

[23] Razmjoo A A, Sumper A, Investigating energy sustainability indicators for developing countries, International Journal of Sustainable Energy Planning and Management, 21 (2019) pages 59-76, https://doi.org/10.5278/ijsepm.2019.21.5

[24] Connolly D, Mathiesen B V, A technical and economic analysis of one potential pathway to a 100% renewable energy systems, International Journal of Sustainable Energy Planning and Management, 1 (2014) pages 7-28, https://doi.org/10.5278/ijsepm.2014.1.2

[25] Hansen Kenneth, Christian Breyer, Henrik Lund, Status and perspectives on 100% renewable energy systems, Energy, 175 (2019) pages 471-480, https://doi.org/10.1016/j.energy.2019.03.092

[26] Østergaard P A, Lund H, Mathiesen B V, Energy system impacts of desalination in Jordan, International Journal of Sustainable Energy Planning and Management, 1 (2014) pages 29-40, https://doi.org/10.5278/ijsepm.2014.1.3

[27] Caldera U, Bogdanov D, Breyer Ch, Local cost of seawater RO desalination based on solar PV and wind energy: A global estimate, Desalination, 385 (2016) pages 207-216, https://doi.org/10.1016/j.desal.2016.02.004

[28] Aghahosseini A, Bogdanov D, Ghorbani N, Breyer Ch, The role of a 100% renewable energy system for the future of Iran: Integrating solar PV, wind energy, hydropower and storage, International Journal of Environmental Science and Technology, 15 (1) (2017) pages 17-36, http://dx.doi.org/10.1007/s13762–017–1373–4

[29] Ghorbani N, Aghahosseini A, Breyer Ch, Transition to a 100% renewable energy system and the role of storage technologies: A case study of Iran, Energy Procedia, 135 (2017) pages 23-36, https://doi.org/10.1016/j.egypro.2017.09.484

[30] Ghorbani N, Aghahosseini A, Breyer C, Assessment of a cost-optimal power system fully based on renewable energy for Iran by 2050 - Achieving net-zero greenhouse gas emissions and overcoming the water crisis, Renewable Energy 146 (2020) pages 125-148, https://doi.org/10.1016/j.renene.2019.06.079

[31] Bogdanov D, Farfan J, Sadovskaia K, Aghahosseini A, Child M, Gulagi A, A S Oyewo, Barbosa L de S N S, Breyer C, Radical transformation pathway towards sustainable electricity via evolutionary steps, Nature Communications 10 (2019) (1077), https://doi.org/10.1038/s41467–019–08855–1

[32] Breyer Ch, Bogdanov D, Gulagi A, Aghahosseini A, Barbosa L S N S, Koskinen O, Barasa M, Caldera U, Afanasyeva S, Child M, Farfan J, Vainikka P, On the Role of Solar Photovoltaics in Global Energy Transition Scenarios, Progress in Photovoltaics: Research and Applications, 25 (2017) pages 727-745, https://doi.org/10.1002/pip.2885

[33] [CAT] - Center for Alternative Technology , Who is getting ready for zero? A report on the state of play of zero carbon modelling, Powys in Wales, United Kingdom 2015, http://zerocarbonbritain.org/en/ready-for-zero

[34] Caldera U, Breyer Ch, Learning curve for seawater reverse osmosis desalination plants: Capital cost trend of the past, present, and future, Water Resources Research, 53 (12) (2017) pages 10523-10538, https://doi.org/10.1002/2017WR021402

[35] Gassert F, Luck M, Landis M, Reig P, Shiao T, Aqueduct Global Maps 2.1: Constructing Decision-Relevant Global Water Risk Indicators. Working Paper. Washington, DC: World Resources Institute 2014. https://www.wri.org/publication/aqueduct-global-maps-21-indicators

[36] Faramarzi M, Abbaspour C K, Schulin R, Yang H, Modelling blue and green water resources availability in Iran, Hydrological Processes, 23 (2009) pages 486-501, https://doi.org/10.1002/hyp.7160

[37] Karbassi A, Bidhendi G N, Pejman A, Bidhendi M E, Environmental impacts of desalination on the ecology of Lake Urmia. In: Journal of Great Lakes Research, 36 (3) (2010) pages 419-424, https://doi.org/10.1016/j.jglr.2010.06.004

[38] Mirchi A, Madani K, A grand but faulty vision for Iran's water problems, Tehran Bureau, Guardian, London, United Kingdom 2016, https://www.theguardian.com/world/2016/may/09/iran-desalination-water

[39] Spang E S, Moomaw W R, Gallagher K S, Kirshen P H, Marks D H , The water consumption of energy production: an international comparison, Environmental Research Letters, 9 (105002) (2014) pages 14 , https://doi.org/10.1088/1748-9326/9/10/105002

[40] [ETIP-PV] European Technology and Innovation Platform Photovoltaics, The true competitiveness of solar PV - A European case study. ETIP-PV, Munich 2017, https://etip-pv.eu/publications/etip-pv-publications/

[41] Fraunhofer ISE, Current and Future Cost of Photovoltaics. Long-term Scenarios for Market Development, System Prices and LCOE of Utility-Scale PV Systems, study on behalf of Agora Energiewende, Freiburg and Berlin 2015, https://www.ise.fraunhofer.de/en/publications/studies/studie-current-and-future-cost-of-photovoltaics-long-term-scenarios-for-market-development-system-prices-and-lcoe-of-utility-scale-pv-systems.html

[42] Amante C, B W Eakins, ETOPO1 1 Arc-Minute Global Relief Model: Procedures, Data Sources and Analysis, NOAA Technical Memorandum NESDIS NGDC-24. National Geophysical Data Center, NOAA, 2009, https://www.ngdc.noaa.gov/mgg/global/relief/ETOPO1/docs/ETOPO1.pdf

[43] Stackhouse PW, Whitlock CH (eds), Surface meteorology and solar energy (SSE) release 6.0, NASA SSE 6.0, Earth Science Enterprise Program, National Aeronautic and Space Administration (NASA), Langley (2008). http://eosweb.larc.nasa.gov/sse/

[44] Stackhouse PW, Whitlock CH (eds), Surface meteorology and solar energy (SSE) release 6.0 methodology, NASA SSE 6.0, Earth Science Enterprise Program. National Aeronautic and

Space Administration (NASA), Langley (2009). http://eosweb.larc.nasa.gov/sse/documents/SSE6Methodology.pdf

[45] Stetter D, Enhancement of the REMix energy system model: global renewable energy potentials optimized power plant siting and scenario validation. Dissertation, Faculty of Energy,Process- and Bio-Engineering, University of Stuttgart (2012)

[46] Luck M, Landis M, Gassert F, Aqueduct Water Stress Projections: Decadal projections of water supply and demand using CMIP5 GCMs. Washington DC, World Resources Institute, 2015, www.wri.org/sites/default/files/aqueduct-water-stress-projections-technical-note.pdf

[47] [IPCC] – Intergovernmental Panel on Climate Change, Climate Change 2015: Synthesis Report – Summary for Policymakers. IPCC, Geneva, 2014, www.ipcc.ch

[48] Food and Agricultural Organisation of the United Nations , AQUASTAT database, FAO, Rome, Italy, 2015, www.fao.org/nr/water/aquastat/data/query/index.html?lang=en

[49] Marjanizadeh S , Fraiture de C, Loiskandl W, Food and water scenarios for the Karkheh River Basin, Iran, Water International, 35 (2010) pages 409-424, https://doi.org/10.1080/02508060.2010.506263

[50] Gohari A, Eslamian S, Mirchi A, Abedi-Koupaei J, Bavani A M, Madani K, Water transfer as a solution to water shortage: A fix that can Backfire, Journal of Hydrology, 491 (2013) 23 – 39, https://doi.org/10.1016/j.jhydrol.2013.03.021

[51] David Z, Desalination and the commons: tragedy or triumph? International Journal of Water Resources Development, 33 (6) (2015) pages 890-906, https://doi.org/10.1080/07900627.2016.1235015

[52] Jones E, Qadir M, Vliet M T H V, Smakhtin V, Kang S, The state of desalination and brine production: A global outlook. Science of the Total Environment, 657 (2019) pages 1343-1356, https://doi.org/10.1016/j.scitotenv.2018.12.076

[53] Saleki S, Introducing multi-stage qualification for micro-level decision-making (MSQMLDM) method in the energy sector – a case study of photovoltaic and wind power in Tehran, International Journal of Sustainable Energy Planning and Management, 17 (2017) pages 61 – 78, https://doi.org/10.5278/ijsepm.2018.17.6

Publication III

Caldera, U., Bogdanov D., Afanasyeva S. and Breyer, C.
Role of seawater desalination in the management of an integrated water and 100% renewable energy based power sector in Saudi Arabia

Reprinted with permission from
Water
Vol. 10, pp 1 – 32, 3, 2017

water

MDPI

Article

Role of Seawater Desalination in the Management of an Integrated Water and 100% Renewable Energy Based Power Sector in Saudi Arabia

Upeksha Caldera *, Dmitrii Bogdanov, Svetlana Afanasyeva and Christian Breyer

School of Energy Systems, Lappeenranta University of Technology, Skinnarilankatu 34, 53850 Lappeenranta, Finland; dmitrii.bogdanov@lut.fi (D.B.); svetlana.afanasyeva@lut.fi (S.A.); christian.breyer@lut.fi (C.B.)

* Correspondence: upeksha.caldera@lut.fi

Received: 19 November 2017; Accepted: 20 December 2017; Published: 22 December 2017

Abstract: This work presents a pathway for Saudi Arabia to transition from the 2015 power structure to a 100% renewable energy-based system by 2050 and investigates the benefits of integrating the power sector with the growing desalination sector. Saudi Arabia can achieve 100% renewable energy power system by 2040 while meeting increasing water demand through seawater reverse osmosis (SWRO) and multiple effect distillation (MED) desalination plants. The dominating renewable energy sources are PV single-axis tracking and wind power plants with 243 GW and 83 GW, respectively. The levelised cost of electricity (LCOE) of the 2040 system is 49 €/MWh and decreases to 41 €/MWh by 2050. Corresponding levelised cost of water (LCOW) is found to be 0.8 €/m^3 and 0.6 €/m^3. PV single-axis tracking dominates the power sector. By 2050 solar PV accounts for 79% of total electricity generation. Battery storage accounts for 41% of total electricity demand. In the integrated scenario, due to flexibility provided by SWRO plants, there is a reduced demand for battery storage and power-to-gas (PtG) plants as well as a reduction in curtailment. Thus, the annual levelised costs of the integrated scenario is found to be 1–3% less than the non-integrated scenario.

Keywords: 100% renewable energy; Saudi Arabia; energy transition; desalination; solar PV; wind energy; sector integration

1. Introduction

The Kingdom of Saudi Arabia (KSA) is the largest country in the Arabian Peninsula and is the 13th largest in the world. As of 2015, the Kingdom had a population of approximately 31,540,000—the highest among the Gulf Cooperation Council (GCC) countries [1,2]. Located between the Persian Gulf and the Red Sea, Saudi Arabia is also one of the largest arid countries without any permanent rivers or lakes. While the global average renewable water resource per capita per year is 6000 m^3, Saudi Arabia has only 84.8 m^3/(capita·a) [3]. In spite of the water scarcity, Saudi Arabia has the third highest water consumption per capita at 250 L/(capita·d) [3]. This is only behind the United States and Canada. The country's water demand is expected to increase by 56% by 2035. Meanwhile, at the current rate of water withdrawal, ground water aquifers are expected to provide potable water only for the next 10–30 years [4].

To augment the fresh water resources, Saudi Arabia relies on seawater desalination, particularly to meet the municipal and industrial water demands. In 2010, 58% of the country's total water demand was met through non-renewable ground water resources, 33.5% by surface water and renewable ground water, 6% by desalinated water and 2.2% by waste water reuse [5]. In 2014, desalinated water is estimated to have met 60% of KSA's municipal water demand [6]. By the end of 2015, Saudi Arabia accounted for 15% of the global installed desalination capacity [5]. With the diminishing of fresh water resources, seawater desalination is expected to play a pivotal role in meeting Saudi Arabia's future

water demands. However, desalination is an energy intensive process compared to traditional water treatment methods. Saudi Arabia is reported to use 25% of the domestic oil and gas production in desalination plants and the share is expected to increase to 50% by 2030 [7]. A report by General Electric (GE) suggests that Saudi Arabia requires 300,000 barrels of oil per day for the desalination plants on the country's Eastern and Western coasts [8].

Saudi Arabia has 1/5th of the world's proven oil reserves and is the largest producer and exporter of petroleum products [9]. In addition, KSA is the 9th largest exporter of natural gas [9]. Saudi Arabia's economy is based on oil revenues and during the time period 2010–2013, oil revenues contributed up to 91% of the country's national income [10]. This is reflected in the recent low oil prices and the resulting slower growth of the Saudi economy. Al Bassam [10] explains that although the government has had plans to diversify the economy and decouple economic growth from oil, there has in fact been an increase in dependence on oil revenues over the last few years. In addition to the low oil prices, growing concern is the share of local fossil fuel reserves, driven by increasing income and population, being used to meet the country's energy demand. According to the King Abdullah City for Atomic and Renewable Energy (KACARE) [11], the country's demand for fossil fuels is expected to grow from 3.8 million barrels of oil equivalent in 2010 to 8.3 million barrels of oil equivalent in 2028. Moser et al. [12] suggests that at the current rate of consumption, Saudi Arabia could become an oil importer by 2030. By 2015, Saudi Arabia's power plants capacities were almost equally separated into oil-based thermal power plants and gas-based power plants [13].

Economic reforms have been discussed in the past but it is only recently that reforms have been discussed with haste. A report in the Guardian [14] suggests that swift actions were triggered by the 100 billion € deficit the Saudi government incurred in 2015. Consequently, in April 2016, King Salman bin Abdulaziz presented details of the Saudi vision 2030 plan and heralded a Saudi future without oil [14]. A key component of the new vision is the growth of Saudi Arabia's renewable energy sector for both power and water desalination. It is planned to have 9.5 GW of renewable capacity by 2023, as an initial stage to meet the country's increasing energy demands [15]. According to a recent article [16], the Saudi Energy Minister has discussed the Kingdom's visions to push installed renewable energy (RE) capacities higher to 10 GW by 2023.

In spite of the country's wealth of solar and wind resources, Saudi Arabia had only 83 MW of renewable power plants, all solar photovoltaic installations, by early 2015 [13]. Figure 1 presents the total installed capacities, by the beginning of 2015, in Saudi Arabia and illustrates the almost complete reliance on oil and gas in the current power sector [13]. The country lies within the sunbelt region of the world and the average population weighted global horizontal irradiation is estimated to be 2158 kWh/(m^2·a) [17,18]. According to Yamada [19], the potential for solar energy in Saudi Arabia is finally being acknowledged with the Saudi government referring to solar energy as 'yellow oil'. The recent bids for 300 MW of solar PV in Saudi Arabia is set to end with an electricity production cost as low as 1.78 USD cents/kWh—the lowest bid to date [20]. With 7 out of the 8 bids placed for the 300 MW installation being less than 3 USD cents/kWh, the new threshold for large scale projects in the MENA region is being discussed to be as little as 3 USD cents/kWh [21]. Further to these developments, the Saudi Public Investment Fund together with the SoftBank Vision Fund, has confirmed the construction of a 3 GW solar and storage project in 2018 [22]. This would enable to meet one-third of Saudi Arabia's renewable energy capacity of 9.5 GW by 2023.

Table 1 illustrates the energy consumption of the most prevalent desalination technologies in Saudi Arabia [23]. In the past, Saudi Arabia has relied on thermal desalination technologies. However, due to the lower energy consumption and improvement in technology, reverse osmosis is expected to dominate the Saudi market in the future [5].

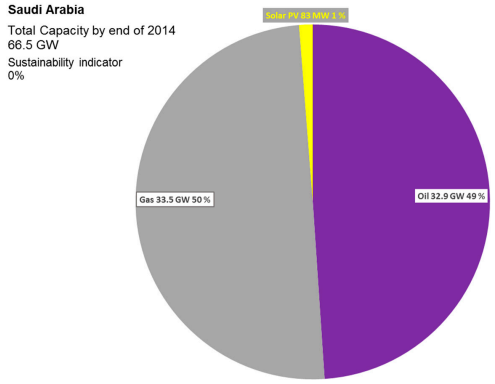

Figure 1. Total Installed Capacities by the beginning of 2015 in Saudi Arabia [13].

Table 1. Average energy consumption of prevalent seawater desalination technologies in the KSA [23].

Desalination Technology	Electrical Energy Consumption (kWh_e/m^3)	Thermal Energy Consumption (kWh_{th}/m^3)
Seawater Reverse Osmosis (SWRO)	4.0	-
Multi Stage Flash (MSF)	2.5–5.0	85
Multiple Effect Distillation (MED)	2.0–2.5	65

In Caldera et al. [24], it was shown that the global water demand of 2030 can be met by seawater reverse osmosis (SWRO) plants powered by 100% hybrid renewable energy power plants at a cost level competitive with that of fossil powered SWRO plants today. This system eliminates the reliance of SWRO desalination plants on non-renewable fossil fuels and concerns about greenhouse gas emissions. Meanwhile, reflecting the Saudi government's vision of high renewable energy capacities, there is recent literature that discusses the 100% renewable energy transition of different countries and regions [25–32], as well as detailed visualization of respective electricity systems [33].

In this paper, motivated by the growing demand for seawater desalination in Saudi Arabia and transition towards 100% renewable energy power systems, we pose the following research question: What are the impacts on Saudi Arabia's electricity and water production costs when the seawater desalination demand is integrated into the country's 100% renewable energy (RE)-based power sector? The energy transition pathway, for Saudi Arabia, from the current fossil-based power system to a 100% RE-based system is first found. Then, the seawater desalination demand is integrated into the power system, to understand the impacts on the cost of the power and water sectors. The excess heat present in the energy system is utilized for the thermal desalination plants during the transition

In addition, the transition accounts for the non-energetic industrial gas demand of Saudi Arabia. During the transition, the non-energy demand for natural gas by the Saudi industry is increasingly met through synthetic natural gas production (SNG). Power to gas plants (PtG) are used to produce SNG from renewable electricity generation [34,35] and integrated into the power system. During the production of the SNG, there may be excess heat produced that can contribute to the operation of thermal desalination plants.

Thus, the results will present an optimal transition path for Saudi Arabia to manage the country's future electricity, water and gas demands through a 100% RE system.

2. Methodology

2.1. Overview

The key objective of our work is to understand the role that seawater desalination can play in the optimal transition of Saudi Arabia's 2015 power sector a 100% renewable energy power sector by 2050. The approach that was taken to answer this research question can be summarized as follows:

1. The energy transition from the current (as of the beginning of 2015) fossil-based power system in KSA to a 100% renewable energy-based power system by 2050, in 5 year time steps, is found. After 2015, there are no new fossil powered thermal plants allowed in order to achieve the target of a 100% RE-based power system. The existing fossil-based power systems are phased out based on their lifetimes. The increase in total electricity demand and population over the years is accounted for. The optimal mix of renewable power systems to replace the phased out fossil power systems are found and the resulting system's levelised cost of electricity (LCOE) is found for every time step.
2. The non-energy industrial gas demand of Saudi Arabia, from 2015 to 2050 is found and integrated into the power system. Figure 6 presents the projected growth in the industrial gas demand in Saudi Arabia. To attain a 100% renewable energy future, our work assumes that over time the industrial gas demand is met from synthetic natural gas (SNG). This can be achieved through power-to-gas plants (PtG) that comprise of two processes already used in industry: electrolysis and methanation [34,35]. PtG plants convert renewable electricity to renewable methane that can be stored in the existing gas infrastructure and used as conventional natural gas or for the industry.
3. Seawater desalination demand in KSA from 2015 to 2050 is determined and the corresponding desalination capacities integrated into the system. After 2015, the model is allowed to only install SWRO plants. This is based on the increasing dominance of the technology in the Saudi Arabian desalination market. MED plants are considered due to the low thermal consumption and lower electricity demand than SWRO [23,36]. The heat from the power system is used to meet the thermal demand of MED plants. Multi stage flash (MSF) desalination capacities that were online up to 2015 are included and phased out based on the lifetimes. MSF stand alone plants are excluded due to the relatively higher thermal consumption compared to MED plants [23,36]. In addition, MED and MSF cogeneration plants are excluded due to the requirement for fossil powered thermal power plants [37]. According to a Water Desalination Report [38], the Ras Al Khair IWPP plant, the largest desalination plant in the world, is expected to be the last new MSF plant in KSA.
4. The energy transition for KSA from the 2015 fossil-based power system to the 100% renewable energy-based power system by 2050 is found with the gas sector and seawater desalination integrated. Ultimately, the total cost of the power, gas and water sectors are compared to determine the impacts of integrated seawater desalination in the energy system.

For the design and analysis of the energy transition, the energy model, used and further developed at LUT, is used [29,39–41]. The LUT Energy System Transition model is based on the linear optimization method with interior point optimization, and is designed in an hourly temporal and $0.45^\circ \times 0.45^\circ$ spatial resolution. The energy model allows for the design of local, national, regional or global energy systems. It is composed of all relevant power generation and storage technologies, respective installed capacities and different operation modes of these technologies. A key feature of the model is its flexibility and expandability besides the hourly resolution for a full real year.

The sections that follow present an overview of the technical and financial assumptions of the energy model, the power plants and seawater desalination plants. The data assumed for the time period from 2015–2050 are presented.

2.2. Model Overview

A key requirement of the LUT Energy Systems model is to match the power generation and demand for every hour of the applied year. The hourly modeling enables a more accurate system description including synergy effects of different system components for power system balance [29]. The aim of the system optimization is to minimize the total annual cost of the installed capacities of the different technologies, cost of energy generation and generation ramping. The full description of the model, its input data including RE resources and technical assumptions can be found in Bogdanov and Breyer [29] and Barbosa et al. [39].

The three main components of the energy model can be listed as:

- Technologies for the conversion of RE into electricity;
- Energy storage technologies;
- Energy sector bridging technologies enable the coupling of different electricity demand sectors. This provides further flexibility to the complete energy system, bringing down the overall system cost.

Aghahosseini et al. [40] describe the various components of the LUT Energy System model and how the model determines the optimal 100% renewable energy mix for Iran for the year 2030.

For Saudi Arabia, the model described by Aghahosseini et al. [40] was modified with the addition of thermal desalination technologies as another desalination technologies and a subsequent energy transition, i.e., the system setup found for one period had been adjusted by the capacities being beyond their technical lifetime as a starting value for incremental optimization for the new period. Figure 2 illustrates the modified energy model. For the energy transition, the model determines the optimal combination of the components that meets the electricity demand of every hour for the time period from 2015 to 2050, in 5 year time steps.

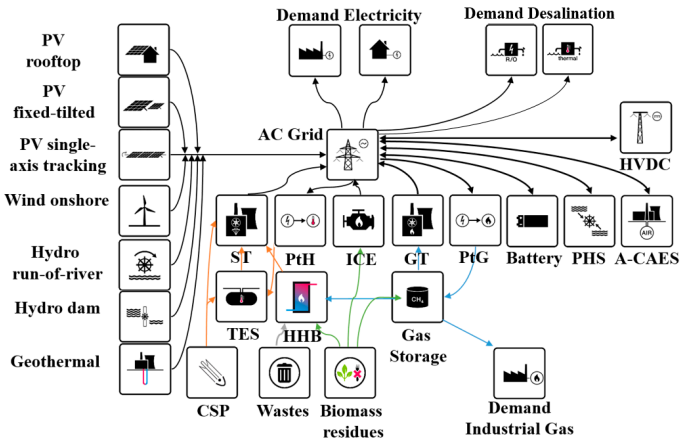

Figure 2. Block diagram of the LUT Energy Systems model used for Saudi Arabia.

2.3. Power Plant Capacities—Technical and Financial Assumptions

The average rate of increase in electricity demand in KSA is 6% and as of 2015, for a total population of 32,540,000, the total electricity consumption of the country was 289 TWh [42,43]. To determine the future energy system, the forecasted total energy demand numbers are required. The International Energy Agency assumes a compound annual growth rate of 2.7% for the Middle East [44]. This growth rate was applied to Saudi Arabia to project the future electricity consumption, as presented in Table 2. Figure 3 illustrates the hourly load profile for Saudi Arabia assumed for

2015 [42,43]. As expected, during the summer period of May to September, the highest loads occur. For the subsequent time periods, the load profile presented is varied depending on the total electricity consumption for the period. The capacity factor on the right y-axis indicates the percentage of the maximum load that is being required for a given point in time.

Table 2. Variation in the electrical energy consumption of Saudi Arabia from 2015 up to 2050 [44].

Year	Total Electricity Consumption (TWh)
2015	289
2020	330
2025	377
2030	431
2035	492
2040	563
2045	643
2050	734

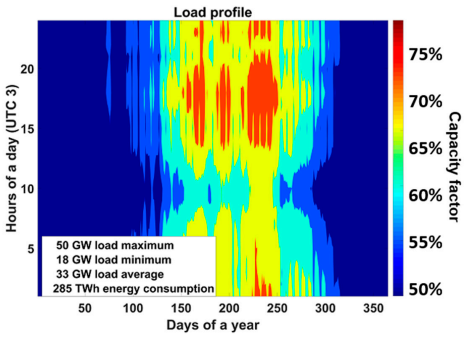

Figure 3. Aggregated load curve for the year 2015 for Saudi Arabia.

The model takes the 2015 installed power plant capacities, presented in Figure 1, corresponding lifetimes, total electrical energy demand, and optimizes the mix of renewable energy plants needed to be installed to achieve a 100% renewable energy power system by 2050. The optimization for each time period is carried out on basis of assumed costs and technological status of the renewable energy technologies. In the integrated scenario, the RE plants are optimized to also cater for the energy demands of the desalination and gas sectors.

The capital expenditures (capex), operational expenditures (opex) and efficiency variations of all the power sector components, from 2015 up to 2050, assumed in the model are presented in Appendix A (Tables A1 and A3). Figure 4 is a visual representation of the capex numbers. A learning curve approach based on several references, is used to identify the variation in capex for the different components. The references for the different components are presented in the Appendix A (Table A1).

The capex and opex numbers generally refer to a kW of electrical power. For the case of water electrolysis the capex and opex numbers refer to a kW of hydrogen thermal combustion energy, and for CO_2 direct air capture, methanation and gas storage to a kW of methane thermal combustion energy. The financial assumptions for storage systems refer to a kWh of electricity, and gas storage refers to a thermal kWh of methane at the lower heating value. Weighted average cost of capital (WACC) is set to 7% for all years. The technical assumptions concerning power to energy ratios for storage technologies, and efficiency numbers for generation and storage technologies are provided in the Appendix A (Tables A1 and A2).

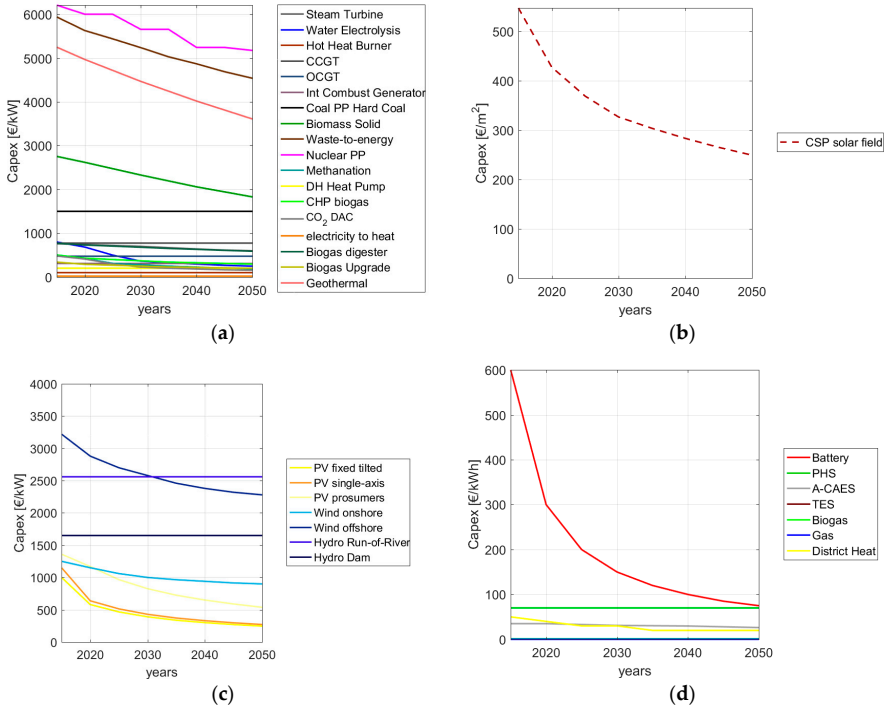

Figure 4. Variation in capex of power system components (**a**), CSP solar field (**b**), RE components (**c**) and storage components (**d**) assumed in the model.

To determine the capacities of the different renewable energy power plant components, it is necessary to understand the local resources available. The solar irradiation components and wind speed data, in a 0.45° × 0.45° spatial and hourly temporarily resolution, is obtained from the NASA [45,46] and reprocessed by the German Aerospace Center [29]. The wind speed data is provided for a height of 50 m. In the LUT Energy Systems model, due to higher performance, ENERCON 3 MW wind turbines (E-101, Enercon, Aurich, Germany), with a hub height of 150 m, are used [29]. The wind speed data from the German Aerospace Center is converted to the relevant wind speed at 150 m using the logarithmic wind shear law [29]. The approach discussed by Aghahosseini et al. [40] is used to identify the biomass and geothermal potential available in KSA. Table 3 presents the biomass and geothermal potential results for KSA and it is assumed that these are the amounts available for every time period from 2015 to 2050.

Table 3. Estimation of biomass potentials and geothermal energy potential for Saudi Arabia from 2015–2050.

Solid Waste (TWh_{th}/a)	Solid Biomass (TWh_{th}/a)	Biogas Sources (TWh_{th}/a)	Geothermal Potential (TWh_{th}/a)
1.92	4.14	1.97	57.53

Feed-in full load hours (FLH) for Saudi Arabia is also computed, as described in Bogdanov and Breyer [29], on the basis of the 0.45° × 0.45° spatially resolved data. The average FLH for CSP solar field, PV optimally tilted, PV single-axis tracking and wind power plants in Saudi Arabia are presented in Table 4. The average full load hours represent the number of hours in a year with the equivalent

maximum generation for the annually obtained yield, which is identical to the capacity factor derived by the average full load hours divided by 8760, the numbers of all hours in a year. Wind energy has the highest FLH, followed by PV single-axis tracking, CSP solar field and PV optimally tilted. Figure 5 presents the aggregated profiles of CSP solar field, wind energy power generation, solar PV generation (optimally tilted and single-axis tracking). The profiles represent the weighted average of the RE resource available as a percentage of the total respective RE resource potential of the country.

Table 4. Average full load hours (FLH) for CSP solar field, PV optimally tilted, PV single-axis tracking and wind onshore power plants in Saudi Arabia.

PV Single-Axis	PV Optimally Tilted	CSP	Wind Onshore
FLH	FLH	FLH	FLH
2443	1830	2382	2618

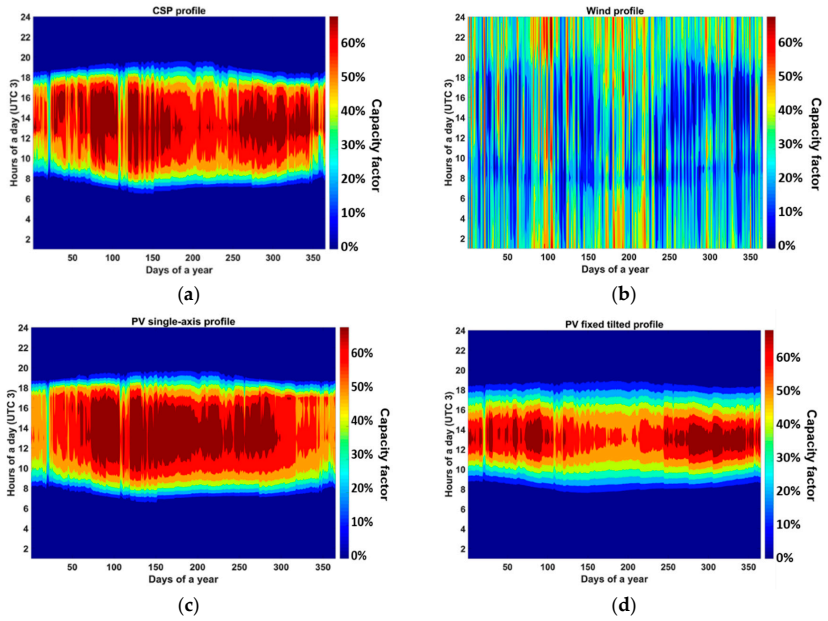

Figure 5. Aggregated feed in profiles in KSA for CSP solar fields (**a**), wind power plants (**b**), single-axis tracking PV (**c**) and optimally tilted PV (**d**).

The model specifies the upper limits and lower limits for the renewable energy power plant capacities. Lower limits are the installed capacities of renewable energy plants by 2015. For Saudi Arabia this is only 81.6 MW of solar PV plants as listed in Table 5. In periods after 2015, the lower limit is set to the capacity of the previous period adjusted by the capacities reached the end of their technical lifetime. The upper limits are calculated according to Bogdanov and Breyer [29] and the relevant results for KSA are listed in Table 6. For solid biomass residues, biogas and waste-to-energy plants it is assumed, due to energy efficiency reasons, that the available and specified amount of the fuel is used during the year.

Table 5. Lower limits of installed capacities [MW] considered in this study for Saudi Arabia.

Country	Solar PV
KSA	81.6

Table 6. Upper limits on installable capacities in Saudi Arabia in units of GW_{th} for CSP and GW_{el} for all other technologies.

Country	Area (1000 km^2)	Solar CSP	Solar PV	Wind
KSA	446.5	19347	9673	722

Tables A1 and A2, in the Appendix A, provide detailed technical and financial assumptions, from 2015 to 2050, for the energy system components used in this research for Saudi Arabia.

2.4. Seawater Desalination Capacities—Technical and Financial Assumptions

Table 7 represents the total online capacities of seawater desalination in Saudi Arabia by 2015 [47].

Table 7. Online capacities of seawater desalination in Saudi Arabia by 2015.

Desalination Technology	Total Online Capacity (m^3/day)
SWRO	2,736,238
MSF Stand Alone	1,519,777
MSF Cogeneration	2,727,021
MED Stand Alone	1,507,074
MED Cogeneration	975,371
Other technologies, including those that use brackish water	220,324

The desalination capacity required for the time period from 2015–2050 is determined using the methodology described in Caldera et al. [24]. The approach is based on the water stress and the water demand values in Saudi Arabia for an optimistic future scenario. The desalination capacities are calculated assuming a 100% utilization of the available renewable water resource. The National Water Strategy (NWS) for Saudi Arabia outlines specific amounts of non-renewable water to be consumed from 2015 up to 2040, such that by 2040 there is 5 billion m^3 of non-renewable water resource being withdrawn annually [48]. Therefore, the actual desalination demand also should take into account the usage of non-renewable water resources. For the model, the non-renewable water resource being withdrawn is deducted from the modelled desalination capacity to find the actual desalination capacity required. However, the non-renewable water resource numbers found in the NWS are based on a percentage of renewable water resource used. In the model, the desalination capacities are based on optimal use of the available renewable freshwater resource. As a result, the actual non-renewable water resource withdrawal decreases. This is ultimately used to find the actual desalination capacity required for the Kingdom of Saudi Arabia from 2015–2050. Table 8 represents the numbers and the final desalination capacities needed. In addition, the capacities online by 2015 are presented. This is less than the actual desalination demand in 2015. It has to be noted that other desalination technologies, such as brackish water reverse osmosis (BWRO), have been excluded from the present study. The desalination capacities in the following years are optimized by the model.

Table 8. Desalination capacities required to meet KSA's increasing total water demand.

	Unit	2015	2020	2025	2030	2035	2040	2045	2050
Population	mill	31.50	34.40	36.85	39.13	41.24	43.14	44.76	46.06
Total water demand	mill m^3/day	65.4	68.5	75.6	81.0	88.6	96.7	105.0	112.6
Desalination demand based on [21]	mill m^3/day	19.1	21.8	27.5	32.0	38.4	45.2	53.8	58.7
Final non-renewable water resource used	mill m^3/day	8.9	7.9	5.8	3.9	6.2	8.5.	0	0
Actual desalination demand	mill m^3/day	10.2	13.9	21.7	28.2	32.3	36.7	53.8	58.7
Installed capacities									
SWRO	mill m^3/day	2.7							
MSF Stand Alone	mill m^3/day	1.52							
MSF Cogeneration	mill m^3/day	2.73							
MED Stand Alone	mill m^3/day	1.57							
MED Cogeneration	mill m^3/day	0.95							

From 2015 onwards, SWRO and MED stand alone desalination plants are optimized to meet the increasing desalination demand. The thermal energy required for the MED stand alone plants are provided through excess heat in the system. The excess heat may be generated from the gas turbines, internal combustion generators, municipal waste incinerators and power-to-gas units. Based on the availability of heat in the system and the cost of required heat generation, the model optimizes the water production from MED stand alone plants.

MSF standalone plants are not installed after 2015. This is due to the higher thermal consumption compared to MED stand alone plants, as highlighted in Table 1. Similar to the MED stand alone plants, the already installed MSF standalone capacities utilize heat from the energy system. Mehzer et al. [49] explain the dependence of the MSF water production costs on the fuel cost. The water production cost has been reported to be 1 USD/m^3 for an oil price of 20 USD/barrel and 4 USD/m^3 for an unsubsidized oil price of 100 USD/barrel. As a result of technological improvements and lower energy consumption, Mehzer et al. [49] discuss the potential for MED to substitute MSF in future desalination markets. MED and MSF cogeneration plants online by 2015 are powered through natural gas, and depending on the cost effectiveness, the cogeneration plants are run to produce water and electricity. Gradually, the MSF desalination plants and MED cogeneration plants are decommissioned based on lifetime.

It has to be noted that there are other desalination technologies with smaller scale applications such as vapor compression and electro-dialysis [49,50]. There are more technologies being researched and developed such as forward osmosis and membrane distillation [46]. Gude and Nirmalakhandan [50,51] have developed a desalination technology that utilizes low grade heat, at about 60 °C, coupled with thermal energy storage, to produced potable water continuously. Meanwhile Inoue et al. [52] and Arnau et al. [53] present a means to desalinate and transport seawater using the difference in seawater and inland temperature. In this study, however, only the seawater desalination technologies that have the largest market shares and used in large scale applications are considered.

The technical and financial parameters of the desalination technologies from 2015–2050 are presented in the Appendix A (Table A2). Similarly, the capex, opex and energy consumption of the water transportation and water storage are presented. There is no variation in the latter numbers from the time period 2015 to 2050.

The future capex of the desalination technologies and the corresponding energy consumption was estimated as follows:

2.4.1. SWRO

1. Using the Global Water Intelligence (GWI) Desal Database, the average capex of plants of the capacity range of 10,000 m^3/day up to 50,000 m^3/day, contracted in all years from 1980–2015, was found [47]. It is assumed that all the plants to be built in Saudi Arabia in the future, would have a capacity of 50,000 m^3/day or higher. Then, the methodology discussed by Loutatidou et al. [54] to determine the EPC costs for SWRO desalination plants up to 2030 was utilized. In our study, this methodology was used to estimate the capex costs for SWRO plants of a capacity 50,000 m^3/day from 2020 up to 2050. The average capex value for 2015 was estimated from the GWI Desal Database.
2. Al Zahrani et al. [55] illustrate the energy consumption of SWRO plants with hydraulic turbines for seawater of different salinity levels. For 35 parts per million (ppm) salinity level, the energy consumption is approximately 3.1 kWh/m^3. Assuming that the other processes such as seawater intake, pretreatment, post-treatment and brine discharge take 1 kWh/m^3, the total energy consumption is 4.1 kWh/m^3. This is in line with a presentation [56] on the desalination plants in Masdar, UAE, where energy consumption of SWRO plants is estimated at 4.5 kWh/m^3. However, test plants built recently have an energy consumption of 3.3 kWh/m^3. These low energy consumption trends are also observed in recently built large SWRO plants such as Ghlalilah, in the United Arab Emirates [57]. The total energy consumption of this plant is estimated to

be just under 3 kWh/m^3 [57]. However, the larger scale plants built recently use a pressure exchanger as the energy recovery device (ERD). For the purpose of our work, it is assumed that, after 2015, all SWRO plants will utilize pressure exchangers. According to Al Zahrani [55], the energy consumption with a pressure exchanger is about 2.6 kWh/m^3. Thus, by 2020, it is assumed that the total energy consumption of the plants will drop to 3.6 kWh/m^3. This is feasible as there are currently large scale plants with similar or lower energy consumption values. Meanwhile, Elimelech et al. [58] present the optimal energy consumption of the SWRO plants from 1970–2008. It is shown that the decrease in energy consumption between 2004 and 2008 is 5%. From 2020 onwards, there is assumed to be about a 5% decrease in energy consumption every 5 years. Elimelech et al. [58] explain that the practical minimum energy consumption of a SWRO plant with a 50% recovery rate and seawater salinity of 35 ppm, is 1.56 kWh/m^3. Assuming 1 kWh/m^3 for the other processes, the total minimum energy consumption is about 2.56 kWh/m^3. Thus, by 2050, a total energy consumption of 2.6 kWh/m^3 is assumed.

2.4.2. MED

1. Reddy et al. [59] and Al-Mutaz et al. [60] discuss the advantages of MED with thermal vapor compression (TVC) over MED without vapor compression. For our model, it was assumed that the MED plants installed are MED-TVC plants due to the lower thermal energy consumption and the recent growth in MED-TVC installations. A report by Fichtner explains that MED-TVC plants are approximately 25% higher in capex than SWRO plants [36]. Thus, for every time period, the capex of MED-TVC was assumed to be 25% more than the corresponding SWRO capex. Moser et al. [61] explain that operating costs of MED-TVC are usually 3–3.3% of the capex. For our study, the opex was taken to be 3.3% of the capex.
2. The average Gain Output Ratio (GOR) of MED-TVC plants in 2015 was obtained from the GWI Desal database [47]. Fath et al. illustrate how the GOR of MED plants will improve in the coming decades [62]. Palenzuela et al. [63] explain that the GOR of MED-TVC plants are generally 20% higher than MED plants. Thus, for this work, the GOR numbers presented by Fath et al. were increased by 20%. From 2040 to 2050 there is assumed to be no increase in the GOR.

The thermal energy consumption in kWh/m^3 is determined from the corresponding GOR. The electrical energy consumption is assumed to be 1.5 kWh/m^3 for all the years as found in Fath et al. [62].

2.4.3. MSF

1. The MSF capex number for 2015 is obtained as an average of all MSF plants built in 2015 [47]. The general value of the GOR is about 8 for MSF plants located in Saudi Arabia, based on the GWI Desal Database.
2. It is assumed that all cogeneration plants in KSA are a combination of a MSF desalination plant and OCGT—unfired with Heat Recovery Generator System (HRGS) [37].
3. The power-to-water ratio (PWR) is specific for cogeneration plants and indicate the amount of power produced per m^3 of water produced a day. For MSF plants with an OCGT power plant and HRGS, this is about 2.25 kW/(m^3·d) [37]. The profits gained through the electricity produced by the cogeneration plants are used to offset the input gas costs. This applies to both the MSF and MED cogeneration plants.

The water production cost presented in this research takes into account the water transportation costs. In [24], we determined the 2030 desalination demand for the whole world on a 0.45° × 0.45° spatial resolution. In addition, we found the optimized vertical and horizontal water transportation distances for every desalination demand node. The optimized horizontal distance is the shortest distance from the desalination demand node to the coast line. The vertical height is the elevation between the desalination demand node and the optimized location on the coast line. The same

procedure was used to determine the desalination demand as well as optimized horizontal and vertical transportation distances, for every 5 year time step from 2015 to 2050, for Saudi Arabia.

For the current transition study we used the total desalination demand for every 5 year time step and the corresponding weighted average horizontal and vertical transportation distance. Table 9 illustrates the optimized horizontal and vertical distances for Saudi Arabia.

Table 9. Weighted average horizontal and vertical water pumping distances.

	Unit	2015	2020	2025	2030	2035	2040	2045	2050
Horizontal distance	km	280	273	269	265	266	267	268	269
Vertical distance	m	711	721	729	736	743	749	754	758

2.5. Synthetic Natural Gas Production—Technical and Financial Assumptions

Figure 6 illustrates the expected growth in non-energy industrial gas demand in Saudi Arabia [64]. In our model the aim is to ensure that by 2050, the non-energy industrial gas demand is met from renewable energy. In 2015, the industrial gas demand is met with fossil natural gas. However, over time, PtG plants produce the SNG required. The increase in cost of fossil natural gas over time and the decrease in cost of PtG plants, makes it viable to produce SNG.

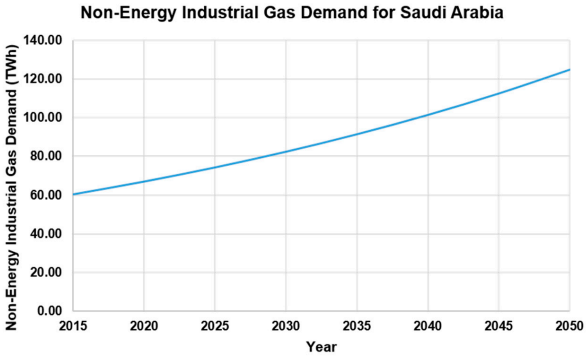

Figure 6. Industrial gas demand projection for Saudi Arabia from 2015 to 2050 [52].

3. Results

The following two scenarios are simulated by the model:

1. Non-integrated scenario

In this scenario, the model determines the optimal transition pathway for Saudi Arabia's power sector, discussed in Section 2.3, and the power plant capacities required for seawater desalination demand, discussed in Section 2.4. The gas sector is integrated with the power sector throughout from 2015 to 2050. Thus, the sum of the power plant capacities required for the three sectors present the total power capacities required to meet KSA's power, water and gas demands in the energy transition.

2. Integrated scenario

In this scenario, the seawater desalination demand and the gas demand are integrated into Saudi Arabia's power sector, throughout the transition from the fossil-based power system in 2015 up to a 100% renewable energy-based system in 2050. The desalination plants, integrated into the power system, will allow for the optimal use of the hourly energy produced by the renewable energy power plants. The excess energy produced by the renewable energy power plants can be stored as desalinated

water and, at times of low energy production, the stored water can be used. Thus, the desalination plants offer additional flexibility to the energy system.

The model determines the power capacities required for the integrated scenario and the two scenarios are compared to understand the impacts of the integrated desalination plants. The integration of the gas sector with the power sector in both scenarios, enables to identify the integration benefits, if any, of the desalination plants only.

In the following sections, the technical and financial results of the energy transition for the integrated scenario are presented. The financial results are ultimately compared with that of the non-integrated scenario to learn the impacts of integrated seawater desalination plants.

3.1. Integrated Scenario—Power Sector

Figure 7a presents the installed capacities of the different types of power plants required for the energy transition from 2015 up to 2050. The colors from top to bottom in the legend are shown from bottom to top in the figure. In 2015, the total power capacity was 66.4 GW, out of which 32.9 GW were internal combustion engines and 33 GW were gas turbines. The model is restricted from installing more fossil fuels thermal power plants after 2015 and can only install renewable technologies to meet the growing electricity demand. However, power-to-gas-based gas turbines are not restricted. Internal combustion generators are eliminated from the system by 2040 after exceeding their technical lifetime. Thermal power plants running on natural gas are also eliminated from the system by 2040. Power-to-gas-based electrolyser and methanation plants are used to produce synthetic natural gas (SNG) that is then used as fuel for existing open cycle gas turbines (OCGT) or combine cycle gas turbines (CCGT). The total capacity of all plants required by 2050 is about 600 GW. PV single-axis tracking accounts for 377 GW and wind power plants account for 83 GW of the 600 GW required by 2050. Figure 7b presents the electricity production of the different power plant categories. After 2030, electricity production from wind power plants remain constant at 217 TWh. The installed capacities of PV single-axis tracking continue to grow and start to dominate the Saudi power sector. By 2050, PV single-axis tacking contributes 922 TWh out of the total annual electricity generation of 1163 TWh, representing 79%. CSP plants for electricity generation are added from 2030 onwards but, by 2050, only account for 0.6% of the total electricity generation share. This is attributed to the higher costs of CSP for electricity generation compared to solar PV, based on the technical and financial assumptions in Appendix A (Table A1). Figure 7b also illustrates the diminishing use of fossil oil and gas in the energy system. The power capacities required for the energy transition can be found in the Appendix A (Table A4).

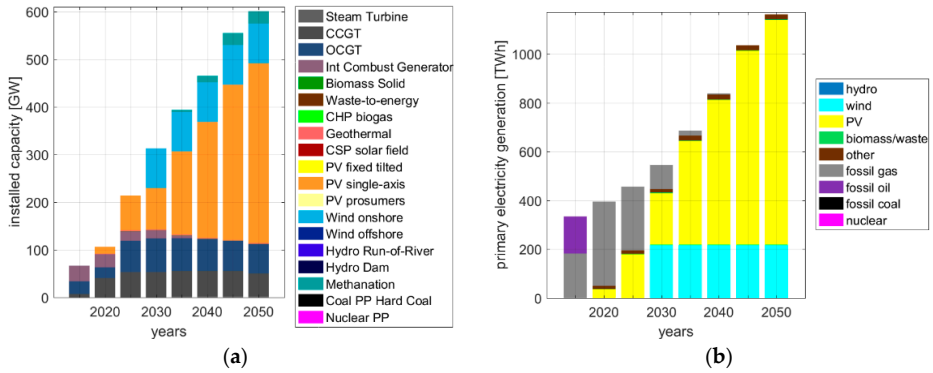

Figure 7. Installed capacities (**a**) and electricity produced (**b**) of the different power plants required from 2015 to 2050.

Figure 8a illustrates the full load hours (FLH) of the different power plants utilized by the model. The FLH of PV single-axis tracking, PV fixed tilted and wind onshore plants are constant at 2443, 1830 and 2618 h. The model determines the optimal FLH and the capacities of the power plants. The FLH of the internal combustion generator rapidly diminishes from 4625 to almost none by 2020. The high cost of oil renders the existing oil powered thermal power plants too expensive to run, since world market prices are taken into account to avoid subsidies for the energy system. In addition, the FLH of the OCGT reduces from 4756 FLH to zero FLH by 2030. The lower cost of the natural gas, in contrast to oil, still enables natural gas powered CCGT plants to be cost effective. However, after 2040, as shown in Figure 7b, there is no more contribution from natural gas powered thermal plants. The remaining CCGT plants are used with SNG to store and produce electricity as required in the Saudi power system.

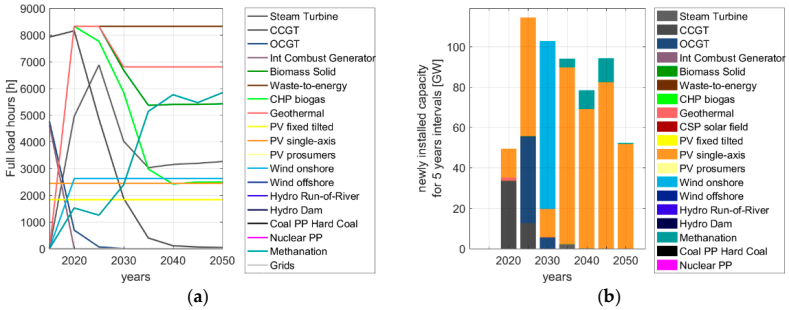

Figure 8. FLH variation of the different power plants used in model (**a**) and additional capacities of different power plants required from 2015 to 2050 (**b**).

Figure 8b represents the additional capacities of different power plants necessary to meet the growing electricity demand and to replace the fossil-based thermal power plants that are being phased out. Initially, there are more wind power plant installations than PV power plants. However, after 2030, the installation of wind power plants cease and PV single-axis tracking start to dominate the power sector. Methanation units are added for the first time in 2035, with additional capacities added until 2050, to meet the gas demands of the energy system and industrial gas demand through SNG.

Figure 9a represents the additionally installed storage capacities for every 5 years period. The large capacity of gas storage is required in 2045, and thereafter, less additional storage is required. Figure 9b represents the ratio of the total storage output for every time period. By 2025, electricity storage systems come into effect as it becomes a more cost effective option to balance the power system than the use of fossil powered thermal plants. By 2050, batteries provide a total output of about 413 TWh_{el} which accounts for about 41% of the total electricity demand and about 58% of the direct electricity supply.

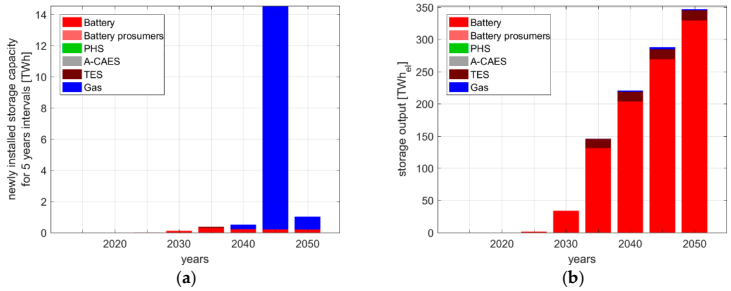

Figure 9. Additional storage capacity (**a**) and storage output (**b**) required from 2015 to 2050.

The total levelised cost of electricity of the system is the sum of the levelised cost of primary electricty generation (LCOE primary), levelised cost of storage (LCOS), levelised cost of curtailment (LCOC), fuel cost and the carbondioxide emission cost (CO_2 cost). Figure 10a represents the contribution of the different components to the total LCOE from 2015 to 2050. In 2015, the fuel cost accounts for the largest contribution due to the fuel prices of 52.50 €/MWh_{th} for oil and 21.8 €/MWh_{th} for gas. As the FLH of the fossil powered thermal plants decrease, as illustrated in Figure 8a, the fossil fuel consumption and consequently the contribution to the LCOE decreases. The OCGT storage and CCGT storage plants in Figure 8a refer to the gas plants utilising SNG.

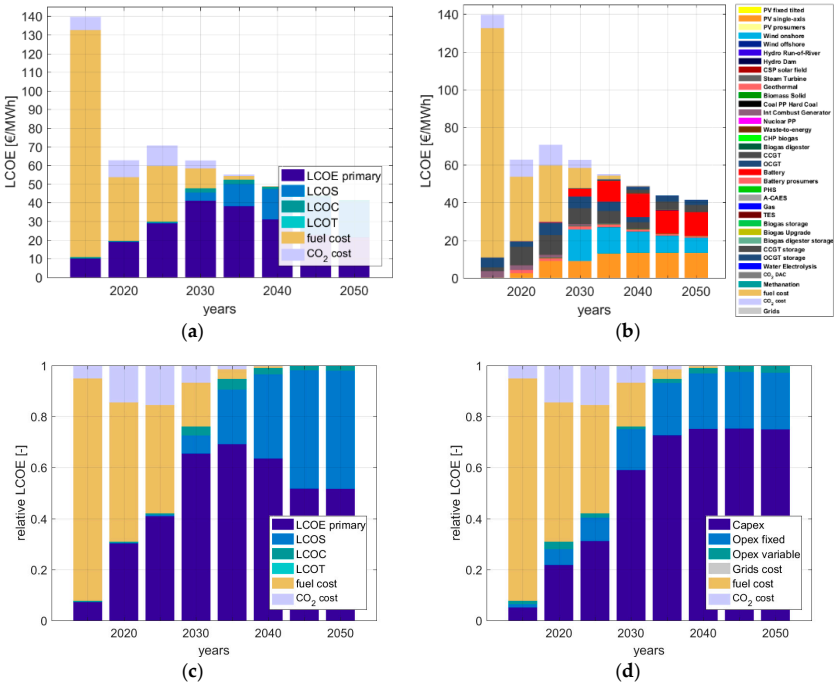

Figure 10. Contribution of different components (**a**), detailed contribution of components (**b**) relative contribution of different components (**c**) and relative contribution of financial components (**d**) to the total LCOE from 2015 to 2050.

The LCOC is as a result of curtailment of the excess energy produced by the renewable energy power plants. The remaining thermal power plants contribute to the CO_2 emissions cost. The batteries and gas storage contribute to the LCOS of the power system. The figure illustrates that with the transition to renewable power plants and the phasing out of the thermal powered plants, the total LCOE of the system decreases. By 2050, the LCOE is estimated to be about 41 €/MWh as opposed to 139 €/MWh in 2015. Figure 10b separates the LCOE primary and LCOS to the individual components and presents the specific contributions towards the LCOE. The rapid drop in LCOE from 2015 to 2020 is due to the phasing out of unsubsidized expensive oil power plants. This eliminates the large fuel cost that contribute towards the LCOE cost in 2015, as shown in Figure 10a,b. In 2020, the oil power plants are substituted by more economical solar PV and gas plants. By 2050, the largest contributors to the cost will be the PV single-axis tracking and battery plants. The contribution of wind decreases after 2030, due to no more wind plant installations and a highly competitive combination of hybrid PV-battery plants, as already found by Afanasyeva et al. for the case of Morocco [65]. However, there

is still a substantial contribution from wind to the LCOE in 2050 due to the large installed capacities of wind power plants in 2030.

Figure 10c presents the relative contribution of the different components to the LCOE. It can be seen that over time, the LCOE primary increasing accounts for the final LCOE. The relative contribution of the fossil fuel cost, and therefore also the CO_2 emission costs, disappear. From 2030 onwards, the relative contribution of the storage increases and ultimately by 2050, the LCOS and LCOE primary have almost equal contributions to the LCOE. This is also reflected in Figure 10d. Figure 10c presents the relative contribution of the financial components to the LCOE. In 2015, the fossil fuel costs determine the LCOE. As the fossil fuel usage diminishes, the total capex of the power system is the largest relative contributor to the LCOE. From 2040 onwards, when there is a 100% renewable energy system, the capex of the system contributes up to 75% of the LCOE. The fixed opex of the energy system components mostly account for the remainder of the LCOE.

Figure 11 illustrates the annual CO_2 emissions during the energy transition illustrated in the previous figures. The annual CO_2 emissions are reduced from about 250 Mton/a to 0 by 2040. The red line diagram represents the ratio of CO_2 emitted for every kWh of electricity produced. In 2015, this value is at about 800 g of CO_2 per kWh and drops to 0 by 2040. The CO_2 emission calculations are explained in [65].

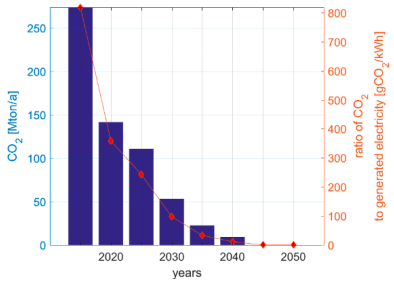

Figure 11. Annual CO_2 emissions during the energy transition and the ratio (blue bars) and CO_2 emissions per kWh of electricity produced (red line).

Figure 12 provides an overview of the gas sector after integration with the power sector. Figure 12a shows how the levelised cost of gas (LCOG) varies over time, while the non-energetic industrial gas demand increases. The LCOG increases from 23 €/MWh_{th} in 2015 to 95 €/MWh_{th} in 2045. After 2045, the LCOG decreases and by 2050, the LCOG is 90 €/MWh_{th}. There is a steep increase in the LCOG from 2030 to 2035. This due to the production of SNG in 2035, as shown by Figure 12b. By 2040, the gas utilized in the system is fully renewable SNG.

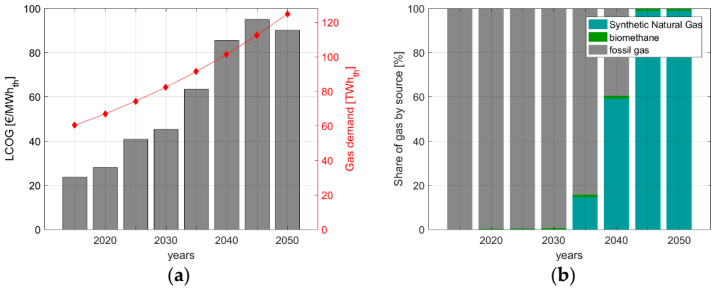

Figure 12. The increase in industrial gas demand (red line) and the variation in levelised cost of gas (LCOG) (grey bars) (**a**) and gas in the system by source (**b**) from 2015 to 2050.

3.2. Integrated Scenario—Desalination Sector

Figure 13 illustrates the growth of the Saudi Arabian desalination sector assumed in the model. The difference between the total water demand and the installed desalination capacity is met by renewable water sources and non-renewable groundwater sources. As explained in Section 2.4, the desalination demand increases to meet the growing total water demand and is met through SWRO and MED stand alone plants. The model optimizes the installed capacities of SWRO and MED depending on the electricity costs and availability of heat in the system.

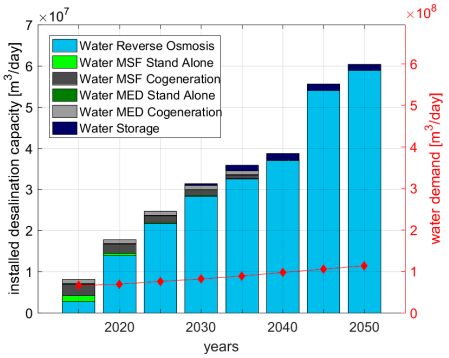

Figure 13. Water desalination capacities required to meet KSA's total water demand from 2015 to 2050.

The MSF and MED cogeneration plants are phased out based on the lifetime of the plants. By 2050, it is expected that there is a total water demand of 112 million m^3/day and SWRO plants meet 52% of the total water demand. MED stand alone provides less than 1% of the total water demand. This is due to the lower excess heat available in the system. In addition, water storage is found to vary daily after 2020. Figure 14 illustrates the variation in water storage for the year 2030. Thus, the water storage acts a daily or seasonal storage optimizing the operation of the desalination plants. With the increase in SWRO desalination capacity there is an increase in water storage capacity.

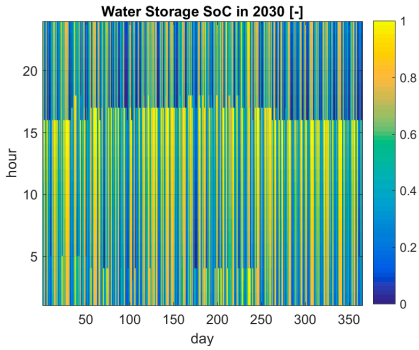

Figure 14. Water storage relative state of charge in 2030.

Figure 15a presents the capex breakdown of the desalination plant capacities installed for the 5 year intervals. The contribution of water transportation increases as the installed desalination capacities increase. By 2050, the transportation infrastructure is the largest contributor to the capex. The total capex required for the period from 2015 up to 2050 for the desalination sector is 1125 b€.

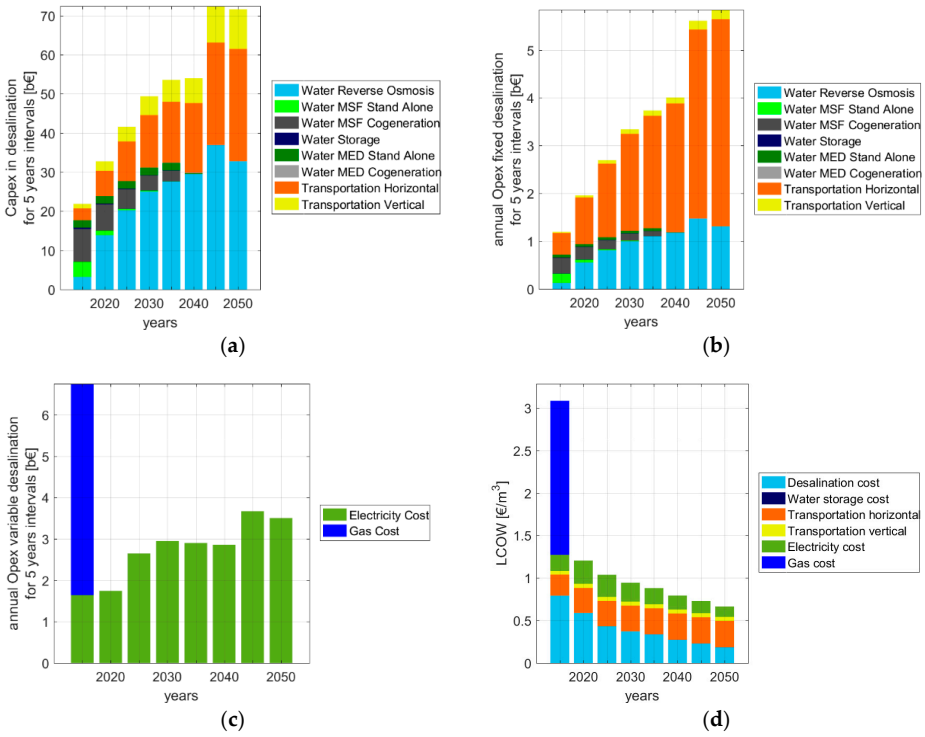

Figure 15. Capex of all desalination sector components (**a**), annual fixed opex for desalination sector components (**b**), annual variable opex for desalination sector components (**c**) and LCOW variation (**d**) from 2015 to 2030.

Figure 15b presents the variation in the annual fixed opex of the desalination capacities. With the increase in desalination capacities, the fixed opex increases. The fixed opex excludes the electricity consumption of the desalination plants and water transportation infrastructure. Figure 15c represents the variation in the annual variable opex. The annual variable opex accounts for both the gas and electricity consumption of the desalination plants. In 2015, due to the electricity produced by the cogeneration plants, there is no resulting electricity costs—the variable cost is finally the gas cost. The increase in the electricity cost maybe explained by the considerable increase in installed SWRO capacities with time and the variation in energy efficiency of the plants. There is only a minimal gas cost for existing cogeneration plants. SWRO and MED stand-alone plants utilize electrical energy and heat from the energy system as required.

Finally, Figure 15d illustrates the contribution of the different aspects of the desalination system to the final LCOW for every time period. The LCOW of the final system decreases from 3.29 €/m^3 in 2015, assuming non subsidized oil and gas prices, to 0.66 €/m^3 in 2050. The costs reduction is mainly due to the elimination of gas consumption and decrease in electricity costs, but also in an increase in the efficiency of RO and MED desalination plants in the decades to come.

Table 10 shows the energy consumption of the different desalination technologies during the transition. The total electricity consumption of the SWRO plants increase due to the high installed capacities. The MSF and MED cogeneration plants only produce water up to 2030 and then are decommissioned due to end of lifetime. The MED stand alone plants continue to produce water but at lower volumes than in 2015. This is because of the low availability of heat in the energy system.

Table 10. Energy Consumption of the desalination technologies during the transition.

	Unit	2015	2020	2025	2030	2035	2040	2045	2050
SWRO electricity cons	GWh	4496.5	22,622.5	29,622.5	37,033.8	40,996.5	45,209.6	64,212.8	63,011.9
MSF-S electricity cons	GWh	1386.8	0	0	0	6.5	0	0	0
MSF-C electricity cons	GWh	2153.8	0	0	0	0	0	0	0
MED-S electricity cons	GWh	114.6	0	0	0	19.4	0	0	0
MED-C electricity cons	GWh	689.2	0	0	0	0	0	0	0
MSF-S heat cons	GWh_{th}	47,151.0	0	0	0	219.4	0	0	0
MSF-C gas cons	GWh_{th}	174,456.5	0	0	0	0	0	0	0
MED-S heat cons	GWh_{th}	3898.6	2.3	1.9	4.7	309.8	1.7	1.5	4
MED-C gas cons	GWh_{th}	59 809.7	0	0	0	0	0	0	0

Table A4, in the Appendix A, summarises the key power capacities determined for the energy transition pathway for KSA from 2015 to 2050.

3.3. Comparison of the Integrated and Non-Integrated Scenarios

As discussed in Section 3, the model was run for a non-integrated scenario where the power capacities to meet the electricity demand and the desalinated water sector are found separately. To compare the integrated and non-integrated scenarios, the annual levelised cost for both scenarios from 2020 to 2050 was found. This is represented in Figure 16a. The annual levelised cost for the non-integrated scenario is higher than that for the integrated scenario. It is found that the approximate percentage benefit of the integrated scenario is between 1% and 3%, as a consequence of increased flexibility to the integrated energy system.

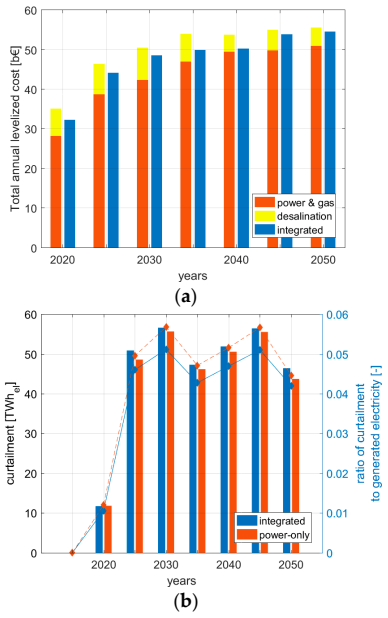

Figure 16. Comparison of total annual levelised cost (**a**) and the curtailed electricity (**b**) for the integrated and non-integrated scenarios.

Figure 16b illustrates the curtailment of electricity for the two scenarios, for the time period from 2015 to 2050. The bars represent the value of the energy curtailed and the dashed lines represent the ratio of the curtailed energy to the total generated electricity. It can be seen that there is more curtailed energy in the integrated scenario. However, the ratio of the curtailed energy to the total electricity

generated is lower in the integrated scenario. This can be attributed to the increased flexibility provided by the desalination plants and therefore better utilization of the hourly produced renewable energy, hence the integrated energy system can be run in a more efficient way than the separated systems.

It has to be mentioned that in the integrated scenario, for the total time period of 2015 to 2050, the power-to-gas (PtG) electrolyser capacity is reduced by 1%, compared to the separated scenario. For the integrated scenario, the PtG electrolyser capacity was estimated to be 73.6 GW_e, respectively. For the non-integrated scenario, the corresponding values was estimated to be 75.4 GW_e.

4. Discussion

The results show how the integration of seawater desalination with power and gas sectors contribute to the least cost transition path to achieving a 100% renewable energy sector in Saudi Arabia before the proposed year 2050.

Figure 7b illustrates that this milestone is feasible for Saudi Arabia by 2040. By 2040, PV single-axis tracking and wind power plants will dominate the Saudi power sector with 243 GW of the former and 83 GW of the latter. However, by 2050, due to the steeper decrease in the PV single-axis tracking and battery capex than the wind onshore plants, as presented in Figure 4c, it is more economical to have PV single-axis tracking as the dominant energy source in the power sector of Saudi Arabia. By 2050, about 377 GW of PV single-axis tracking are required while the capacities of wind power plants remain at 83 GW. Thus, there are no further installations in wind power plants after 2030. This result documents the outstanding impact of low cost solar PV supported by low cost battery storage that lead to a solar PV electricity generation share of 79%, which is significantly higher than the average of about 40% found in the global average assumptions for the year 2030 [25], but also higher than the 48% solar PV share for the MENA region [66]. However, comparable results had been found already earlier for the case of Israel [30], where the solar PV share had be found for cost optimized systems to about 90% of the total electricity supply. It has to be noted that Israel has less good wind conditions as in Saudi Arabia, and [30] was done for assumptions about the year 2030. Breyer et al. [41] discuss the significant role of solar photovoltaics, estimated to have an electricity generation share of 69% by 2050, in the global energy transition. The low cost for solar PV and battery storage can be explained by the standard experience curves in Figure 4 [67–69].

With the phasing out of fossil fueled thermal power plants, battery storage comes into play by 2025. By this time period, about 22% of the energy generation share is accounted for by fossil fueled thermal power plants. As the electricity demand increases and the share of renewables in the system increases, the battery storage required continues to increase. By 2050, batteries provide a total output of about 329 TWh_{el} accounting for approximately 40% of the total electricity demand. For a 100% RE scenario by 2040, the required battery storage output is 203 TWh_{el} accounting for approximately 32% of the total electricity demand. Between, 2025 and 2050, the battery full charge cycles required are between 300 and 330 cycles a year, indicating the almost daily usage of the battery capacity.

PtG plants come into effect in 2035 with 12 GW_{el} of input capacity and increases to 73 GW_{el} by 2050. Similarly, the FLH of the PtG plants increase from about 4313 h in 2035 to 4900 h by 2050. However, the gas storage output contributes about 2.3% towards the total electricity demand by 2050, significantly less than the 40% of batteries. The PtG plants also produce the SNG required to meet the industrial gas demand, as highlighted in Figure 12a.

The LCOE of the energy system is dominated by the high fuel cost in 2015. However, with the phasing out of the fossil powered thermal plants and the decreased consumption of fossil fuel, the LCOE of the energy system reduces from 139 €/MWh_{el} in 2015 to 43 €/MWh_{el} in 2040 and further to 41 €/MWh_{el} in 2050.

Figure 10c illustrates that by 2020 onwards, the dominating contributor to the LCOE is the $LCOE_{primary}$. With the increase in storage capacities, both the $LCOE_{primary}$ and LCOS are the largest contributors to the system LCOE. Figure 9d further shows that by 2050, the largest contributors are PV single-axis tracking and battery storage. However, by 2040, there is still a significant contribution by

the existing wind power plants to the LCOE. This is in spite of the fact that new installations of wind power plants cease after 2030, due to the arising competitiveness of hybrid PV-battery plants.

Figure 13 presents the increasing desalination demand in the Kingdom of Saudi Arabia and the desalination capacities installed to meet the total water demand. The difference between the total water demand and desalination capacity is to be met through renewable water resources and some non-renewable ground water resources. SWRO and MED stand alone desalination plant capacities are optimized to meet the increasing desalination demand. The heat demand of the MED stand alone plants are met through the energy system. The existing MSF cogeneration and stand alone plants are phased out by 2035. After 2015, MSF stand alone plants are not allowed in the model due to the high thermal energy consumption. Similarly, MSF and MED cogeneration plants are not modelled due to the need for fossil powered gas plants. In an integrated scenario, the desalination capacities are used to better utilize the hourly renewable energy production of the power system. Figure 15 presents the variation in the average LCOW from 3.3 €/m^3 in 2015 to 0.66 €/m^3 in 2050.

The reduction in the LCOE of the system, contributes to the rapid decrease of the LCOW. The electricity costs for the desalination sector includes the energy consumption for water production at the desalination plant and transportation of water (vertical and horizontal transportation) to the demand site. By 2050, the transportation costs is the highest contributor to the LCOW followed by the desalination costs. Due to the low availability of heat losses in the system, there is a dominance of SWRO desalination plants which utilize no thermal energy.

To understand the impacts of integrating the desalination and power sectors in KSA, the LUT energy systems model was used to analyse both an integrated and non-integrated scenario. Thus, for the non-integrated scenario, the same desalination capacities are required, but they are not used to increase the flexibility of the power system. Figure 16a illustrates that the annualized levelised cost of the non-integrated scenario is higher than that of the integrated scenario for all time periods from 2020 to 2050. In fact, it is found that between 2040 and 2050, this reduction is between 1% and 3%, representing an annual cost decrease between 0.5 and 1.6 bn€. The lower cost is attributed to the reduced amounts of electricity storage, in the form of power-to-gas, required in the integrated scenario. Figure 16b highlights the lower curtailed energy ratio in the integrated scenario and the better utilization of the hourly renewable energy production.

Therefore, the above work presents a pathway for Saudi Arabia to transition to a 100% renewable energy power sector and shows that the integration of the country's power and desalination sectors provides the least cost solution for both sectors.

It may be argued that the current electricity production costs in Saudi Arabia are lower than what this research presents for 2015. However, the artificially low fossil fuel prices in Saudi Arabia are a result of the high subsidies which, according to Al-Iriani et al. [70], account for 10% of the country's GDP. As the energy consumption increases, the economic price the country has to pay increases. This is due to the heavily subsidized fuel prices that result in economic losses in the form of opportunity costs, since the export value of fuel would be much higher than the subsidized domestic consumption. With the decrease in oil prices and resulting revenue, as well as concerns about availability of fossil fuel resources to meet the country's growing energy demand, Saudi Arabia has started the transition to less or no subsidies. Thus, our work offers a solution for Saudi Arabia to meet its growing energy demands through renewable energy, without hindering the future economic growth of the country. In addition, as demonstrated in this work, KSA can meet its own industrial gas demands by exploiting the country's wealth of solar and wind resources.

This research also addresses how Saudi Arabia can meet the country's growing water demand through the use of 100% renewable energy powered SWRO desalination plants. The average LCOW of KSA is found to be 0.66 €/m^3 by 2050. This includes the cost for water desalination, water transportation to the demand site and water storage. Fthenakis et al. [71] estimated the current LCOW of a 190,000 m^3/day SWRO plant, located in Al-Khajfi, on the east coast of KSA, powered by fixed-tilted PV to be 0.70 €/m^3. Current water production costs of fossil powered SWRO plants in KSA lie between

0.65 €/m^3–1.90 €/m^3 [36]. However, this excludes the cost of transporting the desalinated water to the demand site and water storage.

There is a fast growing number of publications on 100% renewable energy-based energy systems [72], which helps to overcome the past concern that such systems would be neither technically feasible nor economically viable. This research on the case of Saudi Arabia is another confirmation of the high competitiveness of 100% RE systems. Recently Clack et al. [73] claimed that fossil-CCS and nuclear should be part of an energy system solution, which attracted stark criticism by Jacobson et al. [74]. One of the motivations for the critique was the fact that no single one of the about 60 existing articles on 100% RE systems had been mentioned in [73]. This reveals an imbalanced literature basement of the authors. Recent publications of IPCC researchers [75,76] also emphasize the substantial shares of renewable energy, and in particular on solar PV. Breyer et al. [41], recently presented an energy transition scenario for the world structured in 145 regions and simulated in full hourly resolution for the period 2015 to 2050 in 5 years steps. The research showed that 100% RE in the power system is possible, for lower global averaged cost than for the energy system of the year 2015. The energy transition has been further investigated by Ram et al. [77] who show that the transition also implies zero greenhouse gas emissions and a drastic increase in jobs in the power sector.

5. Conclusions

There is growing interest in the energy transition towards a 100% renewable energy-based power system in many countries and regions. Meanwhile, as the global renewable freshwater resource diminishes, seawater reverse osmosis desalination is expected to play a key role in securing future water supplies.

Saudi Arabia is the world's largest producer of crude oil and the 11th largest consumer. Economic growth of the country is tied closely to oil prices. To secure the country's economy, the government recently heralded a future without oil. The new vision calls for increase in renewable energy capacities and at least 9 GW of installed RE capacity by 2023. Saudi Arabia is also the largest producer of desalinated water in the world and desalination will remain vital to the country's future water supply.

The purpose of this research is to analyse the impact of integrating the large desalination demand into the country's 100% RE-based power system by 2050. The power sector is integrated with the non-energy industrial gas sector of Saudi Arabia. Thus, RE is used to produce SNG to satiate the industrial gas demands. The increasing desalination demand is met through SWRO and MED stand alone plants.

It is found that the integration of the power, gas sector and the desalinated water sector, allows for a reduction of 1–3% of the levelised annual costs, in comparison to the non-integrated scenario. The LCOE and LCOW for Saudi Arabia by 2050, in the integrated scenario, is estimated to be 41 €/MWh and 0.66 €/m^3, respectively. By 2050, PV single-axis tracking dominates the power sector in Saudi Arabia with about 79% of total generated electricity due to the further reduction in capex of solar PV and supporting battery technology over wind power plants. In addition, SWRO plants produce most of the desalinated water required. MED stand alone plants contribute when there is sufficient heat available in the energy system. In future research, it is planned to integrate the heat sector into the model. This may lead to more free heat in the energy system resulting in an increase in the MED capacities installed. In the presence of cheap heat source, MED is favourable to SWRO due to its lower electricity consumption.

Thus, the results present a least cost transition path for Saudi Arabia to meet the country's future electricity and water demands through a 100% RE system.

However, there are gaps in the research methodology and data for Saudi Arabia that could be summarised as below:

1. Better understanding of the potential for geothermal and CSP heat use for MED desalination in Saudi Arabia.

2. No well-defined learning curve for SWRO desalination plants: This makes it difficult to project the future SWRO costs.

By filling in the gaps in our research, we can further refine our results and provide the optimal transition pathway for Saudi Arabia to finally start the country's future without oil. By capitalising on the country's excellent solar and wind resources through the implementation of renewable energy, Saudi Arabia can indeed meet the country's future electricity, water and gas demands in a lucrative manner.

Acknowledgments: The authors gratefully acknowledge the scholarship offered by the Reiner Lemoine-Foundation and public financing of Tekes, the Finnish Funding Agency for Innovation, for the 'Neo-Carbon Energy' project under the number 40101/14.

Author Contributions: Upeksha Caldera carried out the research, including collecting the input data, implementing the energy system modelling, generating and analysing the results, and writing the manuscript. Dmitrii Bogdanov did the coding for the model used in this research. Svetlana Afanasyeva visualized and developed the figures. Christian Breyer framed the research questions and scope of the work, checked the results, facilitated discussions, and reviewed the manuscript.

Conflicts of Interest: The authors declare no conflict of interest. The founding sponsors had no role in the design of the study; in the collection, analyses, or interpretation of data; in the writing of the manuscript, and in the decision to publish the results.

Nomenclature

a	annum
d	day
A-CAES	adiabatic compressed air storage
BWRO	brackish water reverse osmosis
Capex	capital expenditures
CCGT	combined cycle gas turbine
CSP	concentrating solar power
crf	capital recovery factor
GCC	Gulf Corporation Council
GOR	gain output ratio
GWI	global water intelligence
HRSG	heat recovery steam generator
IWPP	independent water and power project
KSA	Kingdom of Saudi Arabia
LCOC	levelised cost of curtailment
LCOE	levelised cost of electricity
LCOG	levelised cost of gas
LCOW	levelised cost of water
MSF	multi stage flash
MED	multi effect distillation
NWS	national water strategy
OCGT	open cycle gas turbine
Opex	operational expenditures
PtG	power-to-gas
PtH	power-to-heat
PV	photovoltaic
RE	renewable energy
SEC	specific energy consumption
SoC	state of charg
SNG	synthetic natural gas
SWRO	seawater reverse osmosis
WACC	weighted average cost of capital

Appendix A

Table A1. Technical and Financial Assumptions of all energy system components used in the energy transition from 2015 to 2050 for KSA. Assumptions are taken from Pleßmann et al. [78] and European Commission [79] and further references are individually mentioned.

Name of Component		Unit	2015	2020	2025	2030	2035	2040	2045	2050	Reference
PV optimally tilted	Capex	€/kWp	1000	580	466	390	337	300	270	246	[80,81]
	Opex fix	€/(kWp·a)	15	13.2	11.8	10.6	9.6	8.8	8.0	7.4	
	Opex var	€/(kWh)	0	0	0	0	0	0	0	0	
	Lifetime	years	30	30	35	35	35	40	40	40	
PV single-axis tracking	Capex	€/kWp	1150	638	513	429	371	330	297	271	[80,81]
	Opex fix	€/(kWp·a)	17.3	15.0	13.0	12.0	11.0	10.0	9.0	8.0	
	Opex var	€/(kWh)	0	0	0	0	0	0	0	0	
	Lifetime	years	30	30	35	35	35	40	40	40	
Wind onshore	Capex	€/kW	1250	1150	1060	1000	965	940	915	900	[82]
	Opex fix	€/(kW·a)	25	23	21	20	19	19	18	18	
	Opex var	€/(kWh)	0	0	0	0	0	0	0	0	
	Lifetime	years	25	25	25	25	25	25	25	25	
CSP (solar field, parabolic trough)	Capex	€/m^2	270	240	220	200	180	170	150	140	[83,84]
	Opex fix	%	2.3	2.3	2.3	2.3	2.3	2.3	2.3	2.3	
	Opex var	-	0	0	0	0	0	0	0	0	
	Lifetime	years	25	25	25	25	30	30	30	30	
Geothermal	Capex	€/kW	5250	4970	4720	4470	4245	4020	3815	3610	[79,85]
	Opex fix	€/(kW·a)	80.0	80.0	80.0	80.0	80.0	80.0	80.0	80.0	
	Opex var	€/(kWh)	0	0	0	0	0	0	0	0	
	Lifetime	years	40	40	40	40	40	40	40	40	
Water electrolysis	Capex	€/kW	800	685	500	380	340	310	280	260	[86,87]
	Opex fix	€/(kW·a)	32	27	20	15	14	12	11	10	
	Opex var	€/(kWh)	0.0012	0.0012	0.0012	0.0012	0.0012	0.0012	0.0012	0.0012	
	Lifetime	years	30	30	30	30	30	30	30	30	
Methanation	Capex	€/kW	492	421	310	234	208	190	172	160	[86,87]
	Opex fix	€/(kW·a)	10	8	6	5	4	4	3	3	
	Opex var	€/(kWh)	0.0015	0.0015	0.0015	0.0015	0.0015	0.0015	0.0015	0.0015	
	Lifetime	years	30	30	30	30	30	30	30	30	
CO_2 direct air capture	Capex	€/kW	749	641	470	356	314	286	258	240	[86,87]
	Opex fix	€/(kW·a)	29.9	25.6	18.8	14.2	12.6	11.4	10.3	9.6	
	Opex var	€/(kWh)	0.0013	0.0013	0.0013	0.0013	0.0013	0.0013	0.0013	0.0013	
	Lifetime	years	30	30	30	30	30	30	30	30	

Table A1. *Cont.*

Name of Component		Unit	2015	2020	2025	2030	2035	2040	2045	2050	Reference
CCGT	Capex	€/(kW_{el})	775	775	775	775	775	775	775	775	[88]
	Opex fix	€/(kW_{el}·a)	19.4	19.4	19.4	19.4	19.4	19.4	19.4	19.4	
	Opex var	€/(kWh)	0	0	0	0	0	0	0	0	
	Efficiency	%	58	58	58	58	59	60	60	60	
	Lifetime	years	35	35	35	35	35	35	35	35	
OCGT	Capex	€/(kW_{el})	475	475	475	475	475	475	475	475	[88]
	Opex fix	€/(kW_{el}·a)	14.25	14.25	14.25	14.25	14.25	14.25	14.25	14.25	
	Opex var	€/(kWh)	0	0	0	0	0	0	0	0	
	Efficiency	%	43	43	43	43	43	43	43	43	
	Lifetime	years	35	35	35	35	35	35	35	35	
Steam turbine (CSP)	Capex	€/(kW_{el})	760	740	720	700	670	640	615	600	[88,89]
	Opex fix	€/(kW_{el}·a)	15.2	14.8	14.4	14	13.4	12.8	12.3	12	
	Opex var	€/(kWh)	0	0	0	0	0	0	0	0	
	Efficiency	%	42	42	42	43	44	44	45	45	
	Lifetime	years	25	25	25	25	30	30	30	30	
Steam turbine (coal-fired PP)	Capex	€/(kW_{el})	1500	1500	1500	1500	1500	1500	1500	1500	[88,89]
	Opex fix	€/(kW_{el}·a)	20	20	20	20	20	20	20	20	
	Opex var		0	0	0	0	0	0	0	0	
	Efficiency	%	45	45	45	45	46	46	47	47	
	Lifetime	years	40	40	40	40	40	40	40	40	
Biomass CHP	Capex	€/kW	3400	2900	2700	2500	2300	2200	2100	2000	
	Opex fix	€/(kW·a)	238	203	189	175	161	154	147	140	
	Opex var	€/(kWh)	0.001	0.001	0.001	0.001	0.001	0.001	0.001	0.001	
	Efficiency	%	36	37	40	43	45	47	47.5	48	
	Lifetime	years	30	30	30	30	30	30	30	30	
Biogas CHP	Capex	€/kW	503	429	400	370	340	326	311	296	
	Opex fix	€/(kW·a)	20.1	17.2	16.0	14.8	13.6	13.0	12.4	11.8	
	Opex var	€/(kWh)	0.001	0.001	0.001	0.001	0.001	0.001	0.001	0.001	
	Efficiency	%	35	36	39	42	44	46	46	47	
	Lifetime	years	30	30	30	30	30	30	30	30	
Waste incinerator	Capex	€/kW	5940	5630	5440	5240	5030	4870	4690	4540	
	Opex fix	€/(kW·a)	267.3	253.35	244.8	235.8	226.35	219.15	211.05	204.3	
	Opex var	€/(kWh)	0.0069	0.0069	0.0069	0.0069	0.0069	0.0069	0.0069	0.0069	
	Efficiency	%	27	31	32.5	34	35.5	37	29.5	42	
	Lifetime	years	30	30	30	30	30	30	30	30	

Table A1. *Cont.*

Name of Component		Unit	2015	2020	2025	2030	2035	2040	2045	2050	Reference
Biogas digester	Capex	€/kW	771	731	706	680	653	632	609	589	
	Opex fix	€/(kW·a)	30.8	29.2	28.2	27.2	26.1	25.3	24.3	23.6	
	Opex var	€/(kWh)	0	0	0	0	0	0	0	0	
	Efficiency	%	100	100	100	100	100	100	100	100	
	Lifetime	years	20	20	20	20	25	25	25	25	
Biogas upgrade	Capex	€/kW	340	290	270	250	230	220	210	200	[90]
	Opex fix	€/(kW·a)	27.2	23.2	21.6	20	18.4	17.6	16.8	16	
	Opex var	€/(kWh)	0	0	0	0	0	0	0	0	
	Efficiency	%	98	98	98	98	98	98	98	98	
	Lifetime	years	20	20	20	20	25	25	25	25	
Battery, Li-ion	Capex	€/(kWh_{el})	600	300	200	150	120	100	85	75	[91]
	Opex fix	€/(kWh_{el}·a)	24	12	8	6	4.8	4	3.4	3	
	Opex var	€/($kWh_{throughput}$)	0.0002	0.0002	0.0002	0.0002	0.0002	0.0002	0.0002	0.0002	
	Efficiency	%	90	91	92	93	94	95	95	95	
	Lifetime	years	15	20	20	20	20	20	20	20	
Thermal Energy Storage (TES)	Capex	€/(kWh_{th})	50	40	30	30	20	20	20	20	
	Opex fix	€/(kWh_{th}·a)	0.75	0.6	0.45	0.45	0.3	0.3	0.3	0.3	
	Opex var	€/($kWh_{throughput}$)	0	0	0	0	0	0	0	0	
	Lifetime	years	25	25	25	25	30	30	30	30	
Adiabatic compressed air energy storage (A-CAES)	Capex	€/kWh	35.0	35.0	33.0	31.1	30.4	29.8	28.0	26.3	
	Opex fix	€/(kWh·a)	0.46	0.46	0.43	0.40	0.40	0.39	0.36	0.34	
	Opex var	€/(kWh)	0.0012	0.0012	0.0012	0.0012	0.0012	0.0012	0.0012	0.0012	
	Efficiency	%	54	59	65	70	70	70	70	70	
	Lifetime	years	40	55	55	55	55	55	55	55	
Gas storage	Capex	€/kWh_{th}	0.05	0.05	0.05	0.05	0.05	0.05	0.05	0.05	
	Opex fix	€/(kWh·a)	0.001	0.001	0.001	0.001	0.001	0.001	0.001	0.001	
	Opex var	€/(kWh)	0	0	0	0	0	0	0	0	
	Lifetime	years	50	50	50	50	50	50	50	50	

Table A2. Technical and financial parameters of the seawater desalination technologies from 2015–2050 [36,37,47,54–62].

Name of Component			2015	2020	2025	2030	2035	2040	2045	2050
Sea Water Reverse Osmosis	Capex	€/(m^3·day)	1150	960	835	725	630	550	480	415
	Opex fix	€/(m^3·day)	46	38	33	29	25	22	19	17
	Energy consumption	kWh/m^3	4.1	3.6	3.35	3.15	3	2.85	2.7	2.6
	Lifetime	years	25	25	30	30	30	30	30	30
Multi Effect Distillation—Thermal Vapor Compression for stand alone	Capex	€/(m^3·day)	1437	1200	1043	906	787	687	600	519
	Opex fix	€/(m^3·day)	10	13.2	15.6	18	21.6	24	24	24
	Thermal energy consumption	kWh_{th}/m^3	68	51	44	38	32	28	28	28
	Electrical energy consumption	kWh_{el}/m^3	1.5	1.5	1.5	1.5	1.5	1.5	1.5	1.5
	Lifetime	years	25	25	25	25	25	25	25	25
Multi Effect Distillation—Thermal Vapor Compression for cogeneration	Capex	€/(m^3·day)	1437	1437	1437	1437	1437	1437	1437	1437
	Opex fix	€/(m^3·day)	47.4	47.4	47.4	47.4	47.4	47.4	47.4	47.4
	Thermal energy consumption (Total gas input required for water and electricity)	kWh_{th}/m^3	168	168	168	168	168	168	168	168
	Electrical energy consumption	kWh_{el}/m^3	1.5	1.5	1.5	1.5	1.5	1.5	1.5	1.5
	Lifetime	years	25	25	25	25	25	25	25	25
Multi Stage Flash for cogeneration Gain Output Ratio: 8 Power-to-Water: 2.25 kW/(m^3·day)	Capex	€/(m^3·day)	2000	2000	2000	2000	2000	2000	2000	2000
	Opex fix	€/(m^3·day)	100	100	100	100	100	100	100	100
	Thermal energy consumption (Total gas input required for water and electricity)	kWh_{th}/m^3	202.5	202.5	202.5	202.5	202.5	202.5	202.5	202.5
	Electrical energy consumption	kWh_{el}/m^3	2.5	2.5	2.5	2.5	2.5	2.5	2.5	2.5
	Lifetime	years	25	25	25	25	25	25	25	25
Multi Stage Flash for stand alone Gain Output Ratio: 8	Capex	€/(m^3·day)	2000	2000	2000	2000	2000	2000	2000	2000
	Opex fix	€/(m^3·day)	100	100	100	100	100	100	100	100
	Thermal energy consumption	kWh_{th}/m^3	85	85	85	85	85	85	85	85
	Electrical energy consumption	kWh_{el}/m^3	2.5	2.5	2.5	2.5	2.5	2.5	2.5	2.5
	Lifetime	years	25	25	25	25	25	25	25	25
Water Transportation										
Piping	Capex	€/(m^3·a·km)	0.053	0.053	0.053	0.053	0.053	0.053	0.053	0.053
	Fixed Opex	€/(m^3·a·100 km)	0.023	0.023	0.023	0.023	0.023	0.023	0.023	0.023
	Lifetime	years	30	30	30	30	30	30	30	30
Vertical Pumping	Capex	€/(m^3·h·m)	15.4	15.4	15.4	15.4	15.4	15.4	15.4	15.4
	Fixed Opex	€/(m^3·h·m)	0.3	0.3	0.3	0.3	0.3	0.3	0.3	0.3
	Energy consumption	kWh/(m^3·h·100 m)	0.36	0.36	0.36	0.36	0.36	0.36	0.36	0.36
	Lifetime	years	30	30	30	30	30	30	30	30
Horizontal Pumping	Capex	€/(m^3·h·km)	19.26	19.26	19.26	19.26	19.26	19.26	19.26	19.26
	Fixed Opex	€/(m^3·h·km)	0.4	0.4	0.4	0.4	0.4	0.4	0.4	0.4
	Energy consumption	kWh/(m^3·h·100 km)	0.04	0.04	0.04	0.04	0.04	0.04	0.04	0.04
	Lifetime	years	30	30	30	30	30	30	30	30
Water Storage	Capex	€/m^3	65	65	65	65	65	65	65	65
	Fixed Opex	€/m^3	1.3	1.3	1.3	1.3	1.3	1.3	1.3	1.3
	Lifetime	years	30	30	30	30	30	30	30	30

Table A3. Energy to power ratio of the storage technologies.

Technology	Energy/Power Ratio (h)	Self-Discharge
Battery	6	0
TES	10	0.002
A-CAES	100	0.001
Gas Storage	80 × 24	0

Table A4. Key power capacities required for the energy transition pathway for KSA from 2015 to 2050.

Technology	Unit	2015	2020	2025	2030	2035	2040	2045	2050
PV single-axis tracking	GWp	0	14	73	87	174	243	326	378
PV optimally tilted	GWp	0.08	0.08	0.08	0.08	0.08	0.07	0.07	0.002
Wind power plants	GW	0	0	0	83	83	83	83	83
Geothermal	GW	0	1.6	1.7	2	2	2	2	2
Battery storage output	TWh	0	0	1.4	33.7	131	203	269	329
PtG electrolyser input	GW_e	0	0	0	0	12	39	72	74
Gas Storage	TWh_{th}	0	0.002	0.002	0.003	0.005	0.5	15	16

References

1. United Nations. *Probabilistic Population Projections Based on the World Population Prospects: The 2015 Revision. Population Division*; United Nations Department of Economic and Social Affairs (DESA): New York, NY, USA, 2015; Available online: http://esa.un.org/unpd/ppp/ (accessed on 12 February 2017).
2. Salam, A.A.; Elsegaey, I.; Khraif, R.; Al-Mutairi, A. Population distribution and household conditions in Saudi Arabia: Reflections from the 2010 Census. *SpringerPlus* **2014**, *3*. [CrossRef]
3. DeNicola, E.; Aburizaiza, S.O.; Siddque, A.; Khwaja, H.; Carpenter, O.D. climate change and water scarcity: The case of Saudi Arabia. *Ann. Glob. Health* **2015**, *81*, 342–352. [CrossRef] [PubMed]
4. Drewes, J.E.; Garduno, R.P.C.; Amy, G. Water reuse in the Kingdom of Saudi Arabia–status, prospects and research needs. *Water Sci. Technol. Water Supply* **2012**, *12*, 926–936. [CrossRef]
5. Global Water Intelligence Desal Data, Country Profile Saudi Arabia. 2016. Available online: https://www.desaldata.com/countries/31 (accessed on 12 August 2016).
6. Global Water Intelligence. Top Market Opportunities Saudi Arabia. In *Global Water Market 2017: Meeting the World's Water and Wastewater Needs until 2020*; Middle East and Africa; Media Analytics Publication: Oxford, UK, 2016; Volume 4, pp. 1379–1400.
7. United Nations World Water Assessment Programme. *The United Nations World Water Development Report 2014: Water and Energy*; The United Nations Educational, Scientific and Cultural Organization (UNESCO): Paris, France, 2014; Available online: http://unesdoc.unesco.org/images/0022/002257/225741E.pdf (accessed on 2 February 2017).
8. GE Power Water & Process Technologies. *Saudi Digital Water Opportunities*; General Electric (GE): Boston, MA, USA, 2016.
9. World Energy Council. *Global Energy Transitions: A Comparative Analysis of Key Countries and Implications for the International Energy Debate*; World Energy Council: Berlin, Germany, 2014; Available online: www.atkearney.com/documents/10192/5293225/Global+Energy+Transitions.pdf/220e6818-3a0a-4baa-af32-8bfbb64f4a6b (accessed on 5 February 2017).
10. Albassam, A.B. Economic diversification in Saudi Arabia: Myth or reality? *Resour. Policy* **2015**, *44*, 112–117. [CrossRef]
11. King Abdullah City for Atomic and Renewable Energy. The Vision: Energy Sustainability for Future Generations, Riyadh, Saudi Arabia. 2016. Available online: www.kacare.gov.sa/en/FutureEnergy/Pages/vision.aspx (accessed on 10 March 2017).
12. Moser, S.; Swain, M.; Alkhabbaz, H.M. King Abdullah Economic City: Engineering Saudi Arabia's post-oil future. *Cities* **2015**, *45*, 71–80. [CrossRef]
13. Farfan, J.; Breyer, C. Structural changes of global power generation capacity towards sustainability and the risk of stranded investments. *J. Clean. Prod.* **2016**, *141*, 370–384. [CrossRef]

14. Black, I. *Saudi Arabia Approves Ambitious Plan to Move Economy beyond Oil*; The Guardian: London, UK, 2016; Available online: www.theguardian.com/world/2016/apr/25/saudi-arabia-approves-ambitious-plan-to-move-economy-beyond-oil (accessed on 10 March 2017).
15. Apricum—The Cleantech Advisory. *Saudi Arabia Unveils New Plan Including 9.5 GW of Renewable Energy*; Apricum: Berlin, Germany, 2016; Available online: www.apricum-group.com/saudi-arabia-announces-9-5-gw-renewable-energy-target-new-king-salman-renewable-energy-initiative (accessed on 15 March 2017).
16. New Energy Update. *Saudi Arabia Seeks $50bn of Solar, Wind Investments; Jordan Agrees $60/MWh PV Price*; New Energy Update: London, UK, 2017; Available online: http://analysis.newenergyupdate.com/energy-storage-pv-insider/photovoltaics/saudi-arabia-seeks-50bn-solar-wind-investments-jordan-agrees?utm_campaign=NEP%20PV%2018JAN17%20Newsletter&utm_medium=email&utm_source=Eloqua&elqTrackId=d8920d61149f4391a67ef77264a80a02&elq=6fc7d88267b9474780f52583e043cd34&elqaid=24874&elqat=1&elqCampaignId=11380 (accessed on 15 March 2017).
17. Almasoud, A.H.; Gandayh, H.H. Future of solar energy in Saudi Arabia. *J. King Saud Univ. Eng. Sci.* **2014**, *27*, 153–157. [CrossRef]
18. Breyer, C.; Schmid, J. Population density and area weighted solar irradiation: Global overview on solar resource conditions for fixed-tilted, 1-axis and 2-axis PV systems. In Proceedings of the 25th EUPVSEC/5th World Conference on Photovoltaic Energy Conversion, Valencia, Spain, 6–10 September 2010; Available online: http://bit.ly/2kEpz8w (accessed on 20 March 2017).
19. Yamada, M. Vision 2030 and the Birth of Saudi Solar Energy, Middle East Institute Policy Focus 2016-15. 2016. Available online: www.mei.edu/sites/default/files/publications/PF15_Yamada_Saudisolar_web.pdf (accessed on 10 November 2017).
20. Magazine, P.V. Saudi Arabia's 300 MW Solar Tender May Conclude with Lowest Bid Ever. 2017. Available online: www.pv-magazine.com/2017/10/04/saudi-arabias-300-mw-solar-tender-may-conclude-with-lowest-bid-ever/ (accessed on 4 October 2017).
21. Magazine, P.V. Interview: After Saudi Arabia, How Low Can Solar Prices Go? 2017. Available online: www.pv-magazine.com/2017/10/06/interview-after-saudi-arabia-how-low-can-solar-prices-go/ (accessed on 6 October 2017).
22. Magazine, P.V. SoftBank Vision Fund to Build 3GW of Solar and Storage in Saudi Arabia. 2017. Available online: www.pv-magazine.com/2017/10/24/softbank-vision-fund-to-build-3-gw-of-solar-and-storage-in-saudi-arabia/ (accessed on 24 October 2017).
23. Al-Kharaghouli, A.; Kazmerski, L.L. Energy consumption and water production cost of renewable energy powered desalination processes. *Renew. Sustain. Energy Rev.* **2013**, *24*, 343–356. [CrossRef]
24. Caldera, U.; Bogdanov, D.; Breyer, C. Local cost of seawater RO desalination based on solar PV and wind energy: A global estimate. *Desalination* **2016**, *385*, 207–216. [CrossRef]
25. Breyer, C.; Bogdanov, D.; Gulagi, A.; Aghahosseini, A.; Barbosa, L.S.N.S.; Koskinen, O.; Barasa, M.; Caldera, U.; Afanasyeva, S.; Child, M.; et al. On the Role of Solar Photovoltaics in Global Energy Transition Scenarios. *Prog. Photovolt. Res. Appl.* **2017**, *25*, 727–745. [CrossRef]
26. Breyer, C.; Koskinen, O.; Bogdanov, D. A low-cost power system for Europe based on renewable electricity. In Proceedings of the European Utility Week, Barcelona, Spain, 15–17 November 2016.
27. Bogdanov, D.; Breyer, C. Eurasian Super Grid for 100% Renewable Energy power supply: Generation and storage technologies in the cost optimal mix. In Proceedings of the ISES Solar World Congress 2015, Daegu, Korea, 8–12 November 2015; Available online: http://bit.ly/1IP8AeN (accessed on 24 October 2017).
28. Gulagi, A.; Bogdanov, D.; Choudhary, P.; Breyer, C. Electricity system based on 100% renewable energy for India and SAARC. *PLoS ONE* **2017**, *12*, e0180611. [CrossRef] [PubMed]
29. Bogdanov, D.; Breyer, C. North-East Asian Super Grid for 100% Renewable Energy supply: Optimal mix of energy technologies for electricity, gas and heat supply options. *Energy Convers. Manag.* **2016**, *112*, 176–190. [CrossRef]
30. Bogdanov, D.; Breyer, C. The Role of Solar Energy towards 100% Renewable power supply for Israel: Integrating solar PV, wind energy, CSP and storages. In Proceedings of the 19th Sede Boqer Symposium on Solar Electricity Production, Sede Boqer, Israel, 23–25 February 2015; Available online: http://bit.ly/1JlaiDI (accessed on 25 October 2017).
31. Connolly, D.; Mathiesen, B.V. A technical and economic analysis of one potential pathway to a 100% renewable energy systems. *Int. J. Sustain. Energy Plan. Manag.* **2014**, *1*, 7–28.

32. Center for Alternative Technology. *Who is Getting Ready for Zero? A Report on the State of Play of Zero Carbon Modelling*; Center for Alternative Technology: Powys, UK, 2015; Available online: http://zerocarbonbritain.org/en/ready-for-zero (accessed on 25 October 2017).
33. Neo-Carbon Energy. *Internet of Energy–Online Visualization Tool*; Lappeenranta University of Technology: Lappeenranta, Finland, 2016; Available online: http://neocarbonenergy.fi/internetofenergy/# (accessed on 25 October 2017).
34. Sterner, M. Bioenergy and Renewable Power Methane in Integrated 100% Renewable Energy Systems. Ph.D. Thesis, Faculty of Electrical Engineering and Computer Science, University of Kassel, Kassel, Germany, 2009.
35. Lehner, M.; Tichler, R.; Steinmüller, H.; Koppe, M. *Power-to-Gas: Technology and Business Models*; Springer: Heidelberg, Germany, 2014.
36. Fichtner. *MENA Regional Water Outlook Part 2 Desalination Using Renewable Energy Final Report*; Fichtner: Stuttgart, Germany, 2011.
37. El-Nashar, A.M. Cogeneration for power and desalination–state of the art review. *Desalination* **2001**, *134*, 7–28. [CrossRef]
38. Water Desalination Report. Saudi Arabia Desal Market Re-Ignited. 2017. Available online: www.desaldata.com/news/saudi-arabia-desal-market-re-ignited (accessed on 25 October 2017).
39. Barbosa, L.S.N.S.; Bogdanov, D.; Vainikka, P.; Breyer, C. Hydro, wind and solar power as a base for a 100% Renewable Energy supply for South and Central America. *PLoS ONE* **2017**, *12*, e173820. [CrossRef] [PubMed]
40. Aghahosseini, A.; Bogdanov, D.; Ghorbani, N.; Breyer, C. The role of a 100% renewable energy system for the future of Iran: Integrating solar PV, wind energy, hydropower and storage. *Int. J. Environ. Sci. Technol.* **2016**. [CrossRef]
41. Breyer, C.; Bogdanov, D.; Aghahosseini, A.; Gulagi, A.; Child, M.; Oyewo, A.S.; Farfan, J.; Sadovskaia, K.; Vainikka, P. Solar photovoltaics demand for the global energy transition in the power sector. *Prog. Photovolt. Res. Appl.* **2017**, 1–19. [CrossRef]
42. Al-Saleh, Y.; Upham, P.; Malik, K. *Renewable Energy Scenarios for the Kingdom of Saudi Arabia*; Tyndall Climate Change Research Center: Norwich, UK, 2008; Available online: www.tyndall.ac.uk/sites/default/files/wp125.pdf (accessed on 26 October 2017).
43. Engelhard, M.; Hurler, S.; Weigand, A.; Giuliano, S.; Puppe, M.; Schenk, H.; Hirsch, T.; Moser, M.; Fichter, T.; Kern, J.; et al. Techno-economic analysis and comparison of CSP with hybrid PV-Battery Power Plants. In Proceedings of the 22nd Solar PACES, Abu Dhabi, United Arab Emirates, 12 October 2016; Available online: http://bit.ly/2ig0ZOE (accessed on 12 October 2017).
44. IEA—International Energy Agency. *World Energy Outlook 2014*; IEA Publishing: Paris, France, 2014.
45. Stackhouse, P.W.; Whitlock, C.H. (Eds.) Surface meteorology and solar energy (SSE) release 6.0. In *NASA SSE 6.0, Earth Science Enterprise Program*; National Aeronautic and Space Administration (NASA): Washington, DC, USA, 2008. Available online: http://eosweb.larc.nasa.gov/sse/ (accessed on 12 October 2017).
46. Stackhouse, P.W.; Whitlock, C.H. Surface meteorology and solar energy (SSE) release 6.0 Methodology. In *NASA SSE 6.0, Earth Science Enterprise Program*; National Aeronautic and Space Administration (NASA): Washington, DC, USA, 2009. Available online: http://eosweb.larc.nasa.gov/sse/documents/SSE6Methodology.pdf (accessed on 12 October 2017).
47. Global Water Intelligence Desal Data. Plant Database. 2016. Available online: www.desaldata.com/projects (accessed on 13 October 2017).
48. Ministry of Water and Electricity. National Water Strategy: The Roadmap for Sustainability, Efficiency and Security of the Water Future in the KSA National Water Strategy, Presentation for Water Arabia 2013. 2013. Available online: www.sawea.org/pdf/waterarabia2013/Tue_Panel_Discussion/National_Water_Strategy.pdf (accessed on 13 October 2017).
49. Mehzer, T.; Fath, H.; Abbas, Z.; Khaled, A. Techno-economic assessment and environmental impacts of desalination technologies. *Desalination* **2011**, *266*, 263–273. [CrossRef]
50. Ghaffour, N.; Missimer, T.M.; Amy, G.L. Technical review and evaluation of the economics of water desalination: Current and future challenges for better water supply sustainability. *Desalination* **2013**, *309*, 197–207. [CrossRef]
51. Gude, G.V.; Nirmalakhandan, N. Desalination at low temperatures and low pressures. *Desalination* **2009**, *244*, 239–247. [CrossRef]

52. Inoue, K.; Abe, Y.; Murakami, M.; Mori, T. Feasibility study of desalination technology utilizing the temperature difference between seawater and inland atmosphere. *Desalination* **2006**, *197*, 137–153. [CrossRef]
53. Arnau, D.A.P.; Onatwe, I.D.N.E.; Hanganu, D.A. System and Method for Desalinating Seawater. European Patent Application No. EP2011038219820110615, 19 November 2012.
54. Loutatidou, S.; Chalermthai, B.; Marpu, P.R.; Arafat, H. Capital cost estimation of RO plants: GCC countries versus southern Europe. *Desalination* **2014**, *347*, 103–111. [CrossRef]
55. Al-Zahrani, A.; Orfi, J.; Al-Suhaibani, Z.; Salim, B.; Al-Ansary, H. Thermodynamic analysis of a reverse osmosis desalination unit with energy recovery system. *Procedia Eng.* **2012**, *33*, 404–414. [CrossRef]
56. M+W Group. Solar Seawater Desalination. In *Visit of the MASDAR Test Plants in Ghantoot, UAE*; M+W Central Europe GmbH Global Business Unit Energy: Stuttgart, Germany, 2016.
57. Water Online. Ghalilah Desalination Plant Honored with Distinction Award for Desalination Plant of the Year at 2016 Global Water Awards. 2016. Available online: www.wateronline.com/doc/ghalilah-desalination-plant-honored-plant-of-the-year-at-global-water-awards-0001 (accessed on 13 October 2017).
58. Elimelech, M.; Phillip, A.W. The future of seawater desalination: Energy, technology and the environment. *Science* **2011**, *333*, 712–717. [CrossRef] [PubMed]
59. Reddy, K.V.; Ghaffour, N. Overview of the cost of desalinated water and costing methodologies. *Desalination* **2007**, *205*, 340–353. [CrossRef]
60. Al-Mutaz, I.S.; Wazeer, I. Current status and future direction of MED-TVC technology. *Desalin. Water Treat.* **2015**, *55*. [CrossRef]
61. Moser, M.; Trieb, F.; Fichter, T.; Kern, J.; Hess, D. A flexible techno-economic model for the assessment of desalination plants driven by renewable energies. *Desalin. Water Treat.* **2015**, *55*, 3091–3105. [CrossRef]
62. Fath, H.; Sadik, A.; Mehzer, T. Present and future trends in the production and energy consumption of desalinated water in GCC countries. *Int. J. Therm. Environ. Eng.* **2013**, *5*, 155–165.
63. Palenzuela, P.; Alarcon-Padilla, D.C.; Zaragoz, G.; Blanco, J. Comparison between CSP+MED and CSP+RO in Mediterranean area and MENA region: Techno-economic analysis. *Energy Procedia* **2015**, *69*, 1938–1947. [CrossRef]
64. IEA—International Energy Agency. *Key World Energy Statistics*; IEA: Paris, France, 2015.
65. Afanasyeva, S.; Breyer, C.; Engelhard, M. The Impact of Cost Dynamics of Lithium-Ion Batteries on the Economics of Hybrid PV-Battery-GT Plants and the Consequences for Competitiveness of Coal and Natural Gas-Fired Power Plants. *Energy Procedia* **2016**, *99*, 157–173. [CrossRef]
66. Aghahosseini, A.; Bogdanov, D.; Breyer, C. The MENA Super Grid towards 100% Renewable Energy Power Supply by 2030. In Proceedings of the 11th International Energy Conference, Tehran, Iran, 30–31 May 2016; Available online: http://bit.ly/2iYvZCO (accessed on 13 October 2017).
67. Kittner, N.; Lill, F.; Kammen, M.D. Energy storage deployment and innovation for the clean energy transition. *Nat. Energy* **2017**, *2*. [CrossRef]
68. Schmidt, O.; Hawkes, A.; Gambhir, A.; Staffell, I. The future cost of electrical energy storage based on experience rates. *Nat. Energy* **2017**, *2*. [CrossRef]
69. Breyer, C.; Afanasveya, S.; Brakemeier, D.; Engelhard, M.; Giuliano, S.; Puppe, M.; Schenk, H.; Hirsch, T.; Moser, M. Assessment of mid-growth of assumptions and learning rates for comparative studies of CSP and hybrid PV-battery power plants. *AIP Conf. Proc.* **2017**, *1850*. [CrossRef]
70. Al-Iriani, A.M.; Trabelsi, M. The economic impact of phasing out energy consumption subsidies in GCC countries. *J. Econ. Bus.* **2016**, *87*, 35–49. [CrossRef]
71. Fthenakis, V.; Atia, A.A.; Morin, O.; Bkayrat, R.; Sinha, P. New prospects for PV powered water desalination plants: Case studies in Saudi Arabia. *Prog. Photovolt. Res. Appl.* **2016**, *24*, 543–550. [CrossRef]
72. Brown, T.W.; Bischof-Niemz, T.; Blok, K.; Breyer, C.; Elliston, B.; Lund, H.; Mathiesen, B.V. Response to 'Burden of Proof: A Comprehensive Review of the Feasibility of 100% Renewable-Electricity Systems'. *Renew. Sustain. Energy Rev.* **2017**. under review. Available online: https://arxiv.org/pdf/1709.05716.pdf (accessed on 13 October 2017).
73. Clack, C.T.M.; Qvist, S.A.; Apt, J.; Bazilian, M.; Brandt, A.R.; Caldeira, K.; Davis, S.J.; Diakov, V.; Handschy, M.A.; Hines, P.D.H.; et al. Evaluation of a proposal for reliable low-cost grid power with 100% wind, water, and solar. *Proc. Natl. Acad. Sci. USA* **2017**, *114*, 6722–6727. [CrossRef] [PubMed]

74. Jacobson, M.Z.; Delucchi, M.A.; Cameron, M.A.; Frew, B.A. The United States can keep the grid stable at low cost with 100% clean, renewable energy in all sectors despite inaccurate claims. *Proc. Natl. Acad. Sci. USA* **2017**, *114*, 5021–5023. [CrossRef] [PubMed]
75. Creutzig, F.; Agoston, P.; Goldschmidt, C.J.; Luderer, G.; Nemet, G.; Pietzcker, R.C. The underestimated potential of solar energy to mitigate climate change. *Nat. Energy* **2017**, *2*. [CrossRef]
76. Pehl, M.; Arvesen, A.; Humpenöder, F.; Popp, A.; Hertwich, E.G.; Luderer, G. Understanding future emissions from low-carbon power systems by integration of life-cycle assessment and integrated energy modelling. *Nat. Energy* **2017**, *2*, 939–945. [CrossRef]
77. Ram, M.; Bogdanov, D.; Aghahosseini, A.; Oyewo, S.; Gulagi, A.; Child, M.; Fell, H.-J.; Breyer, C. *Global Energy System Based on 100% Renewable Energy—Power Sector*; Lappeenranta University of Technology and Energy Watch Group: Lappeenranta, Finland; Berlin, Germany, 2017; Available online: http://bit.ly/2hU4Bn9 (accessed on 14 October 2017).
78. Pleßmann, G.; Erdmann, M.; Hlusiak, M.; Breyer, C. Global energy storage demand for a 100% renewable electricity supply. *Energy Procedia* **2014**, *46*, 22–31. [CrossRef]
79. Joint Research Center. *Energy Technology Reference Indicator Projections for 2010–2050*; Joint Research Center Science and Policy Reports; Joint Research Center Institute for Energy and Transport: Petten, The Netherlands, 2014.
80. ETIP-PV—European Technology and Innovation Platform Photovoltaics. *The True Competitiveness of Solar PV—A European Case Study*; ETIP-PV: Munich, Germany, 2017.
81. Fraunhofer Institute for Solar Energy Systems ISE. *Current and Future Cost of Photovoltaics—Long-Term Scenarios for Market Development, System Prices and LCOE of Utility-Scale PV Systems (Study on behalf of Agora Energiewende, Freiburg and Berlin)*; Fraunhofer Institute for Solar Energy Systems ISE: Freiburg, Germany, 2015.
82. Neij, L. Cost development of future technologies for power generation—A study based on experience curves and complementary and bottom-up assessments. *Energy Policy* **2008**, *36*, 2200–2211. [CrossRef]
83. Haysom, J.E.; Jafarieh, O.; Anis, H.; Hinzer, K.; Wright, D. Learning curve analysis of concentrated photovoltaic systems. *Prog. Photovolt. Res. Appl.* **2014**, *23*, 1678–1686. [CrossRef]
84. Kutscher, C.; Mehos, M.; Turchi, C.; Glatzmaier, G.; Moss, T. *Line-Focus Solar Power Plant Cost Reduction Plant*; National Renewable Energy Laboratory: Golden, CO, USA, 2010.
85. Sigfusson, B.; Uihelein, A. *Joint Research Center Geothermal Energy Status Report*; European Commission; Joint Research Center Institute for Energy and Transport: Petten, The Netherlands, 2015.
86. Agora Energiewende. Stromspeicher in der Energiewende. 2014. Available online: www.agora-energiewende.de/fileadmin/Projekte/2013/speicher-in-der-energiewende/Agora_Speicherstudie_Web.pdf (accessed on 14 October 2017).
87. Breyer, C.; Tsupari, E.; Tikka, V.; Vainikka, P. Power-to-Gas as an emerging profitable business through creating an integrated value chain. *Energy Procedia* **2015**, *73*, 182–189. [CrossRef]
88. International Energy Agency. *World Energy Investment Outlook*; International Energy Agency: Paris, France, 2003.
89. McDonald, A.; Schrattenholzer, L. Learning rates for energy technologies. *Energy Policy* **2001**, *29*, 255–261. [CrossRef]
90. Urban, W.; Lohmann, H.; Girod, K. *Abschlussbericht für das BMBF-Verbundprojekt Biogaseinspeisung*; Fraunhofer UMSICHT: Oberhausen, Germany, 2009.
91. Hoffmann, W. Importance and evidence for cost effective electricity storage. In Proceedings of the 29th European Photovoltaic Solar Energy Conference, Amsterdam, The Netherlands, 22–26 September 2014.

Publication IV

Caldera, U., and Breyer, C.
The role that battery and water storage play in Saudi Arabia's transition to an integrated 100% renewable energy power system

Reprinted with permission from
Journal of Energy Storage
Vol. 17, pp 299-310, 2018

Journal of Energy Storage 17 (2018) 299–310

Contents lists available at ScienceDirect

Journal of Energy Storage

journal homepage: www.elsevier.com/locate/est

The role that battery and water storage play in Saudi Arabia's transition to an integrated 100% renewable energy power system

Upeksha Caldera*, Christian Breyer

Lappeenranta University of Technology, Skinnarilankatu 34, 53850 Lappeenranta, Finland

ARTICLE INFO

Article history:
Received 3 October 2017
Received in revised form 28 December 2017
Accepted 18 March 2018
Available online 3 April 2018

Keywords:
100% renewable energy
Saudi Arabia
Energy transition
Battery
Water storage
Flexibility

ABSTRACT

Saudi Arabia can transition to a 100% renewable energy system by 2040 including the integration of the power, desalination and non-energetic industrial gas sectors. Single-axis tracking PV and battery storage contribute the highest to the final LCOE of the system. By 2050, single-axis tracking PV accounts for 79% of the total electricity generation. Battery storage accounts for 30% of the total electricity demand. Battery storage and desalination plants provide additional flexibility to the energy system. Through sensitivity analysis, it is found that decreasing the capex of desalination plants results in lower full load hours (FLH) and a decrease in battery storage output. This results in lower energy system costs. However, the SWRO capex has to be reduced by 50% to achieve a reduction of 1% in SWRO FLH and a 2.1% in the annualised energy system costs. This is because it is preferable to run the expensive SWRO plants in baseload operation for total energy system cost reasons. Flexibility to the energy system can be provided at a lower cost by solar PV and battery storage than by SWRO plants and water storage. Decreasing battery capex reduces the flexibility of desalination plants further, increases single-axis tracking PV capacities, decreases wind and CCGT capacities, and ultimately results in lower LCOE. These insights enable to establish the least cost pathway for Saudi Arabia to achieve net zero emissions by mid-century.

1. Introduction

Energy storage is seen as a cornerstone of the green energy revolution [1,2]. The intermittent nature of solar and wind resources can be overcome with different types of flexibility (supply side management, demand side management, grids, sector coupling, storage), thereof energy storage is regarded as one of the most important, enabling a faster transition towards a 100% renewable energy system [3–5]. With the increase in global installed capacities of renewable energy power plants, there is a surge in demand for energy storage capacities. The Bloomberg New Energy Finances (BNEF) New Energy Outlook 2016 report forecasts the storage capacity to increase to 25 GW by 2028 from the 1 GW installed today [6].

Luo et al. [2] provides an overview of the current storage technologies and explains that pumped hydro storage (PHS) accounts for 99% of the global storage capacities. However, with improved power to energy ratios, Lithium-ion batteries are currently experiencing by far the fastest growth of all storage options and being used in small and utility-scale applications [2]. Consequently, there has been a sharp decline in the capex of batteries as presented by Liebreich from BNEF [7]. The price of the electric vehicle (EV) lithium ion battery price is estimated to have fallen from 770 €/kWh in 2010 to 243 €/kWh in 2015 [7]. The report forecasts the cost to plunge even more sharply to 162 €/kWh by 2018, a 77% fall in cost between 2010 and 2018. Based on the discussed learning curve rate of 14% - 19%, the capital cost of electric vehicles is expected to arrive at parity with internal combustion engine cars by 2022 [7]. Tesla is reported to project even steeper cost reductions with cost of electric vehicle battery packs dropping to 100 USD/kWh by 2020 [8]. These projections are further supported by Kittner et al. [9], who based on their model, expect electric vehicles to be cost competitive with combustion engine vehicles as early as 2017 and no later than 2020. The core technology of Li-ion batteries does not differ substantially between mobile and stationary applications. Thus, cost reductions in one type of battery storage also translates to cost reductions in other applications. Schmidt et al. [10] analyses future cost projections for electrical energy storage, based on learning curves. The learning rate for lithium ion battery storage in electric vehicles is estimated to be 16%. Meanwhile, lithium ion battery storage in electronics has the steepest learning rate with 30%. Utility and residential scale applications had a lower learning rate of 12% in the past. Breyer

* Corresponding author.
E-mail addresses: upeksha.caldera@lut.fi (U. Caldera), christian.breyer@lut.fi (C. Breyer).

https://doi.org/10.1016/j.est.2018.03.009
2352-152X/

et al. [11] have assessed the impact of learning rates for lithium ion battery storage on battery system cost and base their analysis on a learning rate of 15–20%.

In a recent study, we investigated the least cost pathway for Saudi Arabia to transition from the current fossil-based power sector to a 100% renewable energy based system by 2050, whilst integrating the increasing desalination sector with the power sector [12]. This study was motivated by the Saudi government's new vision to embrace the country's renewable energy resources and build a future without reliance on oil. Salam and Khan [13] explain that in order to achieve energy security and minimise energy costs, Saudi Arabia has to adopt higher shares of renewable energy. In addition, Saudi Arabia has consented to achieving 'net zero emissions' by mid-21st century at the Conference of the Parties (COP21) in Paris [14]. A pathway towards achieving this vision, agreed upon by almost all nations on the planet, is what we present. The energy transition pathway discussed aims to fulfill three main criteria: i) only existing technology is used; (ii) no conflict to the Paris Agreement; (iii) low cost pathway.

In the study in [12] it was found that Saudi Arabia can achieve a 100% renewable energy power system by 2040 with a power sector dominated by PV single-axis tracking and battery storage. Single-axis tracking PV contributed 210 GW out of the total 403 GW by 2040. The contribution increased to 369 GW out of a total of 520 GW by 2050. Battery storage contributed up to 30% of the total electricity demand in 2040 and the contribution increases to 48% by 2050. The combination of PV and battery storage provided the least cost option to meet Saudi Arabia's power and desalination sector demands. This was mainly due to the sharp anticipated decrease in PV and battery storage.

In addition, the integration of the power and water desalination sector provided the least cost transition pathway as opposed to the independent transition of the two sectors. The desalination plants and water storage provide additional flexibility to the system, enabling better utilization of the renewable energy generated. This leads to a reduction in the demand for battery and power-to-gas (PtG) storage in the transition. The study [12] highlights the relationship between water and battery storage in the energy transition pathway for Saudi Arabia. Al-Nory and El-Beltagy [15] have modelled the role of water storage when high shares of renewable energy capacities are integrated into the Saudi Arabian electricity grid. The model was simulated for 7 days, on a daily resolution. A 12% reduction in total costs was determined, compared to the integration of renewable energy capacities without water storage. This study further contributes to the understanding of the role that seawater desalination and water storage can play in a 100% renewable energy power system. Similarly, Bognar et al. [16] found that the integration of SWRO plants in a hybrid wind and diesel energy system, for Cape Verde, resulted in the least electricity and water costs. These views are further supported by Lopes et al. [17]. Strang [18] discusses the benefits of storing excess electricity in water and presents an example of tidal power plant design in Australia utilising desalination plants and water storage.

Located between the Persian Gulf and the Red Sea, Saudi Arabia is one of the largest arid countries without any permanent rivers or lakes. Whilst the global average renewable water resource per capita per year is 6000 m^3, Saudi Arabia has only 84.8 m^3/(capita·a) [19]. In spite of the water scarcity, Saudi Arabia has the third highest water consumption per capita at 250 liters/(capita·d). This is only behind the United States and Canada. The country's water demand is expected to increase by 56% by 2035. Meanwhile, at the current rate of water withdrawal, ground water aquifers are expected to provide potable water only for the next 10–30 years [20].

To augment the fresh water resources, Saudi Arabia relies on seawater desalination, particularly to meet the municipal and industrial water demands. In 2010, 58% of the country's total water demand was met through non-renewable ground water resources, 33.5% by surface water and renewable ground water, 6% by desalinated water and 2.2% by waste water reuse [21]. In 2014, desalinated water is estimated to have met 60% of KSA's municipal water demand [22]. By the end of 2015, Saudi Arabia accounted for 15% of the global installed desalination capacity [21]. With the diminishing of fresh water resources, seawater desalination is expected to play a pivotal role in meeting Saudi Arabia's future water demands.

The Saudi Vision 2030 document, released in April 2016, illustrates the Saudi government's road map to ensure the country's development and security [23]. The document, together with the more detailed National Transformation Program 2020 document [23], highlights the government's urgency to secure the country's water resources. In addition to better management of existing renewable water resources and more water from desalination, one of the objectives is to increase the strategic water storage from 0.4 days at present to 3 days by 2020 [23]. However, this is much lower than the water storage capacities planned for by other countries in the Gulf region. The United Arab Emirates (UAE) have recently completed an underground water reservoir that can provide 180 liters of water per person per day for 90 days [24,25]. Similarly, the Water Security Mega Reservoirs Project in Qatar is expected to provide 7 days of water storage. After the final phase of construction, the reservoirs are expected to store 14,384,520 m^3 of water [26], as opposed to the current water storage capacity of 1,097,766 m^3. Research on food and water security in Saudi Arabia by Future Directions International highlight the importance of long term water storage in water-scarce Saudi Arabia [27].

Saudi Arabia's increasing demand for water storage, and the results in [12], which suggest an interplay between battery and water storage, provide the motivation for the current study: How do the technical and financial parameters of battery and water storage influence the least cost transition path to a 100% RE based power system? The research answers will demonstrate if it is cost-effective for Saudi Arabia to harness the increasing desalination and water storage demand to reduce the requirements for battery storage in the energy transition. Or, will battery storage remain the lower cost storage option for the Saudi energy transition? Existing literature discuss the potential role of desalination and water storage in hybrid energy systems on a smaller scale. In this manuscript, a more detailed study of the role of desalination plants and water storage in a full energy system is conducted.

In the sections that follow, a cost-optimised energy transition pathway for Saudi Arabia to achieve a 100% RE based power sector, seawater desalination and industrial gas sector, by 2050, is presented. A sensitivity analysis is then carried out on the pathway to understand the interplay between battery and water storage. This will enable to further optimise the energy transition pathway for Saudi Arabia.

2. Methodology

2.1. Overview

The objective of our work is to understand the features of battery and water storage that will allow for the optimal transition of Saudi Arabia's 2015 power, seawater desalination and industrial gas sector to a 100% renewable energy based system by 2050.

The approach taken to answer the research question is similar to that in [12] and additionally accounts for KSA's multiple effect distillation (MED) desalination plants and the industrial gas sector. In addition, the water storage plants are now located at the

desalination site rather than at the demand site. The methodology maybe summarized as follows:

1. The energy transition from the current (as of the beginning of 2015) fossil based power system in KSA to a 100% renewable energy based power system by 2050, in 5-years time steps, is found. After 2015, there are no new fossil powered thermal plants allowed, except gas turbines, which can be shifted from firing fossil gas to RE-base synthetic natural gas (SNG), or biomethane. The existing fossil based power systems are phased out based on their lifetimes. The increase in total electricity demand and population over the years is accounted for. The optimal mix of renewable power systems to replace the phased out fossil power systems are found and the resulting system's levelised cost of electricity (LCOE) is found for every time step. The industrial gas and desalination sectors are integrated with the power sector.
2. The non-energetic industrial gas demand of Saudi Arabia, from 2015 to 2050 is found and integrated into the power system.
3. Fig. 2 presents the projected growth in the industrial gas demand in Saudi Arabia. To attain a 100% renewable energy future, our work assumes that over time the industrial gas demand is met from SNG. This can be achieved through power-to-gas plants (PtG) that comprise of two processes already used in industry: electrolysis and methanation [28,29]. PtG plants convert renewable electricity to renewable methane that can be stored in the existing gas infrastructure and used as per conventional natural gas or used for the industry.
4. Seawater desalination demand in KSA from 2015 to 2050 is determined and the corresponding desalination capacities integrated into the system. After 2015, seawater reverse osmosis plants are allowed to be installed due to the dominance of the technology in the Saudi Arabian desalination market. Multiple Effect Distillation (MED) plants are considered due to the low thermal consumption and lower electricity demand than seawater reverse osmosis (SWRO) [30,31]. The waste heat from the power system is used to meet the thermal demand of the MED plants.
   Multi stage flash (MSF) desalination capacities that were online up to 2015 are included and phased out based on the lifetimes. MSF stand alone plants are excluded due to the relatively higher thermal consumption compared to MED plants [30,31]. MED and MSF cogeneration plants are excluded due to the requirement for fossil powered thermal power plants [32].
5. Once the successful energy transition has been set up, the capex of the battery storage and SWRO desalination plant is varied, separately, to identify the impacts on the total system costs. Thus a sensitivity analysis is carried out to understand the relationship between battery and water storage.

The final results of the integration of the power, desalination and gas sectors is discussed in [26]. In this paper, we focus on the battery and water storage aspects of the energy transition.

2.2. Model overview

The LUT Energy System Transition model is utilised for the design and analysis of the energy transition as discussed in [12]. The energy model is based on the linear optimization method with interior point optimization and designed in an hourly temporal and 0.45° x 0.45° spatial resolution. The model optimises the installed RE capacities, cost of electricity generation and generation ramping such that the total annual cost of the energy system is minimised.

It is composed of all relevant power generation and storage technologies, respective installed capacities and different operation modes of these technologies. A key feature of the model is its flexibility and expandability besides the hourly resolution for a full real year. Detailed information on the construction and operation of the hourly linear optimisation model is presented in [33–36].

Fig. 1 illustrates the LUT model. For the energy transition, the model determines the optimal combination of the components that meets the electricity demand of every hour for the time period from 2015 to 2050, in 5-years time steps.

2.3. Input data – power, desalination and the industrial gas sector in KSA

The input data is similar to the data presented in [12] except for the adjusted PV capex assumptions, additional MED desalination capacities and the non-energetic industrial gas sector. Thus, this section provides an overview of the data with details of the additional input data. Table 1 presents the updated PV capex numbers used for this paper, based on recent PV capex projections from [37].

Table 2 illustrates the increase in electricity demand assumed for Saudi Arabia from 2015–2050 [38–40]. The electricity demand

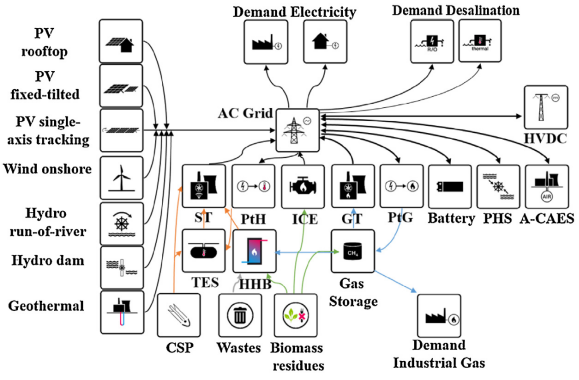

Fig. 1. Block diagram of the LUT Energy System Transition model used for Saudi Arabia.

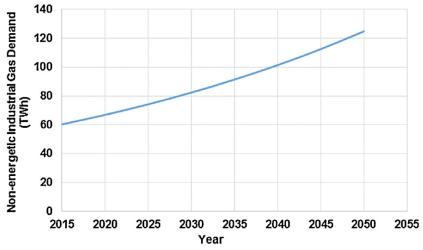

Fig. 2. Variation in non-energetic industrial gas demand for Saudi Arabia.

in 2015 was taken from [38,39]. The World Energy Outlook [39] projects a compound annual growth rate of 2.7% for the Middle East. This was then applied to the demand of 289 TWh in 2015 to project the Saudi electricity demand in the years to come. The LUT model optimises the renewable energy power plants necessary to meet the increasing electricity demand over time.

Table 3 presents an overview of the desalination demand from 2015 to 2050 and the installed capacities by 2015. The methodology used to determine the desalination demand is described in [12]. The table also accounts for the MED technologies online by 2015. After 2015, the model optimises the SWRO and MED stand alone desalination plants required to meet the desalination demand. The optimization is based on the availability of excess heat in the energy system and the cost effectiveness. The cost of the desalination technologies is presented in Appendix A (Table A1). Cost projections for SWRO is based on the model described by Loutatidou et al. [41]. The projections display a learning rate of 15%, as explained in the maiden paper on learning rates of SWRO [42] and an annual growth of desalination capacity slightly higher than 20%. The methodology used to project the technical and financial parameters of SWRO is presented in [12]. All the technical and financial parameters of the power plant technologies utilised by the model are also provided in [43]. Fig. 2 presents the expected growth in non-energetic industrial gas demand in Saudi Arabia [44]. In our model the aim is to ensure that by 2050, the non-energetic industrial gas demand is met from renewable energy. In 2015, the industrial gas demand is met with fossil natural gas. However, over time, PtG plants produce the SNG required. The increase in cost of fossil natural gas over time and the decrease in cost of PtG plants, makes it viable to produce SNG.

3. Results

The three scenarios modelled are described below. The objective of each simulation scenario is to determine the energy system with the least total annualised cost, based on section 2.2 and the technical and financial assumptions of all components presented in Fig. 1. Conducted as a sensitivity analysis, the difference between the simulation scenarios are the SWRO and battery capex values. Different capex values result in different optimised energy systems and system costs. By studying the resulting energy systems and costs, discussed in the following subsections, it is possible to understand the flexibility provided by SWRO and battery plants to the energy system.

Table 1
Updated PV capex assumed in this research [37].

		2020	2025	2030	2035	2040	2045	2050
PV fixed-tilted	€/kWp	580	466	390	337	300	270	246
PV single-axis	€/kWp	638	513	429	371	330	297	271

Table 2
Variation in the electrical energy consumption of Saudi Arabia from 2015 to 2050.

	Total Electricity Consumption (TWh)
2015	289
2020	330
2025	377
2030	431
2035	492
2040	563
2045	643
2050	734

1. Integrated scenario: This section presents an overview of the optimal transition pathway for the power, desalination and non-energetic industrial gas sectors in Saudi Arabia. The objective of each simulation scenario is to determine the energy system with the least total annualised cost, based on section 2.2. The water storage behavior and desalination plant operation is illustrated. Detailed discussions of the technologies and costs for the optimised transition pathway for Saudi Arabia is provided in [43].
2. Integrated scenario with decrease in SWRO capex: In this scenario, the same simulation as in point 1 is run, but for different SWRO capex values. This helps to understand the impact of SWRO plants on the optimal energy transition path.
3. Integrated scenario with decrease in battery capex: In this scenario, the same simulation as in point 1 is run, but for different battery capex values. This helps to understand the impact of battery storage on the optimal energy transition path.

3.1. Integrated scenario

Fig. 3 (left) presents the variation in the LCOE during the energy transition and the contribution of the different components to the LCOE. The LCOE decreases from 139.7 €/MWh in 2015 to 41.5 €/MWh in 2050. KSA achieves a 100% renewable energy system by 2040 with an LCOE of 48.9 €/MWh. Single-axis tracking PV and battery storage is the largest contributor to the LCOE by 2050, followed by wind power plants. As shown in Fig. 3 (right), by 2050, single-axis tracking PV accounts for 377.5 GW out of the total power plant capacity of 600 GW. Battery storage provides a total output of 329 TWh_{el} that accounts for 30.3% of the total system electricity demand.

Fig. 4 (left) illustrates the increase in water desalination and storage capacities to meet the desalination demand. SWRO desalination is the preferred technology due to the low electricity consumption. MED stand alone plants account for less than 1% of the desalination demand due to the low availability of excess heat in the system. By 2050, there is 58 880 614 m^3/day of SWRO plants and 1 531 649 m^3 of water storage. At times of excess electricity production, larger volumes of water can be desalinated and stored in water storage. When there is lower electricity production, the water in storage can be pumped to meet the water demand. In 2050, water storage capacity is 3% of the daily desalination demand. Fig. 4 (right) illustrates the variation in the water storage for 2030. The water storage fluctuates on a daily basis, although not a large variation. The water storage is used mostly in the evening hours. The full load hours of the SWRO desalination plants is estimated to be 8707 h, which is baseload operation. Water from storage is used to supplement the remaining 53 h.

Table 3
Desalination demand and capacities required to meet KSA's increasing total water demand. The desalination capacities after 2015 will be determined by the model.

		2015	2020	2025	2030	2035	2040	2045	2050
Population	mill	31.50	34.40	36.85	39.13	41.24	43.14	44.76	46.06
Total water demand	mill m^3/day	65.4	68.5	75.6	81.0	88.6	96.7	105.0	112.6
Desalination demand based on	mill m^3/day	19.1	21.8	27.5	32.0	38.4	45.2	53.8	58.7
Final non-renewable water resource used	mill m^3/day	8.9	7.9	5.8	3.9	6.2	8.5.	0	0
Actual desalination demand	mill m^3/day	10.2	13.9	21.7	28.2	32.3	36.7	53.8	58.7
Installed capacities									
SWRO	mill m^3/day	2.7							
MSF stand alone	mill m^3/day	1.52							
MSF cogeneration	mill m^3/day	2.73							
MED stand alone	mill m^3/day	1.57							
MED cogeneration	mill m^3/day	0.95							

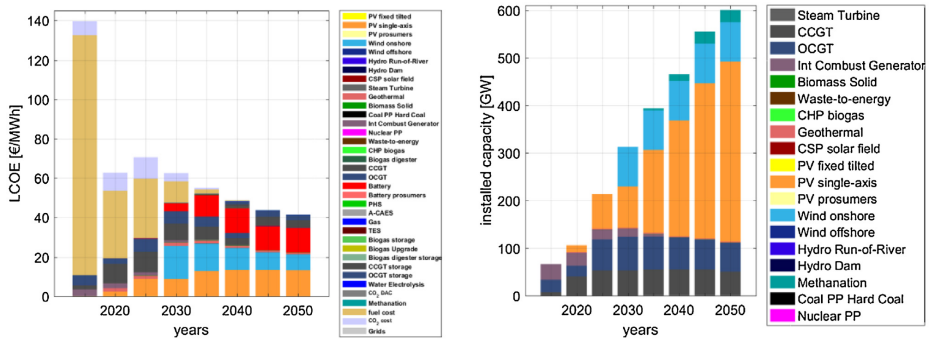

Fig. 3. Variation of LCOE (left) and installed capacities of the different power plants required (right) for the energy transition from 2015 to 2050.

Fig. 4 (bottom) illustrates the further reduced use of water storage in 2050. The SWRO plant full load hours increase to 8733, implying that the water storage is used only for 27 h. It was found that the integration of the desalination plants into the transition enabled a decrease between 1% and 6% in the annual levelised costs of the total energy system. This can be attributed to the additional flexibility offered by the SWRO plants and water storage.

3.2. Integrated scenario with decreasing SWRO capex

The SWRO capex was reduced to different percentages of the original capex in 2030 and the model re-run. Similar to section 3.1, the model establishes the least cost energy transition pathway. However, this time based on the reduced SWRO capex in 2030. All other parameters are the same as that utilised in section 3.1. The procedure was repeated for the year 2050 and the corresponding energy system analysed.

Tables 4 and 5 illustrates some of the key observations of the energy system for the year 2030 and 2050 respectively. The initial SWRO capex is estimated to be 725 €/(m^3·day) for 2030 and 415 €/(m^3·day) for 2050. In 2030, as the SWRO capex is reduced, the FLH of the desalination plants decrease and consequently water storage capacity increases. Concurrently, there is a reduction in the output of the battery storage. This is due to the increased flexibility provided by the reduced capex of SWRO and water storage plants. When the SWRO capex is reduced by 50%, the FLH of the desalination plants decreased from 8707 h to 8432 h – a reduction of 3%. The water storage capacity increased from 506 577 m^3 to 1 647 112 m^3 – accounting for 6% of the 2030 daily desalination demand. The flexibility of the water storage and desalination plants allow for a decrease in battery energy output of almost 6%. In 2050, at 50% of the SWRO capex, the SWRO FLH dropped to 8638 h from 8733 h – a reduction of 1%. The water storage capacity increased from 1 531 649 m^3 to 2 817 521 m^3 – accounting for 4.6% of the 2050 daily desalination demand. The relatively lower flexibility of SWRO plants and water storage in 2050 meant that battery storage output only reduced by 0.6%.

The reduced battery storage output and the desalination capex leads to a reduction in the total system costs. The total annualised system cost is the sum of the annualised cost of the power system and the desalination system. When the SWRO capex is halved, the annualised costs of the system decreases by about 2%. The results indicate that a large and unrealistic drop in SWRO capex is required to obtain concrete benefits for the energy system costs. It has to be noted that throughout this work a weighted average cost of capital (WACC) of 7% is assumed.

Fig. 5 (top) illustrates the variation in the SWRO FLH with the variation in capex. As can be seen for both years 2030 and 2050, there is a decrease in the FLH as the capex decreases. This is because at higher capex, the desalination plants have to be run at higher FLH to enable lower water production costs. There is a slightly steeper decrease in FLH in 2030. Fig. 5 (bottom) illustrates the variation in the battery output with the capex. The battery output decreases with the decrease in SWRO capex. This is attributed to the increasing flexibility of the SWRO plants with the decrease in SWRO capex.

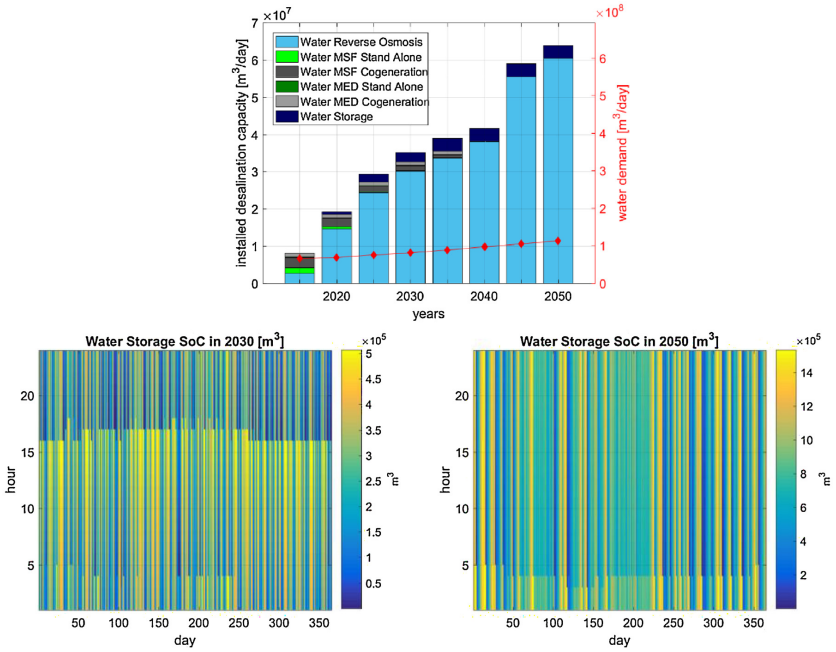

Fig. 4. Water desalination capacities required to meet the desalination demand from 2015 to2050 (top), water storage relative state of charge in 2030 (bottom left) and in 2050 (bottom right).

Table 4
Key observations for the transition year 2030 when SWRO capex is reduced (WACC assumed is 7%).

		100% SWRO Capex	80% SWRO Capex	75% SWRO Capex	50% SWRO Capex
Desalination Demand	m^3/day	28 200 000			
SWRO capacity	m^3/day	28 371 078	28 681 559	28 752 164	29 291 681
Water storage capacity	m^3	506 577	1 145 083	1 175 160	1 647 112
Relative increase in storage to 100% case			638 506	668 583	1 140 535
% of daily demand	%	2%	4%	4%	6%
SWRO FLH	hrs	8707	8612	8591	8432
Relative decrease in FLH to 100% case	%		1.1%	1.3%	3.0%
Battery output	TWh	34	33	33	32
SWRO capex	€/(m^3·day)	725	580	544	363
Battery capex	€/kWh	150	150	150	150
Desalination capex	b€	49	45	43	38
Gas storage output	TWh	0.57	0.57	0.57	0.57
Thermal energy storage output electricity	TWh	0.01	0.01	0.02	0.02
System capex	b€	280	275	274	267
Total capex	b€	329	320	317	305
Relative decrease in total capex to 100% case	%		2.7%	3.6%	7.0%
Total annualised system cost	b€	43.2	42.8	42.7	42.3
Relative decrease in annualised cost to 100% case	%		0.82%	1.03%	2.03%

The role played by gas storage and thermal energy storage is minimal compared to that of battery storage in the energy transition. As illustrated in Tables 4 and 5, the output of gas storage in 2030 is approximately 0.57 TWh_{th} and thermal energy storage is between 0.01–0.02 TWh_{th} for all SWRO capex values. Similarly in 2050, the output of gas storage is between 2.8–2.9 TWh_{th} and thermal output is between 14–16 TWh_{th}. The output of gas and thermal energy storage increase from 2030 to 2050, due to the increase in electricity demand. However, there is no influence from the decreasing SWRO capex.

3.3. Integrated scenario with decreasing battery capex

To determine the impacts of battery capex, the energy transition was modelled for 90% and 80% of the full battery capex. The SWRO capex was not modified. Table 6 illustrates some of the key observations for the 2030 energy system.

Table 5
Key observations for the transition year 2050 when SWRO capex is reduced (WACC assumed is 7%).

		100% SWRO Capex	80% SWRO Capex	75% SWRO Capex	50% SWRO Capex
Desalination Demand	m^3/day	58 699 992			
SWRO capacity	m^3/day	58 880 614	59 020 730	59 093 596	59 522 416
Water storage capacity	m^3	1 531 649	2 080 367	2 440 161	2 817 521
Relative increase in storage to 100% case			548 718	908 512	1 285 872
% of daily demand	%	3%	4%	4%	5%
SWRO FLH	hrs	8733	8712	8701	8638
Relative decrease in FLH to 100% case	%		0.2%	0.4%	1.0%
Battery output	TWh	329	328	327	327
SWRO capex	€/(m^3·day)	415	332	311	208
Battery capex	€/kWh	75	75	75	75
Desalination capex	b€	71	65	63	56
Gas storage output electricity	TWh	2.9	2.9	2.9	2.8
Thermal energy storage output electricity	TWh	16	16.1	16.2	16.1
System capex	b€	465.9	459.4	457.7	449.4
Total capex	b€	536.9	524.4	520.7	505.4
Relative decrease in system capex to 100% case	%		1.4%	1.8%	4.0%
Total annualised system cost	b€	58.9	58.4	58.2	57.6
Relative change in annualised cost to 100% case	%		0.88%	1.09%	2.13%

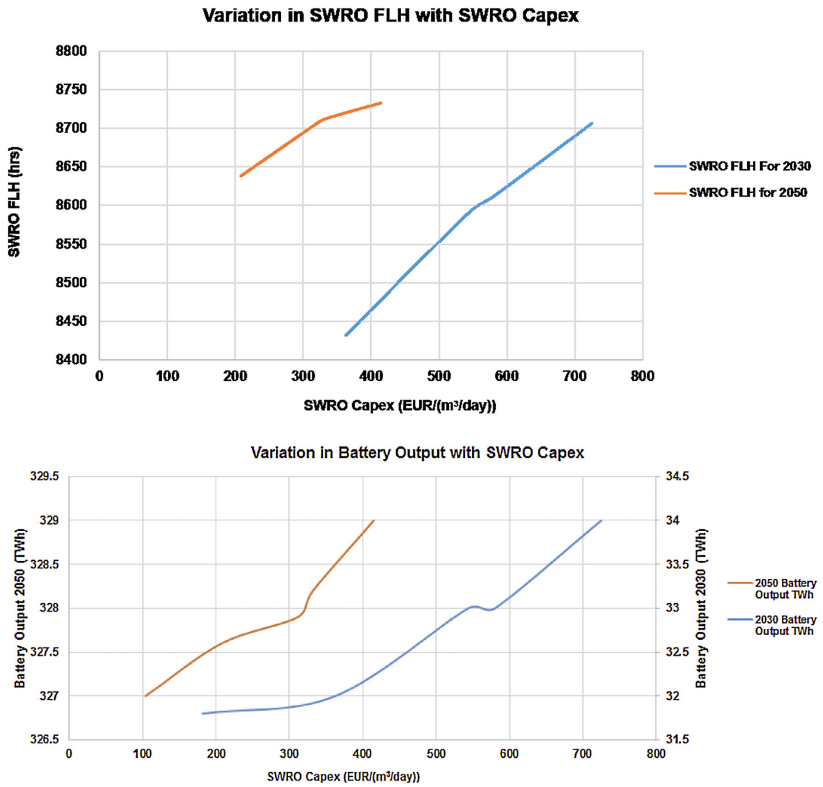

Fig. 5. Variation of SWRO FLH (top) and variation of battery output (bottom) with the SWRO Capex for the years 2030 and 2050. Expected SWRO capex are 725 and 415 €/(m^3·day) for 2030 and 2050 respectively.

Table 6
Key observations for the transition year 2030 when battery capex is reduced (WACC assumed is 7%).

		100% Battery Capex	90% Battery Capex	80% Battery Capex
Battery output	TWh	34	46	61.3
Relative change in Battery output	%		35%	80%
Battery capex	€/kWh	150	135	120
SWRO capacity	m^3/day	28 371 078	28 213 180	28 204 192
Relative change in SWRO capacity	%		−1%	−1%
Water storage capacity	m^3	506 577	53 629	36 343
SWRO FLH	hrs	8707	8756	8758
Relative change in SWRO FLh	%		0.6	0.6
Gas storage output	TWh	0.57	0.56	0.54
Relative change in gas storage output	%		−2%	−5%
Thermal energy storage output	TWh	0.01	0.009	0.008
Relative change in thermal energy output	%		−99%	−99%
Generation share – renewables	%	81.8%	83.0%	84.7%
Total Capex	b€	329	332	336
Relative change in total capex	%		1%	2%
Curtailment loss	%	3.9%	3.6%	3.4%
LCOE	€/MWh	62.5	62.4	62.1

As the battery capex is reduced, the electricity output from battery storage increases. At 80% of the battery capex, which is 120 €/kWh, the battery output increased by 80% to 61 TWh. This was accompanied by a slight increase of 1% in the full load hours of the SWRO plants. As the battery capex drops, it is beneficial to increase the output from battery storage and run the capex intensive SWRO plants on baseload. The latter approach enables lower water production costs for the SWRO plants of 0.6% in 2030. In addition, due to the increase in full load hours, the installed capacity of the SWRO plants reduced slightly. Water storage capacity dropped by 93%, due to the increase in full load hours of the SWRO plants.

For 80% of the battery capex, the gas storage output, utilised at the gas turbines, reduced by 5%. Thermal energy storage, although has the least output, decreased drastically by 99%. This can be attributed to the lower heat loss in the system due to the increase in battery storage output and consequent decrease in output from thermal power plants. The heat loss from thermal power plants is stored in thermal energy storage and used as required.

The total capex of the system accounts for the capex of the power and desalination sectors. Despite the decrease in battery capex, there is a slight increase in total capex of the system. At 80% of the capex, there is an increase of 2% in the total system capex. This slight increase can be attributed to the increase in battery storage. With the increase in battery storage, there is an increase in single-axis tracking PV power plants from 86.7 GW to 104.3 GW. This is illustrated in Fig. 6. However, the increase in capex is offset with a reduction in curtailment losses resulting in a slightly lower LCOE with the decrease in battery capex.

Fig. 6 illustrates the variation of installed capacities with the decrease in battery capex in 2030. Single-axis tracking PV experiences the largest increase in installed capacity while wind power plants decrease from 83.1 GW to 72.9 GW. Geothermal and fixed-tilted PV capacities remain the same. CCGT capacities and generation decrease from 53.1 GW to 51.9 GW and 99.9 TWh to 83.9 TWh respectively. OCGT capacities increase from 70.7 GW to 77.9 GW, but generation is zero GWh. This is attributed to the zero full load hours of the OCGT plants.

Table 7 illustrates the impacts of the decreasing battery capex on the energy system in 2050. Similar to 2030, the decrease in battery capex resulted in an increase in battery output. However, in 2050, the relative increase in battery storage output, for 80% of the battery capex was 8%. The relative increase in battery storage output, in 2030, for 80% for the battery capex, was 80%. Furthermore, the decreasing battery capex resulted in a decrease in the total system capex. This is in contrast to 2030 where the decrease in the battery capex resulted in an increase in the total system capex. The water production costs of the SWRO plants are lowered by 1.1% in 2050. This can be explained by the fact that by 2050, the Saudi Arabian energy system is run solely on 100% renewable energy. The decrease in battery capex increases the battery storage output and single-axis tracking PV capacities as shown in Fig. 7. However, the increase in single-axis tracking PV from 377.5 GW to 386.4 GW is 2% for a 20% decrease in battery

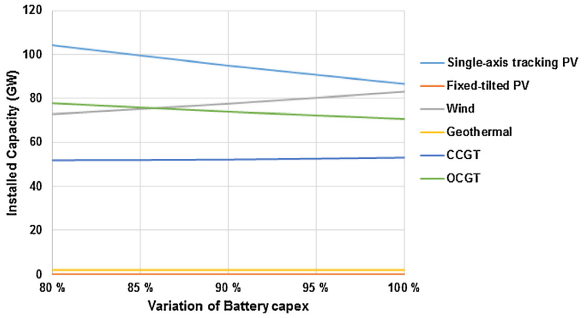

Fig. 6. Variation in installed capacities with decrease in battery capex for 2030.

Table 7
Key observations for the transition year 2050 when battery capex is reduced (WACC assumed is 7%).

		100% Battery Capex	90% Battery Capex	80% Battery Capex
Battery output	TWh	329	343	356.3
Relative change in Battery output	%		4%	8%
Battery capex	€/kWh	75	67.5	60
SWRO capacity	m^3/day	58 880 614	58 828 536	58 763 836
Relative change in SWRO capacity	%		−0.1%	−0.2%
Water storage capacity	m^3	1 531 649	1 275 466	894 929
SWRO FLH	hrs	8733	8741	8750
Relative change in SWRO FLh	%		0.1%	0.2%
Gas storage output	TWh	2.9	2.05	1.52
Relative change in gas storage output	%		−29%	−48%
Thermal energy storage output	TWh	16	5.79	0.09
Relative change in thermal energy output	%		−64%	−91%
Generation share - renewables	%	100%	100%	100%
Total Capex	b€	537	529	520
Relative change in total capex	%		−1%	−3%
Curtailment loss	%	3.9	4.3	4.5
LCOE	€/MWh	41.4	40.9	40.4

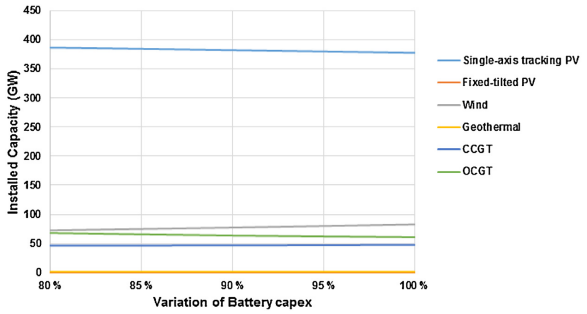

Fig. 7. Variation in installed capacities with decrease in battery capex for 2050.

capex. In contrast, the single-axis tracking PV capacities increased by 20% for the same decrease in battery capex in 2030. The capacity and generation of wind power plants reduced from 83.1 GW to 77.9 GW and 217.7 TWh to 191.1 TWh respectively. The capacity and generation of CCGT plants decreased from 48.1 GW to 46.9 GW and from 1697 GWh to 883 GWh respectively. The combination of lower capex of battery storage, single-axis tracking PV, increase in PV and battery storage capacity, decrease in wind and CCGT capacities, results in a lower total system capex. This translated to a further reduction in the LCOE from 41.4 €/MWh to 40.4 €/MWh. In addition, the low capex of battery and PV allowed for slightly higher curtailment losses. If the capex of single-axis tracking PV reduced further with the battery capex, then there may be a higher increase in installed capacity of PV and battery storage output. The scenario would then lead to steeper reduction in the LCOE (Table 7).

The flexibility of the SWRO plants reduced from 8733 FLH to 8750 FLH while water storage capacity reduced by 42%. Similarly, so did the output of the gas and thermal energy storage. The reasons for the behavior are similar to that in 2030.

4. Discussion

The reduction in the capex of the SWRO plants enables the desalination plants, together with water storage, to run on lower full load hours without increasing the water production costs. This adds another dimension of flexibility to an energy system where the desalination sector is integrated with the power sector.

At times when there is excess energy, it may be more economical to store the excess as water and utilize the water when there is not enough renewable energy in the system. This in turn leads to a decrease in the requirement for battery storage but also more installed desalination capacity.

It was found that when the SWRO capex is decreased by 50%, the relative decrease in total system capex is 7% in 2030 and 4% in 2050. This can be attributed to the reduction in desalination capex and the battery storage output. The battery storage output is reduced by 6% in 2030 and 0.6% in 2050.

In addition, Fig. 5 illustrates that the decrease in the SWRO capex affects the 2030 and 2050 transition in different ways. The decrease in capex causes the SWRO FLH to decrease more sharply in 2030 compared to 2050. In addition, the battery storage output decreases more sharply in 2030 than in 2050. This can be attributed to the fact that battery storage and single-axis tracking PV is increasingly cost competitive in 2050 as opposed to 2030. Therefore, as opposed to the 2030 system, it is more cost effective to run the SWRO plants at higher full load hours with higher battery storage output in 2050.

Meanwhile, the decrease in battery capex results in a reduction in the LCOE for 2030 and 2050, but the impact is more pronounced in 2050. In 2030, when the battery capex is reduced, there is an increase in battery storage output, installed capacity of single-axis

tracking PV and a decrease in wind and CCGT capacities. The increase in capacity of single-axis tracking PV is due to the compatibility with battery storage. At 80% of the battery capex, the output from battery storage and installed capacity of single-axis tracking PV increased by 80% and 20% respectively. This resulted in an increase in total capex of the system although there was a decrease in wind and CCGT capacities. However, the increase in capex was offset by a decrease in curtailment losses, resulting in a decrease in LCOE from 62.5 €/MWh to 62.1 €/MWh. Simultaneously, there was an increase in renewable energy generation share from 81.8% to 84.7%. In addition, varying battery capex decreases the SWRO full load hours by less than 1%.

In 2050, the renewable energy generation share is 100%. The increase in battery output with the decrease in battery capex is not as significant as in 2030. At 80% of battery capex, the output increased by 8%. Meanwhile, the installed capacities of single-axis tracking PV increased by 2%. Coupled with the low PV, battery capex and the reduction in wind and CCGT capacities, the total capex of the system decreased. This results in an LCOE reduction from 41.4 €/MWh to 40.4 €/MWh. If the capex of single-axis tracking PV decreased together with the battery capex, the impacts on the final system cost and behavior will be more significant. For the given single-axis tracking PV capex of 271 €/kWp by 2050, it does not seem cost effective to increase battery storage output significantly. Decreasing battery capex results in a reduction in the total cost of the energy system and enables a faster growth of the renewable energy generation share. However, the results are more pronounced with decrease in cost of PV technologies which is very likely due to the compatibility of the two technologies.

The results demonstrate that, for Saudi Arabia, battery storage together with single-axis tracking PV provides the least cost flexibility option in the energy transition pathway. SWRO plants and water storage are not flexible because of the relatively higher capex and it is cost effective to operate these plants in baseload mode. In addition, steeper reduction in battery capex negates any flexibility provided by the SWRO plants as demonstrated in Tables 6 and 7. However, for more drastic reduction in energy system costs, the decrease in battery capex has to be accompanied by a similar drop in the capex of PV plants.

5. Conclusion

In this work we presented a study on the impacts of battery and water storage on the energy transition pathway for the Kingdom of Saudi Arabia.

The least cost pathway to achieve a 100% renewable energy system through the integration of the power, desalination and non-energetic industrial gas sectors is presented. A sensitivity analysis is carried out on the SWRO plant and battery capex values to understand the impacts on the energy transition costs.

The reduction in the SWRO capex leads to a decrease in the total system capex. However, the maximum decrease is 2.1%, observed in 2050, for a reduction of 50% of the SWRO capex. The lower SWRO capex enables desalination plants to run on lower full load hours, leading to an increase in water storage and consequently a decrease in battery storage output. The reduction in battery storage output results in a lower total system capex.

The results suggest that the relatively high capex of SWRO desalination plants does not allow this component to be operated in a more flexible way, but rather in a baseload mode. This can be explained by the fact that the energy system flexibility can be offered on a lower cost level by PV power plants and battery storage. A drastic decrease in capex, of about 50% - which is not foreseeable - by 2050, would lead to a reduction of 2.1% in the total annualised energy system cost. Therefore, SWRO plants and water storage cannot compete with the flexibility provided by the combination of PV and battery storage.

Similar to the analysis of the capex of SWRO plants, the battery capex were varied. The decrease in battery capex results in an increase in battery storage output, higher single-axis tracking PV capacities and reduced wind and CCGT capacities. The LCOE reduced by a maximum of 2.4% for a 20% reduction in the battery capex in 2050. The results suggest that the impact of decreasing battery capex alone does not lead to steep decrease in the LCOE. The reduction could be more significant if costs of single-axis tracking PV plants reduced accordingly. In addition, faster reduction in battery capex further renders the flexibility offered by SWRO plants and water storage minimal.

For a more comprehensive study the following aspects should be studied further:

1. The impacts of lower battery cost and PV cost on the energy system.
2. The impacts of having a minimum water storage capacity.
3. With the integration of the heat sector of Saudi Arabia, the thermal desalination technology, MED, may play a more prominent role. The use of free heat in the energy system for MED might result in more flexible MED desalination plants.

By understanding the interplay between battery and water storage better, it is possible to further optimise the energy transition pathway for Saudi Arabia. These insights enable to establish the least cost pathway for Saudi Arabia to achieve net zero emissions by mid-century. In addition, the study contributes to the understanding and development of battery and water storage, not only in Saudi Arabia's energy transition, but within the context of the much needed global energy transition.

Acknowledgements

The authors gratefully acknowledge the public financing of Tekes, the Finnish Funding Agency for Innovation, for the 'Neo-Carbon Energy' project under the number 40101/14. The first author would like to thank Reiner Lemoine-Foundation for the valuable scholarship. The authors would like to thank Michael Child for proofreading.

Appendix A.

Table A1
Technical and financial parameters of the seawater desalination technologies from 2015–2050.

			2015	2020	2025	2030	2035	2040	2045	2050
Seawater Reverse Osmosis	Capex	€/(m^3·day)	1150	960	835	725	630	550	480	415
	Opex fix	€/(m^3·day)	46	38	33	29	25	22	19	17
	Energy consumption	kWh/m^3	4.1	3.6	3.35	3.15	3	2.85	2.7	2.6
	Lifetime	years	25	25	30	30	30	30	30	30
Multi Effect Distillation – Thermal Vapor Compression for stand alone	Capex	€/(m^3·day)	1437	1200	1043	906	787	687	600	519
	Opex fix	€/(m^3·day)	10	13.2	15.6	18	21.6	24	24	24
	Thermal energy consumption	kWh_{th}/m^3	68	51	44	38	32	28	28	28

Table A1 (*Continued*)

			2015	2020	2025	2030	2035	2040	2045	2050
	Electrical energy consumption	kWh_{el}/m^3	1.5	1.5	1.5	1.5	1.5	1.5	1.5	1.5
	Lifetime	years	25	25	25	25	25	25	25	25
Multi Effect Distillation – Thermal Vapor	Capex	€/(m^3·day)	1437	1437	1437	1437	1437	1437	1437	1437
Compression for cogeneration	Opex fix	€/(m^3·day)	47.43	47.4	47.4	47.4	47.4	47.4	47.4	47.4
	Thermal energy consumption (Total gas input required for water and electricity)	kWh_{th}/m^3	168	168	168	168	168	168	168	168
	Electrical energy consumption	kWh_{el}/m^3	1.5	1.5	1.5	1.5	1.5	1.5	1.5	1.5
	Lifetime	years	25	25	25	25	25	25	25	25
Multi Stage Flash	Capex	€/(m^3·day)	2000	2000	2000	2000	2000	2000	2000	2000
for cogeneration Gain Output Ratio: 8	Opex fix	€/(m^3·day)	100	100	100	100	100	100	100	100
Power-to-Water: 2.25 kW/(m^3·day)	Thermal energy consumption (Total gas input required for water and electricity)	kWh_{th}/m^3	202.5	202.5	202.5	202.5	202.5	202.5	202.5	202.5
	Electrical energy consumption	kWh_{el}/m^3	2.5	2.5	2.5	2.5	2.5	2.5	2.5	2.5
	Lifetime	years	25	25	25	25	25	25	25	25
Multi Stage Flash	Capex	€/(m^3·day)	2000	2000	2000	2000	2000	2000	2000	2000
for stand alone	Opex fix	€/(m^3·day)	100	100	100	100	100	100	100	100
Gain Output	Thermal energy consumption	kWh_{th}/m^3	85	85	85	85	85	85	85	85
Ratio: 8	Electrical energy consumption	kWh_{el}/m^3	2.5	2.5	2.5	2.5	2.5	2.5	2.5	2.5
	Lifetime	years	25	25	25	25	25	25	25	25
Water Transportation										
Piping	Capex	€/(m^3·a·km)	0.053	0.053	0.053	0.053	0.053	0.053	0.053	0.053
	Fixed Opex	€/(m^3·a·100 km)	0.023	0.023	0.023	0.023	0.023	0.023	0.023	0.023
	Lifetime	years	30	30	30	30	30	30	30	30
Vertical Pumping	Capex	€/(m^3·h·m)	15.4	15.4	15.4	15.4	15.4	15.4	15.4	15.4
	Fixed Opex	€/(m^3·h·m)	0.3	0.3	0.3	0.3	0.3	0.3	0.3	0.3
	Energy consumption	kWh/(m^3·h·100 m)	0.36	0.36	0.36	0.36	0.36	0.36	0.36	0.36
	Lifetime	years	30	30	30	30	30	30	30	30
Horizontal Pumping	Capex	€/(m^3·h·km)	19.26	19.26	19.26	19.26	19.26	19.26	19.26	19.26
	Fixed Opex	€/(m^3·h·km)	0.4	0.4	0.4	0.4	0.4	0.4	0.4	0.4
	Energy consumption	kWh/(m^3·h·100 km)	0.04	0.04	0.04	0.04	0.04	0.04	0.04	0.04
	Lifetime	years	30	30	30	30	30	30	30	30
Water Storage	Capex	€/m^3	65	65	65	65	65	65	65	65
	Fixed Opex	€/m^3	1.3	1.3	1.3	1.3	1.3	1.3	1.3	1.3
	Lifetime	years	30	30	30	30	30	30	30	30

References

[1] Greenpeace, Energy Revolution A Sustainable World Energy Outlook 2015, Amsterdam, (2015) . www.greenpeace.org/international/Global/international/publications/climate/2015/Energy-Revolution-2015-Full.pdf.

[2] X. Luo, J. Wang, M. Dooner, J. Clarke, C. Krupke, Overview of current development in electrical energy storage technologies and the application potential in power system operation, Appl. Energ. 137 (2015) 511–536.

[3] M. Child, Breyer Ch, Vision and initial feasibility analysis of a recarbonised finnish energy system, Renewable Sustainable Energy Rev. 66 (2016) 517–536.

[4] M. Child, Breyer Ch, The role of energy storage solutions in a 100% renewable Finnish energy system, Energy Procedia 99 (2016) 25–34.

[5] A.B. Gallo, J.R. Simoes-Moreira, H.K.M. Costa, M.M. Santos, E. Moutinho dos Santos, Energy storage in the energy transition context: a technology review, Renewable Energy Sustainable Rev. 65 (2016) 800–822.

[6] PV Magazine, Estorage Market to Grow to USD250 Billion by 2040, Berlin, (2016) . www.pv-magazine.com/2016/06/13/energy-storage-market-to-grow-to-usd250-billion-by-2040_100024952/.

[7] M. Liebreich, Bloomberg New Energy Finance Summit In Search of the Miraculous, Bloomberg New Energy Finance, London, (2016) .

[8] F. Lambert, Electric Vehicle Battery Cost Dropped 80% in 6 Years down to $227/kWh ?Tesla Claims to Be Below $190/kWh, Fremont, California, (2017) . (Accessed 5 June 2017) https://electrek.co/2017/01/30/electric-vehicle-battery-cost-dropped-80-6-years-227kwh-tesla-190kwh/https://electrek.co/2017/01/30/electric-vehicle-battery-costdropped-80-6-years-227kwh-tesla-190kwh/.

[9] N. Kittner, F. Lill, M.D. Kammen, Energy storage deployment and innovation for the clean energy transition, Nature Energy 2 (2017) 17125.

[10] O. Schmidt, A. Hawkes, A. Gambhir, I. Staffell, The future cost of electrical energy storage based on experience rates, Nat. Energy 2 (2017) 17110.

[11] C. Breyer, S. Afanasveya, D. Brakemeier, M. Engelhard, S. Giuliano, M. Puppe, H. Schenk, T. Hirsch, M. Moser, Assessment of mid-growth of assumptions and learning rates for comparative studies of CSP and hybrid PV-battery power plants, AIP Conference Proceedings 1850 (2016) 160001.

[12] U. Caldera, D. Bogdanov, S. Afanasyeva, Ch. Breyer, Integration of reverse osmosis seawater desalination in the power sector, based on PV and wind energy, for the Kingdom of Saudi Arabia, 32nd European Photovoltaic Solar Energy Conference, Munich, June 20–24, 2016 (http://bit.ly/2iVKP97).

[13] M.A. Salam, S.A. Khan, Transition towards sustainable energy production –A review of the progress for solar energy in Saudi Arabia, Energy Explor. Exploit. 36 (1) (2018) 3–27.

[14] [UNFCCC] - United Nations Framework Convention on Climate Change, Adoption of the Paris Agreement—Proposal by the President, UNFCCC, Paris France, 2015.

[15] M. Al-Nory, M. El-Beltagy, An energy management approach for renewable energy integration with power generation and water desalination, Renew. Energ. 72 (2014) 377–385.

[16] K. Bognar, R. Pohl, F. Behrendt, Seawater reverse osmosis (SWRO) as deferrable load in microgrids, Desalin. Water Treat. 51 (4–6) (2013) 1190–1199.

[17] A.S. Lopes, R. Castro, J.M. Ferreira de Jesus, Contributions to the preliminary assessment of a water pumped storage system in terceira island (Azores), J. Energy Storage 6 (2016) 56–69.

[18] K.D. Strang, Feasibility of a hidden renewable energy hydro power storage battery, J. Energy Storage 13 (2017) 164–175.

[19] E. DeNicola, S.O. Aburizaiza, A. Siddque, H. Khwaja, O.D. Carpenter, Climate change and water scarcity: the case of Saudi Arabia, Ann. Global Health 81–83 (2015) 342–352.

[20] J.E. Drewes, R.P.C. Garduno, G. Amy, Water reuse in the Kingdom of Saudi Arabia –status, prospects and research needs, Water Sci. Technol.: Water Supply 12 (2012) 926–936.

[21] Global Water Intelligence Desal Data, 2016. Country Profile Saudi Arabia, London, https://www.desaldata.com/countries/31.

[22] Global water intelligence, top market opportunities Saudi Arabia, Global Water Market, vol. 4, Middle East and Africa, Media Analytics Publication, London, 2017 pp 1379–1400.

[23] King Abdullah City for Atomic and Renewable Energy, The Vision: Energy Sustainability for Future Generations, Riyadh, Saudi Arabia, (2016) . www.kacare.gov.sa/en/FutureEnergy/Pages/vision.aspx.

[24] [GIZ] - Deutsche Gesellschaft für Internationale Zusammenarbeit, An underground water reservoir for Abu Dhabi, Eschborn, Germany, www.giz.de/international-services/en/html/1729. html.

[25] Khaleej Times, 2015. Abu Dhabi aquifer to store water for 100 years, Dubai, United Arab Emirates, www.khaleejtimes.com/nation/general/abu-dhabi-aquifer-to-store-water-for-100-years.

[26] Global Water Intelligence, Top Market Opportunities Qatar, In: Global Water Market, 2017. Volume 4: Middle East and Africa, Media Analytics Publication, pp 1351–1366, London.
[27] Future Directions International, 2015. Strategic Analysis Paper Food and Water Security in the Kingdom of Saudi Arabia, Perth, WA, http://futuredirections.org.au/wp-content/uploads/2015/07/Food_and_Water_Security_in_the_Kingdom_of_Saudi_Arabia.pdf.
[28] M. Sterner, Bioenergy and Renewable Power Methane in Integrated 100% Renewable Energy Systems, Faculty of Electrical Engineering and Computer Science, University of Kassel, 2009 (PhD thesis).
[29] M. Lehner, R. Tichler, H. Steinmüller, M. Koppe, Power-to-Gas: Technology and Business Models, Springer Heidelberg, 2014.
[30] A. Al-Karaghouli, L.L. Kazmerski, Energy consumption and water production cost of renewable energy powered desalination processes, Renew. Sustain. Energy Rev. 24 (2013) 343–356.
[31] Fichtner, MENA Regional Water Outlook Part 2 Desalination Using Renewable Energy Final Report, (2011) .
[32] A.M. El-Nashar, Cogeneration for power and desalination –state of the art review, Desalination 134 (2001) 7–28.
[33] D. Bogdanov, Breyer Ch, North-East Asian Super Grid for 100% renewable energy supply: optimal mix of energy technologies for electricity, gas and heat supply options, Energy Convers. Manage. 112 (2016) 176–190.
[34] L.S.N.S. Barbosa, D. Bogdanov, P. Vainikka, Breyer Ch, Hydro, wind and solar power as a base for a 100% Renewable Energy supply for South and Central America, PLoS One 12 (2017) e0173820.
[35] A. Aghahosseini, D. Bogdanov, N. Ghorbani, Breyer Ch, The role of a 100% renewable energy system for the future of Iran: integrating solar PV, wind energy, hydropower and storage, Int. J. Environ. Sci. Technol. (2016), doi:http://dx.doi.org/10.1007/s13762-017-1373-4.
[36] Ch Breyer, D. Bogdanov, A. Aghahosseini, A. Gulagi, M. Child, A.S. Oyewo, J. Farfan, K. Sadovskaia, P. Vainikka, Solar photovoltaics demand for the global energy transition in the power sector, Prog. Photovoltaics Res. Appl. (2017) 1–19, doi:http://dx.doi.org/10.1002/pip.2950.
[37] E. Vartiainen, G. Masson, C. Breyer, The True Competitiveness of Solar PV, A European Case Study, European Technology and Innovation Platform ? Photovoltaic, Munich, 2017. http://bit.ly/2qxV9Y6.
[38] Y. Al-Saleh, P. Upham, K. Malik, Renewable Energy Scenarios for the Kingdom of Saudi Arabia, Tyndall Climate Change Research Center, Norwich, UK, 2008. www.tyndall.ac.uk/sites/default/files/wp125.pdf.
[39] M. Engelhard, S. Hurler, A. Weigand, S. Giuliano, M. Puppe, H. Schenk, T. Hirsch, M. Moser, T. Fichter, J. Kern, F. Trieb, D. Brakemeier, J. Kretschmann, U. Haller, R. Klingler, C. Breyer, S. Afanasyeva, Techno-economic analysis and comparison of CSP with hybrid PV-Battery Power Plants, 22nd Solar PACES, Abu Dhabi, Oct 12, 2016. http://bit.ly/2ig0ZOE.
[40] [IEA] –International Energy Agency, World Energy Outlook 2014, IEA Publishing, Paris, 2014.
[41] S. Loutatidou, B. Chalermthai, P.R. Marpu, H. Arafat, Capital cost estimation of RO plants: GCC countries versus southern Europe, Desalination 347 (2014) 103–111.
[42] U. Caldera, Ch Breyer, Learning curve for seawater reverse osmosis desalination plants: capital cost trend of the past, present, and future, Water Resour. Res. 53 (2017), doi:http://dx.doi.org/10.1002/2017WR021402.
[43] U. Caldera, D. Bogdanov, S. Afanasyeva, C. Breyer, Role of seawater desalination in the management of an integrated water and 100% renewable energy based power sector in Saudi Arabia, Water 10 (2018) 3.
[44] [IEA] –International Energy Agency, Key World Energy Statistics Paris, (2015) .

Publication V

Caldera, U., and Breyer, C.
Learning curve for seawater reverse osmosis desalination plants: capital cost trend of the past, present and future

Reprinted with permission from
Water Resources Research
Vol. 53, pp 10,523-10,528, 2017

AGU PUBLICATIONS

Water Resources Research

RESEARCH ARTICLE
10.1002/2017WR021402

Learning Curve for Seawater Reverse Osmosis Desalination Plants: Capital Cost Trend of the Past, Present, and Future

Upeksha Caldera[1] **and Christian Breyer**[1]

[1] School of Energy Systems, Lappeenranta University of Technology, Lappeenranta, Finland

Key Points:
- First learning curve established for the capital costs of SWRO plants
- SWRO capex has decreased by 15% for every doubling of cumulative online SWRO capacity. This implies a learning rate of 15% for SWRO plants
- Based on 20% annual growth rate, 2030 SWRO capex is estimated to be 1,340 USD/(m^3/d)

Correspondence to:
U. Caldera,
upeksha.caldera@lut.fi

Citation:
Caldera, U., & Breyer, C. (2017). Learning curve for seawater reverse osmosis desalination plants: Capital cost trend of the past, present, and future. *Water Resources Research*, *53*, 10,523–10,538. https://doi.org/10.1002/2017WR021402

Received 27 JUN 2017
Accepted 29 NOV 2017
Accepted article online 4 DEC 2017
Published online 15 DEC 2017

Abstract Seawater reverse osmosis (SWRO) desalination is expected to play a pivotal role in helping to secure future global water supply. While the global reliance on SWRO plants for water security increases, there is no consensus on how the capital costs of SWRO plants will vary in the future. The aim of this paper is to analyze the past trends of the SWRO capital expenditures (capex) as the historic global cumulative online SWRO capacity increases, based on the learning curve concept. The SWRO capex learning curve is found based on 4,237 plants that came online from 1977 to 2015. A learning rate of 15% is determined, implying that the SWRO capex reduced by 15% when the cumulative capacity was doubled. Based on SWRO capacity annual growth rates of 10% and 20%, by 2030, the global average capex of SWRO plants is found to fall to 1,580 USD/(m^3/d) and 1,340 USD/(m^3/d), respectively. A learning curve for SWRO capital costs has not been presented previously. This research highlights the potential for decrease in SWRO capex with the increase in installation of SWRO plants and the value of the learning curve approach to estimate future SWRO capex.

Plain Language Summary Seawater desalination is expected to play a pivotal role in helping to secure future global water supply as water demand surges and freshwater resources diminish. While there are various seawater desalination technologies, the dominant desalination technology is expected to be seawater reverse osmosis (SWRO). The aim of this paper is to understand how the capital cost of SWRO plants has changed in the past as more plants were built and operated. This is based on the "learning by doing" concept that illustrates the relationship between cost reduction in industries and the increase in production output. The relevance for SWRO plants is studied by assessing 4,237 plants that were operated from 1977 to 2015. It is found that as the cumulative global capacity of SWRO plants doubled, the average capital cost reduced by 15%. The results suggest that for every future doubling of SWRO capacity, the capital cost will reduce by 15%. This is the first such observation presented for SWRO plants and can be used to project the future capital costs of SWRO plants.

1. Introduction

Seawater desalination is growing in acceptance as a solution to the increasing gap between global water supply and demand (Ghaffour et al., 2013; Gude, 2016). The driving factors are the diminishing freshwater resources, decreasing desalination costs, and increasing efficiency of desalination technologies (Ghaffour et al., 2013). While the global population has increased linearly, the installed seawater desalination capacity has grown exponentially (Gude, 2016). The growth is observed not only in the Middle East and North Africa (MENA) region, which accounted for 47% of the 2015 global installed desalination capacity (Global Water Intelligence (GWI), 2016a), but in countries within Asia and Sub-Saharan Africa. Until recently, in already water stressed countries such as South Africa and India, desalination has not been a contributor to the water supply (GWI, 2017a, 2017b; Virgili, 2016).

The online desalination capacity at the end of 2016 is estimated to be around 79,789,000 m^3/d (Virgili,2017a). The membrane technology, reverse osmosis, accounts for 66% of the online capacity, followed by the thermal technologies multistage flash (MSF) and multieffect distillation (MED). MSF and MED accounts for 20% and 7% of the online capacities, respectively. Seawater constitutes 58% of the global feed water source, while seawater reverse osmosis (SWRO) accounted for 30% of the installed capacity.

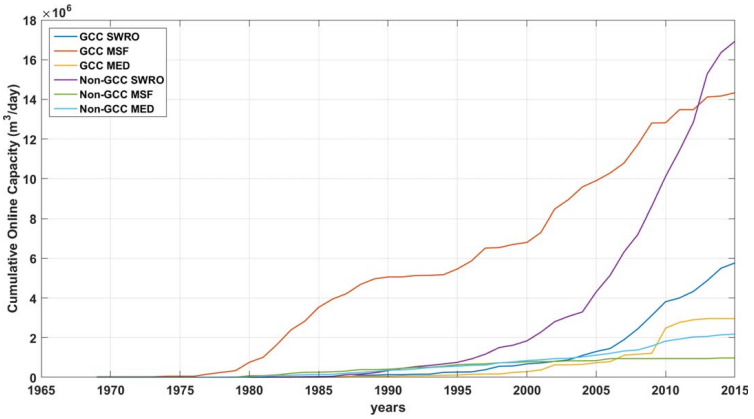

Figure 1. Cumulative SWRO Online Capacity from 1969 to 2015 (Fichtner, 2011; Virgili 2017a).

Figure 1 illustrates the growth of the desalination capacities in the Gulf Cooperation Council (GCC) countries and non-GCC countries from 1969 to 2015 (Fichtner, 2011). The graph builds on the illustration of online desalination capacities from 1950 to 2010 presented in the MENA Regional Water Outlook report by Fichtner (2011). The figure shows the rapid increase of SWRO and the plateauing of MSF capacities in both the GCC and non-GCC countries. The decline of MSF is reflected in recent decision by the Saudi Arabian government to not build any MSF plants after the Ras Al Khair IWPP plant, the largest desalination plant in the world (Water Desalination Report, 2017). Similarly, the 164,000 m^3/d Ras Abu Fontas (RAF) A3 plant, commissioned in 2017, is the first SWRO plant in Qatar and heralds a new era in the Qatari desalination market (Waste & Water International, 2017).

The rise of SWRO is attributed to the lower energy consumption and vast improvements in performance (Ghaffour et al., 2013; Loutatidou et al. 2014). The least energy intensive SWRO desalination plants in operation today consume around 3.0 kWh_{el}/m^3 (Water Online, 2016). In contrast, the heat demand of thermal desalination plants are much higher, ranging from 40 to 80 kWh_{th}/m^3, and additional electrical energy requirements range from 2.5 to 5 kWh_{el}/m^3, depending on the desalination technology (Al-Kharaghouli & Kazmerski, 2013).

RO is expected to maintain the highest global market share due to the low unit water production cost and suitability for all countries (Ghaffour et al., 2013; Gude, 2016). Ghaffour et al. (2013) discuss the improvements in membrane performance and reduction in energy consumption that have decreased the average water cost of SWRO plants from 1.30 USD/m^3 in 1996 to 0.50 USD/m^3 in 2003. In addition, the enhanced membranes enable a higher recovery ratio even in the more saline waters of the Arabian Sea, Red Sea, and Eastern Mediterranean Sea (Ghaffour et al., 2013). The higher recovery ratio contributes to lower RO train, intake, and outfall capacities ultimately contributing to lower capital costs. The decrease in water production costs have been further supported by reduction in pumping energy demand and chemical consumption enabling lower operating costs. According to Ghaffour et al. (2013), the increase in plant capacities, estimated to be a factor of 10 from 1995 to 2010, have also contributed to the decrease in capital costs.

Reflecting similar views, Loutatidou et al. (2014) present a model that estimates the capital expenditures (capex) of RO plants located in the Gulf Cooperation Council (GCC) and Southern Europe. The model determines the capex based on the nominal plant capacity, year of commissioning, type of RO plant based on whether feedwater use is brackish or seawater and the region of the desalination plant. Loutatidou et al. (2014) show that it is the capacity of the plant that most influences the capex. With the increase in plant capacity, the capex reduces, showing the trend of scale-economy. In addition, the research projects the

capex of SWRO plants located in the GCC region from 2014 to 2030, assuming the same trends from 1985 to 2013. According to the projection, the capex will decrease by 2.25% every year.

Voutchkov (2013) also discusses the potential for further improvements in the RO process and estimates that the unit cost of desalinated water will decrease by 20% in the next 5 years. Similar views were presented by the Almar Water Solutions organization (Almar Water Solutions, 2016) who attribute the decrease in the cost of SWRO to the improvements in the technology and production over the last two decades.

However, not everyone foresees a continued decrease in SWRO costs. Literature and market reports indicate an increase in the water production cost of SWRO plants. Ghaffour et al. (2013) predicts an increase in membrane costs, higher electricity prices due to unstable crude oil costs, currency fluctuations, increase in cost of raw materials, equipment, shipping, and tighter environmental regulations. These factors may contribute to higher water production costs. GWI (2017b) expects the cost of reverse osmosis to continue to decrease, but the decrease will be offset by an increase in energy cost and material prices.

The referenced literature (Almar Water Solutions, 2016; Ghaffour et al., 2013; GWI Desal Data, 2017c; Voutchkov, 2013) make projections for both the capital and operational expenditures of the SWRO plants. Capital costs comprise of the procurement, planning, construction, installation of physical infrastructure, and the indirect costs associated with realizing the project. The indirect costs include the engineering, administrative, permitting and funding costs (Voutchkov, 2013). Meanwhile, the operational expenditures (opex) include the costs for energy consumption, chemicals, labor, membrane replacement, maintenance, and concentrate disposal (Voutchkov, 2013).

As the desalination demand and installed capacities increase, there is growing interested in how the cost of desalination plants and water production costs will vary in the future (Loutatidou et al., 2014). However, there is no consensus on how the costs will vary. The aim of this research is to project capital costs of SWRO plants based on the learning curve model. The learning curve model, draws on the concept of learning by doing, illustrates the relationship between cost reduction in industries and the increase in production output (Nemet, 2006). Learning curves have been used to project costs for various industries, ranging from airplane manufacturing in 1936 to the more recent solar photovoltaic (PV) and battery capex (Hoffmann, 2014; International Technology Roadmap for Photovoltaic (ITRPV), 2017; Kersten et al., 2011; Nemet, 2006; Nykvist & Nilsson, 2015).

This research is driven by the need to assess the relationship between global SWRO capex trend and increase in SWRO online capacity. The understanding of how SWRO capex has been influenced by the development of SWRO plants can be used to project the global average capex as the demand for seawater desalination increases.

In the following sections, the learning curve concept is introduced, applied, and discussed to SWRO plants from 1977 to 2015.

2. The Learning Curve Concept

The learning curve concept was first observed and discussed for the aircraft industry by the aeronautic engineer Wright in 1936 (Wright, 1936). It was shown that as more aircrafts were constructed, the unit cost reduced. The decrease in costs was attributed to the experiences gained during the production process. For instance, the improvement in efficiency of the labor, use of more machinery for production of more units, and reduction in material wastage and overheads (Wright, 1936). The second time the same empirical economic coincidence had been observed by Rapping in the shipbuilding industry in the 1940s (Rapping, 1965).

In 1968, Henderson (1968) elaborated on the learning curve concept discussed by Wright and Rapping, and applied it to several industries. These included transistors, integrated circuits, televisions receivers, and facial tissues. It was found that for all the industries studied, the learning rate lay between 20% and 30%. This means when the cumulative production was doubled, there was a decrease in the unit costs of about 20%–30%.

Neij (1997) and Swanson (2006) applied the learning curve concept for solar photovoltaic modules and derived a learning rate of about 20%. Kersten et al. (2011) presented a learning curve for photovoltaic

module costs, based on unit cost data from 1976 to 2010. It was observed that the learning rate for PV modules is about 17% for crystalline silicon modules and for silicon-based PV systems about 16%. Similarly, Breyer et al. (2017a) projected the capex for solar energy technologies and batteries up to the year 2030. The learning rates varied from 10% up to 20%, depending on the different technologies. Both PV plants and battery plants had the highest learning rates of about 20% in the past.

Equation (1) presents the log-linear learning curve concept and highlights how the future cost can be calculated based on the learning rate.

$$cost_{new} = cost_{initial} \times \left(\frac{production_{new}}{production_{initial}}\right)^{-b} \tag{1a}$$

$$PR = (2)^{-b} \tag{1b}$$

$$LR = 1 - PR \tag{1c}$$

$$production_{new} = \sum_{t=0}^{T} production_t \tag{1d}$$

$$production_t = production_{t-1} \times (1 + GR_t) \text{ for } t \geq 1 \tag{1e}$$

$$production_{new} = production_0 \times \prod_{t=0}^{T} (1 + GR_t) \tag{1f}$$

Equation (1): Log-linear learning curve concept. Here, $cost_{new}$ is cost at the global cumulative capacity for the specific year, $cost_{initial}$ is the cost at the historical global cumulative capacity for the initial year, $production_{new}$ is the historical global cumulative production output for the specific year, $production_{initial}$ is the historical global cumulative production output for the initial year, LR is the learning rate that can be determined by plotting the cost against the cumulative production on a log-log scale as discussed in section 3, PR is the progress ratio and is unity—LR, T is the year by which $production_{new}$ occurs, $production_t$ is the production for the specific year number t, GR_t is the growth rate for the year number t, and $production_0$ is the production at the initial year.

The conventional log-linear model used and discussed in this study is based on the concept of "learning by doing." A modification of the log-linear model is the two-factor learning curve which attempts to highlight the impacts of "learning by doing" and "learning by searching." In this model, the cumulative cost of production is assessed against the increase in production and the accumulated knowledge stock (Wiesenthal et al., 2012). This model has not been widely used and proven as the log-linear model. Also there are different factors that can highlight the accumulated knowledge stock such as research and development funding and patent activity (Kittner et al., 2017; Wiesenthal et al., 2012). However, there is no consensus on the most relevant factors. In addition, this is data that is less readily available as opposed to the increase in the cumulative production output used for the log-linear model. Given the historical record, proven accuracy of the log-linear model and available data, it was decided to use the log-linear model for the assessment of the learning rate for the capex of SWRO plants.

2.1. Learning Curves for Capex of SWRO Plants

The objective of this research is to estimate the learning rate for the capex of SWRO desalination plants enabling future projections of capex based on empiric data. The learning curve will illustrate how the unit capital cost (USD/[m^3/d]) of the SWRO plants has varied with the increase in cumulative online desalination capacity (m^3/d).

Sood and Smakhtin (2014) have presented a learning curve for the cost of water desalination. It was determined that the learning rate for the capital and fixed operational expenditures of all desalination technologies was 29%. These numbers were based on the assumptions that the capex and opex of all desalination plants are 40% and 60% of the desalination total cost, respectively. Energy costs are assumed to be 46% of the opex. The assumptions of the capex and opex accounting for 40% and 60% of the total cost, respectively, for every desalination plant and year makes it difficult to analyze the impact of the actual capex and the energy-related costs.

Table 1
SWRO 2030 Capex Based on Annual Growth Rate of 15%

Cumulative capacity in 2015	$production_{initial}$	m^3/d	24,334,000
Capex in 2015	$cost_{initial}$	USD/(m^3/d)	1,000
Growth rate per year	GR_t	%	10
Learning rate	*LR*		15
Cumulative capacity in 2030	$production_{new}$	m^3/d	101,649,000
Capex in 2030	$cost_{new}$	USD/(m^3/d)	715

Note. The capex is calculated based on equation (1). In addition, the corresponding variables from equation (1) are listed (Ghaffour et al. 2013; Virgili 2017a).

For a thorough analysis of LCOW projections, the capital expenditures and electricity costs of SWRO plants have to be studied separately. The LCOW is mainly driven by the capital and energy consumption costs. The cost of electricity varies significantly among regions depending on the local conditions. By separating the projections for the capital expenditures of SWRO plants and electricity costs of a region, the LCOW variations for the relevant region can be better represented.

In this study, the focus is on the capex of SWRO plants, as the technology is expected to retain most of the future market share. Armed with information on the SWRO capex projections, one can project how the water costs from SWRO will vary in the future by adding the respective electricity demand and cost of electricity. The relevance of the learning rate for the capex of SWRO plants is illustrated via equation (2), Tables 1 and 2.

Equation (2), adapted from Caldera et al. (2016), is used to determine the levelized cost of water (LCOW) of the SWRO plants. The LCOW is one of the key economic indicators used to analyze and compare desalination plants (Fichtner, 2011). As can be seen from the equation, both the capex and levelized cost of electricity (LCOE) has an impact on the LCOW.

$$LCOW_{desal} = \frac{Capex_{desal} \times crf_{desal} + opex_{fixed\ \ desal}}{Total\ \ water\ \ produced\ \ in\ \ a\ \ year} + (LCOE \times SEC) \quad (2)$$

Equation (2): Levelized cost of water (LCOW). Here, $capex_{desal}$ is the capex of the desalination plant in €/(m^3·a) and crf_{desal} is the annuity factor for desalination plant. Total water produced in a year is in m^3, $opex_{fixeddesal}$ is the fixed opex of the desalination plant in €/(m^3·a), and *LCOE* is the levelized cost of electricity and is in €/kWh. SEC is the specific energy consumption in kWh/m^3. The product of the LCOE and SEC is the energy cost of the desalination plant in €/(m^3 a).

Table 1 demonstrates how the SWRO capex for a specific year, in this example 2030, can be calculated using equation (1). A learning rate of 15% and annual growth rate of 10% from 2015 to 2030 is assumed. The SWRO capex for 2015 is based on the range presented by Ghaffour et al. (2013). The cumulative SWRO capacity by 2015 is estimated to be 24,334,000 m^3/d (Virgili, 2017a). A different learning rate will result in a different capex by 2030.

Table 2 presents the corresponding LCOW for Saudi Arabia in 2015 and 2030 based on equation (2). Caldera et al. (2016) presents a transition toward 100% renewable energy for Saudi Arabia by 2050. According to Caldera et al. (2016), the LCOE for Saudi Arabia in 2015 is 129 €/MWh_{el}, assuming CO_2 cost of 9 €/ton, unsubsidized oil fuel cost of 52.5 €/MWh_{th} and gas fuel cost of 21.8 €/MWh_{th}. Fthenakis et al. (2016) reports an unsubsidized cost of grid electricity in Saudi Arabia of 210 USD/MWh_{el}. Similarly, the Energy Collective explains that the opportunity cost for oil being used domestically in Saudi Arabia is 139 USD/MWh (The Energy Collective, 2014). Due to lack of transparency of the actual electricity cost in Saudi Arabia, the more conservative LCOE of 129 €/MWh_{el} presented by Caldera et al. (2016) is used in Table 2. The modeled 2030 LCOE is about 62 €/MWh_{el} and used in Table 2. Based on the 2015 exchange rate of 1.10 USD/€ (Organisation for Economic Co-operation and Development (OECD), 2017a), the corresponding LCOE is 143 USD/MWh_{el} in 2015 and 67 USD/MWh_{el} in 2030. With the

Table 2
Influence of the Capex and LCOE in 2015 and 2030 on the Final LCOW

	Capex (USD/[m^3/d])	LCOE (USD/MWh_{el})	LCOW (USD/m^3)
2015	1000	143	1.25
2030	715	62	0.77

Note. The LCOW is calculated based on equation (2). WACC of 7% nd SWRO lifetime of 30 years is assumed (Caldera et al. 2016).

decrease in SWRO capex and LCOE, the LCOW is slashed from 1.25 USD/m^3 in 2015 to 0.77 USD/m^3 by 2030. The LCOW decrease by 38.4%, however it would decrease by 18% if the LCOE were unchanged, and 19% if the capex were unchanged. A weighted average cost of capital (WACC) of 7% and lifetime of 30 years for the SWRO plant is assumed (Caldera et al., 2016). The specific energy consumption is assumed to be 3.0 kWh_{el}/m^3 for 2015 and 2030.

2.2. Learning Curves for Renewable Energy Technologies

By the end of 2014, renewable energy accounted for 30% of the installed global power capacity (Farfan & Breyer, 2017). While hydropower capacities have been the dominant renewable energy resource, growing concerns about the high costs, environmental consequences, availability of the hydro resource and climate change have questioned further massive development of the technology (Ansar et al. 2014; Vest 2015). Meanwhile, solar PV, which accounted for 3% of the installed global capacity in 2014 (Farfan & Breyer, 2017), is experiencing rapid growth with an increase of at least 50% in many regions of the world (Werner et al., 2017). By the end of 2016, the global installed capacity of solar PV was estimated to be 305.8 GWp and 24% of the capacity was added in 2016 (Werner et al., 2017). In addition, the total installed capacity of wind power plants globally was approximately 433 GW at end of 2015, an increase of 17% from the previous year (Global Wind Energy Council, 2015). Farfan and Breyer (2017) estimates that in 2014, the growth rate of nonhydro renewable energy capacities was 36%, where solar PV capacities had a relatively lower growth rate of 17%. The surge in solar PV installations from 2014 to 2016 highlights the global drive toward cleaner, cheaper renewable energy power plants.

Literature and reports extensively discuss the learning curve for renewable energy technologies. The solar PV learning rates presented by Neij (1997), Swanson (2006), Kersten et al. (2011), and Breyer et al. (2017a) were discussed in the previous section. Liebreich et al. (2017) discuss a learning rate of 24% for solar PV modules and states that the cost of solar PV modules has fallen by 80% since 2008. The learning rate for solar PV modules has shown a remarkable acceleration to about 39% for the period of 2006–2016 during which 97% of cumulative historic capacity had been added (ITRPV, 2017). Learning curves also show that the capex decrease for onshore wind power plants is lower than that for solar PV (Liebreich 2016). Williams et al. (2017) estimate a learning rate of 10% for the capex of onshore wind power plants.

Energy storage is vital for energy systems based on abundant but intermittent solar and wind resources. Lithium-ion batteries are currently experiencing by far the fastest growth of all storage options and being used in small and utility-scale applications (Luo et al., 2015). Schmidt et al. (2017) analyze future cost projections for electrical energy storage, based on learning curves. The learning rate for lithium ion battery storage in electric vehicles is estimated to be 16%. Meanwhile, lithium ion battery storage in electronics has the steepest learning rate with 30%. Utility and residential-scale applications had a lower learning rate of 12% in the past. Kittner et al. (2017) suggests a learning rate of 15.47% for lithium-ion battery storage. Breyer et al. (2017a) have assessed the impact of learning rates for lithium ion battery storage on battery system cost and base their analysis on a learning rate of 15–20%.

Various reports and literature discuss the global, regional, and countrywide transition to a 100% renewable energy-based system (Breyer et al., 2017b, 2017c; Jacobson et al., 2017; Teske et al., 2015). The learning curves for renewable energy technologies enable to understand future costs of electricity production from renewable energy power plants during the transition (Breyer et al., 2017a). The corresponding LCOE for the Saudi Arabian energy transition is presented in Table 2. As explained previously, the LCOE in conjunction with the SWRO capex learning curve enables to determine the future cost of desalinated water. Therefore, the SWRO learning curve is instrumental to understand the global potential for SWRO desalination in the decades to come.

Table 3
SWRO Class-Size Distribution (GWI, 2016b)

Size class	Capacity range (m^3/d)
Small	< 1,000
Medium	1,000 – 10,000
Large	10,000 – 50,000
Extra-large	> 50,000

3. Methodology

For this study, all SWRO plants from 1977 to 2015 and relevant data were obtained from the DesalData database (Virgili, 2017b). The subsequent methodology utilized to establish a learning curve can be summarized as follows:

1. A total of 4,237 SWRO plants, awarded between 1977 and 2015 are considered. The status of the plants considered were either online, presumed online, offline, presumed offline, or under construction. All contract types were taken into account. Table 3 explains the size class distribution for the desalination plants (GWI, 2016b).
2. The total capacity that came online for all years from 1977 to 2015, regardless of the current status was found. This was then used to determine the cumulative online capacity increase from 1977 to 2015.
3. The corresponding mean and standard deviation of the capital costs awarded for all years, from 1977 to 2015, was found. All capital cost numbers were inflated to the 2015 USD value based on (OECD, 2017a) and (OECD, 2017b). The capex in USD/(m^3/d) was found using the capital costs and the plant capacity.
4. The mean capex and standard deviation was plotted against the cumulative online capacity on a log-log scale. Equation (1) was then used to determine the progress ratio and the learning rate for different time periods.
5. The steps 2–4 were redone for the database after removing capex values that are clear outliers. The relationship between the capex and SWRO plant parameters outlined by Loutatidou et al. (2014) is used to identify odd capex values for the different plant sizes. Based on the resulting capex range for different sizes according to Table 3, the capex values that deviate from the range were excluded as follows:
   - 5.1 Small plants with capex less than 1,500 USD/(m^3/d) and medium plants with capex less than 1,000 USD/(m^3/d)
   - 5.2 Large or extra-large plants with capex greater than 10,000 USD/(m^3/d)
   - 5.3 Large or extra-large capacities with a capex greater than 5,000 USD/(m^3/d). In this step, large or extra-large plants with capex greater than 10,000 USD/(m^3/d) will also be excluded.

   Figure 2 illustrates the methodology discussed above in a flowchart format. The arrow labeled 1 indicates the use of the full SWRO capex data determined in step 3. The arrow labeled 2 indicates the use of SWRO capex data that meets certain requirements as listed in step 5.
6. The software Origin Pro was used to find the linear fit for the resulting log-log plots and the final results were plotted in Matlab.

4. Results: SWRO Capex Learning Curve

Figure 3 (top) represents the learning curve for all data for the time periods 1977–2015 and 1979–2003. While 1977–2015 represents the full time scale of the observed data, it was noticed that the most uniform decrease in SWRO capex was observed from 1979 to 2003. Thus, both time periods were analyzed. The error bars present the standard deviation for each time period. The learning rate for 1977–2015 is found to be 14.75% and slightly higher at 14.61% for 1979–2003. The results imply that when the global cumulative online capacity was doubled, the unit capex of SWRO plants decreased by about 15%.

From 1979 to 2003, the decrease in capex closely followed the learning curve while almost seven doublings for RO desalination could have been achieved. After 2003, the capex deviated from the learning curve and the standard deviation in the following years increased. The latter indicates the awarding of SWRO plants at a range of different capex values. From 2003 to 2005, the capex plunged from 3,074 USD/(m^3/d) to 1,160 USD/(m^3/d) and increased again from 2009 onward.

The actual average SWRO capex values were plotted against the modeled SWRO capex values obtained from linear fitting the curve to the real values. Figure 3 (bottom) illustrates the relationship. The R^2 value indicates the degree of fit between the model and the real capex values. A 100% R^2 value indicates identical fit. The R^2 value for 1979–2015 is 0.887 and higher than that for 1977–2015 at 0.77. This can be attributed to the odd capex numbers in 1977 and 1978 as can be seen in Figure 3 (top). However, the R^2 value from 1979–2003 is 0.9658, indicating the steady decline in capex based on the learning rate of 15% from 1979 to 2003.

The larger deviation from the actual values is observed for capex less than 2,000 USD/(m^3/d) and higher than 10,000 USD/(m^3/d).

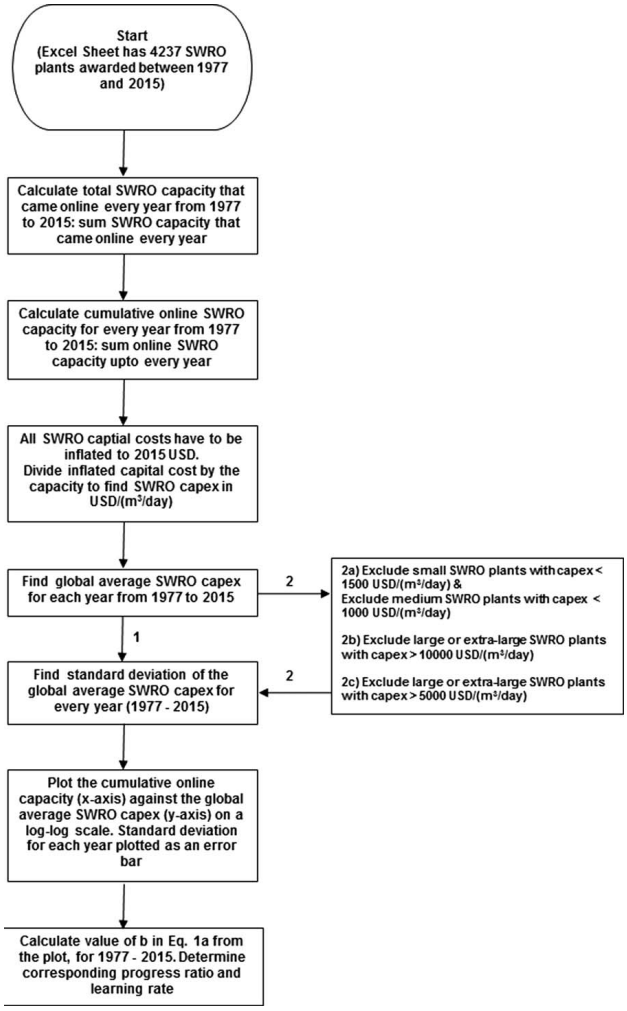

Figure 2. Illustration of methodology to determine the SWRO capex learning rate. Number 1 refers to the use of the full SWRO capex data set. Number 2 refers to the use of SWRO capex that only meets certain capex requirements. First data set in 2a is excluded and the learning rate plotted, then 2a and 2b are excluded, followed by 2a and 2c.

The learning curve establishes the continual decrease in the global average capex of SWRO plants at a learning rate of 15%. Up to 2004, small and medium-sized SWRO plants were the most awarded SWRO plants as illustrated in Figure 4 (top). From 2004 onward, there was a boom in the awarded capacities, in particular the large and extra-large SWRO capacities. However, after 2009, the awarded SWRO capacities reduced globally.

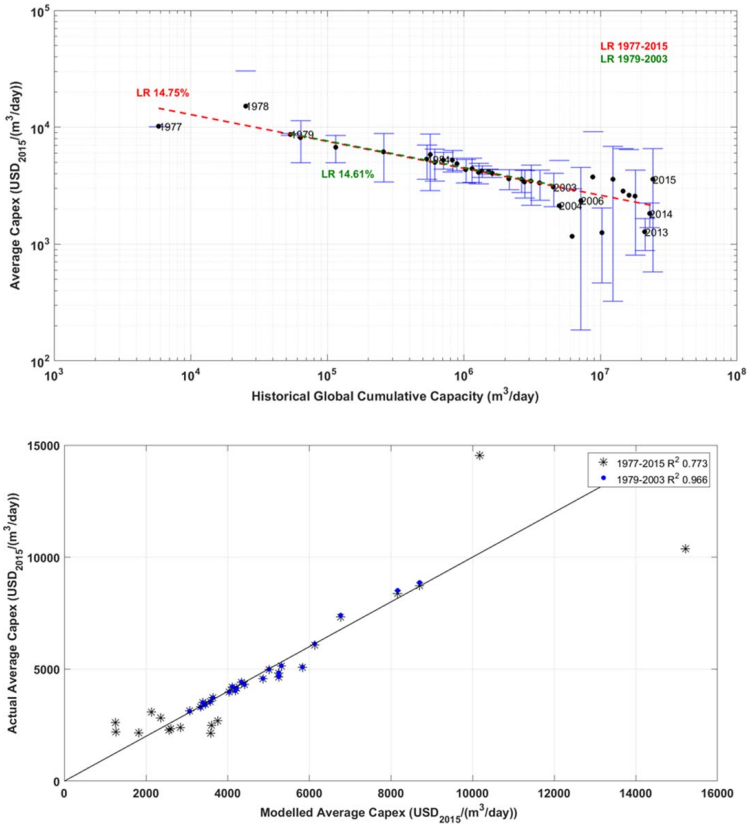

Figure 3. (top) SWRO Capex Learning Curve for 1977–2015 and 1979–2003 and (bottom) fit of the modeled capex values to the actual capex values.

From 1985 to 2003, SWRO plants that came online increased steadily at an average annual growth rate of 12%. Figure 4 (bottom) illustrates the SWRO capacities that came online from 1977 to 2015 in different global regions. The steady increase in global SWRO capacities explains the close fit to the learning curve from 1979 to 2004. Reflecting the increase in awarded capacities post-2004, the SWRO plants that came online increased by 24% from 2004 to 2005. Furthermore, the market spread to all regions, mainly Western Europe and East Asia and not concentrated solely in the Middle East and North Africa. The MENA region dominated the market pre-2004. After 2010, however, the capacities that came online annually decreased, with the exception of 2013.

To project the SWRO capex based on the learning curve, one must understand what market factors caused the sudden dip in 2004, the rise in 2009, and the trend back toward the learning curve pre-2004. Thus, to assess the deviation from the learning curve after 2004, the learning curve with the odd capex numbers excluded is plotted. Figure 5 (top) illustrates the curve when the small and medium-sized plants with low capex numbers (small $<$1,500 and medium $<$1,000 USD/(m^3/d)) are removed. The learning rate from 1977

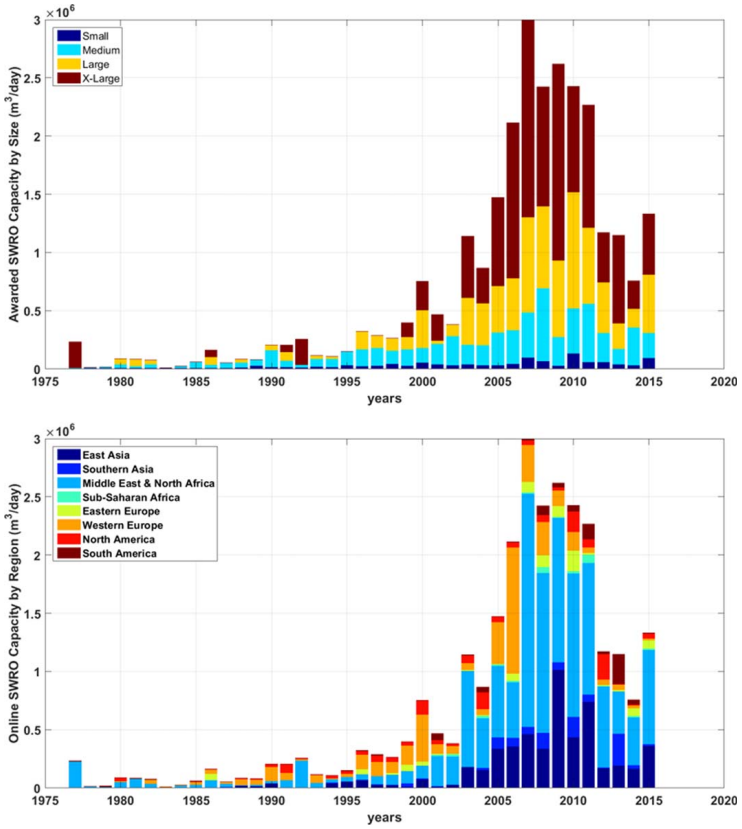

Figure 4. Awarded SWRO capacity from 1977 to 2015 distributed by (top) SWRO plant size and (bottom) online SWRO capacity from 1977 to 2015 distributed by region.

to 2015 decreases slightly to 14.62%. The average capex in the years 2004 and 2005 are pushed up higher due to exclusion of the lower capex numbers.

Figure 5 (middle) illustrates the learning curve after large and extra-large plants with capex greater than 10,000 USD/(m^3/d) are ignored. The learning rate increased to 15.65%. The increase in 2009 is due to extra-large plants awarded in Victoria and South Australia, both Australia, at substantially higher capex. The capex for the 444,000 m^3/d Victorian and 274,000 m^3/d South Australian plants were 7,200 USD/(m^3/d) and 5,600 USD/(m^3/d), respectively. In sharp contrast, the capex for the 500,000 m^3/d Algerian and 25,200 m^3/d Indian plant were 980 USD/(m^3/d) and 680 USD/(m^3/d). These numbers provide insight into the capex intensive Australian SWRO market.

Figure 5 (bottom) presents the learning curve after large and extra-large plants with capex greater than 5,000 USD/(m^3/d) are ignored. The learning rate now increased to 17.50% and the average capex numbers after 2004 lie below the learning curve. Plants awarded in 2004–2007 and 2009–2012 in China, Saudi Arabia, Spain, Cyprus, Chile, and Australia were excluded. The capex jump in 2010 is due to the 3,000 m^3/d in the

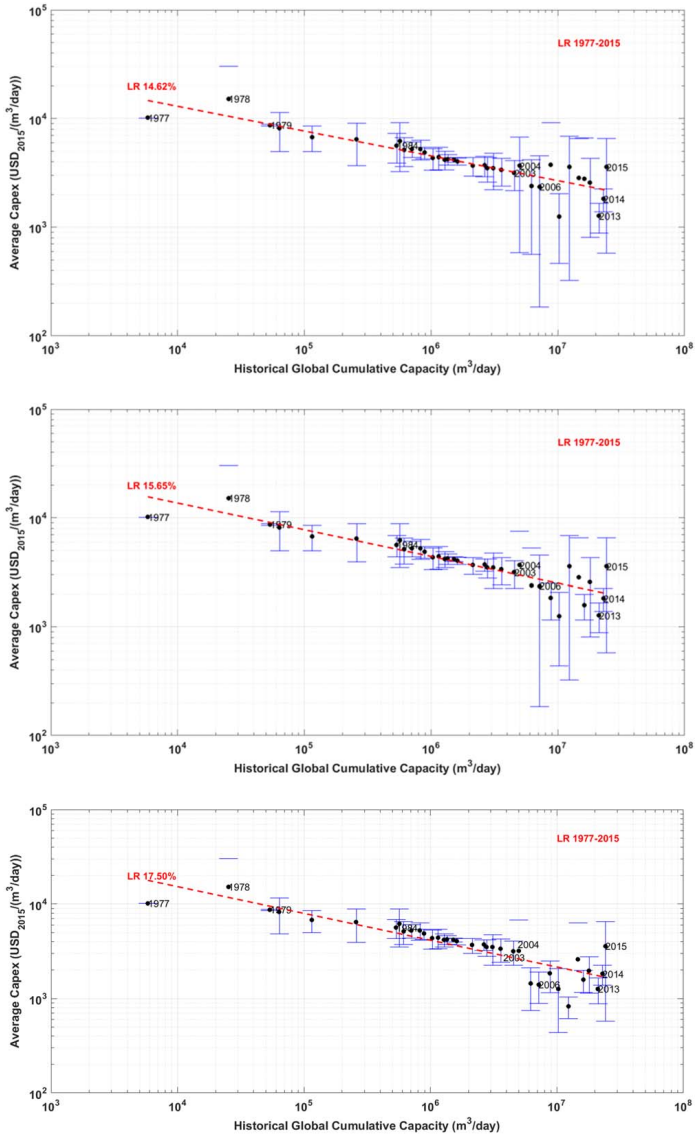

Figure 5. (top) Learning curve from 1977 to 2015 with odd small and medium-sized SWRO plants excluded. (middle) Learning curve from 1977 to 2015 with large and extra-large-sized SWRO plants with capex greater than 10,000 USD/(m^3/d) excluded. (bottom) Learning curve from 1977 to 2015 with large and extra-large-sized SWRO plants with capex greater than 5,000 USD/(m^3/d) excluded.

Table 4
SWRO Capex Projections Based on 15% Learning Rate, 10% and 20% Increase in Annual Online Capacity From 2022 Onwards

		2015	2022	2030	2040	2050
With annual growth rate of 10%						
Global historic cumulative online SWRO capacity	mill m^3/d	24	34	72	188	487
Capex	USD/(m^3/d)	2,070	1,917	1,603	1,282	1,025
With annual growth rate of 20%						
Global historic cumulative online SWRO capacity	mill m^3/d	24	34	145	899	5,567
Capex	USD/(m^3/d)	2,070	1,917	1,361	888	580

Note. The capex for 2022 is based on the forecasted cumulative online capacity (Virgili 2017a) and 15% learning rate.

Maldives with a capex of 15,200 USD/(m^3/d). The average capex in 2015 is pushed higher by the 10,475 m^3/d Charles Meyer plant awarded in California at a capex of 4,300 USD/(m^3/d).

By observing Figure 4 (top) and Figure 4 (bottom), it can be understood that after 2003, most of the plants awarded were large or extra-large capacities. Due to the economy of scale effect, there was a drop in the capex after 2004. However, there were also large and extra-large plants being built at very high capex, as opposed to the lower capex expected for these capacities. The large standard deviation is due to the spread of SWRO plants globally and the location-specific parameters that influence the capex.

In 2010, Voutchkov (2010) estimated the construction costs of SWRO plants to be about 1,032–1,717 USD/(m^3/d) in 2015 and fall further to 528–924 USD/(m^3/d) by 2030. Based on the learning curve, the global average is at 1,824 USD/(m^3/d) in 2014 and increases sharply to 3,581 USD/(m^3/d) in 2015 due to the more expensive plant awarded in California. According to the most recent GWI Desal Data market update (Virgili, 2017a), the desalination market is expected to return to the growth rates prior to the 2010 slump attributed to the global economic slowdown, Arab Spring and low commodity, oil and gas prices. It is projected that by 2022, the total SWRO installed capacity would be 33,777,000 m^3/d. Assuming a cumulative annual growth rate of 10% and an installed capacity of 33,777,000 m^3/d by 2022, the total online capacity by 2030 would be 72,404,200 m^3/d. Based on a 15% learning rate, a starting historic global cumulative capacity of 24,334,000 m^3/d in 2015 and average capex of 2,070 USD/(m^3/d) in 2015, the average SWRO capex would then be 1,580 USD/(m^3/d) in the year 2030, higher than the range specified by Voutchkov (2010). With faster growth of SWRO capacities, spurred on by global water demand, improvements in design and construction, the SWRO capex may decrease even more steeply. Table 4 illustrates the SWRO capex trends for the coming years assuming a 15% learning rate, a 10% and 20% increase in annual online capacity from 2022 onward. It has to be noted that all cost data have been calculated for the currency value of the year 2015.

5. Discussion

The learning curve establishes that as the historic global cumulative online SWRO capacity is doubled, the SWRO capex decreases by approximately 15%. The major components that comprise SWRO plants are the plant intake, pretreatment, reverse osmosis unit, post treatment, and desalination plant discharge management (Voutchkov, 2013). These components contribute in different ratios to the SWRO capex and are dependent on the desalination site parameters.

For instance, SWRO plants that can utilize adjacent power plant's intake and discharge infrastructure may cost half as much as those SWRO plants that require separate intake and outfall infrastructure (Water Reuse Association Desalination Committee, 2012). The difference in cost was observed in the 189, 250 m^3/d Carlsbad facility in Carlsbad, USA, and the ongoing Camp Pendleton project, of similar capacity to Carlsbad, in Camp Pendleton, USA. The latter required construction of dedicated outfall and intake infrastructure and resulted in cost estimations double that of Carlsbad facility (Water Reuse Association Desalination Committee, 2012). Similar example is the 25,200 m^3/d SWRO plant in coastal Gujarat, India, that has a capex of 680 USD/(m^3/d) and located next to a 4 GW coal power plant (Power Online, 2009). Reflecting similar views, Almar Water Solutions presented an example of 100,000 m^3/d plants in Minjur, India, and Qindago, China.

Due to the differences in the feedwater quality, different pretreatment systems are required influencing the capex of the two systems (Almar Water Solutions, 2016).

In Australia, the outfall of the SWRO plants were located in environmentally sensitive marine habitats (Water Reuse Association Desalination Committee, 2012). As a result, complex outfall infrastructure was required to minimize the impact on the environment. It is estimated that these designs may incur an additional 30% of the total desalination project costs. In Figure 2 (top), the resulting high capex in Australia is reflected in the average capex of 2009 and 2010. It is estimated that in most regions, intake and outfall infrastructure account for 10% of total project costs. Thus, site-specific parameters affect the SWRO cost leading to larger standard deviation.

Until 2004, the SWRO market was dominated by small and medium-sized desalination plants, as illustrated in Figure 4 (top). After 2004, there was a spike in both the online and awarded capacities of large and extra-large SWRO plants. This is reflected in the sudden drop in the global average SWRO capex from 3,074 USD/(m^3/d) in 2003 to 1,160 USD/(m^3/d) in 2005. Cost of reverse osmosis plants are influenced by scale of economy more than thermal desalination plants (Loutatidou et al., 2014). Voutchkov (2013) explains that one of the milestones in membrane desalination came around in 2004 when large-diameter RO membranes, suitable for large and extra-large capacities, were developed and commercialized. This was to cater to the growing demand for large desalination capacities. The use of 16 inch membranes, as opposed to the standard 8 inch membranes, implied compact physical structure and RO trains. In addition, there are benefits gained in other SWRO system components such as the high pressure pumps, energy recovery devices, and membrane cleaning systems. These factors explain the spread of large SWRO plant capacities post-2004, decreasing the global average capex. Such technological improvements are exactly the drivers of the learning curve, as identified by Neij (1997) and Nemet (2006), in particular due to their modular nature and industry-wide standard.

However, some of the cost benefits of large SWRO plants may be offset by other reasons such as additional structural costs. The use of larger membranes at the SWRO facility in Gold Coast, Australia, renders the system heavier per unit production capacity. The project site was an inactive landfill site and the low load bearing capacity of the ground necessitated additional foundation structures. As a result, the construction cost benefits of using larger membranes for the 133,000 m^3/d plant would be minimized.

The above described fluctuations from the learning curve help to explain the limitations of the learning curve approach utilized in this research. The learning curve presented is based on the increase in installed SWRO capacity. Therefore, the learning curve does not account for deviations of the global average SWRO capex due to other drivers of costs such as economy of scale of single plants. The limitations of the learning curve approach based solely on the concept of "learning by doing" have already been discussed. Schmidt et al. (2017) explains the drawbacks within the context of electrical energy storage learning curves. Similar issues are discussed by Wiesenthal et al. (2012) for energy technologies.

To overcome the drawbacks and improve the accuracy of SWRO capex projections, the current learning curve should be updated in the coming years to understand future trends and whether two-factor learning curves analyses could improve the understanding. The two-factor learning curve approach will help separate the influence of investments into research and development and increasing installed capacities on the SWRO capex. However, there are other factors such as economy of scale that may still cause divergence from the learning curve trend.

Despite the SWRO capex fluctuations, Figure 3 shows that the average global capex has been reducing at a learning rate of 15% or even more with the increase in construction of large and extra-large capacities. As the development of seawater desalination is driven by factors such as water scarcity, drought, saltwater intrusion due to excessive groundwater pumping and population increase, the SWRO capex costs will decrease (Gude, 2016).

Gude (2016) discusses the factors that may inhibit the development of global desalination markets. These factors comprise of environmental concerns, expensive capital, rising energy costs, water reuse and recycling strategies, political concerns, and uncertainty about droughts. The environmental concern about greenhouse gas emissions and rising energy costs can be tackled through the coupling of renewable energy (RE) power plants and SWRO plants (Caldera et al., 2016). By powering SWRO plants with 100% RE

plants, the dependency on fossil fuel and emission of greenhouse gases is eliminated. With the continual decrease of cost of PV plants and battery storage through the respective learning curves (European Technology & Innovation Platform Photovoltaic, 2017; Hoffmann, 2014; ITRPV, 2017; Kittner et al., 2017; Liebreich, 2016; Nykvist & Nilsson, 2015; Schmidt et al., 2017), concern about rising energy costs can be overcome, as pointed out by Breyer et al. (2017b, 2017c) for very high shares of renewable energy.

Wilder et al. (2016) explains that proponents of seawater desalination perceive the technology as a drought-proof means of meeting a country's water demand and achieving water security. For some water scare countries, desalination is considered to be the only option to meet the country's water demands. The energy consumption and environmental damage can be overcome through the development and use of the right technologies as demonstrated in Israel, Spain, and Australia. These views are further supported by Reyes et al. (2017) who modeled water scarcity mitigation options for the Santa Cruz Island in the Galapagos Archipelago. It was found that by 2044, for a fast population and tourist increase scenario, the business as usual water supply would only meet 20% of the water demand. In the slow growth increase scenario, which is considered unlikely, the business as usual water supply would only meet 70% of the total water demand. Desalination is found to be crucial to ensuring water security for Santa Cruz. Nevertheless, the environmental and energy limitations of desalination are expected to hinder the utilization of desalination. Similarly, El-Sadek (2010) discusses the case for SWRO desalination in achieving water security for Egypt. The paper envisions a renewable energy powered desalination future for Egypt while acknowledging the environmental concerns of brine discharge. Giwa and Dindi (2017) discuss the role of desalination and cloud seeding for United Arab Emirates to achieve water security and sustainability. Ward and Becker (2015) discuss the important role that lower desalination costs can play in contributing toward the peace treaty and environmental protection in Israel and Palestine.

Meanwhile, desalination sceptics believe that water conservation, improved water use efficiency in all sectors, and water management should be initially considered to achieve water security (Wilder et al., 2016). The main concerns are the high capital, operating costs of running desalination plants and the environmental problems. As already highlighted, the high energy consumption and the greenhouse gas emissions can be overcome through 100% renewable energy powered SWRO plants. Brine discharge from desalination plants is a growing area of research with organizations researching the extraction of important minerals from the brine (Drioli et al., 2015), further supporting the use of desalination. Therefore, the main concerns regarding SWRO desalination can be overcome through technological improvements. In a future where two-thirds of the global population is expected to be facing water scarcity (Cosgrove & Loucks, 2015), seawater desalination, coupled with water conservation and management, will play a crucial role in ensuring water security. As depicted in Figure 1, the dominant desalination technology will be seawater reverse osmosis.

This research highlights the potential for decrease in SWRO capex with the increase in installation of SWRO plants. Powering the SWRO plants with 100% renewable energy power plants (Caldera et al., 2016) enables to overcome the concerns with desalination and will pave the way for sustainable and affordable cost of water production.

6. Conclusions

The aim of this paper is to apply the well-established learning curve concept, utilized by various industries, to the SWRO desalination industry and project the capital costs of SWRO plants. It was found that the capex of SWRO desalination plants, from 1977 to 2015, has been decreasing with a learning rate of about 15%. This implies that when the historic global cumulative online SWRO capacity doubled, the SWRO capex decreased by 15%. The decrease of the global average capex aligns with the 15% learning rate until 2004. However, post-2004, driven by the commercialization and demand for larger membrane systems, there is a rise in the number of large and extra-large SWRO capacities awarded. Due to the economy of scale effect, the average capex value drops from the learning curve. However, in some years the capex increased sharply due to site-specific parameters which increased construction costs.

Against a background of increasing desalination demand, the learning curve illustrates the potential for decrease in the SWRO capex. Various market factors may influence the SWRO capex resulting in deviations from the learning curve, as observed from 2004 onward. Coupled with renewable energy power plants,

with rapidly decreasing costs, SWRO plants can rapidly become a more sustainable and cost-effective source of water supply.

Acknowledgements
The first author gratefully acknowledges the scholarship offered by the Reiner Lemoine-Foundation. The authors acknowledge that all data used in this study is available in the references cited.

References

Al-Kharaghouli, A., & Kazmerski, L. L. (2013). Energy consumption and water production cost of renewable energy powered desalination processes. *Renewable and Sustainable Energy Reviews*, *24*, 343–356.

Almar Water Solutions (2016, December 12–14). *Desalination technologies and economics: CAPEX, OPEX, and technological game changers to come*. Paper presented at Mediterranean Regional Technical Meeting, Marseille, France. Retrieved from www.cmimarseille.org/sites/default/files/newsite/library/files/en/1.6.%20C.%20Cosin_%20Desalination%20technologies%20and%20economics_%20capex%2-C%20opex%20and%20technological%20game%20changers%20to%20come%20-ilovepdf-compressed.pdf, accessed March 20, 2017

Ansar, A., Flyvbjerg, B., Budzier, A., & Lunn, D. (2014). Should we build more dams? The actual costs of hydropower megaproject development. *Energy Policy*, *69*, 43–56.

Breyer, C., Afanasveya, S., Brakemeier, D., Engelhard, M., Giuliano, S., Puppe, M., . . . Moser, M. (2017a). Assessment of mid-growth of assumptions and learning rates for comparative studies of CSP and hybrid PV-battery power plants. *AIP Conference Proceedings*, 1850, 160001. https://doi.org/10.1063/1.4984535

Breyer, C., Bogdanov, D., Aghahosseini, A., Gulagi, A., Child, M., Oyewo, A. S., . . . Vainikka, P. (2017b). Solar photovoltaics demand for the global energy transition in the power sector. *Progress in Photovoltaics: Research and Applications*, 1–19. https://doi.org/10.1002/pip.2950

Breyer, C., Bogdanov, D., Gulagi, A., Aghahosseini, A., Barbosa, L. S. N. S., Koskinen, O., . . . Vainikka, P. (2017c). On the role of solar photovoltaics in global energy transition scenarios. *Progress in Photovoltaics: Research and Applications*, *25*, 727–745. https://doi.org/10.1002/pip.2885

Caldera, U., Bogdanov, D., Afanasyeva, S., & Breyer, C. (2016, June 21–24). *Integration of reverse osmosis seawater desalination in the power sector, based on PV and wind energy, for the Kingdom of Saudi Arabia*. Paper presented at 32nd EUPVSEC, Munich, Germany. Retrieved from http://bit.ly/2iVKP97

Caldera, U., Bogdanov, D., & Breyer, C. (2016). Local cost of seawater RO desalination based on solar PV and wind energy: A global estimate. *Desalination*, *385*, 207–216.

Cosgrove, J. W., & Loucks, D. P. (2015). Water management: Current and future challenges and research directions. *Water Resources Research*, *51*, 4823–4839. https://doi.org/10.1002/2014WR016869

Drioli, E., Ali, Macedonia, A. F., & Quinst-Jensen, C. A. (2015). Minerals, energy and water from the sea: A new strategy for zero liquid discharge in desalination. *JSM Environmental Science and Ecology*, *3*(2), 1018.

El-Sadek, A. (2010). Water desalination: An imperative measure for water security in Egypt. *Desalination*, *250*, 876–884.

European Technology and Innovation Platform Photovoltaic (ETIP-PV) (2017). *The true competitiveness of solar PV. A European case study*. European Technology and Innovation Platform Photovoltaic. Munich, Germany: ETIP-PV. Retrieved from http://bit.ly/2yH0QJ7

Farfan, J., & Breyer, C. (2017). Structural changes of global power generation capacity towards sustainability and the risk of stranded investments supported by a sustainability indicator. *Journal of Cleaner Production*, *141*, 370–384.

Fichtner (2011). *MENA Regional Water Outlook Part 2: Desalination using renewable energy* (final report). Stuttgart, Germany: Fichtner.

Fthenakis, V., Atia, A. A., Morin, O., Bkayrat, R., & Sinha, P. (2016). New prospects for PV powered water desalination plants: Case studies in Saudi Arabia. *Progress in Photovoltaics: Research and Applications*, *24*, 543–550.

Ghaffour, N., Missimer, M. T., & Amy, L. G. (2013). Technical review and evaluation of the economics of water desalination: Current and future challenges for better water supply sustainability. *Desalination*, *309*, 197–207.

Giwa, A., & Dindi, A. (2017). An investigation of the feasibility of proposed solutions for water sustainability and security in water-stressed environment. *Journal of Cleaner Production*, *165*, 721–733.

Global Water Intelligence (GWI) (2016a). *Desalknowledge: Global market development*. Oxford, UK: GWI. Retrieved from www.desaldata.com/desalination-markets-2016/subsection-235, accessed March 26, 2016

Global Water Intelligence (GWI) (2016b). *Desalknowledge: Plant size*. Oxford, UK: GWI. Retrieved from www.desaldata.com/desalination-markets-2016/subsection-238, accessed March 26, 2016

Global Water Intelligence (GWI) (2017a). *Global Water Market 2017 Volume 4: Middle East and Africa*. Oxford, UK: Media analytics.

Global Water Intelligence (GWI) (2017b). *Global Water Market 2017 Volume 5: Asia Pacific*. Oxford, UK: Media Analytics.

Global Water Intelligence Desal Data (GWI) (2017c). *Desalknowledge. Forecast trends*. Oxford, UK: GWI Desal Data. Retrieved from www.desaldata.com/desalination-markets-2016/subsection-245, accessed February 22, 2017

Global Wind Energy Council (2015). Global wind report. Annual market update. Brussel, Belgium: Global Wind Energy Council. Retrieved from www.gwec.net/wp-content/uploads/vip/GWEC-Global-Wind-2015-Report_April-2016_19_04.pdf, accessed February 28, 2017

Gude, V. G. (2016). Desalination and sustainability: An appraisal and current perspective. *Water Research*, *89*, 87–106.

Henderson, B. (1968). *Perspectives on experience*. Boston, MA: Boston Consulting Group.

Hoffmann, W. (2014, September 22–26). *Importance and evidence for cost effective electricity storage*. Paper presented at 29th EUPVSEC, Amsterdam, the Netherlands.

International Technology Roadmap for Photovoltaic (ITRPV) (2017). *International technology roadmap for photovoltaic 2016 results* (8th ed.). Frankfurt, Germany: ITRPV.

Jacobson, M. Z., Delucchi, M. A., Bauer, Z. A., Goodman, S. C., Chapman, W. E., Cameron, M. A., . . . Erwin, J. R. (2017). 100% clean and renewable wind, water, and sunlight all-sector energy roadmaps for 139 countries of the world. *Joule*, *1*(1), 108–121.

Kersten, F., Doll, R., Kux, A., Huljić, D. M., Görig, M. A., Breyer, C., . . . Wawer, P. (2011, September 5–9). *PV-learning curves: Past and future drivers of cost reduction*. Paper presented at 26th EU PVSEC, Hamburg, Germany. Retrieved from http://bit.ly/2iYu0OO

Kittner, N., Lill, F., & Kammen, M. D. (2017). Energy storage deployment and innovation for the clean energy transition. *Nature Energy*, *2*, 17125. https://doi.org/10.1038/nenergy.2017.125

Liebreich, M. (2016, April 5). *Bloomberg new energy finance summit in search of the miraculous*. New York, NY: Bloomberg New Energy Finance. Retrieved from www.bbhub.io/bnef/sites/4/2016/04/BNEF-Summit-Keynote-2016.pdf

Loutatidou, S., Chalermthai, B., Marpu, P. R., & Arafat, H. (2014). Capital cost estimation of RO plants: GCC countries versus southern Europe. *Desalination*, *347*, 103–111.

Luo, X., Wang, J., Dooner, M., Clarke, J., & Krupke, C. (2015). Overview of current development in electrical energy storage technologies and the application potential in power system operation. *Applied Energy*, *137*, 511–536.

Neij, L. (1997). Use of experience curves to analyse the prospects for diffusion and adoption of renewable energy technology. *Energy Policy*, *23*, 1099–1107.
Nemet, F. G. (2006). Beyond the learning curve: Factors influencing cost reductions in photovoltaics. *Energy Policy*, *34*, 3218–3232.
Nykvist, B., & Nilsson, M. (2015). Rapidly falling costs of battery packs for electric vehicles. *Nature Climate Change*, *5*(4), 329–332.
Organisation for Economic Co-operation and Development (OECD) (2017a). *OECD.Stat*, Paris, France: OECD. Retrieved from http://stats.oecd.org/index.aspx?queryid=169, accessed April 28, 2017
Organisation for Economic Co-Operation and Development (OECD) (2017b). *Inflation (CPI) (indicator)*. Paris, France: OECD. Retrieved from https://data.oecd.org/price/inflation-cpi.htm, accessed March 23, 2017
Power Online (2009). *Aquatech awarded a major desalination contract for India's first ultramega power project*. Retrieved from www.power-online.com/doc/aquatech-awarded-a-major-desalination-0001?VNETCOOKIE=NO, accessed May 2, 2017
Rapping, L. (1965). Learning and World War II production functions. *The Review of Economics and Statistics*, *47*, 81–86.
Reyes, M. F., Trifunovic, N., Sharma ,S., Behzadian, K., Kapelan, Z., & Kennedy, M. D. (2017). Mitigation options for future water scarcity: A case study in Santa Cruz Island (Galapagos Archipelago). *Water*, *9*(8), 597. https://doi.org/10.3390/w9080597
Schmidt, O., Hawkes, A., Gambhir, A., & Staffell, I. (2017). The future cost of electrical energy storage based on experience rates. *Nature Energy*, *2*, 17110. https://doi.org/10.1038/nenergy.2017.110
Sood, A., & Smakhtin, V. (2014). Can desalination and clean energy combined help to alleviate global water scarcity. *Journal of the American Water Resources Association*, *50*(5), 1111–1123. https://doi.org/10.1111/jawr.12174
Swanson, R. M. (2006). A vision for crystalline silicon photovoltaics. *Progress in Photovoltaics*, *14*, 443–453.
Teske, S., Sawyer, S., Schäfer, O., Pregger, T., Simon, S., Naegler, T., . . . Kleiner, F. (2015). *Energy [R]evolution: A sustainable world energy outlook 2015* (5th ed.). Amsterdam, the Netherlands: Greenpeace International, GWEC and SolarPowerEurope; Greenpeace. Retrieved from http://bit.ly/1MCqbY3
The Energy Collective (2014). *Eye on the Prize: Solar market potential in Saudi Arabia*. Retrieved from www.theenergycollective.com/anonymous/610831/eye-prize-solar-market-potential-saudi-arabia, accessed March 23, 2017
Vest Charles (2016). *Hydropower in the Mekong: An alternative approach*. Retrieved from www.thethirdpole.net/2016/12/05/hydropower-in-the-mekong-an-alternative-approach/, accessed October 10, 2017
Virgili, F. (2016). *Desalination market update. Third Quarter Assessment*. Oxford, UK: Global Water Intelligence. Retrieved from www.desaata.com/forecasts, accessed May 23, 2017
Virgili, F. (2017a). *Q2 2017 market update*. Oxford, UK: Global Water Intelligence. Retrieved from www.desaldata.com/forecasts, accessed May 28, 2017
Virgili, F. (2017b). *Q3 2016 market update*. Oxford, UK: Global Water Intelligence. Retrieved from www.desaldata.com/forecasts, accessed April 28, 2017
Voutchkov, N. (2010). *How much does seawater desalination cost? A seminar to advance the development and management of innovative water supplies in Texas*. Paper presented at Texas Innovative Water 2010. Water Globe Consulting, Texas. Retrieved from www.twdb.texas.gov/innovativewater/events/tiw2010/doc/How_much_does_seawater_desalination_cost.pptx, accessed March 20, 2017
Voutchkov, N. (2013, June 27). *Cost estimating of SWRO plants. Desalination project costs: Trends, examples and interactive session*. Muscat, Oman: The Middle East Research Centre. Retrieved from www.swim-sm.eu/index.php/en/resources/category/41-training-course-cost-estimating-of-seawater-reverse-osmosis-swro-desalination-plants-25-27-june-2013?download=431:reverseosmosistraining3rdday31-desal-project-cost-trendspdf, accessed March 20, 2017
Voutchkov, N. (2013). *Desalination engineering planning and design*. New York, NY: McGraw-Hill Company.
Ward, F. A., & Becker, N. (2015). Cost of water for peace and the environment in Israel: An integrated approach. *Water Resources Research*, *51*, 5806–5826. https://doi.org/10.1002/2014WR016783
Waste and Water International (2017). *RAF extension starts Qatar's journey from thermal to RO desalination*. Tulsa, OK: Waste and Water International. Retrieved from www.waterworld.com/articles/wwi/2017/05/raf-extension-starts-qatar-s-journey-from-thermal-to-ro-desalination.html, accessed May 28, 2017
Water Desalination Report (2017). *Saudi Arabia desal market re-ignited*. Retrieved from www.desaldata.com/news/saudi-arabia-desal-market-re-ignited, accessed March 26, 2016
Water Online (2016). *Ghalilah desalination plant honored with distinction award for desalination plant of the year at 2016 global water awards*. Retrieved from www.wateronline.com/doc/ghalilah-desalination-plant-honored-plant-of-the-year-at-global-water-awards-0001, accessed May 28, 2017
Water Reuse Association Desalination Committee (2012). *Seawater desalination costs. White paper*. Alexandria, VA: Water Reuse Association. Retrieved from https://watereuse.org/wp-content/uploads/2015/10/WateReuse_Desal_Cost_White_Paper.pdf. Access March 20 2017
Werner, C., Gerlach, A., Breyer, C., & Masson, G. (2017, September). *Growth regions in photovoltaics in 2016: Update on latest global solar market development*. Paper presented at 33rd EUPVSEC, Amsterdam, Netherlands. Retrieved from http://bit.ly/2xT4i6e
Wiesenthal, T., Dowling, P., Morbee, J., Thiel, C., Schade, B., Russ, P., . . . Londo, M. (2012). *Technology learning curves for energy policy support*. Petten, the Netherlands: European Commission Joint Research Center. Retrieved from https://setis.ec.europa.eu/sites/default/files/reports/Technology-Learning-Curves-Energy-Policy-Support.pdf
Wilder, M. O., Aguilar-Barajas, I., Pineda-Pablos, N., Varady, R. G., Megdal, S. B., McEvoy, J., . . . Scott, C. A. (2016). Desalination and water security in the US–Mexico border region: Assessing the social, environmental and political impacts. *Water International*, *41*(5), 756–775. https://doi.org/10.1080/02508060.2016.1166416
Williams, E., Hittinger, E., Carvalho, R., & Williams, R. (2017). Wind power costs expected to decrease due to technological progress. *Energy Policy*, *106*, 427–435.
Wright, P. T. (1936). Factors affecting the cost of airplanes. *Journal of the Aeronautical Sciences*, *3*, 122–128.

Publication VI

Caldera, U., and Breyer, C.
Assessing the potential for renewable energy powered desalination for the global irrigation sector

Reprinted with permission from
Science of the Total Environment
Vol. 694, pp 1-13, 133598, 2019

Science of the Total Environment 694 (2019) 133598

Contents lists available at ScienceDirect

Science of the Total Environment

journal homepage: www.elsevier.com/locate/scitotenv

Assessing the potential for renewable energy powered desalination for the global irrigation sector

Upeksha Caldera *, Christian Breyer

LUT University, Yliopistonkatu 34, 53850 Lappeenranta, Finland

HIGHLIGHTS

- Renewable energy based desalination can be used for irrigation of cereals.
- Water for irrigation of cereals can cost less than 0.63 €/m^3 including pumping.
- Increased irrigation efficiency can reduce total water for irrigation by up to 36%.
- Desalination demand for irrigation can be reduced by up to 80%.

GRAPHICAL ABSTRACT

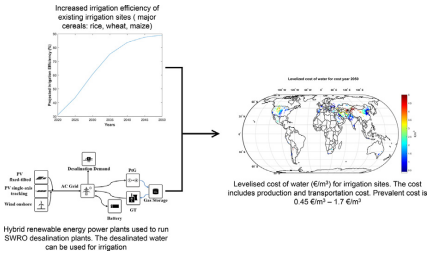

ARTICLE INFO

Article history:
Received 31 January 2019
Received in revised form 23 July 2019
Accepted 24 July 2019
Available online 29 July 2019

Keywords:
Irrigation efficiency
Water stress
Seawater reverse osmosis
Solar photovoltaics
Wind power plants

ABSTRACT

By 2050, it is estimated that the annual cereal production would need to increase by about 140% and total global food production increase by 70%. Meanwhile, total water withdrawals for irrigation are projected to increase by 11%. In contrast, poor management of existing water resources, pollution and climate change has resulted in limited freshwater resources. The aim of this paper is to assess how improved irrigation efficiency and renewable energy based desalination maybe used to secure future water supplies for the growth of rice, wheat and maize. The efficiencies of the existing irrigation sites were obtained and improved based on a logistic curve. The growth was projected such that by 2050, all existing irrigation sites would have an efficiency of 90%. The new irrigation efficiencies were used to obtain the reduced irrigation demand for the years 2030 and 2050. The desalination demand was estimated and an energy system model used to optimise the corresponding renewable energy based power system.

It was found that improving the average irrigation efficiency to 60% by 2030, led to a 64% reduction in total desalination demand. Similarly, an improvement towards 90% irrigation efficiency, by 2050, translates to an 80% reduction in global desalination demand. In 2030, the total water cost is mostly within 0.7 €/m^3–2 €/m^3 including water transportation costs. Literature reports that farmers may be willing to pay up to 0.63 €/m^3 for their irrigation water. The global range in 2050 is estimated to be 0.45 €/m^3–1.7 €/m^3 reflecting the lower system costs in 2050.

The above results indicate that as conventional water prices increase, renewable energy based seawater reverse osmosis desalination, offers a cost effective water supply for the irrigation sector. Adoption of high efficiency irrigation systems alleviate water stress and can eliminate need for additional water supply.

* Corresponding author.
E-mail addresses: upeksha.caldera@lut.fi (U. Caldera), christian.breyer@lut.fi (C. Breyer).

https://doi.org/10.1016/j.scitotenv.2019.133598
0048-9697/

1. Introduction

The conundrum of how to provide food security, at affordable prices, for an increasing global population, on a planet with finite resources, has been addressed by various researchers and organisations (Intergovernmental Panel on Climate Change, 2018; Steduto et al., 2018; Assouline et al., 2015). The recent IPCC SR1.5 report (Intergovernmental Panel on Climate Change, 2018) explains that with the inevitable temperature rise of 1.5 °C above pre-industrial levels, extreme weather events will become common, threatening water and land availability for food production. Failing to achieve net zero emissions by 2050 and thereby overshooting the 1.5 °C limit, will result in even more dire consequences. Therefore, it is crucial to secure land and water resources required for global food production (Intergovernmental Panel on Climate Change, 2018; Steduto et al., 2018; Assouline et al., 2015).

Irrigated agriculture accounts for 70% of the total global water withdrawals and meets 45% of the global food demand (Steduto et al., 2018). Steduto et al. (2018) explain the crucial role that irrigation and water management has played in the last 50 years to enable countries to grow food crops in drier conditions and improve livelihoods. By 2050, the Food and Agricultural Organisation of United Nations (FAO) predicts that annual cereal production should increase by about 140% and total global food production increase by 70% (Food and Agricultural Organisation of the United Nations, 2009). Total water withdrawals for irrigation are projected to increase by 11% (Steduto et al., 2018). The challenge is meeting the water demand, in the face of depleting freshwater resources, climate change and increasing demand from the municipal and industrial sectors (Steduto et al., 2018). It is reported that in the 20th century the global water demand has been growing more than twice the rate of the population growth (Steduto et al., 2018).

Seawater desalination offers a climate-independent alternative to global freshwater resources and is projected to play a crucial role in future water supplies (Jones et al., 2019). The seawater reverse osmosis (SWRO) technology accounts for 30% of the installed global desalination capacities and is projected to retain most of the market share. Literature explains that the increase in SWRO desalination capacities globally is due to improved technologies, decreasing capital costs, energy consumption and increasing water scarcity (Jones et al., 2019; Ghaffour et al., 2013; Caldera and Breyer, 2017). However, according to Jones et al. (2019), 62% of the desalinated water is used for the municipal sector, 30% is used for the industrial sector, and only 1.8% is used for irrigation. Burn et al. (2015) notes that, despite the advancements made, seawater desalination for irrigation is still expensive compared to traditional freshwater sources. However, due to the reducing costs of desalination, potable water is considered economically feasible for cash crops such as vegetables, flowers and fruits. In addition, Burn et al. (2015) summarises the benefits of the use of desalinated water that include reliable supply, consistent quality and recovery of saline soils. Countries that currently use desalination for irrigation are Spain, Canary Islands and Israel (Burn et al., 2015; Martinez-Alvarez et al., 2018). The implementation of desalination for irrigation is also being considered by Chile, China and Australia (Burn et al., 2015).

Burn et al. (2015) report that farmers in Australia are willing to pay up to 0.68 €/m^3 (1 AUD/m^3 at 1.48 AUD/€ exchange rate) for their irrigation water. According to data collected by the FAO (Food and Agricultural Organisation of the United Nations, 2019), the price paid for irrigated water, based on volume, can be as little as 15.3 €/1000 m^3 (20 USD/1000 m^3 at 1.3 USD/€ exchange rate) or as high as 1243/1000 m^3 (1330 USD/1000 m^3 at 1.07 USD/€ exchange rate). The article also notes that in most countries the full cost of water pumping is never recovered. OECD countries, such as Japan, parts of Australia, France, Spain and the Netherlands, are the few exceptions where 100% of the operation and maintenance costs are retrieved. Fischer et al. (2007) show that, due to climate change and increased agricultural withdrawals, the subsidised costs for irrigation water will increase, at a minimum, by 23.8 €/m^3 (30 USD/m^3) to 39.6 €/m^3 (50 USD/m^3). Fischer et al. (2007) note that due to increased competition for water, energy and decreasing subsidies, the future increase in water and energy costs will be much higher than what their research estimates. As freshwater resources become more scarce, the true cost of using water increases. Takatsuka et al. (2018) show how the increased use of ground or surface water in South Florida for irrigation will increase the economic losses. A recent study by Qiu et al. (2018) analyses the economic and environmental impacts of decreasing groundwater levels in the North China Plain (NCP) – one of China's most important agricultural regions. It was found that energy consumption for pumping water has doubled in seven years, rendering irrigation not viable for the farmer. In addition, the total economic cost for energy consumption and corresponding emission reduction is estimated to cost 10.3% of the local GDP. Therefore, the increasing dependence on diminishing groundwater poses a major threat to China's agricultural development. Qiu et al. (2018) suggest to substantially reduce the water withdrawn by using more efficient irrigation technologies, such as pressurized systems which can reduce water consumption by 10%–66%. In addition, the authors propose the use of solar pumps to overcome the fuel costs and greenhouse gas emissions produced by conventional electrical or diesel pumps. Nevertheless, this would still lead to declining groundwater levels, although at reduced rates compared to the present situation. The increments in irrigation efficiency are supported by the United Nations' Sustainable Development Goal 6.4, which targets a substantial increase in water use efficiency across all sectors by 2030 (Vanham et al., 2018).

The conducted literature review highlights the trends of increasing water costs and movement towards improved irrigation to limit the rise in global water demand and costs (Vanham et al., 2018). Jägermeyr et al. (2015) describe the generic concept of irrigation efficiency as the ratio of the water consumed through transpiration, evaporation and interception to the total water withdrawn from the water source. Therefore, irrigation efficiency may imply several definitions in different sources. Beneficial irrigation efficiency is a concept introduced by Jägermeyr et al. This measure of irrigation efficiency is the ratio of the water transpired to the total water withdrawn from the source. Thus, beneficial irrigation efficiency is a precise indicator, but does not account for lost water that may be reused from the basin. The global area weighted beneficial irrigation efficiency, based on the current distribution of different irrigation systems and crops grown, is estimated to be 33%. Jägermeyr et al. (2015) conducted a study on the global water saving potential of improved irrigation systems and noted that water withdrawals can be reduced by up to 68%. It is suggested that changing from the extensive surface irrigation systems to pressurized irrigation systems, namely sprinkler and drip technology, will result in higher irrigation efficiency and increased water savings. The efficiency of surface irrigation systems can lie between 30 and 60%, while that of sprinkler and drip is between 50–70% and 70–90% respectively. Drip irrigation is considered the most efficient and cost effective, particularly in water stressed areas. Fyles and Madramootoo (2016) report that 86% of the global irrigated area has adopted surface irrigation systems, while 11% and 3% of the total area use sprinkler and drip irrigation systems respectively. High shares of surface irrigation are mainly found in Central, South and Southeast Asia due to widespread rice cultivation with low efficiency (Jägermeyr et al., 2015).

Qiu et al. (2018) posit that even with improved irrigation efficiency, there are still declining groundwater levels and increasing water demand from other sectors (Steduto et al., 2018). Multsch et al. (2017) share similar views regarding the availability of water in the Nile Basin. The widening gap between water supply and demand and declining costs present a new role for seawater desalination in the irrigation sector. Vanham et al. (2018) explain that the exclusion of desalination from the definition of the SDG target 6.4 is a drawback and should be accounted for to realistically assess water scarcity. Vanham et al. also note the increasing energy consumption of desalination plants.

Conventional desalination plants are heavily dependent on diminishing and costly fossil fuels, while also resulting in greenhouse gas emissions (Ghaffour et al., 2013). Prior work done by the authors of this manuscript has shown how renewable energy based SWRO desalination can produce potable water at costs comparable with that of current fossil powered SWRO desalination plants (Caldera et al., 2018a). This renders SWRO desalination an attractive water supply source for regions with high water scarcity and increasing demand, while overcoming concerns about greenhouse gas emissions. Furthermore, the rapidly dropping costs of renewable energy power plants portend a reduction in electricity costs, which translate to a corresponding reduction in water production costs. Ghaffour et al. (2013) illustrate the decline in desalinated water costs and the increase in the cost of the use of conventional freshwater resources.

The purpose of this work is to link and establish solutions to meet the increasing water withdrawals for irrigation via improved irrigation efficiency technologies and use of renewable energy (RE) based SWRO plants. The objectives of this study are to: (1) determine the impact of substantial increases in irrigation efficiency on the future water demand; (2) project the SWRO capacities required to supplement the water demand for irrigation sites after improved irrigation efficiency; (3) model the energy system required to power the global SWRO capacities required as supplemental water supply for current irrigation sites; (4) project water production costs with the proposed system. The objectives are analysed for the years 2030 and 2050 to understand the potential for RE-based SWRO desalination in the irrigation sector over time.

2. Methods

The approach utilised for this research can be summarised in the following points:

1. Determine the irrigation efficiency of existing irrigation sites and project efficiency up to 2050.
2. Estimate water withdrawals for irrigation before and after improved irrigation efficiency. Use irrigation site-specific water stress and demand values to project the desalination capacity necessary to augment existing renewable water supplies. The desalination demand for irrigation is projected for the years 2030 and 2050.
3. After establishing the global desalination demand for irrigation sites, the energy system required for the SWRO desalination capacities is modelled and the cost of water production for the irrigation sites projected for the two time periods.

The following sub-sections describe the approach, data input and the model used in detail.

2.1. Global irrigation efficiency

Jägermeyr et al. (2015) model the beneficial irrigation efficiency for different crops on a gridded scale of 0.5°×0.5°. The efficiency is dependent on the irrigation technology (surface, sprinkler or drip) in use and the crops being planted.

For this research, the beneficial irrigation efficiency values of irrigation sites growing the major cereals wheat, maize and rice (Awika, 2011) are obtained from Jägermeyr et al. It is assumed that rice is grown with surface irrigation systems while wheat and maize are grown with sprinkler irrigation systems (Awika, 2011). If a node has both wheat and maize irrigation, it is assumed that the sprinkler area is equally utilised by both wheat and maize. The available data is in a 0.5° × 0.5° spatial resolution, whereas our research is conducted on a spatial resolution of 0.45° × 0.45°. Therefore, based on the latitude and longitude values of the 0.5° × 0.5° grid, the irrigation efficiency values were redistributed to the required 0.45° × 0.45° grid structure. When the latitude and longitude values in the two grid structures did not match, the irrigation efficiency in the nearest 0.5° × 0.5° node was taken. Nodes that had a spatial difference greater than 0.5°, in both latitude and longitude, were not considered.

Fig. 1 presents the area weighted average of the beneficial irrigation efficiency for the crops rice, wheat and maize. The prominent irrigation efficiency range is low and between 20%–40%.

To understand the historical and projected growth in irrigation efficiency for existing irrigation sites, a literature review was done. Hanasaki et al. (2013) collected literature on irrigation efficiency development and suggested the highest growth rate to be 0.3% per year, relative to the respective basis. This helps to explain the currently low irrigation efficiencies found in many regions. Wada et al. (2014) estimate that a linear 1% increase in irrigation efficiency per annum will reduce the water stressed global population by 2% in 2050, compared to a business as usual scenario. For this research, a logistic curve is used to derive a possible development scenario of irrigation efficiency up to 2050, as show in Fig. 2. The scenario is labelled the highest possible irrigation efficiency (HPIE) scenario. Reflecting the use of drip irrigation technology today and the corresponding high efficiencies available, it is assumed that by 2050 all sites will be able to achieve an irrigation efficiency of 90% (Awika, 2011). The efficiency may be higher in some places depending on the implementation and use, but a more conservative value was adopted to be applied globally. Companies like Netafim (2018) show that highly efficient irrigation systems can already be used to grow thirsty crops such as rice and wheat. The compound annual growth rate of the drip irrigation market is estimated to be 15.6%, with marked growth in countries like India and China (Cision PR Newswire, 2018). India is reported to have started using drip irrigation systems for rice production, on a small scale (Soman, 2012).

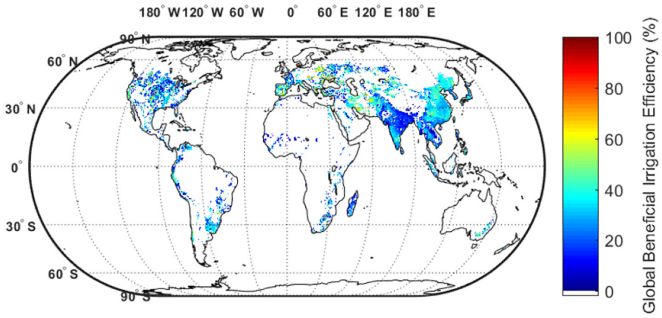

Fig. 1. Global beneficial irrigation efficiency for irrigation sites growing rice, wheat and maize (Awika, 2011).

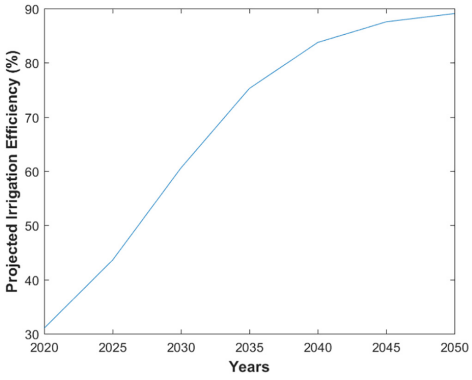

Fig. 2. Projected irrigation efficiency up to 2050 for the HPIE scenario.

Furthermore, Steduto et al. (2018) note that there is an urgent need to transition to highly efficient irrigation systems, and the withholding factor is political will and funding.

The logistic growth of the irrigation efficiency was based on the approach of Breyer et al. (2017a) for the development of renewable energy electricity production globally. Eq. (1) defines the logistic function used for this research.

$$irrigEffHPIE_{(year)} = A + \frac{K - A}{(1 + Qe^{-B\times(t-M)})^{\frac{1}{v}}} \quad (1)$$

where A is the maximum value of efficiency (90%), K is the minimum value of efficiency (20%), B is the growth rate (20%), t is the time in years, v is the factor affecting near which asymptote the maximum growth occurs (14), Q is the scaling parameter depending on f(0) (75) and M is time of maximum growth (2020).

2.1.1. Global water withdrawals for irrigation and corresponding desalination demand

Caldera et al. (2018a) estimate the desalination demand for regions based on the water stress and demand values obtained from the Aqueduct Water Risk Atlas (Luck et al., 2015). The Aqueduct Water Risk Atlas projects the decadal water stress, supply and demand values for 15,006 global water catchments. General circulation models and socioeconomic variables drive the climate variables used in the Atlas. Caldera et al. (2018a) use the water stress and demand values from the Atlas to determine the desalination demand for regions with water stress greater than 40%. The study was done for the year 2030.

The Aqueduct Water Risk Atlas projects the future water demand using irrigation efficiency based on the historically low growth rates. The change in water demand and stress factors is presented for global water catchments for the decades 2020, 2030 and 2040. The water demand change factor accounts for the increase in water withdrawals from 2010 (Food and Agricultural Organisation of the United Nations, 2015) for the municipal, industrial and agricultural sectors. To obtain the change in demand in 2050 for every catchment, the respective data from 2030 to 2040 is extrapolated. For the purpose of this work, the water demand and stress values projected by the Atlas are considered to be a Base scenario.

Table 1 illustrates the total water withdrawals assumed for the period from 2020 to 2050. The compound annual growth rate of 4% from 2030 to 2040 is also observed for the period from 2040 to 2050.

Table 1
Total water demand projections from 2020 to 2050 in the Base scenario.

		2020	2030	2040	2050
Total water demand	Billion m^3/day	14	16	17	19

To project the desalination demand after substantial improvements in irrigation efficiency of existing sites – the HPIE scenario - the following approach was taken. The analysis was carried out for the years 2030 and 2050:

1. Current irrigation water withdrawals of each country are obtained from the FAO Aquastat database (Food and Agricultural Organisation of the United Nations, 2015) and assumed to be distributed equally amongst the current irrigation sites.
2. Current irrigation efficiency for the irrigation site is obtained, as shown in Fig. 1.
3. Water withdrawals for irrigation in the years 2030 and 2050 are projected using the demand change factors presented in the Aqueduct Water Risk Atlas.
4. The irrigation efficiency is increased based on Fig. 2.
5. New irrigation water withdrawals are calculated for the higher irrigation efficiency, as illustrated in Eq. (2).
6. The municipal and industrial sector water withdrawals are the numbers estimated for the specific year in the Base scenario.
7. The corresponding total water demand, is the sum of the municipal, industrial and new irrigation water withdrawal numbers estimated for the specific year.
8. New water stress is found from the Base water stress, Base total water demand and reduced new total demand.
9. Desalination demand for irrigation node is calculated as a logistic function of the new water stress and new irrigation water demand, as described in Caldera et al. (2018a).

$$irrigDemandNew(i,y) = \frac{origirrigDemand}{\left(1 + \left(\frac{irrigEffHPIE_{(y)} - irrigEff(i)}{irrigEff(i)}\right)\right)} \quad (2)$$

where i and y are the 0.45° × 0.45° node and year under consideration respectively, *irrigDemandNew* is the water withdrawal for irrigation at the node i after improved efficiency, *origirrigDemand* is the water withdrawal for irrigation at the node i before improved efficiency, $irrigEffHPIE_{(y)}$ is the irrigation efficiency in the HPIE scenario for the year y, $irrigEff(i)$ is the initial irrigation efficiency for the node obtained from Jägermeyr et al. (2015).

2.1.2. Desalination demand and energy system model

The energy system, based solely on renewable energy resources, required to run the SWRO desalination capacities for irrigation are modelled using the LUT Energy System model. The modelling approach is similar to that described in Caldera et al. (2018a). The results of the modelling will provide the levelised cost of electricity (LCOE), or the cost of electricity production, for each node with desalination demand. The LCOE values can be used, as presented in Eq. (3), to determine the levelised cost of water (LCOW) for nodes with desalination demand. Eq. (3) has been summarised from Caldera et al. (2018a) and Caldera et al. (2016). The LCOW includes the cost of water pumping from the desalination plant on the coast to the irrigation site.

$$LCOW_{desal} = \frac{(capex_{desal} \times crf_{desal} + capex_{water\ storage} \times crf_{water\ storage}) + opex_{fixed}}{Total\ water\ produced\ in\ a\ year} + opex_{var\ desal} \times SEC$$

Table 2
Key assumptions for the SWRO desalination system in 2030 and 2050.

		2030	2050
SWRO desalination system			
CAPEX	€/(m³·a)	2.75	1.17
Fixed OPEX	€/(m³·a)	4% of CAPEX	4% of CAPEX
Mg remineralisation cost	€/m³	0.035	
Energy consumption	kWh_{el}/m^3	3.15	2.6
Lifetime	yrs	30	
Water storage			
CAPEX	€/m³	65	
Fixed OPEX	€/(m³)	2% of CAPEX	
Lifetime	yrs	30	
Horizontal pumping and piping			
Horizontal pipes CAPEX	€/(m³·a·km)	0.053	
Horizontal pipes Fixed OPEX	€/(m³·a·100 km)	0.023	
Horizontal pump CAPEX	€/(m³·hr·km)	19.23	
Horizontal pump Fixed OPEX	€/(m³·hr·km)	2% of CAPEX	
Energy consumption	kWh_{el}/(m³·hr·100 km)	0.04	
Lifetime	yrs	30	
Vertical pumping and piping			
Vertical pipes CAPEX	€/(m³·a·km)	0.053	
Vertical pipes Fixed OPEX	€/(m³·a·100 km)	0.023	
Vertical pump CAPEX	€/(m³·hr·m)	15.40	
Vertical pump Fixed OPEX	€/(m³·hr·m)	2% of CAPEX	
Energy consumption	kWh_{el}/(m³·hr·100 m)	0.36	
Lifetime	yrs	30	

$$LCOW = LCOW_{desal} + LCOT_{desal} \quad (3)$$

$capex_{desal}$ is the capital expenditures of the SWRO desalination plant in €/m³, $capex_{water\ storage}$ is the CAPEX of the water storage tank at the desalination site in €/m³, crf_{desal} is the annuity factor for the desalination plant, $crf_{water\ storage}$ is the annuity factor for water storage, Total water produced in a year is in m³ and $opex_{fixed}$ is the total fixed annual operational expenditures of the desalination system in €/m³. The total fixed OPEX is the sum of the fixed OPEX of the desalination plant in €/m³ and the OPEX of the water storage tank in €/m³. The value $opex_{var\ desal}$ is the variable OPEX of the desalination plant and is equal to the levelised cost of electricity (LCOE) of the plant in €/kWh. SEC is the specific energy consumption in kWh/m³. The product of the LCOE and SEC is the energy cost of the desalination plant in €/m³. $LCOT_{desal}$ is the levelised cost of water transportation from the desalination plant to the irrigation site in €/m³, *LCOW* is the resulting levelised cost of water in €/m³. The horizontal pumping distance is the shortest path from the irrigation site to the coast where the SWRO desalination plants are located. The highest elevation on the path is found using the ETOPO1 global relief model (Amante and Eakins, 2009) and considered to be the vertical pumping distance. For landlocked countries, the desalinated water may have to be transported through other countries.

Table 2 defines the key cost assumptions made for the SWRO desalination system in 2030 and 2050. The costs projections are based on the SWRO capex learning curve defined in Caldera and Breyer (2017). The energy consumption projections of SWRO plants are based on Caldera et al. (2018b). The cost for remineralisation of the desalinated water with Magnesium has been considered as discussed by Yermiyahu et al. (2007). Water storage is located at the site of the desalination plant and allows the SWRO plants to store excess water that may be utilised during times of low electricity production.

The LUT Energy System model is a linear optimisation model that uses the MOSEK ApS optimisation software to determine the least cost renewable energy system required to meet the defined energy demand. The system optimisation is done on an hourly resolution so that the energy demand of every hour is met by renewable energy resources at a minimum cost. In addition, a spatial resolution of $0.45° \times 0.45°$ is considered. The system optimisation minimises the total annual cost of the installed capacities of the different technologies, cost of energy generation and cost of generation ramping. Detailed description of the complete model can be found in Caldera et al. (2018b) and Breyer et al. (2017b).

Fig. 3 is a block diagram of the LUT Energy System model used for this research and illustrates the renewable energy generation technologies, energy storage technologies and energy sector bridging technologies. The hybrid RE power plants modelled are comprised of single-axis tracking PV, fixed-tilted PV, wind, batteries and power-to-gas (PtG) power plant. The hourly and spatially resolved profiles for the RE resources, solar photovoltaics (PV) and wind, are calculated as discussed in Caldera et al. (2018b) and Breyer et al. (2017b).

The key technical and financial parameters of the technologies that are used in the LUT Energy System model are listed in Table 3. The learning curves, based on the historical trends of the relevant technologies, are utilised to project the financial and technical assumptions for 2030 and 2050.

3. Results

3.1. Projected impact of improved irrigation efficiency

Increasing the irrigation efficiency reduces the total water demand and consequently the water stress across the basins. Fig. 4 provides insights into the relationship between irrigation efficiency and water stress in 2030 and 2050.

Fig. 4 (top) presents the water stress in 2030 for a base scenario, where there are no significant improvements in irrigation efficiency. The dependence on fossil groundwater is highlighted in regions where water stress is greater than 100%, such as regions in Northeast China and Central United States. Fig. 4 (center) illustrates the situation in

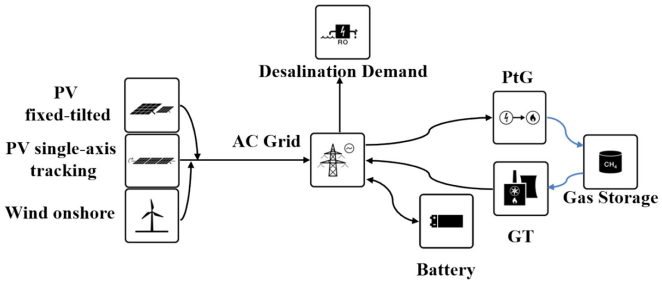

Fig. 3. Block diagram of the LUT Energy System model.

Table 3
Key assumptions for the renewable energy technologies used in the LUT Energy System model (Caldera et al., 2018b).

		2030	2050
Fixed-tilted PV plant			
CAPEX	€/kW	390	246
OPEX	€/(kW·a)	3% of capex	3% of capex
Lifetime	yrs	35	40
Single-axis tracking PV plant			
CAPEX	€/kW	429	271
OPEX	€/(kW·a)	3% of capex	3% of capex
Lifetime`	yrs	35	40
Wind plant			
CAPEX	€/kW	1000	900
OPEX	€/(kW·a)	2% of CAPEX	
Lifetime	yrs	25	
Battery system			
CAPEX	€/kWh_{cap}	150	75
Fixed OPEX	€/(kWh·a)	2.5% of CAPEX	
Lifetime	yrs	20	
PtG			
Water electrolysis CAPEX	€/kW_{H2}	363	248
Water electrolysis Fixed OPEX	€/(kW_{H2}·a)	13	8.7
Lifetime	yrs	30	
CO_2 direct air capture CAPEX	€/tCO_2	356	154
CO_2 direct air capture OPEX	€/(tCO_2·a)	9.1	5.7
Lifetime	yrs	30	
Methanation CAPEX	€/kW_{SNG}	278	190
Methanation OPEX	€/(kW_{SNG}·a)	11.1	7.6
Lifetime	yrs	30	
Gas storage	€/kWh	0.05	
Lifetime	yrs	50	

2030 if the average beneficial irrigation efficiency is improved to about 60%. Marked decreases in water stress levels are observed in India, China, Central Asia, Mediterranean and North America. However, there are still regions of high or extremely high stress in central United States and Northeast China. This could be attributed to the fact that the regions face high water demand from the other sectors, namely industrial and municipal. Fig. 4 (bottom) shows the declining water stress trends in the 2050 HPIE scenario. By this year the beneficial irrigation efficiency is expected to be 90%.

Fig. 5 illustrates the desalination demand for irrigation sites in the HPIE scenario for the years 2030 and 2050. The desalination demand for irrigation sites in 2030 is found to be $8.32 \cdot 10^8$ m^3/day. China, Iran and Pakistan account for approximately 55% of the total demand. In 2050, the total desalination demand decreases to be $6.25 \cdot 10^8$ m^3/day due to the higher irrigation efficiency, illustrated in Fig. 2. The countries China, Iran and Pakistan account for 50% of the total demand.

Table 4 presents the total irrigation water and desalination demand values for 2030 and 2050, in a base and HPIE scenario. If the irrigation efficiency is improved to 60% by 2030, a 27% reduction in total water demand and 64% reduction in total desalination demand is observed. Similarly, an improvement towards 90% irrigation efficiency, by 2050, will result in 36% reduction in total water demand for irrigation. This translates to an 80% reduction in global desalination demand. The remaining demand for desalination can be explained by the increasing total water withdrawals for irrigation in regions of high water stress.

3.2. The modelled RE-based SWRO desalination system

As mentioned in Section 2, the optimal system to produce water from the SWRO capacities show in Fig. 5, is modelled using the LUT Energy System model. Fig. 6 (top) illustrates the estimated LCOW range for the irrigation sites in 2030. The global range is from 0.7 €/m^3–6 €/m^3, while the prevalent range is 0.7 €/m^3–2 €/m^3. Fig. 6 (bottom) shows the corresponding LCOW diagram for 2050. The global range in 2050 is estimated to be 0.45 €/m^3–6 €/m^3 reflecting the lower costs of the SWRO and renewable energy power plants in 2050. The prevalent LCOW range is found to be 0.45 €/m^3–1.7 €/m^3, and particularly low in the sites closer to the coast where water transportation costs are low. Some nodes, such as in central United States, experience an increase in desalination demand, compared to 2030. This requires more pumping capacities, contributing to a slightly higher LCOW in 2050 compared to 2030.

Fig. 7 shows the optimised levelised cost of electricity at the irrigation sites for 2030 and 2050. As illustrated, the LCOE range reduces from 0.08 €/kWh–0.13 €/kWh in 2030 to 0.05 €/kWh–0.10 €/kWh in 2050. The least cost combination of RE power plants for the irrigation sites comprised of single-axis tracking PV, fixed-tilted PV and wind power plants, highlighting the solar and wind resources at the sites. Battery and power-to-gas plants are used to ensure continuous running of the SWRO desalination plants, which would technically not be required, but had been found the least cost operation mode (Caldera and Breyer, 2018). Fig. 8 (top) shows the contribution of PV and wind power plants to the total electricity generated for the year 2050. The global range is from as little as 26% in central regions of North America to as high as 96% in South Asia. The steeper reduction in solar PV costs and the location of most irrigation sites in regions with abundant solar resources can explain the higher share of PV generation. Similar generation shares are observed in 2030.

Fig. 8 (bottom) illustrates the extent to which the electricity cost contribute to the final LCOW. The range is not varied and all values lie between 23% and 42%. Regions that have large desalination demand or have large water pumping distances have higher contribution from the electricity cost. In 2030, the range is larger from 25% to 60%. The higher shares can be attributed to the higher cost of electricity in 2030, compared to 2050.

Table 5 presents key parameters of the modelled system for the countries with the highest desalination demand in 2030 and 2050. China, Iran and United States have higher average LCOW due to the larger pumping distances, in both vertical and horizontal directions. The longer pumping distances are reflected in the slight increase in LCOW from 2030 to 2050, despite the decrease in LCOE. China, Iran and Pakistan account for 53% of the global investment costs.

The technical and financial aspects of the RE systems required to power the SWRO capacities in 2030 and 2050 are summarised in Table 6. The results show that adopting RE-based SWRO systems for the irrigation sector will require 32% and 18% less investment and annualised costs respectively in 2050, relative to 2030. This is due to the projected lower costs in RE and SWRO systems by 2050, compared to 2030. The higher total opex costs in 2050 are due to the increase in demand and pumping distances in some regions.

4. Discussion

The results obtained show that RE-based SWRO desalination can be a cost competitive water supply option for irrigation in many regions in the world. In Australia, where farmers are reluctant to pay more than 0.63 €/m^3 (1 AUD/m^3) (Martinez-Alvarez et al., 2018), Fig. 6 shows that desalinated water can be supplied reliably for less than 1 €/m^3. It should be noted that increasing the efficiency of the irrigation sites on the eastern states decreases the demand for desalination by 50% from 2030 to 2050. This indicates the impact of irrigation on the water stress levels at the sites. The ongoing drought in Australia, stated to be the longest in recent history, has resulted in an increase in demand for desalination capacities to ensure reliable water supply to the eastern states (Water Desalination + Reuse, 2018).

In the North China Plain (NCP), the cost of water for irrigation can be as little as 1 €/m^3 in 2030 and 2050. The issues of farmers, about increasing costs due to declining groundwater levels and fuel costs, can be overcome by the increased irrigation efficiency and RE-based SWRO desalination systems presented. Similarly, in Colorado, Dolan et al. (2018) estimate a cost of 2.4 €/m^3 for produced water, excluding cost of

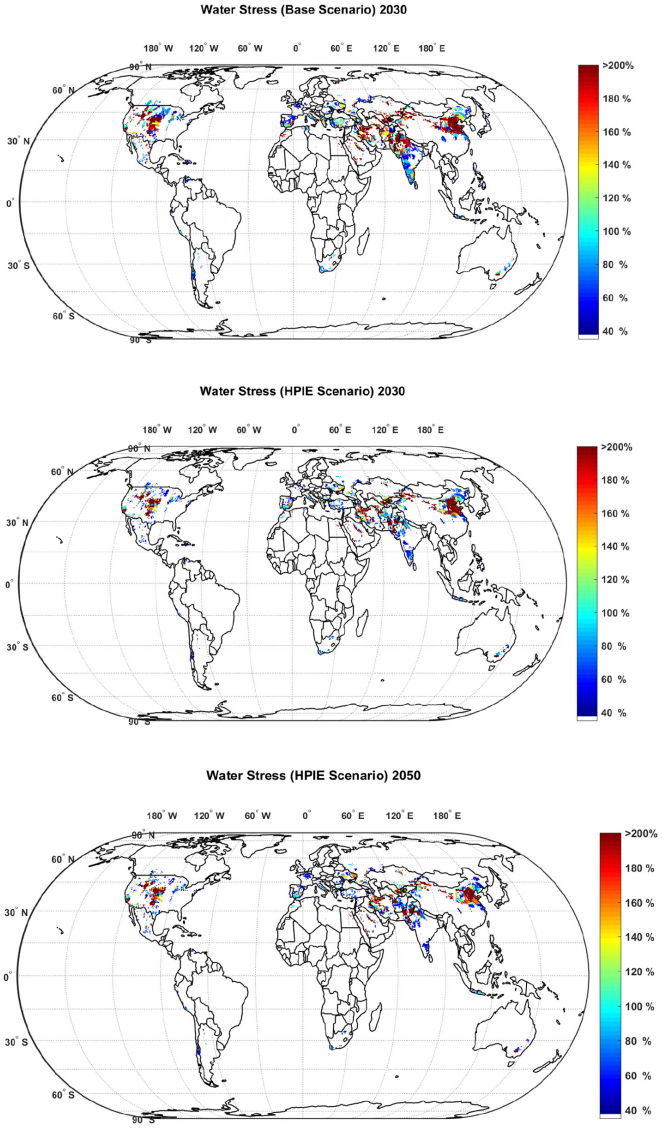

Fig. 4. Water stress of irrigation sites in the year 2030 base scenario (top), water stress of irrigation sites in 2030 HPIE scenario (centre) and water stress of irrigation sites in 2050 HPIE scenario (bottom).

transportation. Based on Fig. 6, the LCOW for this region can range from 2 to 3 €/m^3, including the transportation costs.

The FAO literature survey shows that the prices paid by farmers in countries, in particular developing countries, do not help to recover the operation and maintenance costs. Rosegrant et al. (2003) explain that some countries in Asia subsidise up to 90% of the O&M costs of the irrigation sector. Countries like United States, India, Pakistan and Egypt are reported to spend billions on subsidies for irrigation water a year. While subsidies are supposed to encourage equity and ensure people the basic access to water, the lack of recovery of the full costs of water has resulted in poorly maintained water infrastructure and mismanagement of water for irrigation. Rosegrant et al. present a

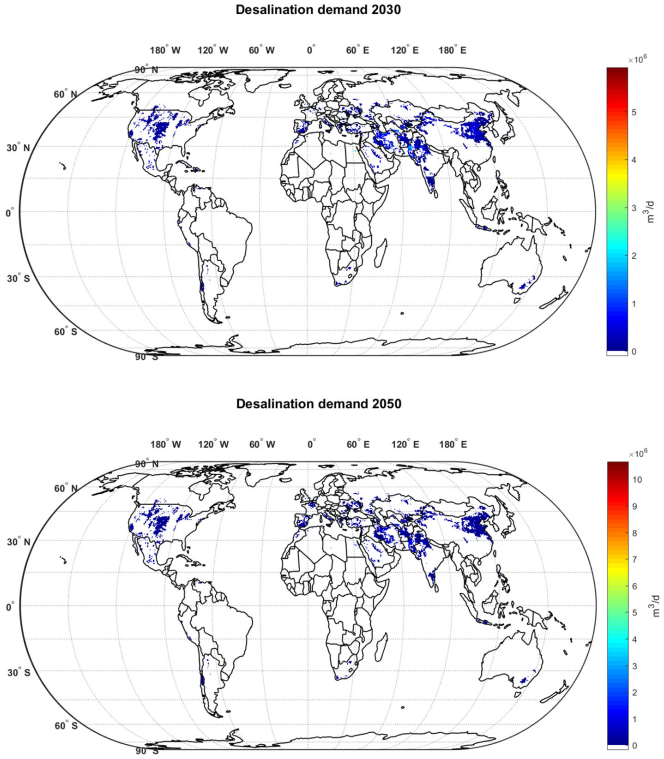

Fig. 5. Desalination demand for irrigation sites in the HPIE scenario for the year 2030 (top) and 2050 (bottom).

sustainable water use scenario, where water resources are managed and made available for people and the environment. The scenario expects the cost of water for the agricultural sector in developed countries to double, compared to a business as usual scenario, by 2025. The cost of water in developing countries is expected to triple. In contrast, in a water crisis scenario, where there is no regulation of the water price and groundwater is overdrafted, sharp increases in the cost of rice, wheat and maize is projected. Ghaffour et al. (2013) also discuss the increase in cost of water from traditional water resources and the growing potential for desalinated water.

Based on the results in Fig. 4, countries with most irrigation sites closer to the coast, such as Algeria, Morocco, Israel, Philippines, Venezuela and Italy, can produce water for costs less than 0.5 €/m^3. Countries with larger desalination demand and pumping distances, such as China and the United States, experience higher water production costs in the range of 0.5 €/m^3–4.5 €/m^3. Countries in Central Asia have the largest average water production costs, ranging from 3 €/m^3–5.8 €/m^3. This is due to the absence of a coastline and therefore longer pumping distances. In addition, desalinated water would need to be transported from regions with access to the sea, between international boundaries, posing further challenges. For regions such as these, water demand management, through techniques such as improved irrigation efficiency, maybe vital to overcoming the water scarcity issues. Fig. 2 already indicate marked decrease in water stress in the regions of Central Asia where rice, wheat or maize is grown. Karimov et al. (2013) provides insights into the ensuing issues between the Central Asian countries over the use of shared water resources. For instance, Tajikistan, as upstream water users, want to use the river water for electricity generation, but this causes conflict with downstream users in Uzbekistan, who want to use the water for cotton irrigation. To avoid potential water conflicts, the authors recommend the adoption of solar PV and wind power for electricity generation and drip irrigation technologies for farming.

The high desalination demand in 2030 and 2050 for some irrigation sites, despite the increase in irrigation efficiency, suggests that these irrigation sites are located in highly water stressed hydrological basins.

Table 4
Global irrigation water demand in base and HPIE scenarios.

		Base scenario 2030	Base scenario 2050	HPIE scenario 2030	HPIE scenario 2050
Water demand for irrigation	m^3/day	$1.10 \cdot 10^{10}$	$1.30 \cdot 10^{10}$	$8.06 \cdot 10^{9}$	$8.32 \cdot 10^{9}$
Desalination demand for irrigation	m^3/day	$2.31 \cdot 10^{9}$	$3.10 \cdot 10^{9}$	$8.32 \cdot 10^{8}$	$6.25 \cdot 10^{8}$

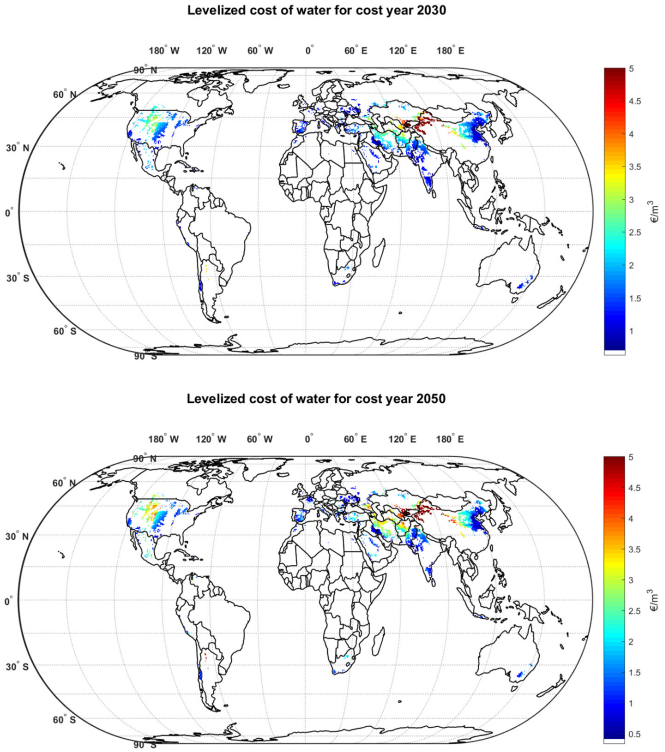

Fig. 6. LCOW in the year 2030 (top) and 2050 (bottom).

This is owing to the demands from the industrial and municipal sectors which are projected to experience an even larger growth by 2050 compared to the agricultural sector. Nevertheless, Fig. 4 shows that in most regions, increasing the beneficial irrigation efficiency results in significant reduction of the water stress and demand for desalination. Therefore, it is imperative that the beneficial irrigation efficiency is improved if water demand is to be controlled in the decades to come. The current average global irrigation efficiency is as little as 33%. The very low growth rates of 0.3% per annum, observed by Hanasaki et al. (2013), do not make a significant dent in the future water withdrawals for irrigation. It has to be noted that the present study only considers the cost of water supply to the irrigation sites and does not account for investments required to upgrade infrastructure at the sites. Various reports have made estimations on the costs involved for irrigation system upgrades in different parts of the world (Rosegrant Mark et al., 2017; Palazzo et al., 2019). For a comprehensive assessment of the costs entailed in high efficiency irrigation scenarios, the costs of improving the irrigation systems have to be accounted for.

The SWRO plants operate in a baseload manner throughout the year, utilising the combination of solar PV and battery storage, to minimise the cost of water production. The higher capital expenditures of SWRO plants entail that the plants are operated at higher full load hours to minimise the LCOW (Caldera and Breyer, 2018). To overcome the seasonal requirements of irrigation water demand, a reservoir maybe used as buffer between the desalination plant and the irrigation site to ensure that the irrigation water is supplied as per the demand throughout the year. Such a strategy has been discussed by Serrano-Tovar et al. (2019) for a local desalination plant in the Canary Islands. This is another aspect that should be considered for a comprehensive cost assessment of upgrading irrigation infrastructure.

Amidst growing global concern over the impacts of climate change, various reports and literature already highlight the global transition towards renewable energy resources (Intergovernmental Panel on Climate Change, 2018). In addition, the costs of renewable energy and storage technologies are projected to decline, securing a cost competitive energy source for desalination plants (Caldera et al., 2018b). Similarly, research has shown that the increase in desalination capacities globally (Caldera and Breyer, 2017) drive the decline of the capital costs of SWRO plants. Therefore, SWRO desalination systems coupled to RE power plants help overcome the environmental concern of greenhouse gas emissions and can be a reliable water supply for irrigation. Various researchers echo similar views on the need to drive the uptake of RE- based desalination (Jones et al., 2019; Ghaffour et al., 2013; Fornarelli et al., n.d.). Jones et al. (2019) shed light on the issue of increasing quantities of concentrated brine from desalination plants being discharged into the marine environment, without proper treatment. This can lead to the pollution of coastal waters, damage of sensitive marine life that will ultimately threaten the food chain. In order to minimise the impact on the environment, more complex infrastructure is required, leading to an increase in the final costs of the project. For instance, in Australia, SWRO plants located in environmentally sensitive areas required the implementation of suitable outfall structures that

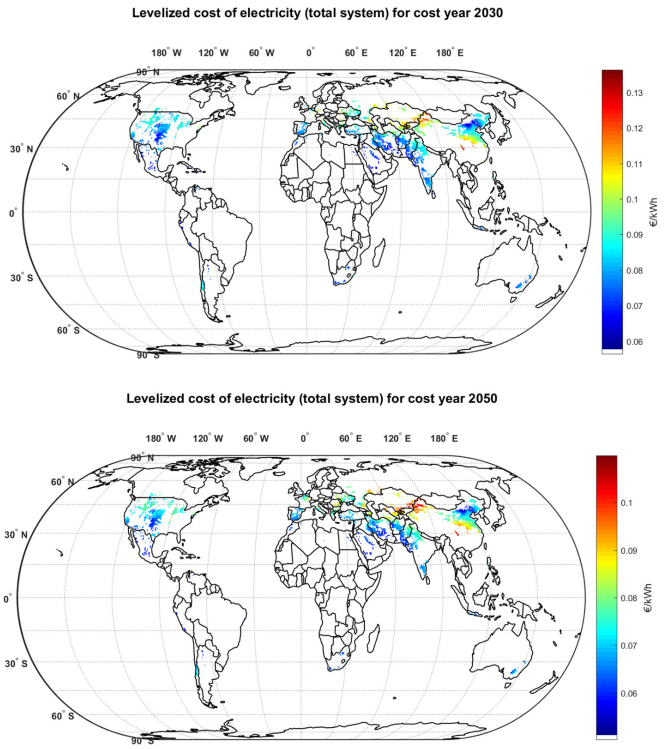

Fig. 7. LCOE in the HPIE scenario for the year 2030 (top) and 2050 (bottom).

led to a 30% increase in the final cost (Water Reuse Association Desalination Committee, 2012). Jones et al. (2019) acknowledge the increasing importance of desalinated water in the future global water supply and suggest using the brine discharge for economic gains. This maybe for new opportunities such as commercial salt production and recovery of precious metals.

Various literature and reports discuss viable ways to secure water supply for irrigation and to ensure global food security. Some of the discussed approaches include investments in improved technologies, removal of subsidies, the use climate resilient crops, off-grid greenhouses watered by desalination systems, uptake of plant-based diets, reductions in losses in the global food systems and efficient usage of nutrients and fertilizers (Steduto et al., 2018; Kahiluoto, 2019; Kahiluoto et al., 2019; Shekarchi and Shahnia, 2018). Other approaches proposed maybe more radical and redefine the conventional concept of food production. Solar Foods (Solarfoods, 2019) is a Finnish enterprise, established in 2017, and provides the means to produce single-cell protein using CO_2, renewable electricity and water as raw materials. The protein, Solein, with a texture similar to that of wheat flour, is reported to consume as little as 10 l of water per kg. According to Solar Foods, the technique can be used to produce food independent of climate, irrigation or soil. These projects highlight the variety of work being done on the topic of achieving global food security in the decades to come.

The purpose of this research is to shed light on how improved irrigation efficiency and RE-based SWRO desalination can help the agricultural sector deal with the yawning gap between water supply and demand. RE-based SWRO can provide water at costs suitable for farmers in various irrigation sites, particularly closer to the coastline. Improved irrigation efficiency is crucial to ensure the sustainability of the water supply. Furthermore, as costs of obtaining ground and surface water increase due to scarcity, fossil fuel-based electricity costs and removal of government subsidies, RE-based SWRO desalination offers a steady and cost-effective water supply.

5. Conclusion

By 2050, it is estimated that the annual cereal production would need to increase by about 140% and total global food production increase by 70%. Total water withdrawals for irrigation are projected to increase by 11%. In contrast, poor management of existing water resources, pollution and climate change has resulted in limited freshwater resources for irrigation.

The aim of this paper is to gauge how improved irrigation efficiency and RE-based SWRO desalination maybe used to secure water supplies for the agricultural sector. Desalination is currently being used in countries like Israel and Spain for cash crops. In this research, the focus was on the use of SWRO desalination for growth of the main cereals: rice, wheat and corn.

Estimates of the beneficial irrigation efficiencies of the current locations were obtained. The irrigation efficiency growth was projected

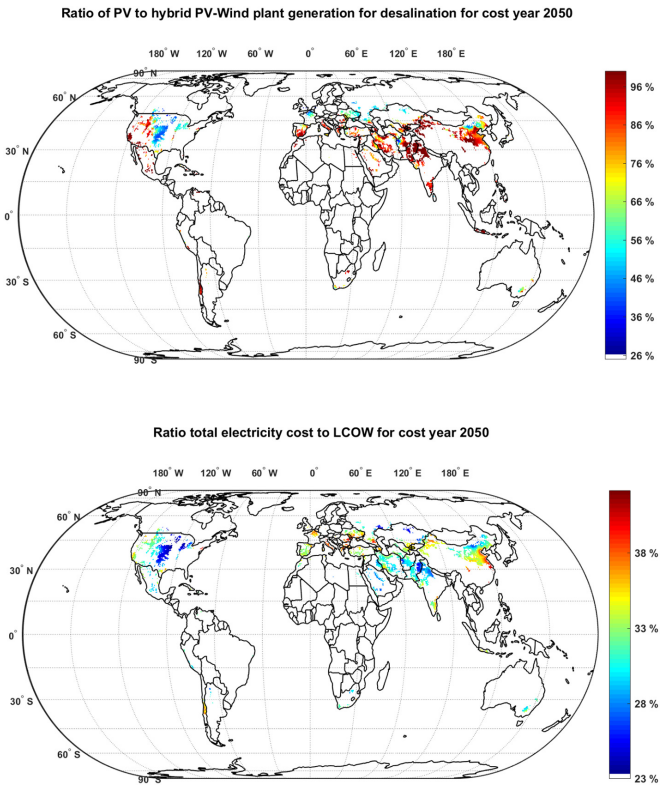

Fig. 8. Ratio of PV to PV-Wind plant generation (top) and ratio of total electricity cost to the LCOW (bottom) both for the year 2050 and the HPIE scenario.

such that by 2050, all existing irrigation sites would have an efficiency of 90%. This was labelled an HPIE scenario. The new irrigation efficiencies were used to obtain the reduced irrigation demand for the years 2030 and 2050.

Based on previous research, the desalination demand for the HPIE scenario was estimated. The LUT Energy System model was used to define a least cost RE power system based on solar PV and Wind resources, to power the estimated desalination demand.

Table 5
Overview of the RE-based SWRO desalination system required for countries with the largest desalination demand in 2030 and 2050.

	2030					
Country	Demand	LCOE	LCOW	Total PV capacity	Total wind capacity	Total investment cost
	m^3/day	€/kWh	€/m^3	GW	GW	b€
China	2.25E+08	0.09	2.23	650	68	1570
India	5.53E+07	0.08	1.53	93	2	249
Iran	1.26E+08	0.07	2.16	349	47	852
Pakistan	1.11E+08	0.07	1.42	185	5	477
United States	4.91E+07	0.07	2.01	82	31	297
	2050					
Country	Demand	LCOE	LCOW	Total PV capacity	Total wind capacity	Total investment cost
	m^3/day	€/kWh	€/m^3	GW	GW	b€
China	1.23E+08	0.08	2.66	391	29	812
India	2.79E+07	0.07	1.51	45	0.20	102
Iran	8.98E+07	0.06	2.65	257	29	566
Pakistan	9.41E+07	0.06	1.36	146	3	317
United States	4.06E+07	0.06	2.14	71	22	215

Table 6
Key parameters of the RE-based power system required to meet the global desalination demand in 2030 and 2050.

		2030 global system	2050 global system
Installed PV capacity	GW	2107	1650
Fixed-tilted PV	GW	1171	801
Single-axis tracking PV	GW	938	848
Installed wind capacity	GW	264	164
Installed battery capacity	GWh_{cap}	4212	2772
Installed PtG capacity	GW_{el}	213	200
Total Capex	b€	5380	3620
Total OPEX	b€	201	249
Annualised costs	b€	644	543

It was found that improving the average irrigation efficiency to 60% by 2030, led to a 64% reduction in total desalination demand. Similarly, an improvement towards 90% irrigation efficiency, by 2050, translates to an 80% reduction in global desalination demand. There was a marked decrease in water stress across many countries, resulting in the lower desalination demand. However, regions in China and USA, where there is increasing demand for the industrial and municipal sectors, still experienced high water stress levels.

In 2030, the global LCOW range is mostly within 0.7 €/m^3–2 €/m^3 including transportation costs. Literature reports that farmers may be willing to pay up to 0.63 €/m^3 for their irrigation water. The global range in 2050 is estimated to be 0.45 €/m^3–1.7 €/m^3 reflecting the lower costs of the SWRO and renewable energy power plants in 2050. Countries in Central Asia have a higher LCOW range of 3 €/m^3–5.8 €/m^3 due to the absence of a coast and long transportation distances.

The above results indicate that as conventional water prices increase, due to scarcity, fossil fuel-based electricity costs and removal of government subsidies, RE-based SWRO desalination offers a steady and cost effective water supply. In addition, a fast transition towards higher irrigation efficiencies will help control the increasing future water demand.

Declaration of Competing Interest

The authors declare no conflict of interest.

Acknowledgements

The first author gratefully acknowledges the scholarship offered by the Reiner Lemoine-Foundation.

References

Amante, C., Eakins, B.W., 2009. ETOPO1 1 Arc-Minute Global Relief Model: Procedures, Data Sources and Analysis. NOAA Technical Memorandum NESDIS NGDC-24. National Geophysical Data Center, NOAA, Colorado, USA.

Assouline, S., Russo, D., Silber, A., Or, D., 2015. Balancing water scarcity and quality for sustainable irrigated agriculture. Water Resour. Res. 51, 3419–3436. https://doi.org/10.1002/2015WR017071.

Awika, J.M., 2011. Advances in Cereal Science: Implications to Food Processing and Health Promotion. ACS Symposium SeriesAmerican Chemical Society, Washington, DC.

Breyer, C., Heinonen, S., Ruotsalainen, J., 2017a. New consciousness: a societal and energetic vision for rebalancing humankind within the limits of planet earth. Technol. Forecast. Societal Change 114, 7–15.

Breyer, Ch., Bogdanov, D., Gulagi, A., Aghahosseini, A., Barbosa, L.S.N.S., Koskinen, O., Barasa, M., Caldera, U., Afanasyeva, S., Child, M., Farfan, J., Vainikka, P., 2017b. On the role of solar photovoltaics in global energy transition scenarios. Prog. Photovolt. Res. Appl. 25, 727–745.

Burn, S., Hoang, M., Zarzo, D., Olewniak, F., Campos, E., Bolto, B., Barron, O., 2015. Desalination techniques – a review of the opportunities for desalination in agriculture. Desalination 364, 2–16.

Caldera, U., Breyer, Ch., 2017. Learning curve for seawater reverse osmosis desalination plants: capital cost trend of the past, present, and future. Water Resour. Res. 53, 10523–10538.

Caldera, U., Breyer, C., 2018. The role that battery and water storage play in Saudi Arabia's transition to an integrated 100% renewable energy power system. J. Energy Storage 17, 299–310.

Caldera, U., Bogdanov, D., Breyer, Ch., 2016. Local cost of seawater RO desalination based on solar PV and wind energy: a global estimate. Desalination 385, 207–216.

Caldera, U., Bogdanov, D., Breyer, C., 2018a. Desalination costs using renewable energy technologies. Renewable Energy Powered Desalination Handbook: Application and Thermodynamics. Butterworth-Heinemann (Elsevier), Oxford, Great Britain.

Caldera, U., Bogdanov, D., Afanasyeva, S., Breyer, C., 2018b. Role of seawater desalination in the management of an integrated water and 100% renewable energy based power sector in Saudi Arabia. Water. vol. 10, p. 3.

Cision PR Newswire, 2018. Global Drip Irrigation Systems Market to 2026 - Increasing Benefits of Drip Irrigation Systems and Rising Agricultural Activities in Emerging Economies. Chicago, United States. https://www.prnewswire.com/news-releases/global-drip-irrigation-systems-market-to-2026--increasing-benefits-of-drip-irrigation-systems-and-rising-agricultural-activities-in-emerging-economies-300763526.html.

Dolan, F.C., Cath, T.Z., Hogue, T.S., 2018. Assessing the feasibility of using produced water for irrigation in Colorado. Sci. Total Environ. 640 – 641, 619–628.

Fischer, G., Tubiello, F.N., Velthuizen, H.V., Wiberg, D.A., 2007. Climate change impacts on irrigation water requirements: effect of mitigation, 1990–2080. Technol. Forecast. Soc. Chang. 74, 1083–1107.

Food and Agricultural Organisation of the United Nations, 2009. Issue Brief: How to Feed the World in 2050. Rome, Italy. http://www.fao.org/wsfs/forum2050/wsfs-background-documents/hlef-issues-briefs/en/.

Food and Agricultural Organisation of the United Nations, 2015. AQUASTAT Database, Rome, Italy. http://www.fao.org/nr/water/aquastat/data/query/index.html?lang=en.

Food and Agricultural Organisation of the United Nations, 2019. Annex 1 Water Charging for Irrigation – Data from Literature, Rome, Italy. http://www.fao.org/docrep/008/y5690e/y5690e0b.htm.

Fornarelli R, Shahnia F, Anda M, Bahri A P, Ho G, Selecting an economically suitable and sustainable solution for a renewable energy-powered water desalination system: a rural Australian case study. In: Desalination, 435, 128 - 139.

Fyles, H., Madramootoo, C., 2016. Water management. Emerging Technologies for Promoting Food Security. Woodhead Publishing (Elsevier), Sawston, United Kingdom.

Ghaffour, N., Missimer, M.T., Amy, L.G., 2013. Technical review and evaluation of the economics of water desalination: current and future challenges for better water supply sustainability. Desalination 309, 197–207.

Hanasaki, N., Fujimori, S., Yamamoto, T., Yoshikawa, S., Masaki, Y., Hijioka, Y., Kainuma, M., Kanamori, Y., Masui, T., Takahashi, K., Kanae, S., 2013. A global water security assessment under shared socio-economic pathways – part 1: water use. Hydrology and Earth System Sciences. vol. 17, pp. 2375–2391.

Intergovernmental Panel on Climate Change, 2018. Global Warming of 1.5°C. An IPCC Special Report on the Impacts of Global Warming of 1.5°C above Pre-industrial Levels and Related Global Greenhouse Gas Emission Pathways, in the Context of Strengthening the Global Response to the Threat of Climate Change, Sustainable Development, and Efforts to Eradicate Poverty. World Meteorological Organization, Geneva, Switzerland.

Jägermeyr, J., Gerten, D., Heinke, J., Schaphoff, S., Kummu, M., Lucht, W., 2015. Water savings potentials of irrigation systems: global simulation of processes and linkages. Hydrol. Earth Syst. Sci. 19, 3073–3091.

Jones, E., Qadir, M., Vliet, M.T.H.V., Smakhtin, V., Kang, S., 2019. The state of desalination and brine production: a global outlook. Sci. Total Environ. 657, 1343–1356.

Kahiluoto, H., 2019. The concept of planetary boundaries. Encyclopedia of Food Security and Sustainability, General and Global Situation. Elsevier, Amsterdam, Netherlands.

Kahiluoto, H., Kaseva, J., Balek, J., Olesen, J.E., Ruiz-Ramos, M., Gobin, A., Kersebaum, K.C., Takáč, J., Ruget, F., Ferrise, R., Bezak, P., Capellades, G., Dibari, C., Mäkinen, H., Nendel, C., Ventrella, D., Rodríguez, A., Bindi, M., Trnka, M., 2019. Decline in climate resilience of European wheat. Proc. Natl. Acad. Sci. 116, 123–128.

Karimov, K.S., Akhmedov, K.M., Abid, M., Petrov, G.N., 2013. Effective management of combined renewable energy resources in Tajikistan. Sci. Total Environ. 461 – 462, 835–838.

Luck, M., Landis, M., Gassert, F., 2015. Aqueduct Water Stress Projections: Decadal Projections of Water Supply and Demand Using CMIP5 GCMs. Technical Note. World Resources Institute, Washington, D.C https://www.wri.org/sites/default/files/aqueduct-water-stress-projections-technical-note.pdf.

Martinez-Alvarez, V., Gonzalez-Ortega, M.J., Soto-Garcia, M., Maestre-Valero, J.F., 2018. Seawater desalination for crop irrigation – current status and perspectives. Emerging Technologies for Sustainable Desalination Handbook. Butterworth - Heinemann.

Multsch, S., Elshamy, M.E., Batarseh, S., Seid, A.H., Fred, H.G., Breuer, L., 2017. Improving irrigation efficiency will be insufficient to meet future water demand in the Nile Basin. J. Hydrol. Reg. Stud. 12, 315–330.

Netafim, 2018. Drip Irrigation for Rice Is Changing the Rules of the Game. Hatzerim, Israel. https://www.netafim.com/en/crop-knowledge/rice/.

Palazzo, A., Valin, H., Batka, M., Havlík, P., 2019. Investment Needs for Irrigation Infrastructure Along Different Socioeconomic Pathways. Policy Research Working Paper. World Bank Group, Washington DC.

Qiu, G.Y., Zhang, X., Yu, X., Zou, Z., 2018. The increasing effects in energy and GHG emission caused by groundwater level declines in North China's main food production plain. Agric. Water Manag. 203, 138–150.

Rosegrant Mark, W., Sulser Timothy, B., Mason-D'Croz, D., Cenacchi, N., Nin-Pratt, A., Dunston, S., Zhu, T., Ringler, C., Wiebe, K.D., Robinson, S., Willenbockel, D., Xie, H., Kwon, H.Y., Johnson, T., Thomas, T.S., Wimmer, F., Schaldach, R., Nelson, G.C., Willaarts, B., 2017. Quantitative Foresight Modeling to Inform the CGIAR Research Portfolio. Project Report for USAID. International Food Policy Research Institute, Washington DC.

Rosegrant, M.W., Cai, X., Cline, S.A., 2003. World water and food to 2025: dealing with scarcity. International Food Policy Research Institute, Washington D.Chttps://reliefweb.int/sites/reliefweb.int/files/resources/1B0BBA6D1080C010C1256C6E002E1D17-ifpri-water2025-16oct.pdf.

Serrano-Tovar, T., Suarez, P.B., Musicki, A., Bencombo, F.A.J., Cabello, V., Giampietro, M., 2019. Structuring an integrated water-energy-food nexus assessment of a local wind energy desalination system for irrigation. Sci. Total Environ. 689, 945–957.

Shekarchi, N., Shahnia, F., 2018. A comprehensive review of solar-driven desalination technologies for off-grid greenhouses. Int. J. Energy Res. 43 (4), 1357–1386.

Solarfoods, 2019. The Revolutionary Protein by Solar Foods. Lappeenranta, Finland. https://solarfoods.fi/.

Soman, P., 2012. Drip Fertigation for Rice Cultivation. Presentation at the Asia Irrigation Forum. Manila, Philippines. https://k-learn.adb.org/system/files/materials/2012/04/201204-drip-fertigation-rice-cultivation.pdf.

Steduto, P., Schultz, B., Unver, O., Ota, S., Vallee, D., Kulkarni, S., Garcia, M.D.-J., 2018. Food security by optimal use of water: synthesis of the 6th and 7th world water forums and developments since then. Irrig. Drain. 67, 327–344.

Takatsuka, Y., Niekus, M.R., Harrington, J., Feng, S., Watkins, D., Mirchi, A., Nguyen, H., Suokp, M.C., 2018. Value of irrigation water usage in South Florida agriculture. Sci. Total Environ. 626, 486–496.

Vanham, D., Hoekstra, A.Y., Wada, Y., Bouraoui, F., Rooa, A., Mekonnen, M.M., Bund, W.J., Batelaan, O., Pavelic, P., Bastiaanssen, W.G.M., Kummu, M., Rockström, J., Liu, J., Bisselink, B., Ronco, P., Pistocchi, A., Bidoglio, G., 2018. Physical water scarcity metrics for monitoring progress towards SDG target 6.4: an evaluation of indicator 6.4.2 "level of water stress". Sci. Total Environ. 613-614, 218–232.

Wada, Y., Gleeson, T., Esnault, G., 2014. Wedge approach to water stress. Nat. Geosci. 7, 615–617.

Water Desalination + Reuse, 2018. Australia's Demand for Desalination Jumps Amidst Drought. West Sussex, UK. https://www.desalination.biz/news/0/Australias-demand-for-desalination-jumps-amid-drought/9090/.

Water Reuse Association Desalination Committee, 2012. Seawater desalination costs. White paper. Water Reuse Association, Virginia, United States of Americahttps://watereuse.org/wp-content/uploads/2015/10/WateReuse_Desal_Cost_White_Paper.pdf.

Yermiyahu, U., Tal, A., Ben-Gal, A., Bar-Tal, A., Tarchitzky, J., Lahav, O., 2007. Rethinking desalinated water quality and agriculture. Science 318, 920–921.

Publication VII

Caldera, U., and Breyer, C.
Strengthening the global water supply through a decarbonised global desalination sector and improved irrigation systems
Reprinted with permission from
Energy
Vol. 200, pp 1-17, 117507, 2020

Energy 200 (2020) 117507

Contents lists available at ScienceDirect

Energy

journal homepage: www.elsevier.com/locate/energy

Strengthening the global water supply through a decarbonised global desalination sector and improved irrigation systems

Upeksha Caldera *, Christian Breyer

LUT University, Yliopistonkatu 34, 53850 Lappeenranta, Finland

ARTICLE INFO

Article history:
Received 4 September 2019
Received in revised form
3 March 2020
Accepted 28 March 2020
Available online 3 April 2020

Keywords:
Irrigation efficiency
Seawater desalination
Solar photovoltaics
Battery storage

ABSTRACT

This study analyses the role that renewable energy based desalination, in conjunction with improvements in water use efficiency in the irrigation sector, can play towards securing future global water supplies. It is found that the global desalination demand by 2050 can be reduced as much as 30% and 60%, depending on the irrigation efficiency growth rate. India, China, USA, Pakistan and Iran account for between 56% and 62% of the global desalination demand. Decarbonising the desalination sector by 2050, will result in global average levelised cost of water decreasing from about 2.4 €/m^3 in 2015, considering unsubsidised fossil fuel costs, to approximately 1.05 €/m^3 by 2050, with most regions in the cost range of 0.32 €/m^3 – 1.66 €/m^3. Low-cost renewable electricity, in particular solar photovoltaics and battery storage, is found to form the backbone of a sustainable and clean global water supply, supported by measures to increase irrigation efficiency. The results show the untapped relationships between the irrigation and decarbonised desalination sector that can be utilised to strengthen the global water supply for the decades to come and meet United Nations Sustainable Development Goals.

1. Introduction

Seawater desalination is increasingly seen as an important element of the global water supply [1,2]. From 2010 to 2016, desalination installations have increased annually by 9%, spreading to regions where desalination was once not necessary or considered too expensive [3]. Market projections up to 2025 expect the upward trend to continue at a cumulative annual growth rate (CAGR) of 7% [4]. This growth has been backed by an exponential increase in research on desalination, with a greater focus on technological improvements [5].

According to the Global Water Intelligence (GWI) [6], 1,522,504 m^3/day of seawater desalination capacity were contracted in 2015, out of which 77% were awarded to seawater reverse osmosis (SWRO) desalination plants. Due to the technological improvements and declining costs, SWRO has dominated the desalination market over the last decade and will continue to do so in the future. This perspective is supported by both academics and industrial analysts [1,2,5].

Whilst there is a clear consensus on the dominance of SWRO in the future desalination market, there is less clarity on what the future demand for desalination may be. Mayor [7] projects the desalination demand up to 2050 based on logistic curves using historical data. The global cumulative capacity projected for 2050 is $1.7 \cdot 10^8$ m^3/day, with RO accounting for about 80% of the total capacity. Meanwhile, total global installed desalination capacity in 2018 is estimated to be $95.37 \cdot 10^6$ m^3/day [6]. Thus, according to Mayor the desalination capacity would increase almost two-fold by 2050, based on past growth trends. Gao et al. [8] estimated the economic feasibility of desalination based on the decreasing SWRO costs and increasing water price in different countries. The authors established that by 2050, the global population dependent on desalination will increase by 3.2 times, compared to the present. Hanasaki et al. [9] link gross domestic product (GDP), aridity and proximity to the shore with demand for seawater desalination. Based on these observed relationships, the production of desalinated water is projected to increase by up to 2.1 times before 2040. The demand is estimated to increase further by 6.7–17.3 times during the years 2041–2070.

Wada et al. [10] applied the concept of stabilization wedges, used in climate change mitigation discourse, to assess the potential for different strategies to mitigate global water stress. It was found that to reduce the global population living in water stressed regions by 2% in 2050, the desalination capacity has to increase by a factor

* Corresponding author.
E-mail addresses: upeksha.caldera@lut.fi (U. Caldera), christian.breyer@lut.fi (C. Breyer).

https://doi.org/10.1016/j.energy.2020.117507

Nomenclature

a	annum
Capex	capital expenditures
CAGR	cumulative annual growth rate
GWI	global water intelligence
HPIE	Highest Possible Irrigation Efficiency
HRSG	heat recovery steam generator
IEP	Irrigation Efficiency Push
IWMI	International Water Management Institute
LCOE	levelised cost of electricity
LCOW	levelised cost of water
MSF	multi stage flash
MED	multi effect distillation
Opex	operational expenditures
PtG	power-to-gas
PV	photovoltaic
RE	renewable energy
SNG	synthetic natural gas
SWRO	seawater reverse osmosis

of 50. Caldera et al. [11] determined the desalination demand for regions based on the projected water stress and water demand for different hydrological basins. A logistic relationship was established to illustrate how the water stress increased, the dependency on desalinated water increased for the municipal, industrial and irrigation sectors. The total desalination demand in 2030 was projected to be $2.6 \cdot 10^9$ m^3/day – a factor of 10 times more than the current installed capacity. The higher desalination demand estimate is due to the consideration of water demand for the global irrigation sector.

The irrigation sector accounts for 70% of the global water withdrawals and the large share may be partly explained through the use of inefficient irrigation systems [12]. Jägermeyr et al. [12] introduced the concept of beneficial irrigation efficiency to be the ratio of the water transpired by the plants to the water withdrawn. The authors estimate the global average to be as little as 33%. Fig. 1 illustrates the derived beneficial irrigation efficiencies for the three major crops rice, wheat and maize [12,13]. The very low efficiency is attributed to the wide-spread use of surface irrigation systems where a large share of the water is lost via conveyance losses, soil evaporation and runoff. It is suggested that changing from the extensive surface irrigation systems to pressurized irrigation systems, namely sprinkler and drip technology, will result in higher irrigation efficiency and increased water savings. The efficiency of surface irrigation systems can lie between 30 and 60%, while that of sprinkler and drip is between 50%–70% and 70%–90% respectively. However, only 11% of the world's irrigated area is equipped with sprinkler technology and an even smaller 3% with drip irrigation systems [14].

At present only 1.8% of the global desalination capacity is used for the irrigation sector and this is attributed to the higher cost of desalinated water [5]. Medeazza et al. [15] highlight the current use of desalination plants for irrigation in Spain and the policies in place to promote crops that are more resistant to saline water. As the cost of water from conventional sources increase over time, as explained by Gao et al. [8], desalinated water becomes a more attractive option for irrigation.

Despite the decreasing costs, desalination is an energy intensive process, in contrast to traditional water treatment methods. The average specific energy consumption (SEC) of the more energy efficient SWRO plants in operation is said to be 3–4 kWh_{el}/m^3 [16]. The low-efficient MSF and MED options typically require thermal energy between 40 and 80 kWh_{th}/m^3 plus electrical energy within the range 2.5–5 kWh_{el}/m^3 [7]. In contrast, water treatment plants for freshwater resources consumes 0.06 kWh/m^3 [11]. As of 2015, all but 1% of the installed desalination capacity was powered by fossil fuels [17]. Martin-Gorriz et al. [18] flag the concerns of the increasing greenhouse gas (GHG) emissions from the growing desalination sector in South-Eastern Spain. Despite the increased reliability provided by seawater desalination, the sector contributes negatively towards water scarcity in the region. In a business as usual scenario GHG emissions are projected to increase by 140% by 2040 [19]. As the global community strives to limit greenhouse gas emissions and avoid runaway climate change [20], it is crucial that the growing desalination sector overcomes its dependency on expensive fossil fuels.

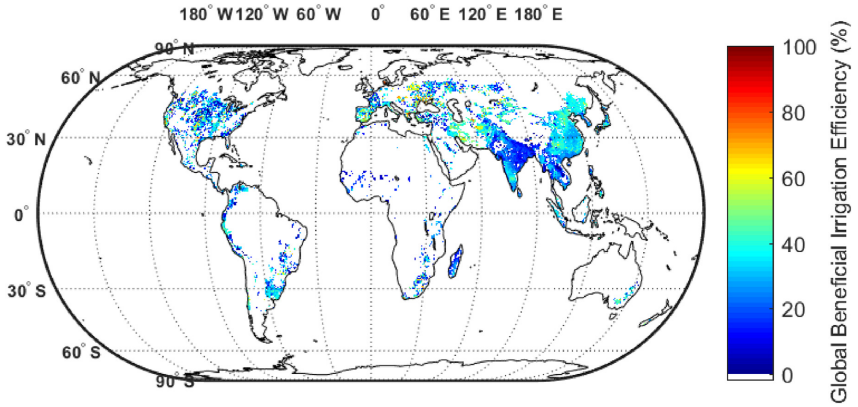

Fig. 1. Global beneficial irrigation efficiency for irrigation sites growing rice, wheat and maize [12,13].

Table 1
Initial and modified desalination demand projections from 2015 to 2050 for the Base scenario.

Desalination capacity		2015	2020	2025	2030	2035	2040	2045	2050
Initial	10^6 m^3/day	40	2790	3060	3340	3590	3850	4120	4400
Modified			89	224	608	1590	3110	4120	4400

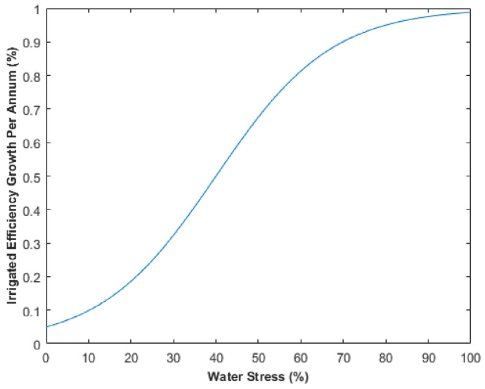

Fig. 2. Irrigation efficiency growth rate per annum for a specific water stress value in the IEP scenario.

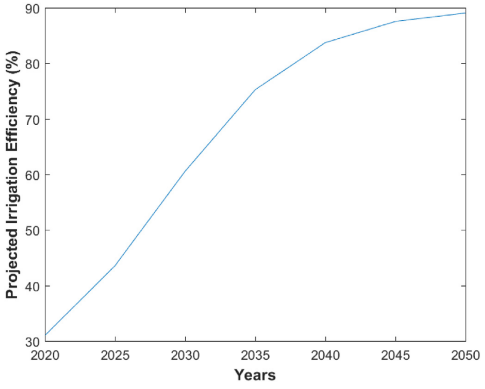

Fig. 3. Projected irrigation efficiency up to 2050 in the HPIE scenario [13].

The large-scale implementation of RE based desalination has been held back by concerns over the need to run desalination plants on high full load hours and the cost of doing so with RE [21]. According to Freyberg [21], the variability of RE, mainly solar photovoltaics (PV) and wind, can be overcome with the use of battery storage, but current costs are not considered to be conducive. However, these concerns do not reflect the present day reality. The costs of solar PV, wind power plants and battery storage have reduced drastically over the last decade and is reflected in recent plans to implement RE-based desalination plants in Dubai [22–26]. A study by Sadiqa et al. [27] further demonstrates how, for the case of Pakistan, future water demand can be supplied through desalination plants powered entirely by low cost renewable energy systems. In addition, cooling water for thermal power plants is reported to account for 15% of the global water withdrawals, with USA and China accounting for the largest shares of 36% and 15% respectively [28,29]. Lohrmann et al. [29] have shown that by transitioning to a RE system, global water withdrawals for cooling can be reduced by as much as 95% by 2050. Thus, from a water-energy nexus perspective, it is critical that the desalination sector built to provide water are run on RE plants rather than thirsty thermal power plants.

In Caldera and Breyer [13], we posed the following question: Can 100% RE-based SWRO desalination, coupled with the use of highly efficient irrigation systems worldwide, be used to provide water for irrigation sites at acceptable costs? An optimistic scenario labelled 'Highest Possible Irrigation Efficiency (HPIE)' was modelled. The results were contrasted with a business as usual scenario (Base). In the HPIE scenario, it was assumed that by 2050 all irrigation sites were at a 90% efficiency level, suggesting the widespread adoption of drip irrigation systems. Using an overnight energy systems study, we determined the cost of desalinated water supply just for irrigation sites in the decades 2030 and 2050. The results showed that RE-based SWRO systems could provide water at a suitable cost range of 0.7 €/m^3 − 2 €/m^3 for particular sites, by as early as 2030. The described system becomes more attractive as the cost of conventional water resources increase.

As the desalination market grows and the world grapples with climate change, we build on the results of Caldera and Breyer [13] to comprehensively analyse the role for RE-based desalination in the global water supply. The objectives of this study are two-fold: First objective is to assess the total desalination demand up to 2050 considering different water use efficiency improvement scenarios in the irrigation sector. This includes a detailed look into the HPIE scenario introduced in Ref. [13]. Furthermore, the desalination demand for the municipal, industrial and irrigation sectors will be considered. Next the research analyses energy system transition pathways in full hourly resolution to determine how the current desalination sector can evolve such that by 2050 all desalination plants are run by RE systems. This builds on the initial overnight study for the years 2030 and 2050 presented in Ref. [13]. By addressing the issues of irrigation efficiency improvement through different scenarios, global water demand management, seawater

Table 2
Initial and modified desalination demand projections from 2015 to 2050 for the IEP scenario.

Desalination capacity		2015	2020	2025	2030	2035	2040	2045	2050
Initial	10^6 m^3/day	40	2630	2730	2850	2880	2940	3000	3040
Modified			84	193	485	1190	2210	2860	3040

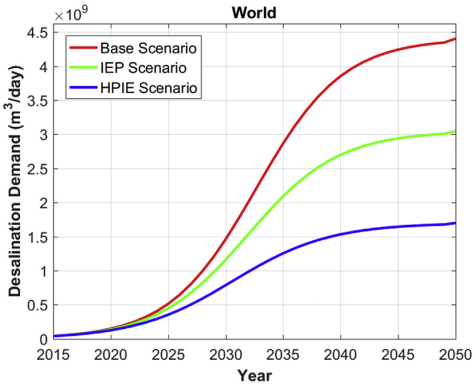

Fig. 4. Desalination demand projection from 2015 to 2050 for the Base, IEP and HPIE scenarios.

desalination powered by RE, the research establishes pathways that can help achieve the United Nations (UN) sustainable development goals (SDGs) 2, 6 and 7 [30].

2. Methods and data

2.1. Overview of methods

The global desalination demand from 2015 to 2050 is projected using the approach presented in Caldera et al. [11]. The desalination demand is estimated in 5-year time steps, taking into account the water demand and stress factors for 15,006 hydrological basins from the Aqueduct Water Risk Atlas [31]. The demand for desalination is a logistic function of the regional water stress and demand [11].

For this study, three scenarios are investigated where the irrigation efficiency, which affects the water demand at the respective basin, is varied over time. This in turn affects the water stress, water demand and ultimately the desalination demand for nodes with irrigation sites. Thus, across the three scenarios, the desalination demand for countries will vary. It has to be noted that the basis of two of the presented scenarios, the Base and HPIE, have been introduced in Caldera and Breyer [13]. Next, the widely used LUT Energy Systems Transition model [32,33] is used to set up the energy transition pathway options for the global desalination sector in the different scenarios. The aim is to present a broadly defined road map for countries to transition away from the fossil fuel dominated desalination sector currently in operation, and achieve a zero-emissions and sustainable desalination sector by 2050.

The three scenarios presented and the energy transition modelling are described in further detail in the following subsections.

2.2. Scenario description

2.2.1. Base scenario

The desalination demand is calculated as defined in Caldera et al. [11], on a 0.45° × 0.45° spatial resolution, for the time period from 2020 to 2050, in 5-year time steps. The initial 2015 desalination demand is set to be the online installed capacity of the three main technologies SWRO, MED and MSF, obtained from the GWI Desal database [6].

Table 1 presents the initial desalination demand projection from 2015 to 2050 in the first row. The demand is estimated for the irrigation, municipal and industrial sectors [11]. The growth required from 2015 to 2050 is unrealistically large, particularly in the first few decades due to the lower installed capacity in 2015. To project a smooth increase from the capacity in 2015 to the required value in 2050, a logistic function is used as presented in Equation (1). The modified demand values are presented in the second row of Table 1 and captures a smoother increase in desalination capacities globally. Fig. 4 illustrates the resulting s-curve for the global desalination demand in the base scenario.

$$Desal_{Demand(year)} = \frac{Peak}{\left(1 + e^{(-1 \cdot \alpha \cdot (year - T_0))}\right)} \quad (1)$$

where *Peak* is the maximum desalination demand ($4400 \cdot 10^6$ m^3/day), *year* is the time period under consideration, α is the steepness of the curve (0.26) and T_0 (2032) is the x co-ordinate of the midpoint of the curve.

2.2.2. Irrigation efficiency push (IEP) scenario

Hanasaki et al. [9] collected literature on irrigation efficiency development and explain that the highest historical growth rate has been about 0.3% per year, relative to the respective basis. This helps to explain the currently low irrigation efficiencies found in many regions as illustrated in Fig. 1. In order for countries to achieve food security, it is crucial that the efficiency of irrigation systems are improved. Wada et al. [10] estimate that a linear 1% increase in irrigation efficiency per annum will reduce the water stressed global population by 2% in 2050, compared to a business as usual scenario. The growth rates of 0.3% and 1% reported by Hanasaki et al. [9] and Wada et al. [10] respectively, were used to stipulate the conditions for the IEP scenario.

The IEP scenario is defined on the premise that irrigation sites with higher water stress require a steeper increase in irrigation efficiency as opposed to sites with lower water stress. Fig. 2 illustrates the relationship envisaged. Regions with water stress greater than 100% have the highest irrigation efficiency growth rate of 1% per annum indicated by Wada et al. [10]. Regions with no indication of water stress endure the minimum irrigation efficiency growth of 0.3% per annum referenced by Hanasaki et al. [9]. Equation (1) is adapted to formulate the irrigation efficiency growth rate, presented in Equation (2).

$$GR_{(water\ \ stress)} = \frac{1\%}{\left(1 + e^{(-\alpha \cdot (year - T_0))}\right)} \quad (2)$$

where *GR* is the growth rate, *Peak* is the maximum irrigation

Table 3
Initial and modified desalination demand projections from 2015 to 2050 for the HPIE scenario.

Desalination capacity		2015	2020	2025	2030	2035	2040	2045	2050
Initial	10^6 m^3/day	40	2280	2070	1730	1570	1550	1610	1700
Modified			74	150	338	758	1290	1610	1700

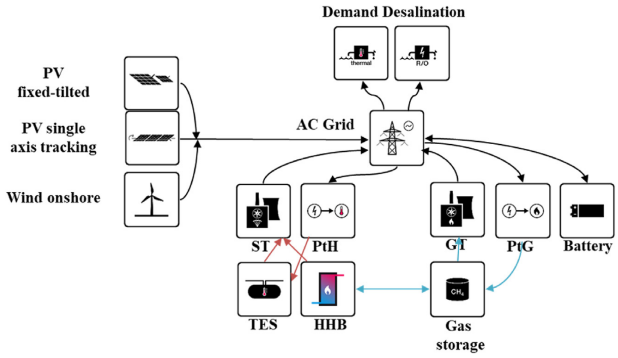

Fig. 5. LUT Energy System Transition Model Adapted to the Desalination Sector. Abbreviation: alternating current, AC, steam turbine, ST, thermal energy storage, TES, power-to-heat, PtH, hot heat burner, HHB, gas turbine, GT, power-to-gas, PtG [32,34].

efficiency growth of 1% per annum, α is 7.36 and T_0 is 0.40.

The reduced irrigation demand is calculated for irrigation nodes with water stress greater than 40% for every 5-year time step using Equation (3). Higher efficiency results in lower water demand, water stress and consequently desalination demand for the specific time period.

$$irrigDemandNew_{(year)} = \frac{origirrigDemand(year)}{\prod_{n=0}^{(year-5-2015)/5}\left(1+GR_{(water\ \ stres\ \ in\ \ 2015+n\cdot 5)}\right)^5} \tag{3}$$

where *irrigDemandNew* is the reduced new irrigation demand, *origirrigDemand* is the original irrigation demand for the year, $GR_{(water\ stress\ in\ 2015\ +\ n\cdot 5)}$ where n is from 0 to $(\text{year} - 5 - 2015)/5$ is the irrigation efficiency growth rate every 5 years from 2015 to the specific year.

The resulting desalination demand for the IEP scenario is the sum of the new demand for the irrigation sector and the municipal and industrial sector. It has to be noted that the demand for the last two sectors remains the same as in the Base scenario due to no relative efficiency improvements considered. The total desalination demand estimations are presented in Table 2. Similar to the Base scenario, the demand growth is steep in the first few time steps. Equation (1) was used to smoothen the data with the corresponding α and T_0 values of 0.25 and 2032 respectively. Fig. 4 illustrates the growth in global desalination demand in the IEP scenario.

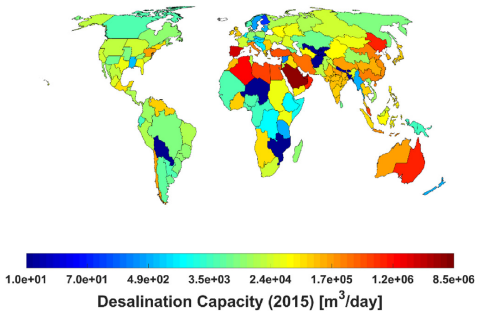

Fig. 6. Total online desalination capacities in 2015 distributed to the 145 regions of the LUT model.

2.2.3. Highest possible irrigation efficiency (HPIE) scenario

The highest possible irrigation efficiency (HPIE) scenario is the most optimistic of the three scenarios presented. The scenario reflects the increasing use of drip irrigation technology. In this scenario, it is assumed that by 2050 all existing irrigation sites will be able to achieve an irrigation efficiency of 90%. Fig. 3 illustrates the assumed behaviour of the scenario: over time, the efficiency of all irrigation sites will increase until a maximum efficiency of 90% is reached. Equation (4) is used to characterise the relationship and is based on the general logistic approach. An initial study on the use of SWRO desalination in the HPIE scenario has been done in Ref. [13].

$$irrigEffHPIE_{(year)} = A + \frac{K-A}{\left(1+Qe^{-B\cdot(year-M)}\right)^{\frac{1}{\nu}}} \tag{4}$$

where *year* is the year at which the irrigation efficiency is being estimated, A is the maximum value of efficiency (90%), K is the minimum value of efficiency (20%), B is the growth rate (20%), ν is the factor affecting near which asymptote the maximum growth occurs (14), Q is the scaling parameter depending on f(0) (75) and M is time of maximum growth (2020) [13].

The new water demand for every irrigation site for the period from 2020 to 2050 in the optimistic HPIE scenario is estimated using Equation (5).

$$irrigDemandNew(i, year) = \frac{origirrigDemand}{\left(\frac{1+(irrigEffHPIE_{(year)} - irrigEff(i))}{irrigEff(i)}\right)} \quad (5)$$

where i and $year$ are the 0.45° × 0.45° node and year under consideration respectively, *irrigDemandNew* is the water withdrawal for irrigation at the node i after improved efficiency, *origirrigDemand* is the water withdrawal for irrigation at the node i before improved efficiency, $irrigEffHPIE_{(year)}$ is the irrigation efficiency in the HPIE scenario for the *year*, *irrigEff(i)* is the initial irrigation efficiency for the node obtained from Jägermeyr et al. [12,13].

Table 3 presents the resulting total desalination demand for the HPIE scenario. The smoothed values of the desalination demand are found using Equation (1) with α and T_0 values of 0.24 and 2031 respectively.

Fig. 4 presents the global desalination demand increase for the three scenarios. By 2050, the IEP and HPIE scenarios have 30% and 60% less desalination demand relative to the Base scenario.

It must be noted that for the IEP and HPIE scenarios, only the water use efficiency of irrigation sites presented in Ref. [12] is increased. Future expansion of irrigation land area is not considered due to the unavailability of data.

2.3. Model description and data overview

The LUT Energy Systems Transition model is a MOSEK based linear optimisation model that has been used to analyse the transition of the global, regional and country wide energy systems [32,34]. The model optimises the cost of the energy system on an hourly resolution for a specific year and given set of conditions. A detailed overview of the model is provided in Bogdanov et al. [32] and Breyer et al. [34], while Hansen et al. [33] gives insights into the status and perspectives of 100% renewable energy systems and the modelling approaches used.

For this study, the LUT Energy Systems Transition model [32,34] is adapted, as per Fig. 5, to determine the energy system evolution needed to power the desalination plants. Implementing an energy transition from 2015 to 2050, in an hourly resolution and spatial resolution of 0.45° × 0.45° requires significant computational prowess. As such, the nodes were merged into 145 regions based on the corresponding latitude and longitude. The 145 regions and 9 major regions are presented in Ref. [32]. For each region the model determines the cost optimised energy transition, considering the regional desalination demand from 2015 to 2050. The desalination demand for every region is the sum of the demand for the nodes that comprise the region. The energy demand for the desalination plants is met through a combination of the solar PV and wind generation technologies, complemented with battery, gas and thermal energy storage. Other forms of renewable energy are assumed to be already fully consumed in other energy sectors and practically limited in substantial high resource potentials, unlike solar and wind resources.

The energy demand to transport the desalinated water from the coast line to the region is also accounted for in each time step. The shortest distance from the coastline to the desalination demand node is taken to be the horizontal pumping distance for every node. The highest elevation on this horizontal path is found using the ETOPO1 global relief model [35] and considered to be the vertical pumping height for the node. For each of the 145 regions, the weighted average pumping distance and height are calculated based on the distance, height and desalination demand of the nodes within the region. The LCOW which includes the cost of desalinating water and transporting the potable water to the region is determined during the transition. Equation (5) quantifies the concept of the LCOW:

$$LCOW_{desal} = \frac{\left(capex_{desal} \times crf_{desal} + capex_{water\ \ storage} \times crf_{water\ storage)} + opex_{fixed}\right.}{Total\ \ water\ \ produced\ \ in\ \ a\ \ year} + opex_{var\ desal} \times SEC \quad (6a)$$

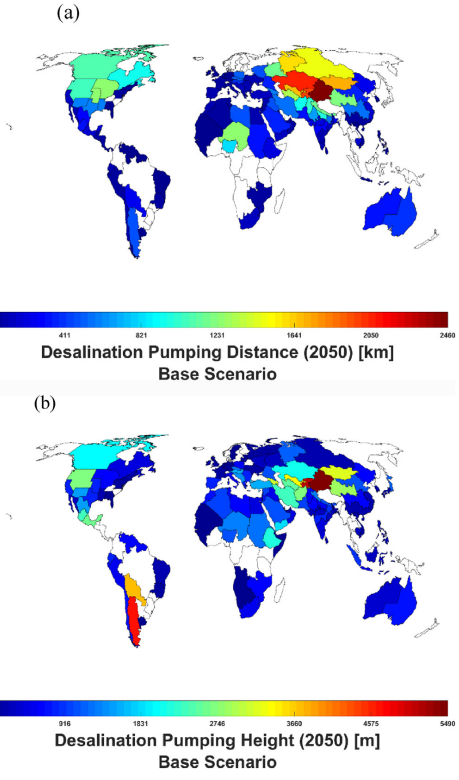

Fig. 7. Weighted average horizontal pumping distances (a) and vertical pumping distances (b) for the Base Scenario in 2050.

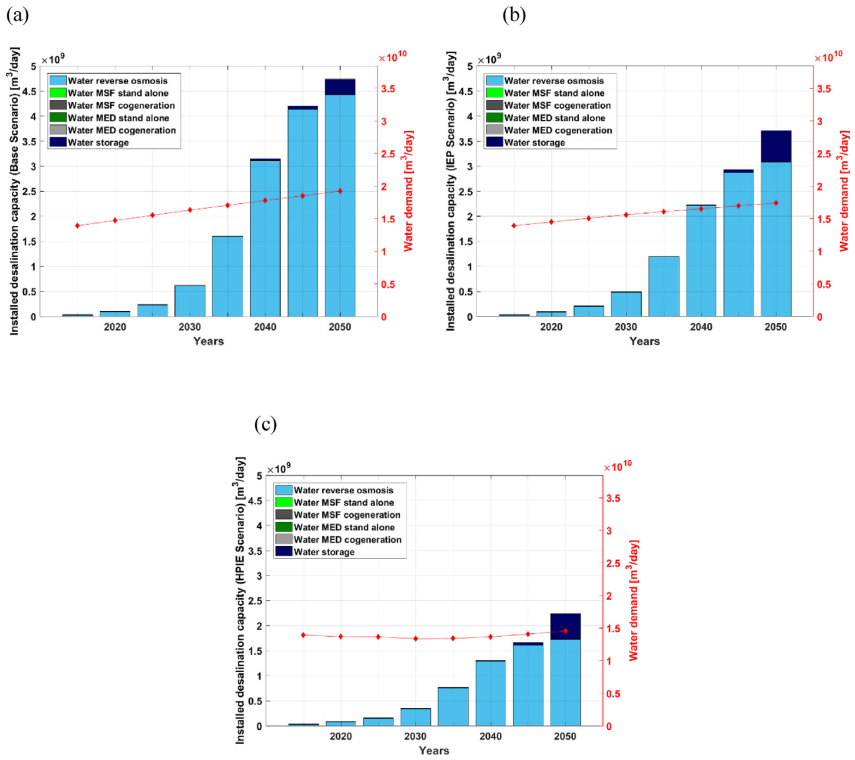

Fig. 8. Desalination capacity growth and total water demand projection from 2015 to 2050 in Base (a), IEP (b), HPIE (c) scenarios.

$$LCOW = LCOW_{desal} + LCOT_{desal} \quad (6b)$$

where $capex_{desal}$ is the capital expenditures of the SWRO desalination plant in €/m^3, $capex_{water\ storage}$ is the *capex* of the water storage tank at the desalination site in €/m^3, crf_{desal} is the annuity factor for the desalination plant, $crf_{water\ storage}$ is the annuity factor for water storage, *Total water produced in a year* is in m^3 and $opex_{fixed}$ is the total fixed annual operational expenditures of the desalination system in €/m^3. The total $opex_{fixed}$ is the sum of the $opex_{fixed}$ of the desalination plant in €/m^3 and the *opex* of the water storage tank in €/m^3. The value $opex_{var\ desal}$ is the variable opex of the desalination plant and is equal to the levelised cost of electricity (LCOE) of the plant in €/kWh. *SEC* is the specific energy consumption in kWh/m^3. $LCOT_{desal}$ is the levelised cost of water transportation from the desalination plant to the demand site in €/m^3, *LCOW* is the resulting levelised cost of water in €/m^3.

A summary of the approach adopted for modelling the energy transition is presented below:

1. The desalination plants that are online by 2015 are considered as the installed capacity for the year. For this study, only installed SWRO, MED and MSF capacities are considered. Out of the total capacity of 43 million m^3/day, 53% was SWRO, 18% was MSF stand-alone, 17% was MSF co-generation, 5% was MED stand-alone and 6% was MED co-generation [36].
2. Fig. 6 illustrates the global spread of the online desalination capacities in 2015. The countries with the largest online capacities of SWRO, MSF and MED plants were United Arab Emirates (8 501 147 m^3/day), Saudi Arabia (8 218 312 m^3/day), Spain (3 319 098 m^3/day), Kuwait (2 072 756 m^3/day) and Qatar (1 664 015 m^3/day). For countries like the United States (379 581 m^3/day), that have been sub-divided into smaller regions, the total desalination capacity has been allocated to the regions based on the respective share of the country's total water demand. Despite the high water stress in countries like India, Pakistan, Iran and China, the installed desalination capacities in 2015 are relatively lower. Regions without any installed capacities are in white.
3. Detailed operation of the desalination technologies are described in Caldera et al. [37]. For stand-alone MED and MSF plants, the thermal energy required is provided by burning gas or by using excess heat available in the energy system. Co-generation plants are assumed to be run with OCGT plants and a heat recovery generator system (HRGS) to produce both water and electricity [37]. The energy consumption, financial and technical parameters of all the desalination technologies utilised are listed in the Supplementary Material (Table S1).

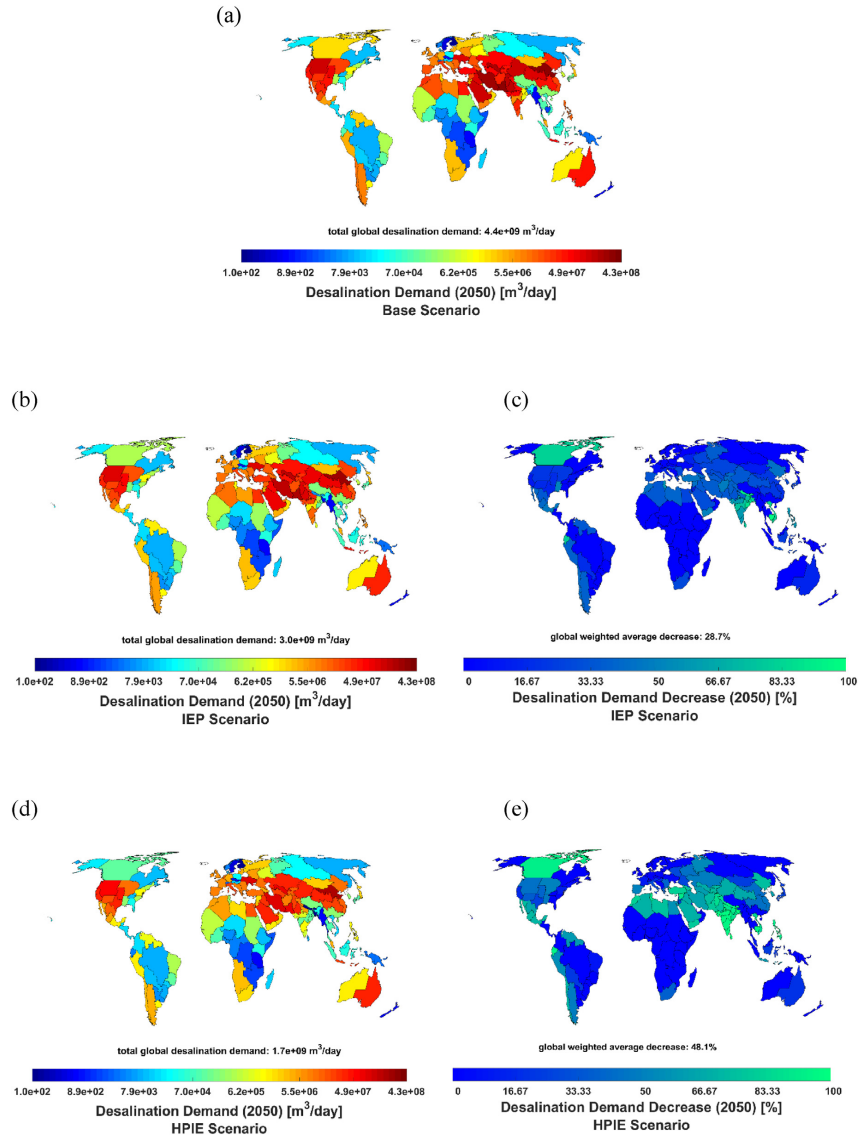

Fig. 9. Desalination demand in 2050 in the Base scenario (a), IEP scenario (b), demand decrease in percent in the IEP scenario (c), desalination demand in 2050 in the HPIE scenario (d), demand decrease in percent in the HPIE scenario (e).

4. The model optimises the installation of different RE systems to run the desalination plants installed from 2020. The financial and technical parameters of the energy system components, illustrated in Fig. 5, are used as input data for the model and provided in the Supplementary Material (Tables S2 and S3). The desalination capacities that are online in 2015 are run based on the average energy, technical and financial parameters [37]. A combination of thermal based power plants is used to meet the

electricity and heat demand of desalination plants in 2015, taking into account unsubsidised oil and gas costs.

5. To meet the desalination demand from 2020 onwards, the model optimises the installation of SWRO or MED stand-alone based on the overall costs of the final system. The model does not install new MSF plants or MED co-generation plants due to the high thermal energy consumption and thus high cost of these technologies.
6. The adoption of solar PV or wind power plants depend on the RE resource profiles and the respective financial and technical parameters. The unsubsidised natural gas cost is used to evaluate the costs of fossil gas in the energy transition for the 145 regions. Other fossil based thermal power plants are not installed during the transition. In addition, a CO_2 cost is accounted for over the time period, as listed in the Supplementary Material (Table S4). The solar PV and wind resource profiles for the 145 regions are obtained as presented in Bogdanov et al. [32].

Fig. 7 indicates the desalinated water pumping distances for the Base scenario in 2050. Fig. 7 (a) illustrates the weighted average horizontal pumping distance for each of the 145 regions. Similarly, Fig. 7 (b) illustrates the weighted average vertical pumping distance. The weighted average distances vary slightly for each time step and between scenarios as the desalination demand distribution changes.

3. Results

3.1. Impacts on water demand due to the use of improved irrigation systems

The bar charts in Fig. 8 illustrate the desalination technologies required to meet the desalination demand from 2020 to 2050, for the three scenarios. From 2020 onwards, SWRO is found to be the preferred technology to meet the increasing desalination demand. There is also an increase in water storage observed over time with the steepest increase occurring in 2050. Water storage supplements the output from the desalination plants during times of low renewable electricity generation.

The second y-axis on Fig. 8 indicates the growth in total water demand for the agricultural, municipal and industrial sectors. In the Base scenario, the total water demand is 19 billion m^3/day by 2050, and 23% of the demand is met by desalination. In contrast, in the IEP scenario, the global water demand decreases to 17 billion m^3/day by 2050 and 18% is met through desalination. The HPIE scenario indicates a decrease in the total water demand from 2015 onwards until 2040, before increasing more than the 2015 estimate of 13 billion m^3/day. The initial decreasing trend is attributed to the immediate effects of the irrigation efficiency improvement. However, after 2040, the increase in water demand overtakes the effects of the efficiency growth, resulting in a slight increase from 2040 to 2050. Desalination plants are required to meet up to 12% of the final water demand in 2050. In an entirely renewable energy run

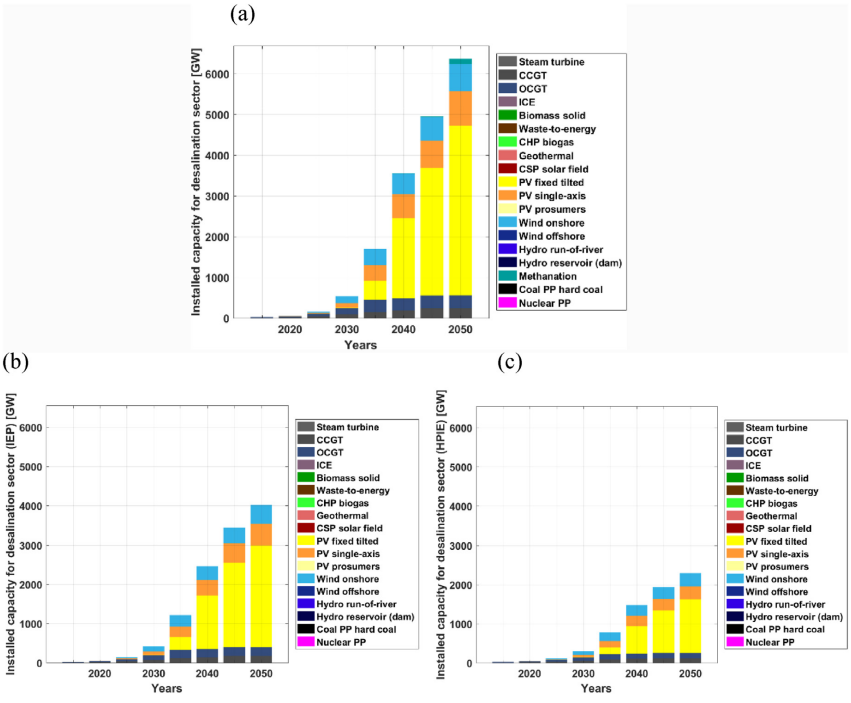

Fig. 10. Power generation capacities required for the desalination transition in the Base (a), IEP (b) and HPIE (c) scenarios in the period 2015 to 2050.

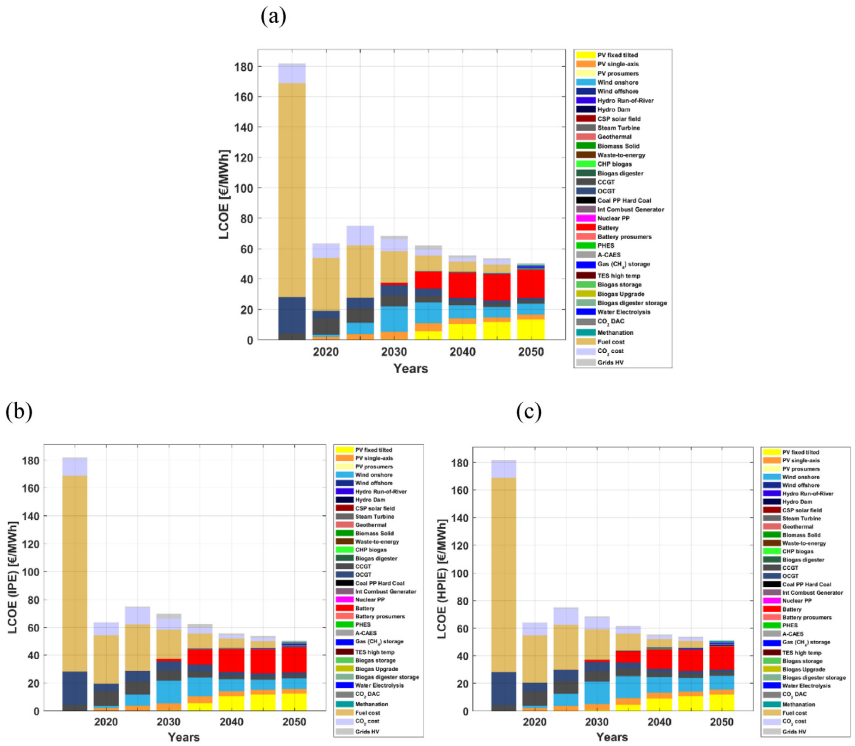

Fig. 11. LCOE during the energy transition from 2015 to 2050 for the Base (a), IEP (b) and HPIE (c) scenarios.

desalination sector in 2050, water storage accounts for less than 1% of the total desalination demand in the Base, IEP and HPIE scenarios.

Fig. 9 presents the desalination demand for the year 2050, across the three scenarios for 145 regions. The scale has been kept the same to aid comparison. For the IEP and HPIE scenarios, the percentage of reduction in desalination demand from the 2050 Base scenario is presented. These figures quantify the impacts of improved irrigation efficiency systems on the desalination demand. In the Base scenario, the countries with the largest desalination demand are China (824 million m^3/day), Pakistan (648 million m^3/day), India (477 million m^3/day) and USA (433 million m^3/day). When the irrigation efficiency is increased in the IEP scenario, as per Fig. 2, the desalination demand reduces by 27% for China, 36% for Pakistan, 17% for United States and 44% for India. The regions Cambodia, Nepal and Bhutan experience nearly 100% reduction in the desalination demand. This indicates that the relatively smaller desalination demand estimated for the regions are due to the irrigation sites. The sub-regions India-East and Canada-West also observed a dramatic decrease of 89% and 83% in desalination demand.

In the most efficient HPIE scenario, the 4 countries with the highest desalination demand were China (381 million m^3/day), USA (275 million m^3/day), Iran (116 million m^3/day) and Pakistan (115 million m^3/day). India and Sri Lanka experienced the largest reduction of 86% and 99% respectively. In fact, with the increase in irrigation efficiency, Sri Lanka has no requirement for desalinated water. The desalination capacity that remains in 2050 is the capacity that has already been online in 2015. As a sub-region, Pakistan-North experienced the largest decrease of 87%. Pakistan-South experienced a slightly lower decrease of 80%. Globally, the weighted average reduction is about 29% and 48% in the IEP and HPIE scenarios respectively. Fig. 9(d) and (e) also show that about half of the 145 regions experience no more than 10% reduction in demand, indicating the lower irrigation water withdrawals in these regions.

The desalination demand growth from 2015 to 2050 for the 145 regions for the Base, IEP and HPIE scenarios are provided in the Supplementary Material (spreadsheet file). Additional parameters, including the results discussed in the following sub-sections, are also presented for the 145 regions in the Supplementary Material (spreadsheet file).

3.2. Energy system transition

The desalination demand increases at different rates for the 145 regions, across the three scenarios, based on the water stress, demand and irrigation efficiency factors. In this section, the results of

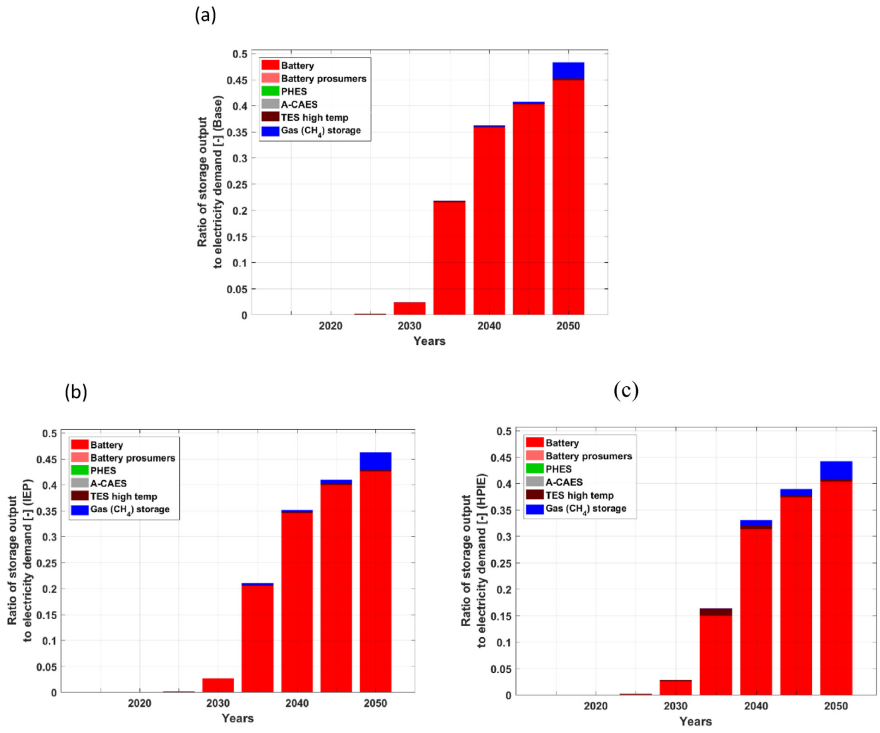

Fig. 12. Ratio of output from different storage options to electricity demand in the Base (a), IEP (b) and HPIE (c) scenarios.

the energy system transition is discussed from both a global and region-specific perspective.

Fig. 10 presents the growth of the power generation capacities required for the global desalination capacity in the three scenarios. Solar PV dominates the installed power capacities with approximately 5015 GW in the Base scenario, 3148 GW in the IEP scenario and 1697 GW in the HPIE scenario. The wind installations do not vary as much across the scenarios with 667 GW required in the Base scenario, 477 GW in the IEP scenario and 340 GW in the HPIE scenario. The total required electricity generation in 2050 is 10460 TWh, 6710 TWh and 3850 TWh in the Base, IEP and HPIE scenarios, whereas the solar PV generation share is 81%, 79% and 73% respectively.

These sets of results highlight that regions with high desalination demand and significant water demand for irrigation also lie in regions with an abundance of solar resources.

Gas turbines are sought throughout the transition to burn fossil natural gas or renewable electricity based synthetic natural gas (SNG) at times of low renewable electricity production. The full load hours of the gas turbines reduce from around 4000 h in 2020 to 500 h in 2050, indicating the decreasing reliance on the output from gas turbines. Reflecting the installed capacities, solar PV has the highest generation share with 80%, 78% and 73% in the Base, IEP and HPIE scenarios respectively. By 2050, there is no use of fossil fuel in the global energy system, thereby achieving an entirely RE based desalination sector.

Fig. 11 presents the average LCOE of the global energy system during the transition. The LCOE decreases drastically from 180 €/MWh to approximately 50 €/MWh for the three scenarios. The initial high cost in 2015 is due to the significant use of fossil fuel, taking into account the unsubsidised costs. During the transition, the cost of fuel diminishes as fossil gas is replaced with RE based power plants. In 2050, solar PV plants and battery storage account for the largest share of the LCOE. The CO_2 cost decreases with increase in RE generation and is eliminated by transitioning to a 100% RE based energy system.

Energy storage capacities are installed during the transition to ensure the operation of the desalination plants when there is insufficient generation from solar and wind resources. In total 13 TWh_{cap}, 8 TWh_{cap}, and 4 TWh_{cap} of battery energy storage capacity, as the major energy storage solution, are required in 2050 for the Base, IEP and HPIE scenarios, respectively. Fig. 12 shows the ratio of the storage output that is used to meet the electricity demand. Battery storage starts to play a significant role after 2035, accounting for 45%, 42% and 40% in the Base, IEP and HPIE scenarios. The role of gas storage, holding synthetic natural gas, increases slightly in the entirely RE based system in 2050. However, gas storage output is only used to meet 5% of the electricity demand, indicating the dominance of battery storage in the transition, which is a regular result in energy system transition analyses [32,34,37].

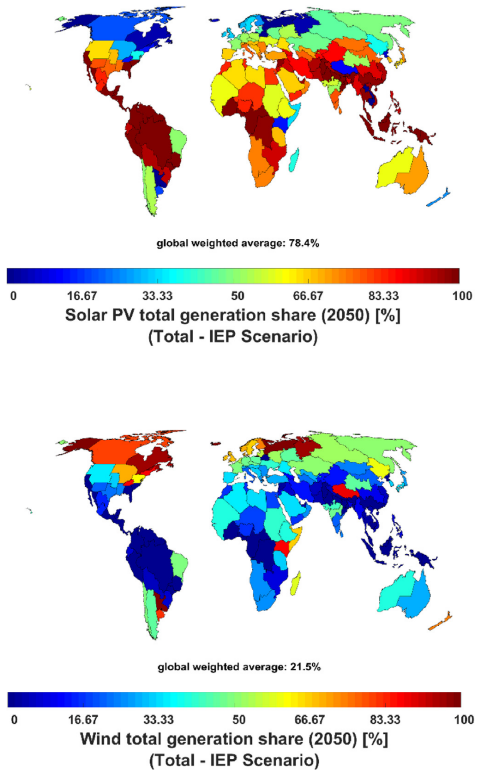

Fig. 13. Generation shares of solar PV (a) and wind turbines (b) in 2050 of the IEP scenario.

The decrease in battery storage output contribution from the Base to the HPIE scenarios, may be attributed to the decrease in desalination demand of irrigation sites that are located in regions with plentiful solar resources.

In order to gain a region wide perspective, Fig. 13(a) and (b) illustrate the total solar PV and wind generation shares in 2050 for the IEP scenario respectively. Solar PV is the dominant electricity generation source in most regions of the world, except for wind resource rich parts of North America, Northern Europe, eastern regions of South America and East Africa. The globally weighted average solar PV and wind generation shares are about 78% and 22% respectively. The regions with high wind generation shares are also regions with relatively lower desalination demand.

The global average LCOW decreases from 2.4 €/m^3 in 2015 to approximately 1.05 €/m^3, across all scenarios, by 2050. Fig. 14 presents the variation in the global average LCOW and the different components that contribute to the final LCOW. The high cost in 2015 is mostly due to the real unsubsidised market price of fossil gas used for electricity and heat production. The electricity production cost decreases throughout the transition, due to the increasing share and decreased costs of RE power plants. To meet the desalination demand, the model opts for SWRO instead of MED stand alone plants, as shown in Fig. 9, thereby overcoming the need to burn gas for heat production. The desalination cost comprises of the decreasing capital and operational expenditures of the desalination plants, mainly the SWRO plants. The increase in the horizontal transportation costs indicates the spread of the desalination demand further inland and the increase in demand for desalination. The water storage cost is minimal in all scenarios.

Fig. 15 highlights the region specific LCOW in 2050 for the three scenarios. Most regions of the world, representing 82%–88% of global desalination demand, achieve an LCOW range of 0.32 €/m^3 – 1.66 €/m^3, including the cost of transporting water from the coast to the demand site. Sub-regions of China, India, Australia and USA mostly have a LCOW less than 1 €/m^3. Regions with larger water transportation distances, such as Iran, Central Asia, and inland regions of China have higher costs. Regions like Papua New Guinea, where the desalination demand is constant throughout the transition due to available installed capacity in 2015 but no specific demand value, obtain a higher LCOW during the transition. This is owing to a slower transition, where 100% RE based desalination sector is specified to be achieved only by 2050.

Table 4 presents the global and country-specific capital expenditures required for the three scenarios by 2050. In comparison to the Base scenario, the global capex requirements for IEP and HPIE scenarios decrease by 32% and 62% respectively. The opex for the IEP and HPIE scenarios decrease also by the same amount. The listed five countries account for 60%, 59% and 59% of the total capex in the Base, IEP and HPIE scenarios. For India, the cumulative system capex requirements, in the IEP and HPIE scenarios, are reduced by 42% and 85% respectively. This was the largest reduction, followed by Pakistan with 38% and 82%. China continues to retain the largest shares of the global investments required.

4. Discussion

In the Base scenario, where irrigation efficiency improvements are discounted, the total water demand of all sectors is projected to increase to 19 billion m^3/day by 2050. This is slightly higher than the 15 billion m^3/day total demand extrapolated from n the water demand numbers in the Aquastat database [38]. India, China, USA, Pakistan and Indonesia account for 51% of the total water demand in 2050. According to Amarasinghe and Smakhtin [38], the listed countries, bar Indonesia, have accounted for 47% of the global water withdrawals between 1995 and 2010. Reflecting the same patterns, the four countries account for 54% of the global desalination demand in 2050. Whilst Indonesia has the 5th highest water demand, the country also has significant renewable water resources, rendering the country as a lower water-stressed country. In contrast, China, India, USA and Pakistan, require 29%, 15%, 25% and 55% respectively, of the country's total water demand to be met with desalination. The higher share in Pakistan highlights the fact that water demand is concentrated in regions of overexploited aquifers. Globally, it is found that in the Base scenario, desalination plants are required to meet 23% of the water demand by 2050.

Dalin et al. [39] show that Pakistan, USA and India account for two-thirds of the groundwater abstractions embedded in international food trade. In contrast with the fact that these nations are the breadbaskets of the world, 100%, 94% and 48% of the irrigated areas are covered by surface irrigation systems [12]. Meanwhile, climate change further threatens existing freshwater resources, and projections anticipate water demand from the municipal and industrial sectors to rise more steeply than that of the irrigation sector [40]. China, whose main agricultural fields lie on some of the world's most water stressed basins in the Northeast, is reported to have already begun investing in improved irrigation systems [38]. However, the report also claims that India is lagging with no

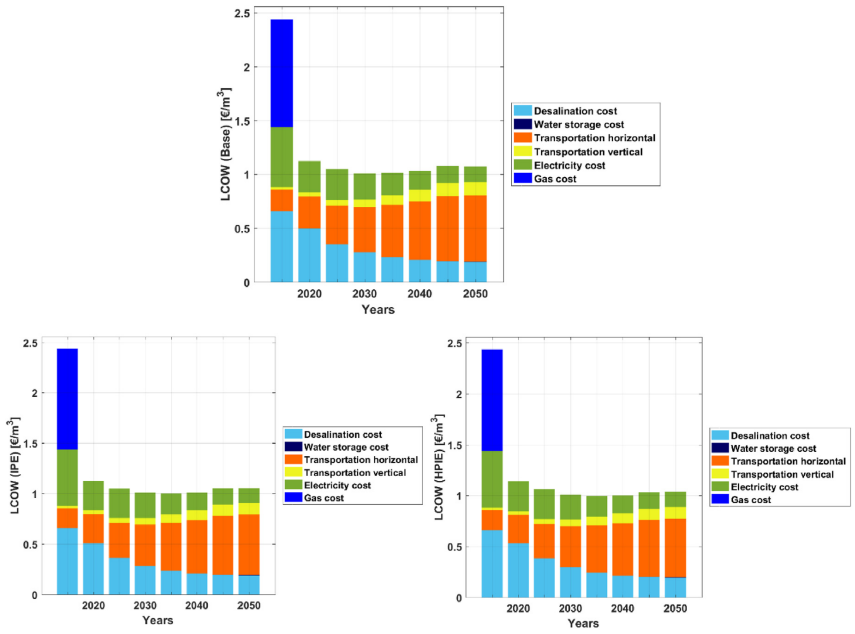

Fig. 14. Variation in the global average LCOW during the energy transition from 2015 to 2050 for the Base (a), IEP (b) and HPIE (c) scenarios.

concrete interest taken by the government to improve the water use efficiency in the irrigation sector. In contrast, Israel is reported to have 75% of the irrigation done by drip technology and have been able to increase the value of crops grown by 1600% over the last 65 years [41].

The improved water use efficiency growth adopted in the IEP and HPIE scenarios result in a 30% and 60% reduction of the total desalination demand respectively. Table 5 breaks down the total water demand in 2050 for the top 5 countries. Table 6 does the same for the desalination demand in 2050. Despite the increase in irrigation efficiency, India, China, USA, Pakistan and Indonesia continue to retain the largest shares of the total global water withdrawals. The cumulative shares of the global water withdrawal decrease slightly from 51% in the Base scenario to 48% in the HPIE scenario.

The countries with the largest shares of the global desalination demand in all three scenarios are China, Pakistan, India and Iran. The cumulative shares of the global desalination demand decrease from 62% in the Base scenario to 56% in the HPIE scenario. In the HPIE scenario, Iran takes over India as the country with the 3rd largest desalination demand. These results highlight the untapped potential of improving irrigation efficiencies across India to better manage the water demand in exploited aquifers. Recent reports discuss the dire circumstances of water supplies in India as monsoon rains become intermittent and groundwater and reservoirs are steadily depleted [42,43]. The think-tank NITI Aayog expect 21 cities in India to runout of groundwater as early as next year, endangering the lives of almost 100 million people. India's water crisis is already at its doorstep. With the adoption of better irrigation systems, India can dent the surge in demand for water by almost 70%. In fact, our results show that by increasing the irrigation efficiency, the total water demand by 2050 can be 8% lower than the current water withdrawals recorded for India [44]. A similar observation from the global perspective is presented in Fig. 8 (c) where the total water projection by 2050 does not increase much more than the current water withdrawals. Furthermore, the 60% decrease in desalination demand in the HPIE scenario, relative to the Base scenario, highlights the fact that most of the world's irrigation sites lie in water scarce regions.

The results presented in Section 3.2 highlight the fact that the combination of solar PV and battery storage play a key role in powering the global desalination demand. These results for the three scenarios confirm what had been found earlier in detailed energy system studies for India, Pakistan, Iran, Saudi Arabia, Israel, and Turkey [33]. The global average solar PV generation supply share of 73–81% is in line to latest findings for the global power sector [32] and the entire global energy system [45], both reaching 69% of solar PV supply share, which is a consequence of the excellent solar resource availability and economics [22]. Fig. 8 also highlights the fact water storage does not provide as much flexibility to the energy system, contributing only up to 1% of the total desalination demand. This is because the combination of solar PV and battery storage provide lower cost flexibility than running the capex intensive SWRO plants at lower full load hours [46].

The slightly higher solar PV supply share in the desalination sector compared to the power sector and total energy system [45] is exemplified by the fact that most of water stressed regions are located in areas with plentiful solar resources. The solar PV and wind generation capacities obtained during the transition are summarised in the Supplementary Material (spreadsheet file). The

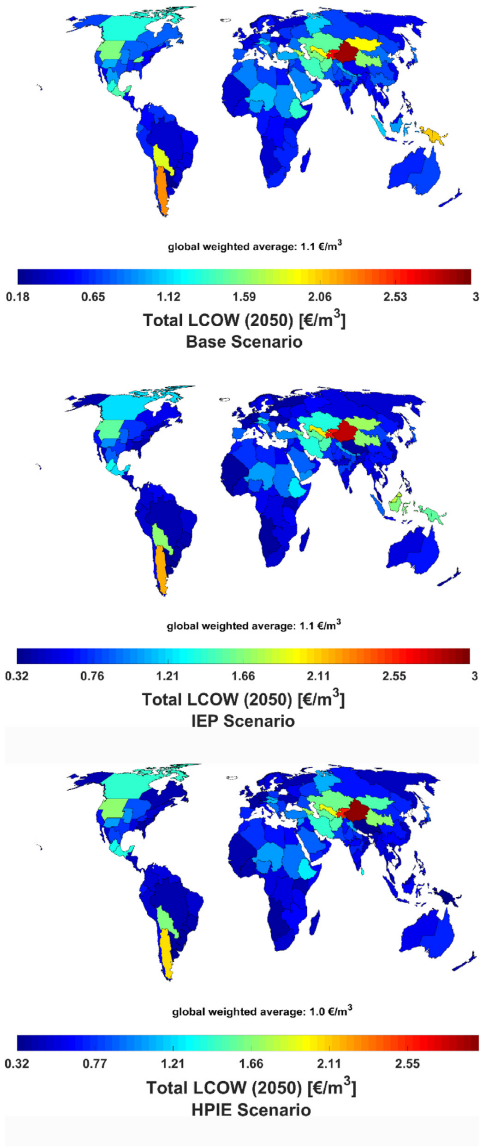

Fig. 15. Regional distribution of the LCOW in 2050 for the Base (a), IEP (b) and HPIE (c) scenarios.

total global solar PV capacity demand of 5015 GW, 3148 GW and 1697 GW in the Base, IEP and HPIE scenarios equals to about 7.9%, 5.0% and 2.7% of the total projected 63,380 GW solar PV capacity demand for a fully sustainable and renewable energy system [45],

Table 4
Total cumulative capex, cumulative opex and annual opex requirements, by 2050, for the Base, IEP and HPIE scenarios.

	Capex b€		Opex b€		Annual Opex b€/a	
	Desalination	Energy	Desalination	Energy	Desalination	Energy
Global						
Base	8769	6416	1019	218	50	25
IEP	5942	4409	693	156	35	25
HPIE	3260	2505	380	81	19	7.5
China						
Base	1993	1231	229	42	40	3
IEP	1373	916	162	32	7.5	3
HPIE	769	548	90	18	2.5	0.5
USA						
Base	917	647	99	22	4.5	2.5
IEP	739	518	81	18	4	3
HPIE	607	420	64	13	7	1
India						
Base	669	695	71	22	10	5
IEP	391	401	41	31	0.3	0.8
HPIE	103	106	10	3	0.05	0.15
Pakistan						
Base	926	849	104	30	24	14
IEP	579	515	64	17	2.5	1.5
HPIE	168	149	19	5	1.0	0.5
Iran						
Base	778	432	99	16	4.5	4
IEP	496	269	63	9	1.5	0.5
HPIE	300	162	38	5	1.0	0.5

which is further supported by Haegel et al. [22].

During the transition, the global average LCOW decreases from about 2.4 €/m^3 in 2015 to approximately 1.05 €/m^3 by 2050, with most regions in the cost range of 0.32 €/m^3 – 1.66 €/m^3. Currently, desalination plants powered by fossil plants produce potable water at a cost range of 0.60 €/m^3 – 1.90 €/m^3, excluding the cost of water transportation [11]. Therefore, the energy transition enables countries to achieve a cost-competitive and greenhouse gas emissions free desalination sector. The relatively higher LCOW estimated globally in 2015, as illustrated in Fig. 14, is due to the large consumption of fossil fuel at unsubsidised costs. When the actual cost of the fuel is considered, it is not lucrative to run lower efficient MSF or MED plants that require large amounts of gas for heat generation. As a result, during the transition, the model rapidly switches to the use of SWRO for water production and phases out the thermal desalination technologies based on the lifetime.

Gao et al. [8] modelled the future municipal water price in 140 countries based on specific socio-economic factors. The average water price is projected to increase and by 2050, lie between 1.2 USD/m^3 - 1.4 USD/m^3 or 0.9 €/m^3 - 1.0 €/m^3, based on a 1.3 USD to 1 € exchange rate. The results show that a decarbonised desalination sector will enable water costs competitive with the municipal water prices, across all the major regions. The LCOW and LCOE variation obtained during the transition for all regions are summarised in the Supplementary Material (spreadsheet file).

An analysis of the global and regional investments required, as presented in Table 4, further explain the benefits of improving the water use efficiency in the irrigation sector. By improving the irrigation systems of these countries, the total investments required to meet the water demand through desalination can be significantly reduced. In countries like India, the investments can be reduced by as much as 85%.

The presented work considers the costs of running desalination plants while improving irrigation efficiency. The results do not account for investments required to upgrade the irrigation infrastructure across the regions. This would be the next step of

Table 5
Countries with the largest total water demand by 2050, in the Base, IEP and HPIE scenarios. The percentage share of the corresponding scenarios' total global water demand in 2050 is also presented.

Base			IEP			HPIE		
Country	Demand million m^3/day	%	Country	Demand million m^3/day	%	Country	Demand million m^3/day	%
India	3 105	16	India	2 673	15	China	2 220	15
China	2 890	15	China	2 599	15	India	1 921	13
USA	1 730	9	USA	1 631	9	USA	1 474	10
Pakistan	1 169	6	Pakistan	926	5	Indonesia	815	6
Indonesia	914	5	Indonesia	881	5	Pakistan	539	4

Table 6
Countries with the largest desalination demand by 2050, in the Base, IEP and HPIE scenarios. The percentage share of the corresponding scenarios' total desalination water demand in 2050 is also presented.

Base			IEP			HPIE		
Country	Demand million m^3/day	%	Country	Demand million m^3/day	%	Country	Demand million m^3/day	%
China	824	19	China	601	10	China	380	22
Pakistan	648	15	Pakistan	413	14	USA	275	16
India	477	11	USA	360	12	Iran	116	7
USA	433	10	India	266	9	Pakistan	111	7
Iran	314	7	Iran	199	6.5	India	64	4

developing a comprehensive study. Various literature exist on the topic of estimating the cost of improving irrigation infrastructure, particularly in developing regions [47,48]. For instance, Rosegrant et al. [47] estimated that to increase irrigation efficiency by 15% in developing countries by 2030, it would cost approximately 4.58 billion USD a year on average between 2015 and 2050. A similar study was carried out by the World Bank Group [48] on investments required to improve irrigation infrastructure for different socioeconomic pathways.

In addition to RE-based desalination, researchers and organisations call for the ramping up of nuclear based desalination to produce potable water [49]. This is because this form of energy generation does not result in greenhouse gas emissions and it delivers base generation electricity. Whilst this is true, the use of nuclear energy poses other financial, sustainable and social threats to society. This includes the significant subsidies used for running nuclear plants, the environmental burden of nuclear waste storage, the significant water withdrawals for cooling the nuclear plants, and the links between nuclear energy and nuclear weapons proliferation [50,51]. In the current environmental and political climate, nuclear based desalination threatens to do more harm than good to society.

By 2050, crop production is expected to increase by 70% to ensure global food security [40]. Meanwhile, renewable and non-renewable water resources are dwindling [11,40], endangering the feasibility of the UN SDGs 2 and 6. Mahlknecht et al. [52] explain, using the case of Latin America and the Caribbean, how food production is dependent on the availability of water and greenhouse gas emissions. The water-energy-food nexus is evaluated using the indicators UN SDGs 2, 6 and 7 that focus on food security, clean water and energy for all respectively. It is found that more attention needs to be paid to fostering relationships between the water, energy and food sectors to secure sustainable development. Vanham et al. [53] analysed the SDG indicator 6.4.2 on blue water stress and noted the substantial increase in water use efficiency required across all sectors and the use of desalination as a viable water resource.

The results of this research illustrate how more efficient irrigation systems and a renewable energy based desalination sector can be a viable solution to closing the gap between global water demand and supply while also eliminating GHGs. By doing so, we shed light on the untapped relationship between the global energy, water and food sectors that can be harnessed to achieve the respective SDGs.

5. Conclusion

This study shows that renewable energy based desalination, together with improvements in water use efficiency in the irrigation sector, can play a pivotal role in securing future global water supplies. The lack of global water supplies to meet the increasing demand, the water use efficiencies in the irrigation sector and the expanding desalination sector are topics of increasing concern in the global community.

With moderate development in the irrigation sector, as in the IEP scenario, the total water demand and desalination demand by 2050 is estimated to decrease by 10% and 30% respectively, relative a Base scenario. By achieving a more optimistic 90% efficiency by 2050, as in the HPIE scenario, the total water and desalination demand are projected to decrease by 30% and 60% respectively. Consequently, the investments required to supply water through desalination is estimated to decrease by 32% and 62% in the IEP and HPIE scenarios respectively.

Meanwhile, the global desalination sector can be powered through a combination of solar PV and wind power by 2050, to produce potable water at costs competitive with current fossil powered desalination plants. Solar PV is expected to emerge as the dominant source of energy supply for desalination due to excellent economics and vast resource availability in regions of desalination demand. Battery storage enables practically baseload operation of desalination plants as the least cost solution. The global LCOW in 2050, including the cost of water transportation, is estimated to lie mostly between 0.32 €/m^3 – 1.66 €/m^3, competing with the municipal water price projections.

Therefore, the results highlight the relationships between the irrigation and decarbonised desalination sector that can be utilised to strengthen the global water supply for the decades to come. United Nations Sustainable Development Goals are strongly

supported by a vast expansion of renewable electricity based desalination for clean water supply.

Declaration of competing interest

The authors declare that they have no known competing financial interests or personal relationships that could have appeared to influence the work reported in this paper.

CRediT authorship contribution statement

Upeksha Caldera: Conceptualization, Methodology, Software, Formal analysis, Visualization, Writing - original draft. **Christian Breyer:** Conceptualization, Methodology, Formal analysis, Writing - review & editing, Supervision.

Acknowledgment

The first author gratefully acknowledges the grant offered by the Finnish Cultural Foundation.

Appendix A. Supplementary data

Supplementary data to this article can be found online at https://doi.org/10.1016/j.energy.2020.117507.

References

[1] World Bank. The role of desalination in an increasingly water-scare world. Washington, DC: World Bank; 2019.
[2] Gude V. Desalination and sustainability – an appraisal and current perspective. Water Res 2016;89:87–106.
[3] Jia X, Klemes JJ, Varbanov PS, Alwi SRW. Analysing the energy consumption, GHG emission, and cost of seawater desalination in China. Energies 2019;12:463.
[4] Water Technology. Growth expected for global water desalination market from 2018 to 2025. Birmingham, Alabama, USA: Endeavour Business Media; 2019. https://www.watertechonline.com/growth-global-water-desalination-market/.
[5] Jones E, Qadir M, Vliet MTHV, Smakhtin V, Kang S. The state of desalination and brine production: a global outlook. Sci Total Environ 2019;657:1343–56.
[6] Virgili F. Q3 2016 market update. Oxford, United Kingdom: Global Water Intelligence; 2017. www.desaldata.com/forecasts.
[7] Mayor B. Growth patterns in mature desalination technologies and analogies with the energy field. Desalination 2019;457:75–84.
[8] Gao L, Yoshikawa S, Iseri Y, Fujimori S, Kanae S. An economic assessment of the global potential for seawater desalination to 2050. Water 2017;9:763–82.
[9] Hanasaki N, Yoshikawa S, Kakinuma K, Kanae S. A seawater desalination scheme for hydrological models. Hydrol Earth Syst Sci 2016;20:4143–57.
[10] Wada Y, Gleeson T, Esnault L. Wedge approach to water stress. Nat Geosci 2014;7:615–7.
[11] Caldera U, Bogdanov D, Breyer Ch. Local cost of seawater RO desalination based on solar PV and wind energy: a global estimate. Desalination 2016;385:207–16.
[12] Jägermeyr J, Gerten D, Heinke J, Schaphoff S, Kummu M, Lucht W. Water savings potentials of irrigation systems: global simulation of processes and linkages. Hydrol Earth Syst Sci 2015;19:3073–91.
[13] Caldera U, Breyer C. Assessing the potential for renewable energy powered desalination for the global irrigation sector. Sci Total Environ 2019;694:133598.
[14] Fyles H, Madramootoo C. Water management. Emerging technologies for promoting food security. Sawston, United Kingdom: Woodhead Publishing (Elsevier); 2016.
[15] Medeazza von MG, Moreau V. Modelling of water-energy systems. The case of desalination. In: Energy, 2007, vol. 32; 2007. p. 1024–31.
[16] Ghaffour N, Missimer MT, Amy LG. Technical review and evaluation of the economics of water desalination: current and future challenges for better water supply sustainability. Desalination 2013;309:197–207.
[17] International Renewable Energy Agency. Water desalination using renewable energy. Technology brief. Abu Dhabi: IRENA; 2012.
[18] Martin-Gorriz B, Soto-Garcia M, Alvarez-Martinez V. Energy and greenhouse-gas emissions in irrigated agriculture of SE (southeast) Spain. Effects of alternative water supply scenarios. Energy 2014;77:478–88.
[19] Global Clean Water Desalination Alliance. $H_2O - CO_2$, concept paper. GCWDA, Abu Dhabi. 2015. https://www.diplomatie.gouv.fr/IMG/pdf/global_water_desalination_alliance_1dec2015_cle8d61cb.pdf.
[20] Intergovernmental Panel on Climate Change. Global warming of 1.5°C. An IPCC special report on the impacts of global warming of 1.5°C above pre-industrial levels and related global greenhouse gas emission pathways, in the context of strengthening the global response to the threat of climate change, sustainable development, and efforts to eradicate poverty. Geneva, Switzerland: World Meteorological Organization; 2018.
[21] Freyberg T. Desalination + Renewables: a long engagement without the wedding? WaterWorld. 2018. Oklahoma, USA.
[22] Haegel MN, Atwater Jr h, Barnes T, Breyer C, Burrell A, Chiang YM, De Wolf S, Dimmler B, Feldman D, Glunz S, Goldschmidt CJ, Hochschild D, Inzunza R, Kaizuka I, Kroposki B, Kurtz S, Leu S, Margolis R, Matsubara K, Metz A, Metzger KW, Morjaria M, Niki S, Nowak S, Peters MI, Philipps S, Reindl T, Richter A, Rose D, Sakurai K, Schlatmann R, Shikano M, Sinke W, Sinton R, Stanbery BJ, Topic M, Tumas W, Ueda Y, van de Lagemaat J, Verlinden P, Vetter M, Warren E, Werner M, Yamaguchi M, Bett A W. Terawatt-scale photovoltaics: transform global energy. Science 2019;364(6443):836–8.
[23] Vartiainen E, Masson G, Breyer C, Moser D, Medina ER. Impact of weighted average cost of capital, capital expenditure and other parameters on future utility-scale. PV Levelised Cost of Electricity; 2019. https://doi.org/10.1002/pip.3189. published online.
[24] Schmidt O, Hawkes A, Gambhir A, Staffell I. The future cost of electrical energy storage based on experience rates. Nat Energy 2017;2:17110.
[25] Publicover B. LCOE for Li-ion batteries has fallen to 187$/MWh – BNEF. Berlin: PV Magazine; 2019. https://www.pv-magazine.com/2019/03/26/lcoe-for-li-ion-batteries-down-35-to-187-mwh-since-2018-bnef/.
[26] Dipaola A. Dubai plans desert city's first solar-powered desalination plant. New York: Bloomberg; 2019. https://www.bloomberg.com/news/articles/2019-02-11/dubai-plans-desert-city-s-first-solar-powered-desalination-plant.
[27] Sadiqa A, Gulagi A, Breyer C. Energy transition roadmap towards 100% renewable energy and role of storage technologies for Pakistan by 2050. Energy 2018;147:518–33.
[28] United Nations World Water Assessment Programme. The united nations world water development report: water and energy. Paris, France: UNESCO; 2014.
[29] Lohrmann A, Farfan J, Caldera U, Lohrmann C, Breyer C. Global scenarios for significant water use reduction in thermal power plants based on cooling water demand estimation using satellite imagery. Nat Energy 2019;4:1040–8.
[30] United Nations. Sustainable development goals knowledge platform. UN, New York, https://sustainabledevelopment.un.org/sdgs.
[31] Luck M, Landis M, Gassert F. Aqueduct Water Stress Projections: decadal projections of water supply and demand using CMIP5 GCMs. Washington DC: World Resources Institute; 2015. http://www.wri.org/sites/default/files/aqueduct-water-stress-projections-technical-note.pdf.
[32] Bogdanov D, Farfan J, Sadovskaia K, Aghahosseini A, Child M, Gulagi A, Oyewo SA, Barbosa SNSL, Breyer C. Radical transformation pathway towards sustainable electricity via evolutionary steps. Nat Commun 2019;10:1077.
[33] Hansen Kenneth, Breyer Christian, Lund Henrik. Status and perspectives on 100% renewable energy systems. Energy 2019;175:471–80.
[34] Breyer Ch, Bogdanov D, Gulagi A, Aghahosseini A, Barbosa LSNS, Koskinen O, Barasa M, Caldera U, Afanasyeva S, Child M, Farfan J, Vainikka P. On the role of solar photovoltaics in global energy transition scenarios. Prog Photovolt Res Appl 2017;25:727–45.
[35] Amante C, Eakins BW. ETOPO1 1 arc-minute global relief model: procedures, data sources and analysis. NOAA technical memorandum NESDIS NGDC-24. NOAA, Colorado, USA: National Geophysical Data Center; 2009.
[36] Virgili F. Q3 2016 market update. Oxford, United Kingdom: Global Water Intelligence; 2017. www.desaldata.com/forecasts.
[37] Caldera U, Bogdanov D, Afanasyeva S, Breyer C. Role of seawater desalination in the management of an integrated water and 100% renewable energy based power sector in Saudi Arabia. Water 2018;10:3.
[38] Amarasinghe AU, Smakhtin V. Global water demand projections: past, present and future. IWMI Research Report 156, 32. Colombo: International Water Management Institute; 2014.
[39] Dalin C, Wada Y, Kastner T, Puma JM. Groundwater depletion embedded in international food trade. Nat Lett 2017;543:700–4.
[40] United Nations World Water Assessment Programme. The united nations world water development report 2015: water for a sustainable world. Paris: UNESCO; 2015.
[41] Tal A. Rethinking the sustainability of Israel's irrigation practices in the Drylands. Water Res 2016;90:387–94.
[42] Yeung J, Gupta S, Guy M. India has five years to solve its water crisis, experts fear. Otherwise hundreds of millions of lives will be in danger. Georgia, USA: Cable News Network; 2019. https://edition.cnn.com/2019/06/27/india/india-water-crisis-intl-hnk/index.html.
[43] NITI Aayog. Composite water. Management index. A tool for water management. Delhi, India: National Institution for Transforming India; 2018. https://niti.gov.in/writereaddata/files/document_publication/2018-05-18-Water-index-Report_vS6B.pdf.
[44] DownToEarth. 688 billion cubic meters: India's water withdrawals for agriculture is the highest in the world. Down to Earth. 2018. New Delhi, https://www.downtoearth.org.in/news/water/688-billion-cubic-metres-india-s-water-withdrawals-for-agriculture-is-the-highest-in-the-world-60967.
[45] Ram M, Child M, Aghahosseini A, Bogdanov D, Lohrmann A, Breyer Ch. A comparative analysis of electricity generation costs from renewable, fossil

fuel and nuclear sources in G20 countries for the period 2015-2030. J Clean Prod 2018;199:687–704.
[46] Caldera U, Breyer C. The role that battery and water storage play in Saudi Arabia's transition to an integrated 100% renewable energy power system. J Energy Storage 2018;17:299–310.
[47] Rosegrant MW, Sulser TB, Mason-D'Croz D, Cenacchi N, Nin-Pratt A, Dunston S, Zhu T, Ringler C, Wiebe KD, Robinson S, Willenbockel D, Xie H, Kwon HY, Johnson T, Thomas TS, Wimmer F, Schaldach R, Nelson GC, Willaarts B. Quantitative foresight modeling to inform the CGIAR research portfolio. Project Report for USAID. Washington DC: International Food Policy Research Institute; 2017.
[48] Palazzo A, Valin H, Batka M, Havlík P. Investment needs for irrigation infrastructure along different socioeconomic pathways. Policy research working paper. Washington DC: World Bank Group; 2019.
[49] Conca J. How 1500 nuclear-powered water desalination plants could save the world from desertification. New Jersey: Forbes; 2019. https://www.forbes.com/sites/jamesconca/2019/07/14/megadroughts-and-desalination-another-pressing-need-for-nuclear-power/#42c869d37fde.
[50] Ram M, Child M, Aghahosseini A, Bogdanov D, Lohrmann A, Breyer Ch. A comparative analysis of electricity generation costs from renewable, fossil fuel and nuclear sources in G20 countries for the period 2015-2030. J Clean Prod 2018;199:687–704.
[51] Jacobson ZM. Evaluation of nuclear power as a proposed solution to global warming, air pollution, and energy security. In: 100% clean, renewable energy and storage for everything. United Kingdom: Cambridge University Press; 2020. https://web.stanford.edu/group/efmh/jacobson/Articles/I/NuclearVsWWS.pdf.
[52] Mahlknecht J, Gonzalez – Bravo R, Loge FJ. Water-energy-food security: a Nexus perspective of the current situation in Latin America and the Caribbean. Energy 2019;194:116824.
[53] Vanham D, Hoekstra AY, Wada Y, Bouraoui F, Rooa A, Mekonnen MM, Bund WJ, Batelaan O, Pavelic P, Bastiaanssen WGM, Kummu M, Rockström J, Liu J, Bisselink B, Ronco P, Pistocchi A, Bidoglio G. Physical water scarcity metrics for monitoring progress towards SDG target 6.4: an evaluation of indicator 6.4.2 "Level of water stress". Sci Total Environ 2018;613–614:218–32.

ACTA UNIVERSITATIS LAPPEENRANTAENSIS

893. HEKMATMANESH, AMIN. Investigation of EEG signal processing for rehabilitation robot control. 2019. Diss.

894. HARMOKIVI-SALORANTA, PAULA. Käyttäjät liikuntapalvelujen kehittäjinä - Käyttäjälähtöisessä palveluinnovaatioprosessissa käyttäjien tuottama tieto tutkimuksen kohteena. 2020. Diss.

895. BERGMAN, JUKKA-PEKKA. Managerial cognitive structures, strategy frames, collective strategy frame and their implications for the firms. 2020. Diss.

896. POLUEKTOV, ANTON. Application of software-defined radio for power-line-communication-based monitoring. 2020. Diss.

897. JÄRVISALO, HEIKKI. Applicability of GaN high electron mobility transistors in a high-speed drive system. 2020. Diss.

898. KOPONEN, JOONAS. Energy efficient hydrogen production by water electrolysis. 2020. Diss.

899. MAMELKINA, MARIA. Treatment of mining waters by electrocoagulation. 2020. Diss.

900. AMBAT, INDU. Application of diverse feedstocks for biodiesel production using catalytic technology. 2020. Diss.

901. LAAPIO-RAPI, EMILIA. Sairaanhoitajien rajatun lääkkeenmääräämistoiminnan tuottavuuden, tehokkuuden ja kustannusvaikuttavuuden arviointi perusterveydenhuollon avohoidon palveluprosessissa. 2020. Diss.

902. DI, CHONG. Modeling and analysis of a high-speed solid-rotor induction machine. 2020. Diss.

903. AROLA, KIMMO. Enhanced micropollutant removal and nutrient recovery in municipal wastewater treatment. 2020. Diss.

904. RAHIMPOUR GOLROUDBARY, SAEED. Sustainable recycling of critical materials. 2020. Diss.

905. BURGOS CASTILLO, RUTELY CONCEPCION. Fenton chemistry beyond remediating wastewater and producing cleaner water. 2020. Diss.

906. JOHN, MIIA. Separation efficiencies of freeze crystallization in wastewater purification. 2020. Diss.

907. VUOJOLAINEN, JOUNI. Identification of magnetically levitated machines. 2020. Diss.

908. KC, RAGHU. The role of efficient forest biomass logistics on optimisation of environmental sustainability of bioenergy. 2020. Diss.

909. NEISI, NEDA. Dynamic and thermal modeling of touch-down bearings considering bearing non-idealities. 2020. Diss.

910. YAN, FANGPING. The deposition and light absorption property of carbonaceous matter in the Himalayas and Tibetan Plateau. 2020. Diss.

911. NJOCK BAYOCK, FRANCOIS MITERAND. Thermal analysis of dissimilar weld joints of high-strength and ultra-high-strength steels. 2020. Diss.

912. KINNUNEN, SINI-KAISU. Modelling the value of fleet data in the ecosystems of asset management. 2020. Diss.

913. MUSIKKA, TATU. Usability and limitations of behavioural component models in IGBT short-circuit modelling. 2020. Diss.

914. SHNAI, IULIIA. The technology of flipped classroom: assessments, resources and systematic design. 2020. Diss.

915. SAFAEI, ZAHRA. Application of differential ion mobility spectrometry for detection of water pollutants. 2020. Diss.

916. FILIMONOV, ROMAN. Computational fluid dynamics as a tool for process engineering. 2020. Diss.

917. VIRTANEN, TIINA. Real-time monitoring of membrane fouling caused by phenolic compounds. 2020. Diss.

918. AZZUNI, ABDELRAHMAN. Energy security evaluation for the present and the future on a global level. 2020. Diss.

919. NOKELAINEN, JOHANNES. Interplay of local moments and itinerant electrons. 2020. Diss.

920. HONKANEN, JARI. Control design issues in grid-connected single-phase converters, with the focus on power factor correction. 2020. Diss.

921. KEMPPINEN, JUHA. The development and implementation of the clinical decision support system for integrated mental and addiction care. 2020. Diss.

922. KORHONEN, SATU. The journeys of becoming ang being an international entrepreneur: A narrative inquiry of the "I" in international entrepreneurship. 2020. Diss.

923. SIRKIÄ, JUKKA. Leveraging digitalization opportunities to improve the business model. 2020. Diss.

924. SHEMYAKIN, VLADIMIR. Parameter estimation of large-scale chaotic systems. 2020. Diss.

925. AALTONEN, PÄIVI. Exploring novelty in the internationalization process - understanding disruptive events. 2020. Diss.

926. VADANA, IUSTIN. Internationalization of born-digital companies. 2020. Diss.

927. FARFAN OROZCO, FRANCISCO JAVIER. In-depth analysis of the global power infrastructure - Opportunities for sustainable evolution of the power sector. 2020. Diss.

928. KRAINOV, IGOR. Properties of exchange interactions in magnetic semiconductors. 2020. Diss.

929. KARPPANEN, JANNE. Assessing the applicability of low voltage direct current in electricity distribution - Key factors and design aspects. 2020. Diss.

930. NIEMINEN, HARRI. Power-to-methanol via membrane contactor-based CO2 capture and low-temperature chemical synthesis. 2020. Diss.

LUT University

ISBN 978-952-335-580-4
ISBN 978-952-335-581-1 (PDF)
ISSN-L 1456-4491
ISSN 1456-4491
Lappeenranta 2020